

AD-A074 265

AIR FORCE WEAPONS LAB KIRTLAND AFB NM  
ELECTROMAGNETIC PULSE INTERACTION NOTES-EMP 3-39.(U)  
JUL 79 C E BAUM

F/G 20/14

UNCLASSIFIED

AFWL-TR-79-402

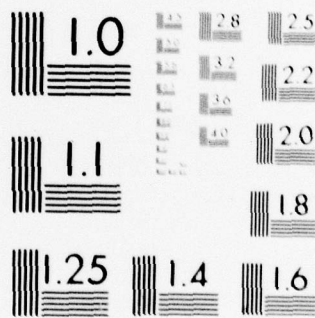
SBIE-AD-E200 363

NL

1 OF 5

AD  
A074265





MICROCOPY RESOLUTION TEST CHART  
NATIONAL BUREAU OF STANDARDS-1963-A

AFWL-TR-79-402

**LEVEL** III

(2) SC

AFWL-TR-  
79-402

1073770

ADC 200 363

**ELECTROMAGNETIC PULSE  
INTERACTION NOTES - EMP 3-39**

July 1979

Final Report



**DISTRIBUTION STATEMENT A**  
Approved for public release;  
Distribution Unlimited

**DDC**  
**RECEIVED**  
SEP 26 1979  
**A**

**AIR FORCE WEAPONS LABORATORY**  
Air Force Systems Command  
Kirtland Air Force Base, NM 87117

**79 09 21 016**

AD A 074265

DDC FILE COPY

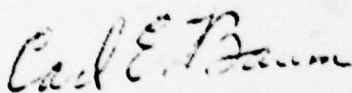
This report is one in the Note Series on EMP and Related Subjects which is an EMP community-wide series of journals on EMP technology related matters. The editor is Dr Carl E. Baum, Air Force Weapons Laboratory (EL), Kirtland Air Force Base, New Mexico, 87117. The editor should be contacted for any matters related to this series. The Laboratory assists in the publication of this series as a service to the technical community.

When US Government drawings, specifications, or other data are used for any purpose other than a definitely related Government procurement operation, the Government thereby incurs no responsibility nor any obligation whatsoever, and the fact that the Government may have formulated, furnished, or in any way supplied the said drawings, specifications, or other data is not to be regarded by implication or otherwise as in any manner licensing the holder or any other person or corporation or conveying any rights or permission to manufacture, use, or sell any patented invention that may in any way be related thereto.

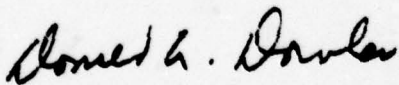
This report has been authored by an employee of the US Government. Accordingly, the US Government retains a nonexclusive royalty-free license to publish or reproduce the material contained herein, or allow others to do so, for the US Government purposes.

This report has been reviewed by the Office of Information (OI) and is releasable to the National Technical Information Service (NTIS). At NTIS it will be available to the general public, including foreign nationals.

This technical report has been reviewed and is approved for publication.

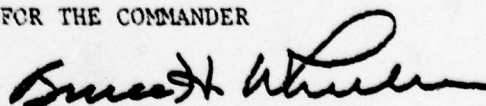


DR CARL E. BAUM  
Editor



DONALD A. DOWLER  
Col, USAF  
Ch, Electromagnetics Division

FOR THE COMMANDER



BRUCE H. WHEELER  
Col, USAF  
Director of Nuclear Technology

---

DO NOT RETURN THIS COPY. RETAIN OR DESTROY.

UNCLASSIFIED

SECURITY CLASSIFICATION OF THIS PAGE (When Data Entered)

REPORT DOCUMENTATION PAGE		READ INSTRUCTIONS BEFORE COMPLETING FORM
1. REPORT NUMBER <b>14</b> AFWL-TR-79-4027	2. GOVT ACCESSION NO.	3. RECIPIENT'S CATALOG NUMBER <b>9</b>
4. TITLE (and Subtitle) <b>6</b> ELECTROMAGNETIC PULSE INTERACTION NOTES—EMP 3-39.	5. TYPE OF REPORT & PERIOD COVERED Final Report	
7. AUTHOR(s) <b>10</b> Carl E. / Baum	6. PERFORMING ORG. REPORT NUMBER	
8. PERFORMING ORGANIZATION NAME (and ADDRESS) Air Force Weapons Laboratory (ELTE) Kirtland Air Force Base, New Mexico 87117	9. CONTRACT OR GRANT NUMBER(s)	
11. CONTROLLING OFFICE NAME AND ADDRESS Air Force Weapons Laboratory (ELTE) Kirtland Air Force Base, New Mexico 87117	10. PROGRAM ELEMENT, PROJECT, TASK AREA & WORK UNIT NUMBERS	
14. MONITORING AGENCY NAME & ADDRESS (if different from Controlling Office) <b>12</b> 415 p.	13. REPORT DATE <b>11</b> Jul 79	
	15. SECURITY CLASS. (of this report) UNCLASSIFIED	
	16. NUMBER OF PAGES 410	
	17. DECLASSIFICATION/DOWNGRADING SCHEDULE	
18. DISTRIBUTION STATEMENT (of this Report) Approved for public release; distribution unlimited.		
19. DISTRIBUTION STATEMENT (of the abstract entered in Block 20, if different from Report) <b>16</b> 9996 <b>17</b> 00		
20. SUPPLEMENTARY NOTES <b>18</b> SBIE <b>19</b> AD-E200 363		
21. KEY WORDS (Continue on reverse side if necessary and identify by block number) EMP		
22. ABSTRACT (Continue on reverse side if necessary and identify by block number) This is a series of five notes on electromagnetic pulse interaction. Subjects covered are: Electromagnetic Penetration Through a Circular Aperture in a Plane Screen Separating a Conducting Medium and Nonconducting Medium; Small Aperture on a Multiconductor Transmission Line Filled with Inhomogeneous Dielectrics; On the Electromagnetic Field Excitation of Unshielded Multiconductor Cables; A Coupling Model for a Pair of Skewed Transmission Lines; On the Analysis of General Multiconductor Transmission-Line Networks; Field Excitation		

DD FORM 1 JAN 73 1473 EDITION OF 1 NOV 65 IS OBSOLETE

UNCLASSIFIED


SECURITY CLASSIFICATION OF THIS PAGE (When Data Entered)

013 150

JM

Continued, Item 20

of Multiconductor Transmission Lines; Diffraction Through a Circular Aperture in a Screen Separating Two Different Media; and The Receiving Properties of the Small Annular Slot Antenna.



UNCLASSIFIED

SECURITY CLASSIFICATION OF THIS PAGE(When Data Entered)

# PREFACE

Much of the existing information on EMP is in the form of notes or semiformal reports and has not been adequately documented or distributed. In particular, there are several series of notes that act as technical journals for various areas related to EMP and other related subjects. These note series are not exclusively for one organization and are run much as technical journals with an editor, Dr. Carl E. Baum.

The Air Force Weapons Laboratory has undertaken to reissue these existing notes in convenient volume units. The present volume is Volume 39 of the Interaction Notes, one of the note series in the Electromagnetic Pulse Note Series. The Interaction Notes have the report designation EMP 3 in the EMP group of note series.

Contributions to this volume, EMP 3-39, have been made by the following individuals at the included organizations:

## Air Force Weapons Laboratory

Carl E. Baum  
J. Philip Castillo  
Clayborne D. Taylor

## Electro Magnetic Applications, Inc.

Roger B. Cook  
Robert Fisher  
David E. Merewether

## Eyring Research Institute

Harvey J. Fletcher  
Alan Harrison

## LuTech, Inc.

Steve K. Chang<sup>+</sup>  
David V. Giri<sup>+</sup>  
Tom K. Liu<sup>+</sup>  
Fred M. Tesche<sup>+</sup>

## University of Mississippi

Darko Kajfez  
Donald R. Wilton

<sup>+</sup> Formerly at Science Applications, Inc.

Accession For	
NTIS GNA&I	<input checked="" type="checkbox"/>
DDC TAB	<input type="checkbox"/>
Unannounced	<input type="checkbox"/>
Justification	
By _____	
Distribution/	
Availability Codes	
Dist	Avail and/or special
A	

Research for these notes has been funded by the United States Air Force and the Department of Energy.

Contributions to the Note Series are encouraged from all organizations actively engaged in related research. Active participation throughout the community will build a collection of information useful to all. Contributions and questions regarding the Note Series should be directed to:

Dr. Carl E. Baum  
Air Force Weapons Laboratory/ELT  
Kirtland Air Force Base, New Mexico 87117

TABLE OF CONTENTS

- NOTE 346      ELECTROMAGNETIC PENETRATION THROUGH A CIRCULAR  
APERTURE IN A PLANE SCREEN SEPARATING A CONDUCTING  
MEDIUM AND A NON-CONDUCTING MEDIUM  
Harvey Fletcher and Alan Harrison, Eyring Research  
Institute
- NOTE 347      SMALL APERTURE ON A MULTICONDUCTOR TRANSMISSION LINE  
FILLED WITH INHOMOGENEOUS DIELECTRICS  
Darko Kajfez and Donald R. Wilton, University of  
Mississippi
- NOTE 348      ON THE ELECTROMAGNETIC FIELD EXCITATION OF UNSHIELDED  
MULTICONDUCTOR CABLES  
Clayborne D. Taylor and J. Philip Castillo  
Air Force Weapons Laboratory
- NOTE 349      A COUPLING MODEL FOR A PAIR OF SKEWED TRANSMISSION  
LINES  
David V. Giri, Steve Change, and Fred M. Tesche  
Science Applications, Inc.
- NOTE 350      ON THE ANALYSIS OF GENERAL MULTICONDUCTOR TRANSMISSION-  
LINE NETWORKS  
Carl E. Baum, Tom K. Liu, and Fred M. Tesche  
Air Force Weapons Laboratory and LuTech, Inc.
- NOTE 351      FIELD EXCITATION OF MULTICONDUCTOR TRANSMISSION LINES  
Fred M. Tesche, Tom K. Liu, Steve K. Chang, and David  
V. Giri, LuTech, Inc.
- NOTE 352      DIFFRACTION THROUGH A CIRCULAR APERTURE IN A SCREEN  
SEPARATING TWO DIFFERENT MEDIA  
Harvey J. Fletcher and Alan Harrison, Eyring Research  
Institute
- NOTE 353      THE RECEIVING PROPERTIES OF THE SMALL ANNULAR SLOT  
ANTENNA,  
David E. Merewether, Robert B. Cook, and Robert Fisher  
Electro Magnetic Applications, Inc.

NOTE 346

ELECTROMAGNETIC PENETRATION THROUGH A CIRCULAR  
APERTURE IN A PLANE SCREEN SEPARATING A CONDUCTING  
MEDIUM AND A NON-CONDUCTING MEDIUM

by

Harvey Fletcher  
Alan Harrison

October 1978

ELECTROMAGNETIC PENETRATION THROUGH A CIRCULAR  
APERTURE IN A PLANE SCREEN SEPARATING A CONDUCTING  
MEDIUM AND A NON-CONDUCTING MEDIUM

ABSTRACT

A low frequency approximation is made to the Fourier Transform of EMP in the presence of an infinite conducting screen. A circular aperture is introduced in the screen with air on the shadow side. A particular solution of Maxwell's equations is added to a general solution involving oblate spheroidal coordinates to match the boundary conditions. Analytical expressions are given for the fields on the screen, along the axis, in the aperture and for large distances from the aperture.

The electromagnetic diffraction by a circular aperture in a plane screen between different media was given by D. P. Thomas<sup>1</sup>. He assumed a low frequency incoming wave and no conductivity in either medium and gave an approximate result. C. M. Butler<sup>2</sup> generalized the problem to an arbitrarily shaped aperture and described a numerical procedure by the method of moments but only gave results for an infinite strip. D. R. Marston<sup>6</sup> and others found the currents induced in underground cables by EMP.

In this paper we shall assume a thin, infinite, perfectly conducting screen illuminated by a low frequency plane wave. We seek an exact analytical solution with a conductivity which is not assumed to be zero in the incident medium.

The physical problem which motivates the study is that of an electromagnetic pulse (EMP) coming through the ground and entering an aperture in a silo or a window on a submerged vessel or underground communication center (see Figure 1).

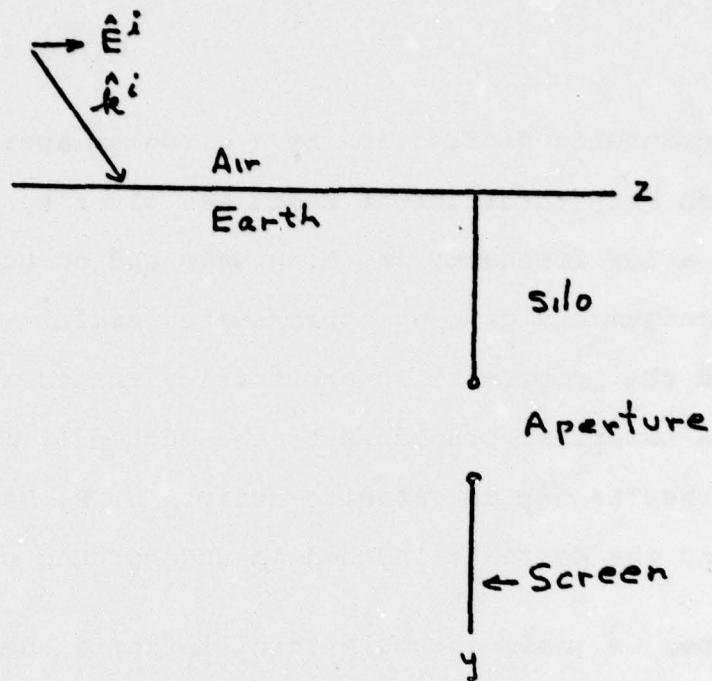


Figure 1A EMP Penetration of a Silo

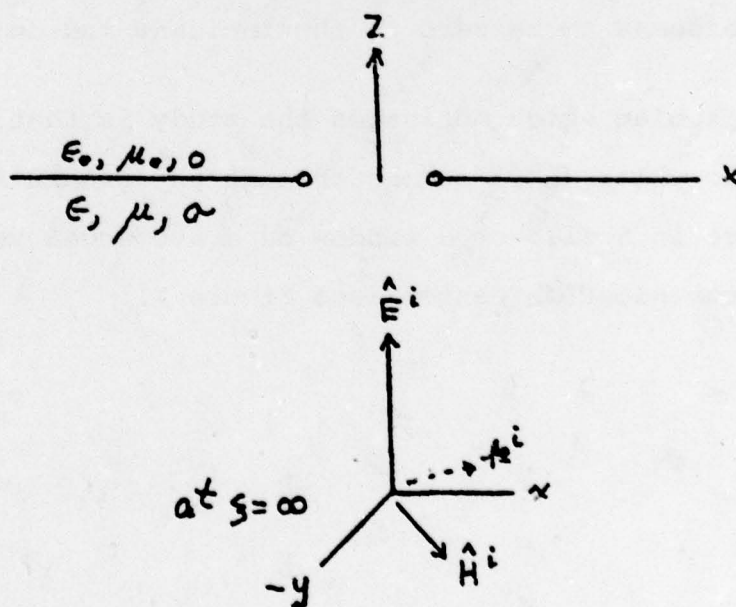


Figure 1B Standardized Coordinate System

The Fourier transform of the electric field in the earth of a plane EMP whose  $\vec{E}$  is parallel to the surface of the ground is given as

$$\vec{E} = \hat{z} E_0(\omega) e^{\frac{-j\omega}{c(\omega)} \hat{k} \cdot \vec{r}}$$

where

$$E_0(\omega) = E_1 \left( \frac{1}{\alpha + j\omega} - \frac{1}{\beta + j\omega} \right) \frac{2 \cos \theta_0}{\cos \theta_0 + \frac{\mu_0}{\mu} \sqrt{\frac{\epsilon \mu}{\epsilon_0 \mu_0} - \frac{j\sigma \omega}{\epsilon_0 \mu_0 \omega} - \sin^2 \theta_0}}$$

$$c(\omega) = \frac{1}{\sqrt{\epsilon \mu - \frac{j\mu\sigma}{\omega}}}$$

$$\beta = 1/\text{rise time of EMP}$$

$$\alpha = 1/\text{fall time of EMP}$$

$$\hat{k} = -k_3 \hat{x} + k_1 \hat{y}$$

$$k_3 = c(\omega) \frac{\sin \theta_0}{c_0}$$

$$c_0 = \frac{1}{\sqrt{\epsilon_0 \mu_0}}$$

$$k_1 = \sqrt{1 - k_3^2}$$

$$\vec{r} = x\hat{x} + y\hat{y} + z\hat{z}$$

The magnetic field is

$$\vec{H} = \frac{\hat{k} \times \vec{E}}{Z(\omega)}$$

where

$$Z(\omega) = \mu c(\omega)$$

If  $\omega \ll \frac{\sigma}{\epsilon}$ , then  $\vec{E}$  and  $\vec{H}$  can be expanded in powers of  $\omega^{1/2}$ . Retaining only the first two terms,

$$\vec{E} = E_z^0 \hat{z} + O(\omega)$$

$$\vec{H} = (H_x^0 - \sigma E_z^0 y) \hat{x} + H_y^0 \hat{y} + O(\omega)$$

where

$$E_z^0 = 2E_1 \left( \frac{1}{\alpha} - \frac{1}{\beta} \right) \sqrt{\frac{j\omega\epsilon_0\mu}{\mu_0\sigma}} \cos \theta_0$$

$$H_x^0 = 2E_1 \left( \frac{1}{\alpha} - \frac{1}{\beta} \right) \sqrt{\frac{\epsilon_0}{\mu_0}} \left( 1 - \sqrt{\frac{j\omega\epsilon_0\mu}{\mu_0\sigma}} \cos \theta_0 \right) \cos \theta_0$$

$$H_y^0 = 2E_1 \left( \frac{1}{\alpha} - \frac{1}{\beta} \right) \epsilon_0 \sqrt{\frac{j\omega}{\mu\sigma}} \sin \theta_0 \cos \theta_0$$

For very small  $\omega$ ,  $E_0$  is zero. Let us consider terms of order  $\omega^{1/2}$  but neglect terms of order  $\omega$ . Maxwell's equations on the conducting side of an aperture are then

$$\nabla \times \tilde{\mathbf{H}} = \sigma \tilde{\mathbf{E}}, \quad \nabla \times \tilde{\mathbf{E}} = 0, \quad \nabla \cdot \tilde{\mathbf{E}} = 0, \quad \nabla \cdot \tilde{\mathbf{H}} = 0$$

This approximation is good if  $|\omega| \ll \sigma/\epsilon$

Price<sup>(5)</sup> gives values  $\sigma = 3 \times 10^{-3}$  mho/m

$$\epsilon = 10 \times 8.854 \times 10^{-12} \text{ f/m}$$

For a frequency of 1 MHz,  $\frac{\omega\epsilon}{\sigma} = .185$ .

On the shadow side of the screen ( $z > 0$ )  $\sigma = 0$  and

Maxwell's equations are

$$\begin{aligned} \nabla \times \tilde{\mathbf{E}} &= 0 & \nabla \times \tilde{\mathbf{H}} &= 0 \\ \nabla \cdot \tilde{\mathbf{E}} &= 0 & \nabla \cdot \tilde{\mathbf{H}} &= 0 \end{aligned}$$

The tildas will be suppressed from this point on.

The natural coordinates to use are oblate spheroidal coordinates  $\xi, \eta, \phi$ , given in Fig. 2.

$$\rho = \sqrt{x^2 + y^2} = \frac{1}{a} \sqrt{(\xi + a^2)(\eta + a^2)} \quad 0 < \xi < \infty$$

$$z = \frac{\text{sign } z}{a} \sqrt{-\xi\eta} \quad -a^2 < \eta < 0$$

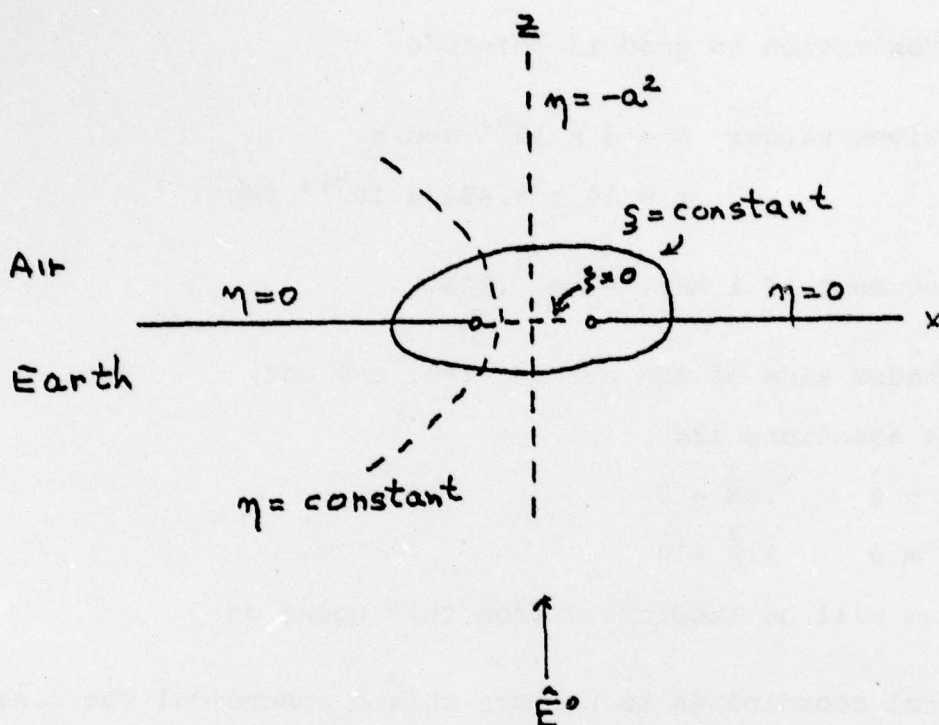


Figure 2 Oblate Spheroidal Coordinates

$\phi$  is the regular polar coordinate.

The boundary conditions are such that the tangential electric field and the normal magnetic field are zero on the screen. Both fields have continuous tangential components at the aperture. The normal component of magnetic induction  $\vec{B}$  is continuous at the aperture. Both fields are zero at  $z = +\infty$  and

$$\vec{E} = E_z^0 \hat{z}, \quad \vec{H} = (H_x^0 - \sigma E_z^0 y) \hat{x} + H_y^0 \hat{y} \quad \text{at } z = -\infty.$$

The boundary condition at the aperture is that the current flowing into the aperture is the increase of surface charge at the aperture:

$$\begin{aligned} J_z^-(0, \eta, \phi) &= \frac{\partial \rho_s}{\partial t} = j\omega \rho_s = j\omega[\epsilon_0 E_z^+(0, \eta, \phi) - \epsilon E_z^-(0, \eta, \phi)] \\ &= \sigma E_z^-(0, \eta, \phi) \end{aligned}$$

Since we have assumed  $\frac{\omega \epsilon}{\sigma} \ll 1$  this is equivalent to  $E_z^-(0, \eta, \phi) = 0$ .

It should be noted that the boundary condition reduces to  $E_z^+(0, \eta, \phi) = E_z^-(0, \eta, \phi)$  if  $\epsilon = \epsilon_0$  and  $\sigma = 0$ . However, if  $\omega$  is allowed to go to zero first, then the boundary condition  $E_z^-(0) = 0$  does not reduce to  $E_z^+(0, \eta, \phi) = E_z^-(0, \eta, \phi)$  and hence the solution of the problem with  $\sigma > 0$  does not reduce to the case of an aperture with both sides in air.

The complete mathematical problem is given as follows:

$$\begin{array}{ll} \nabla \times \vec{E}^- = 0 & \nabla \times \vec{H}^- = \sigma \vec{E}^- \\ \nabla \times \vec{E}^+ = 0 & \nabla \times \vec{H}^+ = 0 \\ \nabla \cdot \vec{E}^- = 0 & \nabla \cdot \vec{H}^- = 0 \\ \nabla \cdot \vec{E}^+ = 0 & \nabla \cdot \vec{H}^+ = 0 \end{array}$$

At  $\xi = 0$ ,

$$E_x^- = E_x^+$$

$$E_y^- = E_y^+$$

$$E_z^- = 0$$

$$H_x^- = H_x^+$$

$$H_y^- = H_y^+$$

$$\mu H_z^- = \mu_0 H_z^+$$

At  $\eta = 0$ ,

$$E_x^- = 0$$

$$E_x^+ = 0$$

$$E_y^- = 0$$

$$E_y^+ = 0$$

$$H_z^- = 0$$

$$H_z^+ = 0$$

At  $\xi = \infty, z < 0$ ,

$$E_x^- = 0$$

$$E_y^- = 0$$

$$E_z^- = E_z^0$$

$$H_x^- = H_x^0 - E_z^0 \sigma y$$

$$H_y^- = H_y^0$$

$$H_z^- = 0$$

At  $\xi = \infty, z > 0$ 

$$E_x^+ = 0$$

$$E_y^+ = 0$$

$$E_z^+ = 0$$

$$H_x^+ = 0$$

$$H_y^+ = 0$$

$$H_z^+ = 0$$

This is a total of 16 equations with 24 boundary conditions. They are sufficient to determine a unique solution. The minus subscript indicates the earth with constants  $\epsilon, \mu, \sigma$ . The plus subscript indicates the shadow side of the screen with constants  $\epsilon_0, \mu_0, 0$ .

The procedure to calculate a solution is outlined as follows.

1. We first formulate the Laplace Equation in oblate spheroidal coordinates. Since  $\nabla \times \vec{E} = 0$ , then  $\vec{E} = -\nabla \phi$  and  $\nabla^2 \phi = 0$ . We label
 
$$\phi = \phi^+ \quad \text{if } z \geq 0$$

$$\phi = \phi^- \quad \text{if } z \leq 0$$
2. We separate variables and find separable solutions.
3. We apply the boundary conditions and determine  $\vec{E}$ . This can be done without using the  $\vec{H}$  equations.
4. We split  $\vec{H}$  into three parts,  $\vec{H} = \vec{H}_1 + \vec{H}_2 + \vec{H}_3$ , such that  $\vec{H}_1$  takes care of  $H_x^0$  and  $H_y^0$  at  $z = -\infty$ ,  $\vec{H}_2$  is the complementary solution and  $\vec{H}_3$  is the particular solution satisfying  $\nabla \times \vec{H}_3 = \sigma \vec{E}^*$ . Then  $\vec{H}_1 = -\nabla \phi_1^*$  and  $\vec{H}_2 = -\nabla \phi_2^*$ , where  $\nabla^2 \phi_1^* = \nabla^2 \phi_2^* = 0$ .  $H_{3x}^-(\xi = 0) = -\sigma E_z^0 y$ , and  $\vec{H}_3^+ \equiv 0$ .
5. We solve for  $\vec{H}_1$  using the boundary condition that  $\mu H_z^- = \mu_0 H_z^+$  at the aperture.
6. We solve for  $\vec{H}_3$  without specifying continuity at the aperture.
7. We solve for  $\vec{H}_2$  without specifying continuity at the aperture.
8. We apply the continuity boundary conditions to the sum of  $\vec{H}_2$  and  $\vec{H}_3$  and evaluate  $\vec{H}$ .

The Laplace equation in oblate spheroidal coordinates is given by

$$\nabla^2 \phi = \frac{4}{\xi - \eta} \left\{ \xi^{\frac{1}{2}} \frac{\partial}{\partial \xi} [\xi^{\frac{1}{2}} (\xi + a^2) \frac{\partial \phi}{\partial \xi}] + \sqrt{-\eta} \frac{\partial}{\partial \eta} [\sqrt{-\eta} (\eta + a^2) \frac{\partial \phi}{\partial \eta}] \right\} + \frac{a^2}{(\xi + a^2)(\eta + a^2)} \frac{\partial^2 \phi}{\partial \phi^2} = 0$$

In order that  $E_z^-(\xi = \infty) = E_z^0$  we shall pick a particular solution for  $\phi$  given by

$$\phi_p^- = -E_z^0 z = +\frac{E_z^0}{a} \sqrt{-\xi \eta}$$

Let us look for a separable complementary solution of the form  $\phi = f(\xi)g(\eta)h(\phi)$ . Then it follows that

$$\xi^{\frac{1}{2}} \frac{d}{d\xi} [\xi^{\frac{1}{2}} (\xi + a^2) \frac{df}{d\xi}] + \left[ \frac{a^2 m^2}{\xi + a^2} - n(n+1) \right] \frac{f}{4} = 0$$

$$\sqrt{-\eta} \frac{d}{d\eta} [\sqrt{-\eta} (\eta + a^2) \frac{dg}{d\eta}] - \left[ \frac{a^2 m^2}{\eta + a^2} - n(n+1) \right] \frac{g}{4} = 0$$

$$\frac{d^2 h}{d\phi^2} + m^2 h = 0$$

The solution to the first two equations can be found by letting  $\frac{i\xi^{\frac{1}{2}}}{a}$  and  $\frac{\sqrt{-\eta}}{a}$  be new variables and recognizing that these are the associated Legendre equations.

$$f(\xi) = AP_n^m \left( \frac{i\xi^{\frac{1}{2}}}{a} \right) + BQ_n^m \left( \frac{i\xi^{\frac{1}{2}}}{a} \right)$$

$$g(\eta) = CP_n^m \left( \frac{\sqrt{-\eta}}{a} \right) + DQ_n^m \left( \frac{\sqrt{-\eta}}{a} \right)$$

$$h(\phi) = E \cos m\phi + F \sin m\phi$$

We are looking for solutions which have period  $2\pi$  in  $\phi$  so that  $m$  is chosen to be an integer. We want solutions which are well behaved at  $\eta=0$  and  $\eta=-a^2$  so that we will choose  $D=0$  and  $n$  is an integer. If  $\phi$  is to be zero at  $\infty$ , then  $A=0$ . Some of the remaining functions are tabulated below:

$$Q_0^0 \left( \frac{i\xi^{\frac{1}{2}}}{a} \right) = -i\alpha$$

$$Q_1^0 \left( \frac{i\xi^{\frac{1}{2}}}{a} \right) = \frac{\xi^{\frac{1}{2}}}{a} \alpha - 1$$

$$Q_2^0 \left( \frac{i\xi^{\frac{1}{2}}}{a} \right) = \frac{i}{2} \left[ \left( \frac{3\xi}{a^2} + 1 \right) \alpha - \frac{3\xi^{\frac{1}{2}}}{a} \right]$$

$$Q_1^1 \left( \frac{i\xi^{\frac{1}{2}}}{a} \right) = \left( 1 + \frac{\xi}{a^2} \right)^{\frac{1}{2}} \left( \alpha - \frac{a\xi^{\frac{1}{2}}}{\xi+a^2} \right)$$

$$Q_2^1 \left( \frac{i\xi^{\frac{1}{2}}}{a} \right) = i \left( 1 + \frac{\xi}{a^2} \right)^{\frac{1}{2}} \left( \frac{3\xi^{\frac{1}{2}}}{a} \alpha - 3 + \frac{a^2}{\xi+a^2} \right)$$

$$Q_2^2 \left( \frac{i\xi^{\frac{1}{2}}}{a} \right) = i \left[ 3 \left( 1 + \frac{\xi}{a^2} \right) \alpha - \frac{3\xi^{\frac{1}{2}}}{a} - \frac{2a\xi^{\frac{1}{2}}}{\xi+a^2} \right]$$

$$\text{where } \alpha = \cot^{-1} \frac{\xi^{\frac{1}{2}}}{a}$$

$$P_0^0 \left( \frac{\sqrt{-\eta}}{a} \right) = 1$$

$$P_1^0 \left( \frac{\sqrt{-\eta}}{a} \right) = \frac{\sqrt{-\eta}}{a}$$

$$P_2^0 \left( \frac{\sqrt{-\eta}}{a} \right) = -1/2 \left( \frac{3\eta}{a} + 1 \right)$$

$$P_1^1 \left( \frac{\sqrt{-\eta}}{a} \right) = - \left( 1 + \frac{\eta}{a^2} \right)^{1/2}$$

$$P_2^1 \left( \frac{\sqrt{-\eta}}{a} \right) = - \frac{3\sqrt{-\eta}}{a} \left( 1 + \frac{\eta}{a^2} \right)^{1/2}$$

$$P_2^2 \left( \frac{\sqrt{-\eta}}{a} \right) = 3 \left( 1 + \frac{\eta}{a^2} \right)$$

The complementary solution where  $z < 0$  is of the form

$$\phi_c^- = \sum Q_n^m \left( \frac{i\xi^{1/2}}{a} \right) P_n^m \left( \frac{\sqrt{-\eta}}{a} \right) (a_{mn} \cos m\phi + b_{mn} \sin m\phi)$$

The x component of the electric field is given by  $E_x^- = -\frac{\partial \phi}{\partial x}$

$$\begin{aligned} = -\sum & \left[ \frac{dQ_n^m}{d\xi} \left( \frac{i\xi^{1/2}}{a} \right) \frac{\partial \xi}{\partial x} P_n^m \left( \frac{\sqrt{-\eta}}{a} \right) h_{mn}(\phi) \right. \\ & + Q_n^m \left( \frac{i\xi^{1/2}}{a} \right) \frac{dP_n^m}{d\eta} \left( \frac{\sqrt{-\eta}}{a} \right) \frac{\partial \eta}{\partial x} h_{mn}(\phi) \\ & \left. + Q_n^m \left( \frac{i\xi^{1/2}}{a} \right) P_n^m \left( \frac{\sqrt{-\eta}}{a} \right) \frac{dh_{mn}(\phi)}{d\phi} \frac{\partial \phi}{\partial x} \right] \end{aligned}$$

where  $\frac{\partial \xi}{\partial x} = \frac{2x\xi}{\xi-\eta}$ ,  $\frac{\partial \eta}{\partial x} = -\frac{2x\eta}{\xi-\eta}$ ,  $\frac{\partial \phi}{\partial x} = -\frac{\sin \phi}{\rho}$

$$h_{mn}(\phi) = a_{mn} \cos m\phi + b_{mn} \sin m\phi$$

In order that this be zero at  $\eta = 0$

we take  $P_n^m(0) = 0$  or  $m + n = \text{an odd integer}$ .

The  $z$  component of the electric field is given by

$$E_z^- = E_z^O - \sum_{\substack{m,n=0 \\ m+n=\text{odd}}}^{\infty} \left[ \frac{dQ_n^m}{d\xi} \left( \frac{i\xi^{\frac{1}{2}}}{a} \right) \frac{\partial \xi}{\partial z} P_n^m \left( \frac{\sqrt{-\eta}}{a} \right) h_{mn}(\phi) \right. \\ \left. + Q_n^m \left( \frac{i\xi^{\frac{1}{2}}}{a} \right) \frac{dP_n^m}{d\eta} \left( \frac{\sqrt{-\eta}}{a} \right) \frac{\partial \eta}{\partial z} h_{mn}(\phi) \right]$$

If this is to vanish at  $\xi = 0$ , then

$$E_z^O = \sum_{\substack{m,n=0 \\ m+n=\text{odd}}}^{\infty} \left[ \frac{dQ_n^m \left( \frac{i\xi^{\frac{1}{2}}}{a} \right)}{d \left( \frac{i\xi^{\frac{1}{2}}}{a} \right)} \frac{i\xi^{\frac{1}{2}}}{2a\xi^{\frac{1}{2}}} \frac{\partial \xi}{\partial z} P_n^m \left( \frac{\sqrt{-\eta}}{a} \right) h_{mn}(\phi) \right]_{\xi=0}$$

Since the left side is independent of  $\phi$ , then  $m = 0$ .

$$\frac{\partial \xi}{\partial z} = \frac{2z(\xi+a^2)}{\xi-\eta} = - \frac{2(\xi+a^2)}{a(\xi-\eta)} \sqrt{-\xi\eta}$$

$$E_z^O = \sum_{\substack{n \\ \text{odd}}} \left[ Q_n' \left( \frac{i\xi^{\frac{1}{2}}}{a} \right) \left( -\frac{i}{a^2} \right) \frac{\sqrt{-\eta}(\xi+a^2)}{\xi-\eta} \right]_{\xi=0} P_n \left( \frac{\sqrt{-\eta}}{a} \right) a_{on} \\ = \sum_{\substack{n \\ \text{odd}}} Q_n'(0) \frac{i\sqrt{-\eta}}{\eta} P_n \left( \frac{\sqrt{-\eta}}{a} \right) a_{on}$$

Since the left side is independent of  $\eta$ , then  $n = 1$ .

Hence

$$\phi_C^- = Q_1 \left( \frac{i\xi^{\frac{1}{2}}}{a} \right) P_1 \left( \frac{\sqrt{-\eta}}{a} \right) a_{01}$$

$$= a_{01} \left[ \frac{\xi^{\frac{1}{2}}}{a} \alpha - 1 \right] \left[ \frac{\sqrt{-\eta}}{a} \right]$$

$$\phi_C^- = -E_z^0 z + C \left( \frac{\xi^{\frac{1}{2}}}{a} \alpha - 1 \right) \sqrt{-\eta}$$

From this it follows that

$$E_x^- = - \frac{Ca^2 x \sqrt{-\eta}}{(\xi - \eta)(\xi + a^2)}$$

$$E_y^- = - \frac{Ca^2 y \sqrt{-\eta}}{(\xi - \eta)(\xi + a^2)}$$

$$E_z^- = E_z^0 + C \left( \alpha - \frac{a\xi^{\frac{1}{2}}}{\xi - \eta} \right)$$

The condition that  $E_z^- = 0$  at  $\xi = 0$  implies that

$$C = - \frac{2}{\pi} E_z^0$$

In order that the tangential electric field be continuous at  $\xi = 0$ , we take

$$\phi^+(x, y, z) = \phi_C^-(x, y, -z)$$

Then

$$E_x^+(x, y, z) = E_x^-(x, y, -z), \quad E_y^+(x, y, z) = E_y^-(x, y, -z)$$

$$E_z^+ = -C \left( \alpha - \frac{a\xi^{\frac{1}{2}}}{\xi - \eta} \right)$$

This is independent of  $\sigma$ ,  $\epsilon_0$ , and  $\epsilon$ . It is interesting that as  $\sigma$  goes to zero and  $\epsilon \rightarrow \epsilon_0$  this solution does not reduce to the case of medium 1 and 2 being the same (as in air).

The latter case has  $E_z^- = E_z^+ = \frac{E_z^0}{2}$  and no surface charge exists at the aperture. In the case of a small  $\sigma$ ,  $E_z^- = 0$  and  $E_z^+ = E_z^0$ . This gives a free surface charge of  $\rho_s = \epsilon_0 E_z^0$  at the aperture. Thus a small change in the parameter  $\sigma$  gives an instantaneous change in  $E_z$  and  $\rho_s$ . There is a singularity in this field at  $\xi = \eta = 0$ , which is the edge of the aperture.

The case of  $\vec{H} = \vec{H}^0 = H_x^0 \hat{x} + H_y^0 \hat{y}$  at  $z = -\infty$  has been treated by Fletcher and Harrison<sup>(3)</sup> and Chen<sup>(4)</sup> for the case when  $\epsilon = \epsilon_0$ ,  $\mu = \mu_0$  and  $\sigma = 0$ . A similar procedure leads to the following solution for  $\vec{H}_1$ :

$$H_{1x}^- = H_x^0 + \frac{A_1 H_x^0}{a^3} \left( \alpha - \frac{a\xi^{\frac{1}{2}}}{\xi + a^2} \right) - \frac{2A_1 x \xi^{\frac{1}{2}} \vec{H}^0 \cdot \vec{\rho}}{(\xi - \eta) (\xi + a^2)^2}$$

$$H_{1y}^- = H_y^0 + \frac{A_1 H_y^0}{a^3} \left( \alpha - \frac{a\xi^{\frac{1}{2}}}{\xi + a^2} \right) - \frac{2A_1 y \xi^{\frac{1}{2}} \vec{H}^0 \cdot \vec{\rho}}{(\xi - \eta) (\xi + a^2)^2}$$

$$H_{1z}^- = \frac{2A_1 H^0 \cdot \vec{\rho} \sqrt{-\eta}}{a(\xi + a^2) (\xi - \eta)}$$

$$H_{1x}^+ = \frac{A_2 H_x^O}{a^3} \left( \alpha - \frac{a\xi^{\frac{1}{2}}}{\xi+a^2} \right) - \frac{2A_2 \vec{H}^O \cdot \vec{\rho} x \xi^{\frac{1}{2}}}{(\xi-\eta)(\xi+a^2)^2}$$

$$H_{1y}^+ = \frac{A_2 H_y^O}{a^3} \left( \alpha - \frac{a\xi^{\frac{1}{2}}}{\xi+a^2} \right) - \frac{2A_2 \vec{H}^O \cdot \vec{\rho} y \xi^{\frac{1}{2}}}{(\xi-\eta)(\xi+a^2)^2}$$

$$H_{1z}^+ = - \frac{2A_2 \vec{H}^O \cdot \vec{\rho} \sqrt{-\eta}}{a(\xi-\eta)(\xi+a^2)}$$

where  $\vec{\rho} = x\hat{x} + y\hat{y}$ . To satisfy the continuity conditions

$$A_1 = - \frac{2a^3 \mu_0}{\pi(\mu + \mu_0)}, \quad A_2 = \frac{2a^3 \mu}{\pi(\mu + \mu_0)}$$

If  $\mu = \mu_0$ , then  $A_1 = -A_2 = -\frac{a^3}{\pi}$  which checks the result of Chen<sup>4</sup>.

This result is independent of  $\epsilon$ ,  $\sigma$ .

We next solve for  $\vec{H}_3$ , which is a particular solution of  $\nabla \times \vec{H}_3 = \sigma \vec{E}$ ,  $\vec{H}_3^+ = 0$ . In this case  $\vec{H}_3$  is not derivable from a potential.

For large  $\xi$  and negative  $z$ ,  $\nabla \times \vec{H}^- = \sigma E_z^O \hat{z}$ .

A particular solution is

$$H_{3x}^- = -E_z^O \sigma y$$

$$H_{3y}^- = 0$$

$$H_{3z}^- = 0$$

For small  $z$ ,  $H_{3x}^-$  must satisfy Laplace's equation. A separable solution is given by

$$A_{mn} Q_n^m \left( \frac{i\xi^{\frac{1}{2}}}{a} \right) P_n^m \left( \frac{\sqrt{-\eta}}{a} \right) \begin{Bmatrix} \sin m\phi \\ \cos m\phi \end{Bmatrix}$$

If  $m=1$  and  $m=1$  this is

$$\begin{aligned} A_{11} Q_1^1 \left( \frac{i\xi^{\frac{1}{2}}}{a} \right) P_1^1 \left( \frac{\sqrt{-\eta}}{a} \right) \begin{Bmatrix} \sin \phi \\ \cos \phi \end{Bmatrix} \\ = -\frac{A_{11}}{a} \begin{pmatrix} y \\ x \end{pmatrix} \left( \alpha - \frac{\xi^{\frac{1}{2}} a}{\xi + a^2} \right) \end{aligned}$$

$A_{11}$  is chosen to satisfy  $\nabla \times \vec{H}^- = \sigma \vec{E}^-$

$$H_{3x}^- = -E_z^0 \sigma y - \frac{E_z^0 \sigma y f(\xi)}{\pi}$$

$$H_{3y}^- = \frac{E_z^0 \sigma x f(\xi)}{\pi}$$

$$H_{3z}^- = 0$$

$$\vec{H}_3^+ = 0$$

where  $f(\xi) = \frac{a\xi^{\frac{1}{2}}}{\xi + a^2} - \alpha$

The last part of  $\vec{H}$  to calculate is  $\vec{H}_2$ , which gives the complementary solution necessary to satisfy the continuity conditions at the aperture.  $\vec{H}_2$  is derivable from a potential since  $\nabla \times \vec{H}_2 = 0$ . The potential can be found in a similar way to that in

which the electric field was found. It is

$$\phi_2^+ = \frac{ia^2A}{3} Q_2^2 \left(\frac{i\xi^{\frac{1}{2}}}{a}\right) P_2^2 (\sqrt{-\eta}/a) \sin 2\phi$$

$$\phi_2^- = \frac{ia^2B}{3} Q_2^2 \left(\frac{i\xi^{\frac{1}{2}}}{a}\right) P_2^2 (\sqrt{-\eta}/a) \sin 2\phi$$

where the coefficients are chosen to simplify later expressions.

m and n were chosen equal to 2 so that at the aperture

$$\phi_2^+ = -3\pi Axy$$

$$\phi_2^- = -3\pi Bxy$$

making the x- and y- components of  $\vec{H}_2$  linear in x and y at the aperture; thus the boundary condition of  $\vec{H}_2$  and  $\vec{H}_3$  can be matched at the aperture.

$$\phi_2^+ = A \left[ -3 \left( 1 + \frac{\xi}{a^2} \right) \alpha + \frac{3\xi^{\frac{1}{2}}}{a} + \frac{2a\xi^{\frac{1}{2}}}{\xi + a^2} \right] (\eta + a^2) \sin 2\phi$$

$$\begin{aligned} \vec{H}_{2x}^+ = & -A \left[ \frac{2x\xi}{\xi - \eta} (\eta + a^2) \sin 2\phi h(\xi) - \frac{2\eta x}{\xi - \eta} \sin 2\phi g(\xi) \right. \\ & \left. - 2 \left( \frac{\eta + a^2}{\rho} \right) \sin \phi \cos 2\phi g(\xi) \right] \end{aligned}$$

$$\begin{aligned} H_{2y}^+ = & -A \left[ \frac{2y\xi}{\xi - \eta} (\eta + a^2) \sin 2\phi h(\xi) - \frac{2\eta y}{\xi - \eta} \sin 2\phi g(\xi) \right. \\ & \left. + 2 \left( \frac{\eta + a^2}{\rho} \right) \cos \phi \cos 2\phi g(\xi) \right] \end{aligned}$$

$$\begin{aligned} H_{2z}^+ = & -\frac{2z}{\xi - \eta} \rho^2 a^2 A \sin 2\phi h(\xi) + \frac{2Az}{\xi - \eta} (\eta + a^2) \sin 2\phi g(\xi) \\ = & -\frac{16A\sqrt{-\eta}}{(\xi - \eta)} \frac{xya^4}{(\xi + a^2)^2} \end{aligned}$$

where

$$h(\xi) = -\frac{3\alpha}{a^2} + \frac{3}{a\xi^{\frac{1}{2}}} + \frac{a(a^2-\xi)}{\xi^{\frac{1}{2}}(a^2+\xi)^2} = g'(\xi)$$

$$g(\xi) = -3(1+\frac{\xi}{a^2})\alpha + \frac{3\xi^{\frac{1}{2}}}{a} + \frac{2a\xi^{\frac{1}{2}}}{\xi+a^2}$$

$H_{2x}^-$ ,  $H_{2y}^-$ ,  $H_{2z}^-$  are the same except that A is replaced by B and the sign of  $H_{2z}$  is changed. On the aperture it follows that

$$H_{2x}^+(\xi=0) = 3\pi Ay \quad H_{2x}^-(\xi=0) = 3\pi By$$

$$H_{2y}^+(\xi=0) = 3\pi Ax \quad H_{2y}^-(\xi=0) = 3\pi Bx$$

$$H_{2z}^+(\xi=0) = \frac{-16Axy}{\sqrt{a^2-\rho^2}} \quad H_{2z}^-(\xi=0) = \frac{16Bxy}{\sqrt{a^2-\rho^2}}$$

$\vec{H}_1$  has already been constrained to satisfy the continuity boundary conditions at the aperture. Applying these boundary conditions to the sum  $\vec{H}_2 + \vec{H}_3$ , one obtains

$$\Delta H_x = 3\pi Ay - 3\pi By + E_z^0 \sigma y - \frac{E_z^0 \sigma y}{2} = 0$$

$$\Delta H_y = 3\pi Ax - 3\pi Bx + E_z^0 \sigma x = 0$$

$$\Delta B_z = -\frac{16Axy\mu_0}{\sqrt{a^2-\rho^2}} - \frac{16Bxy\mu}{\sqrt{a^2-\rho^2}} = 0$$

or

$$A = -\frac{E_z^0 \sigma \mu}{6\pi(\mu_0 + \mu)}$$

$$B = \frac{E_z^0 \sigma \mu_0}{6\pi(\mu_0 + \mu)}$$

This completes the evaluation of all constants. We have thus found the fields which satisfy all twenty-four boundary conditions. The final result and some special cases are tabulated below.

#### Table of Results

$$E_x^- = \frac{2a^2 E_z^0 x \sqrt{-\eta}}{\pi(\xi + a^2)(\xi - \eta)} = E_x^+$$

$$E_y^- = \frac{2a^2 E_z^0 y \sqrt{-\eta}}{\pi(\xi + a^2)(\xi - \eta)} = E_y^+$$

$$E_z^- = E_z^0 \left[ 1 - \frac{2\alpha}{\pi} + \frac{2a\xi^{\frac{1}{2}}}{\pi(\xi - \eta)} \right]$$

$$E_z^+ = \frac{2E_z^0}{\pi} \left( \alpha - \frac{a\xi^{\frac{1}{2}}}{\xi - \eta} \right)$$

$$E_x^+ = \frac{2xE_z^0}{\pi\sqrt{a^2 - \rho^2}}$$

$$E_x^- = \frac{2xE_z^0}{\pi\sqrt{a^2 - \rho^2}}$$

$$E_y^+ = \frac{2yE_z^0}{\pi\sqrt{a^2 - \rho^2}}$$

at a general point  
in space

in the aperture ( $z=0$ ,  
 $\rho \leq a$ ,  $\eta = \rho^2 - a^2$ )

$$E_Y^- = \frac{2yE_z^0}{\pi\sqrt{a^2-\rho^2}}$$

$$E_z^+ = E_z^0$$

$$E_z^- = 0$$

$$\rho_s = \epsilon_0 E_z^0$$

in the aperture ( $z=0, \rho \leq a, \eta = \rho^2 - a^2$ )

$$E_x^- = 0$$

$$E_y^- = 0$$

$$E_z^- = E_z^0 \left[ 1 - \frac{2}{\pi} \left( \sin^{-1} \frac{a}{\rho} - \frac{a}{\sqrt{\rho^2 - a^2}} \right) \right]$$

on the screen

( $z=0^-, \rho > a,$

$\eta=0, \xi = \rho^2 - a^2$ )

$$E_x^+ = 0$$

$$E_y^+ = 0$$

$$E_z^+ = \frac{2E_z^0}{\pi} \left( \sin^{-1} \frac{a}{\rho} - \frac{a}{\sqrt{\rho^2 - a^2}} \right)$$

on the screen

( $z=0^+, \rho > a,$

$\eta=0, \xi = \rho^2 - a^2$ )

$$E_x^- = 0$$

$$E_y^- = 0$$

$$E_z^- = E_z^0 \left[ 1 - \frac{2}{\pi} \left( \cot^{-1} \frac{z}{a} - \frac{az}{z^2 + a^2} \right) \right]$$

along the Z axis

( $x=y=0, z \leq 0$

$\eta = -a^2, \xi = z^2$ )

$$E_x^+ = 0$$

$$E_y^+ = 0$$

$$E_z^+ = \frac{2E_z^0}{\pi} \left( \cot^{-1} \frac{z}{a} - \frac{az}{z^2 + a^2} \right)$$

$$E_x^+ = \frac{2E_z^0 x a^3 \cos \theta}{\pi r^4} = \frac{2E_z^0 a^3 \cos^2 \phi \cos \theta \sin \theta}{\pi r^3}$$

$$E_y^+ = \frac{2E_z^0 y a^3 \cos \theta}{\pi r^4} = \frac{2E_z^0 a^3 \sin \phi \cos \theta \sin \theta}{\pi r^3}$$

$$E_z^+ = -\frac{2E_z^0 a^3}{3\pi r^3} (1 - 3\cos^2 \theta),$$

$$\vec{E}^+ = \frac{3\hat{r}(\hat{r} \cdot \vec{P}_E) - \vec{P}_E}{4\pi\epsilon_0 r^3} \text{ where } \vec{P}_E = \frac{8}{3}\epsilon_0 a^3 E_z^0 \hat{z}$$

$$E_x^- = \frac{2E_z^0 a^3 \cos \phi \cos \theta \sin \theta}{\pi r^3}$$

$$E_y^- = \frac{2E_z^0 a^3 \sin \phi \cos \theta \sin \theta}{\pi r^3}$$

$$E_z^- = E_z^0 \left[ 1 + \frac{2a^3}{3\pi r}, (1 - 3\cos^2 \theta) \right]$$

$$H_x^+ = -\frac{E_z^0 \sigma \mu y}{\pi(\mu_0 + \mu)} \left\{ \alpha - \frac{a\xi^{\frac{1}{2}}}{3(\xi + a^2)^2} \left[ 3\xi + 5a^2 + \frac{8a^4 x^2}{(\xi - \eta)(\xi + a^2)} \right] \right\}$$

$$+ \frac{2\mu H_x^0}{\pi(\mu + \mu_0)} \left( \alpha - \frac{a\xi^{\frac{1}{2}}}{\xi + a^2} \right) - \frac{4a^3 \mu x \xi^{\frac{1}{2}} \vec{H}^0 \cdot \vec{\rho}}{\pi(\mu + \mu_0)(\xi - \eta)(\xi + a^2)^2}$$

along the z axis

(x=y=0, z>0,

$\eta = -a^2$ ,  $\xi = z^2$ )

in the far field

(z>>0,  $\frac{\xi}{r^2} \rightarrow 1$ ,

$\eta \rightarrow -\frac{a^2 z^2}{r^2} = -a^2 \cos^2 \theta$ ),

for the far field

(z<<0,  $\frac{\xi}{r^2} \rightarrow 1$ ,

$\eta = -\frac{a^2 z^2}{r^2} = -a^2 \cos^2 \theta$ ,

$\theta$  measured from positive real axis)

$$H_y^+ = - \frac{E_z^0 \sigma \mu x}{\pi (\mu_0 + \mu)} \left\{ \alpha - \frac{a \xi^{\frac{1}{2}}}{3(\xi + a^2)^2} \left[ 3\xi + 5a^2 + \frac{8a^4 y^2}{(\xi - \eta)(\xi + a^2)} \right] \right\} \\ + \frac{2\mu H_y^0}{\pi (\mu + \mu_0)} \left( \alpha - \frac{a \xi^{\frac{1}{2}}}{\xi + a^2} \right) - \frac{4a^3 \mu y \xi^{\frac{1}{2}} \vec{H}^0 \cdot \vec{\rho}}{\pi (\mu + \mu_0) (\xi - \eta) (\xi + a^2)^2}$$

$$H_z^+ = \frac{8E_z^0 \sigma \mu a^4 xy \sqrt{-\eta}}{3\pi (\mu_0 + \mu) (\xi - \eta) (\xi + a^2)^2} - \frac{4a^2 \mu \vec{H}^0 \cdot \vec{\rho} \sqrt{-\eta}}{\pi (\mu + \mu_0) (\xi - \eta) (\xi + a^2)}$$

$$H_x^- = - E_z^0 \sigma y \left[ 1 - \frac{\alpha}{\pi} + \frac{a \xi^{\frac{1}{2}}}{\pi (\xi + a^2)} \right]$$

$$+ \frac{E_z^0 \sigma \mu_0 y}{\pi (\mu_0 + \mu)} \left\{ \alpha - \frac{a \xi^{\frac{1}{2}}}{3(\xi + a^2)^2} \left[ 3\xi + 5a^2 + \frac{8a^4 x^2}{(\xi - \eta)(\xi + a^2)} \right] \right\} \\ + H_x^0 \left[ 1 - \frac{2\mu_0}{\pi (\mu + \mu_0)} \left( \alpha - \frac{a \xi^{\frac{1}{2}}}{\xi + a^2} \right) \right] + \frac{4a^3 \mu_0 x \xi^{\frac{1}{2}} \vec{H}^0 \cdot \vec{\rho}}{\pi (\mu + \mu_0) (\xi - \eta) (\xi + a^2)^2}$$

$$H_y^- = \frac{E_z^0 \sigma x}{\pi} \left( \frac{a \xi^{\frac{1}{2}}}{\xi + a^2} - \alpha \right) \\ + \frac{E_z^0 \sigma \mu_0 x}{\pi (\mu_0 + \mu)} \left\{ \alpha - \frac{a \xi^{\frac{1}{2}}}{3(\xi + a^2)^2} \left[ 3\xi + 5a^2 + \frac{8a^4 y^2}{(\xi - \eta)(\xi + a^2)} \right] \right\} \\ + H_y^0 - \frac{2\mu_0 H_y^0}{\pi (\mu + \mu_0)} \left( \alpha - \frac{a \xi^{\frac{1}{2}}}{\xi + a^2} \right) + \frac{4a^3 \mu_0 y \xi^{\frac{1}{2}} \vec{H}^0 \cdot \vec{\rho}}{\pi (\mu + \mu_0) (\xi - \eta) (\xi + a^2)^2} \\ H_z^- = + \frac{8E_z^0 \sigma \mu_0 a^4 xy \sqrt{-\eta}}{3\pi (\mu + \mu_0) (\xi - \eta) (\xi + a^2)^2} - \frac{4a^2 \mu_0 \vec{H}^0 \cdot \vec{\rho} \sqrt{-\eta}}{\pi (\mu + \mu_0) (\xi + a^2) (\xi - \eta)}$$

$$H_x^- = -\frac{E_z^0 \sigma \mu y}{2(\mu + \mu_0)} + \frac{\mu H_x^0}{\mu + \mu_0} = H_x^+$$

$$H_y^- = -\frac{E_z^0 \sigma \mu x}{2(\mu + \mu_0)} + \frac{\mu H_y^0}{\mu + \mu_0} = H_y^+$$

$$H_z^+ = \frac{8E_z^0 \sigma \mu xy}{3\pi(\mu + \mu_0) \sqrt{a^2 - \rho^2}} - \frac{4\mu \vec{H}^0 \cdot \vec{\rho}}{\pi(\mu + \mu_0) \sqrt{a^2 - \rho^2}}$$

$$H_z^- = \frac{8E_z^0 \sigma \mu_0 xy}{3\pi(\mu + \mu_0) \sqrt{a^2 - \rho^2}} - \frac{4\mu_0 \vec{H}^0 \cdot \vec{\rho}}{\pi(\mu + \mu_0) \sqrt{a^2 - \rho^2}}$$

$$H_x^+ = \frac{2\mu H_x^0}{\pi(\mu + \mu_0)} \left( \cot^{-1} \frac{z}{a} - \frac{az}{z^2 + a^2} \right)$$

$$H_y^+ = \frac{2\mu H_y^0}{\pi(\mu + \mu_0)} \left( \cot^{-1} \frac{z}{a} - \frac{az}{z^2 + a^2} \right)$$

$$H_z^+ = 0$$

$$H_x^- = H_x^0 - \frac{2\mu_0 H_x^0}{\pi(\mu + \mu_0)} \left( \cot^{-1} \frac{z}{a} - \frac{az}{z^2 + a^2} \right)$$

$$H_y^- = H_y^0 - \frac{2\mu_0 H_y^0}{\pi(\mu + \mu_0)} \left( \cot^{-1} \frac{z}{a} - \frac{az}{z^2 + a^2} \right)$$

$$H_z^- = 0$$

In the aperture

$$(z=0, \rho < a, \xi=0, \eta=\rho^2 - a^2)$$

Along the axis

$$(x=y=0, \eta=-a^2, \xi=z^2)$$

On the screen ( $\eta=0$ ,  $z=0$ ).

$$H_x^+ = - \frac{E_z^0 \sigma \mu y}{\pi(\mu + \mu_0)} \left\{ \sin^{-1} \frac{a}{\rho} - \frac{a^2}{3\rho^4} \sqrt{\frac{\rho^2}{a^2} - 1} \left[ 3\rho^2 + 2a^2 + \frac{8a^4 x^2}{\rho^2(\rho^2 a^2)} \right] \right\} \\ + \frac{2\mu H_x^0}{\pi(\mu + \mu_0)} \left( \sin^{-1} \frac{a}{\rho} - \frac{a^2}{\rho^2} \sqrt{\frac{\rho^2}{a^2} - 1} \right) - \frac{4a^2 \mu x \vec{H}^0 \cdot \vec{\rho}}{\pi(\mu + \mu_0) \rho^4 \sqrt{\frac{\rho^2}{a^2} - 1}}$$

$$H_y^+ = - \frac{E_z^0 \sigma \mu x}{\pi(\mu + \mu_0)} \left\{ \sin^{-1} \frac{a}{\rho} - \frac{a^2}{3\rho^4} \sqrt{\frac{\rho^2}{a^2} - 1} \left[ 3\rho^2 + 2a^2 + \frac{8a^4 y^2}{\rho^2(\rho^2 a^2)} \right] \right\} \\ + \frac{2\mu H_y^0}{\pi(\mu + \mu_0)} \left( \sin^{-1} \frac{a}{\rho} - \frac{a^2}{\rho^2} \sqrt{\frac{\rho^2}{a^2} - 1} \right) - \frac{4a^2 \mu y \vec{H}^0 \cdot \vec{\rho}}{\pi(\mu + \mu_0) \rho^4 \sqrt{\frac{\rho^2}{a^2} - 1}}$$

$$H_z^+ = 0$$

$$H_x^- = - E_z^0 \sigma y \left( 1 - \frac{1}{\pi} \sin^{-1} \frac{a}{\rho} + \frac{a^2}{\pi \rho^2} \sqrt{\frac{\rho^2}{a^2} - 1} \right) \\ + \frac{E_z^0 \sigma \mu_0 y}{\pi(\mu + \mu_0)} \left\{ \sin^{-1} \frac{a}{\rho} - \frac{a^2}{3\rho^4} \sqrt{\frac{\rho^2}{a^2} - 1} \left[ 3\rho^2 + 2a^2 + \frac{8a^4 x^2}{\rho^2(\rho^2 a^2)} \right] \right\} \\ + H_x^0 \left\{ 1 - \frac{2\mu_0}{\pi(\mu + \mu_0)} \sin^{-1} \frac{a}{\rho} - \frac{a^2}{\rho^2} \sqrt{\frac{\rho^2}{a^2} - 1} \right\} \\ + \frac{4a^2 \mu_0 x \vec{H}^0 \cdot \vec{\rho}}{\pi(\mu + \mu_0) \rho^4 \sqrt{\frac{\rho^2}{a^2} - 1}}$$

$$\begin{aligned}
H_y^- = & -\frac{E_z^0 \sigma x}{\pi} \left( \sin^{-1} \frac{a}{\rho} - \frac{a^2}{\rho^2} \sqrt{\frac{\rho^2}{a^2} - 1} \right) + \frac{E_z^0 \sigma \mu_0 x}{\pi(\mu + \mu_0)} \left\{ \sin^{-1} \frac{a}{\rho} \right. \\
& - \frac{a^2}{3\rho^4} \sqrt{\frac{\rho^2}{a^2} - 1} \left[ 3\rho^2 + 2a^2 + \frac{8a^4 y^2}{\rho^2(\rho^2 - a^2)} \right] \} + H_y^0 \\
& - \frac{2\mu^0 H_y^0}{\pi(\mu + \mu_0)} \left( \sin^{-1} \frac{a}{\rho} - \frac{a^2}{\rho^2} \sqrt{\frac{\rho^2}{a^2} - 1} \right) \\
& + \frac{4a^2 \mu_0 y \vec{H}^0 \cdot \vec{\rho}}{\pi(\mu + \mu_0) \rho^4 \sqrt{\frac{\rho^2}{a^2} - 1}} \\
H_z^- = & 0
\end{aligned}$$

Far fields (up to terms of  $\frac{1}{r^3}$ )

$$\begin{aligned}
H_x^+ = & \frac{4a^3 \mu}{3\pi(\mu + \mu_0) r^3} (H_x^0 - 3H_x^0 \sin^2 \theta \cos^2 \phi - 3H_y^0 \sin^2 \theta \sin \phi \cos \phi) \\
& (\theta \text{ measured from positive } z\text{-axis})
\end{aligned}$$

$$H_y^+ = \frac{4a^3 \mu}{3\pi(\mu + \mu_0) r^3} (H_y^0 - 3H_x^0 \sin^2 \theta \cos \phi \sin \phi - 3H_y^0 \sin^2 \theta \sin^2 \phi)$$

$$H_z^+ = \frac{4a^3 \mu \cos \theta \sin \theta (H_x^0 \cos \phi + H_y^0 \sin \phi)}{\pi(\mu + \mu_0) r^3}$$

$$H_x^- = H_x^0 - E_z^0 \sigma y + \frac{2a^3 E_z^0 \sigma y}{3\pi r^3} - \frac{4a^3 \mu_0}{3\pi(\mu + \mu_0) r^3}$$

$$(H_x^0 - 3H_x^0 \sin^2 \theta \cos^2 \phi - 3H_y^0 \sin^2 \theta \sin \phi \cos \phi)$$

$$H_Y^- = H_Y^0 - \frac{2a^3 E_z^0 \sigma x}{3\pi r^3} - \frac{4a^3 \mu_0}{3\pi(\mu + \mu_0)r^3}$$

$$(H_Y^0 - 3H_X^0 \sin^2 \theta \cos \phi \sin \phi - 3H_Y^0 \sin^2 \theta \sin^2 \phi)$$

$$H_Z^- = - \frac{4a^3 \mu_0 \cos \theta \sin \theta}{\pi(\mu + \mu_0)r^3} (H_Z^0 \cos \phi + H_Y^0 \sin \phi)$$

$$\vec{H}^+ = \frac{3\hat{r}(\hat{r} \cdot \vec{P}_M) - \vec{P}_M}{4\pi r^3} \quad \vec{P}_M = - \frac{16a^3 \mu}{3(\mu + \mu_0)} \vec{H}^0$$

The magnetic moment is independent of  $\sigma$ . If  $\mu = \mu_0$ , this is the same value as for the case of an aperture in air. For the incident side, the scattered magnetic far field is the same as a magnetic dipole of moment given by

$$\vec{P}_M = \frac{16a^3 \mu_0 \vec{H}^0}{3(\mu + \mu_0)} + \frac{8a^3 \sigma \vec{E}^0 \times \vec{\rho}}{3}$$

References

1. D. P. Thomas, "Electromagnetic Diffraction by a Circular Aperture in a Plane Screen between Different Media," Canadian Journal of Physics, vol. 47, pp. 921-930, 1969.
2. C. M. Butler and K. R. Umashankar, "Electromagnetic Penetration through an Aperture in an Infinite, Planar Screen Separating Two Half Spaces of Different Electromagnetic Properties," Radio Science, vol. 11, No. 7, pp. 611-619, July 1976.
3. H. J. Fletcher and Alan Harrison, "Fields in a Rectangular Aperture," AFWL Interaction Note 342, June 1978.
4. L. W. Chen, "On Cavity Excitation Through Small Apertures," AFWL Interaction Note 45, January 1970.
5. G. H. Price, "Sub Surface HEMP Field Calculations," AFWL Theoretical Note 232, 1 May 1975.
6. D. R. Marston, "Approximate Method for Calculating the Currents Induced in Underground Cables by a High Altitude Overhead Electromagnetic Field Source," AFWL Interaction Note 21, January 1969. (See also Interaction Notes 19, 24, 25, 37, 39, 50 and 52).

NOTE 347

SMALL APERTURE ON A MULTICONDUCTOR TRANSMISSION  
LINE FILLED WITH INHOMOGENEOUS DIELECTRICS

by

Darko Kajfez  
Donald R. Wilton

November 1977

SMALL APERTURE ON A MULTICONDUCTOR TRANSMISSION  
LINE FILLED WITH INHOMOGENEOUS DIELECTRICS

ABSTRACT

The penetration of the electromagnetic pulse through a small aperture in the conducting plane is studied when a multiconductor transmission line is located behind the aperture. The multiconductor transmission line is filled with inhomogeneous dielectric material, so that the propagating modes have different velocities. The aperture is replaced by a pair of electric and magnetic current moments, and the equivalent multiport for the aperture junction is developed. The accuracy of the dipole moment approach is checked by the continuous spectrum approach, and the limits of validity are established.

## CONTENTS

<u>Section</u>		<u>Page</u>
I	INTRODUCTION	347-6
II	TRAVELING WAVE FORMULATION	347-16
III	EQUIVALENT SOURCES FOR APERTURE EXCITATION	347-28
IV	EXAMPLES OF VOLTAGE WAVEFORMS	347-33
V	FIRST ORDER EQUIVALENT CIRCUIT OF THE SMALL APERTURE	347-50
VI	INTERACTION BETWEEN AN APERTURE AND A SINGLE WIRE	347-67
APPENDIX A	Lumped-element traveling wave source	347-92
APPENDIX B	Matrix algebra in Dirac's notation	347-97
APPENDIX C	Multiconductor-line formulation by simultaneous diagonalization of two matrices	347-102
REFERENCES		347-115

## ILLUSTRATIONS

<u>Figure</u>		<u>Page</u>
1(a)	Multiconductor transmission line with a small aperture.	347-9
1(b)	The aperture is replaced by a pair of dipoles.	347-9
1(c)	Magnetic and electric surface currents which are equivalent to the pair of dipoles.	347-9
2	Excitation fields.	347-12
3	Orientation of coordinates.	347-14
4	Signal flow graph of a MTL section.	347-19
5	Terminated MTL with a source of outgoing waves located at $z=0$ .	347-19
6	Signal flow graph of the MTL from Fig. 5.	347-22
7	Time-table representation of multiple reflections on the terminated MTL.	347-24
8(a)	MTL section of length $\ell$ .	347-27
8(b)	Equivalent circuit for normal modes.	347-27
9(a)	A junction with an aperture.	347-29
9(b)	Normal-mode sources.	347-29
9(c)	Voltage and current sources.	347-29
10	Terminated 2-conductor transmission line with an aperture.	347-34
11	Parallel-plate 2-conductor transmission line.	347-34
12	Evaluation of the electric field on the line from Fig. 11.	347-40
13	Evaluation of the magnetic field on the line from Fig. 11.	347-40
14	Voltage waveforms on a 2-conductor line: moderate mismatch.	347-44

<u>Figure</u>		<u>Page</u>
15	Voltage waveforms on a 2-conductor line: matched load at left-hand terminals.	347-46
16	Voltage waveforms on a 2-conductor line: large mismatch at both ends.	347-47
17	Voltage waveforms on a 3-conductor line: moderate mismatch.	347-48
18	Aperture junction with sources.	347-51
19	Signal flow graph of the aperture junction with sources.	347-51
20	Small parallel admittance perturbation on MTL.	347-54
21	Small series impedance perturbation on MTL.	347-54
22	MTL with both series and parallel perturbations.	347-57
23	Equivalent circuit of the aperture junction with sources.	347-57
24(a)	Impedance perturbation circuit.	347-60
24(b)	Admittance perturbation circuit.	347-60
25	Geometry of wire over a ground screen with equivalent dipole moments representing an aperture.	347-69
26	Magnitude of $t_m$ for a wire of radius $kr = 0.1$ .	347-79
27	Magnitude of $t_e$ for a wire of radius $kr = 0.1$ .	347-80
28	Magnitude of $t_m$ for a wire of radius $kr = 0.01$ .	347-81
29	Magnitude of $t_e$ for a wire of radius $kr = 0.01$ .	347-82
30	Magnitude of $t_m$ for a wire of radius $kr = 0.001$ .	347-83
31	Magnitude of $t_e$ for a wire of radius $kr = 0.001$ .	347-84
32	Magnitude of $t_m$ for a wire of radius $kr = 0.0001$ .	347-85
33	Magnitude of $t_e$ for a wire of radius $kr = 0.0001$ .	347-86
34	Magnitude of $(kd/2)^3 \tilde{t}_m(0, kd, kr)$ .	347-87
35	Magnitude of $(kd/2)^3 \tilde{t}_e(0, kd, kr)$ .	347-88

<u>Figure</u>		<u>Page</u>
36	Branch cuts and contour of integration in the $k_z$ plane.	347-90
37	Deformation of the contour around the branch cut.	347-90
A1	Conventional symbol for traveling-wave source.	347-94
A2(a)	Combination of voltage and current sources.	347-94
A2(b)	Proposed symbol for traveling-wave source.	347-94
C1	Voltages and currents on MTL.	347-103

## SECTION I

### INTRODUCTION

The objective of this report is to study the penetration of an electromagnetic pulse through a small aperture in an aircraft, and to evaluate the induced voltages on multiconductor cables located inside the aircraft. Knowledge of these voltages caused by the electromagnetic pulse is of interest in estimating possible interference with or damage to the electric and electronic systems within the aircraft.

The computational approach used in this report is based on the assumption that the aperture in the metal shell of the aircraft is considerably smaller than the wavelength of the highest spectral component contained in the electromagnetic pulse. Therefore, the small aperture approximation is used in evaluating the electromagnetic field behind the aperture. A bundle of wires is assumed to be located inside the aircraft, passing behind the aperture. The magnitudes of the traveling waves on the individual conductors may then be calculated for given wire dimensions and given dielectric filling. The conventional representation of the induced voltages and currents on individual conductors is in terms of voltage sources and current sources on the individual conductors. In the present report, an alternative representation in terms of traveling wave sources has been utilized. This novel class of sources is formally introduced in Appendix A. The advantage of this representation is that individual sources are not associated with the individual conductors, but they are directly associated with the individual modes.

When the wires are placed in a straight line, running parallel to the metal surface in the aircraft, the bundle can be modeled as a multiconductor transmission line. Because of the presence of various dielectric materials, the individual modes on the multiconductor transmission line differ in their velocities, but the

propagation of each mode is essentially nondispersive. Such transmission-line modes are classified as quasi-TEM waves. The wave propagation on multiconductor transmission lines is best described in terms of matrices. Particularly convenient for that purpose is the Dirac notation. While the notation is widely used in physics, it is not always familiar to engineers. Because of that, the basic principles of the Dirac notation for matrices are reviewed in Appendix B. The advantages of this notation can be clearly seen in Appendix C, in which the wave equations are solved for multiconductor transmission lines filled with inhomogeneous dielectrics. Some matrix operations, which are quite intricate in the conventional matrix notation, become surprisingly simple and obvious in the Dirac notation. Appendix C differs from the conventional derivation also in the fact that the solution is accomplished by simultaneous diagonalization of two real symmetric matrices  $\underline{K}$  and  $\underline{K'}$ , instead of diagonalizing a real but not symmetric matrix  $\underline{KL}$ .

The validity of the quasi TEM approach is closely examined in Section VI. This Section investigates the assumption that coupling of a multiconductor transmission line back into a plane-wave excited aperture can be neglected. The configuration treated consists of a single wire conductor behind an aperture and the relation of this problem to the multiconductor transmission line problem is discussed. The problem is treated from the rigorous Fourier transform approach and hence includes the complete modal spectrum consisting of the TEM mode and continuous spectra of evanescent and propagating modes. It is found that whenever the representation of the aperture by dipole moments is valid, the effects of a transmission line on the strength of those dipole moments is negligible.

Before starting with the presentation in Section II, the small aperture theory will be briefly reviewed. A convenient approximation of the electromagnetic field in the presence of a small aperture is in terms of a pair of dipoles, as originated by Bethe [1]. Assume that the local distribution of the total electric field  $\vec{E}_t(x, z)$  over an aperture in x-z plane, such as in Fig. 1.(a), has been determined by an analytical or a numerical solution of the boundary-value problem. Then, the electromagnetic field in the "internal" region  $y > 0$  remains unchanged if the aperture is closed by a metal lid on top of which there is a magnetic surface current

$$\vec{J}_s^m(x, z) = \vec{E}_t(x, z) \times \vec{a}_y \quad (1)$$

where  $\vec{a}_y$  is the unit vector in y direction.

The coupling to the TEM wave on the system of conductors can then be computed by replacing the aperture with a conducting lid on top of which there are two dipoles,  $\vec{c}_e$  and  $\vec{c}_m$  as shown in Fig. 1.(b). Electric dipole moment  $\vec{c}_e$  is oriented in the y direction:

$$c_{ey} = \iint J_{sx}^m(x, z) dx dz, \quad (2)$$

and the magnetic dipole moment of interest here is oriented in the x direction:

$$c_{mx} = j\omega\epsilon \iint z J_{sx}^m(x, z) dx dz. \quad (3)$$

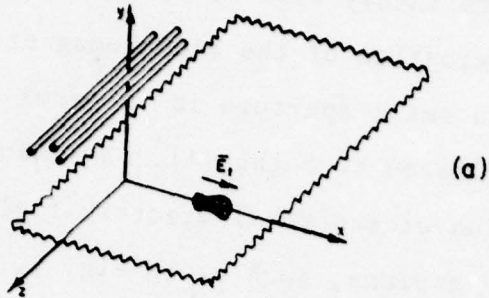


Fig. 1(a) Multiconductor transmission line with a small aperture.

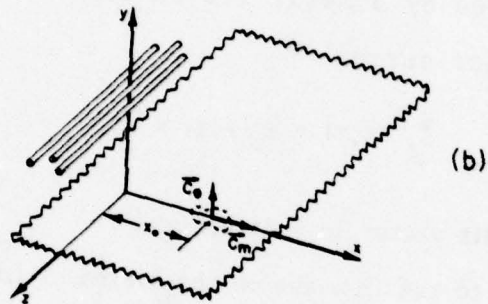


Fig. 1(b) The aperture is replaced by a pair of dipoles.

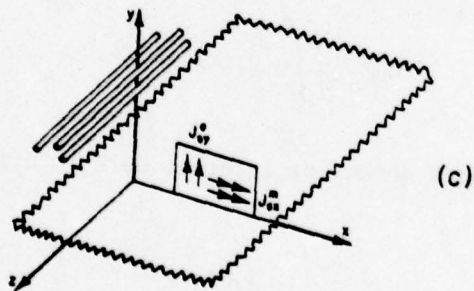


Fig. 1(c) Magnetic and electric surface currents which are equivalent to the pair of dipoles.

The magnetic dipole moment may also have the z-component, but the present report is devoted solely to a coupling of quasi-TEM waves guided along the z direction by a system of conductors as indicated in Fig. 1.(b). Therefore, the z component of the magnetic dipole is of no importance, because it does not interact with these quasi-TEM waves.

In this report, the electric dipole moment  $\vec{C}_e$  (in Ampere·meters) has a meaning of the moment of an electric current element, similar to that given in references [2]-[4]. This current moment should not be confused with the electric charge moment  $\vec{p}$  (in Coulomb·meters) such as is used in references [5]-[7]. The relationship between these two moments, for  $\exp(j\omega t)$  variation, is as follows:

$$\vec{C}_e = j\omega\vec{p}. \quad (4)$$

Similarly, the magnetic dipole moment  $\vec{C}_m$  (in Volt·meters) in this report denotes the moment of the magnetic current element, in the sense as used in references [8]-[10]. The magnetic charge moment  $\vec{m}$  (in Ampere·square-meters), such as used for instance in references [5]-[7] is related to  $\vec{C}_m$  as follows:

$$\vec{C}_m = j\omega\mu\vec{m}. \quad (5)$$

Figure 1.(b) is a first-order equivalent of the original configuration from Fig.1.(a). Sometimes it is convenient to further change Fig. 1.(b) into an equivalent configuration in Fig. 1.(c) in which there is a distribution of the surface magnetic current  $\vec{J}_s^m$  and of the surface electric current  $\vec{J}_s^e$  over the x-y plane. Figures 1.(b) and 1.(c) are equivalent if the surface currents become delta functions as follows:

$$\vec{J}_s^e = \vec{c}_e \delta(x-x_0) \delta(y) , \quad (6)$$

$$\vec{J}_s^m = \vec{c}_m \delta(x-x_0) \delta(y) . \quad (7)$$

For an aperture of general shape, integrations (2) and (3) are to be performed numerically. For several characteristic shapes (circle, ellipse, narrow slit, square, etc.), the dipole moments have been computed or determined experimentally. It is customary to express the moments in terms of the excitation fields  $\vec{E}_s$ ,  $\vec{H}_s$  and in terms of the polarizabilities  $\alpha_e$ ,  $\alpha_m$ . Consider the aperture in Fig. 2 which is to be replaced by the dipole moments so that the field in the "internal" region  $y > 0$  is maintained. The excitation fields (so-called short circuit fields) produced by the sources located in the internal region will be denoted  $\vec{E}_s^{\text{int}}$  and  $\vec{H}_s^{\text{int}}$ . When the excitation comes from the side  $y < 0$ , the short circuit fields will be denoted by  $\vec{E}_s^{\text{ext}}$  and  $\vec{H}_s^{\text{ext}}$ . For the purpose of coupling to the quasi-TEM waves in the internal region, only the components  $E_{ys}$  and  $H_{xs}$  are of interest. Instead of performing the numerical integrations from (2) and (3), the dipole moments of small apertures of characteristic shapes may be computed as follows:

$$c_{mx} = -j\omega\mu\alpha_m (H_{xs}^{\text{ext}} - H_{xs}^{\text{int}}) , \quad (8)$$

$$c_{ey} = j\omega\epsilon\alpha_e (E_{ys}^{\text{ext}} - E_{ys}^{\text{int}}) . \quad (9)$$

The electric polarizability  $\alpha_e$  and the magnetic polarizability  $\alpha_m$  of a circular aperture of diameter  $d$  are:

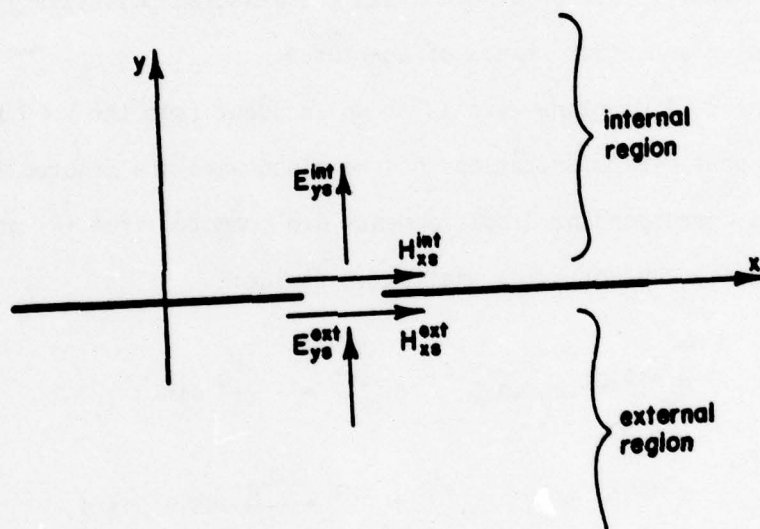


Fig. 2. Excitation fields.

$$\alpha_e = \frac{1}{12} d^3, \quad \alpha_m = \frac{1}{6} d^3. \quad (10)$$

For a square aperture of side  $\ell$ , Cohn [11], [12] has measured the following polarizabilities:

$$\alpha_e = 0.1137\ell^3, \quad \alpha_m = 0.2590\ell^3.$$

The last two references also contain the measured polarizabilities for rectangular and other shapes of apertures.

In Fig. 3, a plane wave is shown incident from the  $y < 0$  region. The two possible polarizations of the plane wave are denoted TE and TM. The corresponding dipole moments are computed from (8) and (9) by substituting the following excitation fields:

$$\text{TM: } E_{ys}^{\text{ext}} = 2E_0 \sin \theta, \quad H_{xs}^{\text{ext}} = -\frac{2E_0}{\eta} \sin \alpha, \quad (11)$$

$$\text{TE: } E_{ys}^{\text{ext}} = 0, \quad H_{xs}^{\text{ext}} = \frac{2E_0}{\eta} \cos \theta \cos \alpha. \quad (12)$$

For this excitation, take  $E_{ys}^{\text{int}} = 0$  and  $H_{xs}^{\text{int}} = 0$ .

When electromagnetic fields in the presence of a ground plane are considered, sometimes it is convenient to remove the plane and replace it by appropriate images. In the present report the ground plane has not been removed and the images have not been invoked.

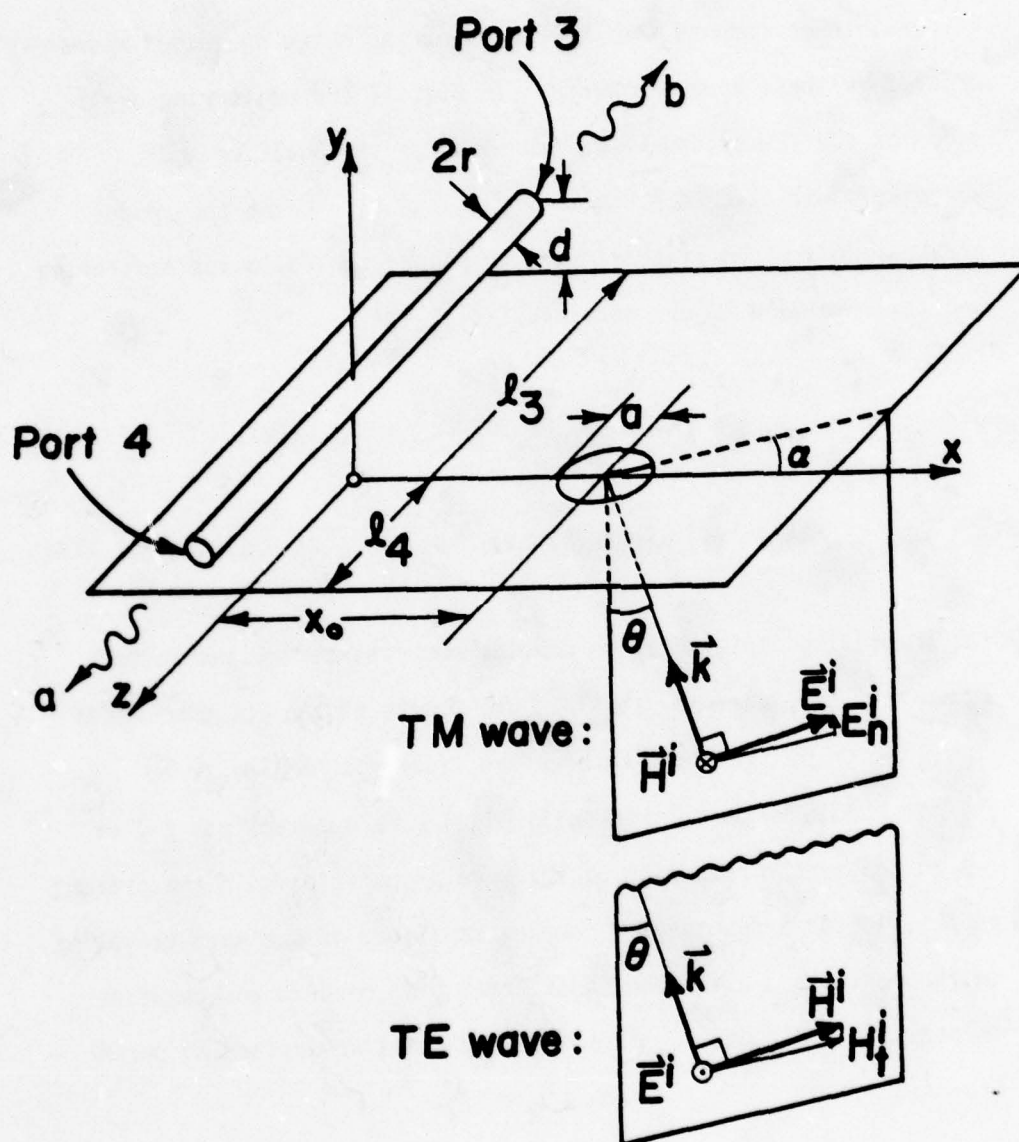


Fig. 3. Orientation of coordinates.

When dipole moments  $c_{mx}$  and  $c_{ey}$  have been determined, it is possible to compute the amplitudes of the outgoing guided waves created by these dipole moments. In Fig. 3, the scattering amplitudes of the TEM guided waves traveling in the positive and negative  $z$  direction are denoted by  $a_s$  and  $b_s$ . Using the appropriate boundary conditions in the  $xy$  plane, the following scattering amplitudes  $a_s$  and  $b_s$  are obtained [13]:

$$a_s = \frac{1}{2} [-c_{mx} h_{xTEM}(x_0, 0) - c_{ey} e_{yTEM}(x_0, 0)], \quad (13)$$

$$b_s = \frac{1}{2} [c_{mx} h_{xTEM}(x_0, 0) - c_{ey} e_{yTEM}(x_0, 0)]. \quad (14)$$

The scattering amplitudes are complex numbers, normalized in such a way that  $|a_s|^2/2$  and  $|b_s|^2/2$  are powers of the outgoing waves traveling in positive and in negative  $z$  directions [14].

It should be noted that Collin [14] uses superscripts (+) or (-) to denote the direction of the wave propagation. In the present report, letter  $a$  denotes the complex amplitude of the wave traveling in the positive  $z$  direction, and letter  $b$  is used for propagation in negative  $z$  direction. These are the familiar scattering parameters [15].

## SECTION II

### TRAVELING WAVE FORMULATION

Lossless multiconductor transmission lines (MTL) with unequal conductors and inhomogeneous dielectrics give rise to multivelocit quasi-TEM waves. As shown in Appendix C, the voltages and currents on a MTL are described by

$$|V(z)\rangle = \sum_{n=1}^N (a_n e^{-j\beta_n z} + b_n e^{j\beta_n z}) |\phi_n\rangle, \quad (15)$$

$$|I(z)\rangle = \sum_{n=1}^N (a_n e^{-j\beta_n z} - b_n e^{j\beta_n z}) |\psi_n\rangle. \quad (16)$$

$|\phi_n\rangle$  and  $|\psi_n\rangle$  are normalized voltage and current eigenvectors, and  $a_n$ 's and  $b_n$ 's are scattering amplitudes of the waves traveling in positive and negative  $z$  direction, respectively. It is assumed that on an  $N$  conductor MTL there are  $N$  normal modes, each of them having a distinct propagation constant  $\beta_n$ .

The notation from (15) and (16) may be made more compact by introducing the vectors of incident and reflected normal-mode amplitudes

$$|a\rangle = \begin{pmatrix} a_1 \\ \vdots \\ a_N \end{pmatrix}, \quad |b\rangle = \begin{pmatrix} b_1 \\ \vdots \\ b_N \end{pmatrix} \quad (17)$$

and by introducing the diagonal matrix  $\underline{E}(z)$  containing the exponential functions

$$\underline{E}(z) = \text{diag. } (e^{j\beta_1 z}, \dots, e^{j\beta_N z}), \quad (18)$$

In the new notation, (15) and (16) become:

$$|V(z)\rangle = \underline{M}_V(\underline{E}^*(z)|a\rangle + \underline{E}(z)|b\rangle) \quad , \quad (19)$$

$$|I(z)\rangle = \underline{M}_I(\underline{E}^*(z)|a\rangle - \underline{E}(z)|b\rangle) \quad , \quad (20)$$

where  $*$  denotes a complex conjugate number, and  $\underline{M}_V$  and  $\underline{M}_I$  are matrices consisting of voltage and current eigenvectors, as defined by (C-42) and (C-43). (19) and (20) may be now solved for  $|a\rangle$  and  $|b\rangle$ :

$$\underline{E}^*(z)|a\rangle = \frac{1}{2}(\underline{M}_I^+|V(z)\rangle + \underline{M}_V^+|I(z)\rangle) \quad , \quad (21)$$

$$\underline{E}(z)|b\rangle = \frac{1}{2}(\underline{M}_I^+|V(z)\rangle - \underline{M}_V^+|I(z)\rangle) \quad . \quad (22)$$

$|a\rangle$  is a constant vector containing the amplitudes of the individual modes as its components. For instance,  $a_i$  is the complex amplitude such that the total power of the  $i$ th mode transmitted in positive  $z$  direction is

$$P_i^+ = \frac{1}{2}|a_i|^2 \quad .$$

The entire power of all the modes traveling in the positive  $z$  direction is

$$P^+ = \frac{1}{2}\langle a|a\rangle \quad (23)$$

where  $\langle a|$  denotes a transpose conjugate of  $|a\rangle$ . Similarly, the total power traveling in the negative  $z$  direction is

$$P^- = \frac{1}{2}\langle b|b\rangle \quad . \quad (24)$$

The net power is the difference of the two. On a uniform MTL there is no exchange of power between different modes. Each mode travels with

constant magnitude, while its phase grows linearly with distance.

The  $z$  dependence of scattering amplitudes may be expressed as

$$|a(z)\rangle = \underline{E}^*(z) |a\rangle \quad (25)$$

and

$$|b(z)\rangle = \underline{E}(z) |b\rangle \quad (26)$$

where  $|a\rangle$  and  $|b\rangle$  are vectors consisting of complex constants. Thus, the  $i$ th component of the vector equation (25) is

$$a_i(z) = e^{-j\beta_i z} a_i,$$

and the corresponding  $i$ th component of (26) is

$$b_i(z) = e^{j\beta_i z} b_i.$$

The signal flow graph [16] of the MTL section of length  $\ell$  is shown in Fig. 4.

The  $i$ th mode has two variables  $a_i(0)$  and  $b_i(0)$  at  $z=0$ . Similarly, at  $z=\ell$  the two variables of the  $i$ th mode are  $a_i(\ell)$  and  $b_i(\ell)$ . The coefficients of matrix  $\underline{E}^*(\ell)$  equal to  $e^{-j\beta_i \ell}$ . Thus,  $a_i(\ell)$  is obtained by multiplying  $a_i(0)$  by the coefficient  $e^{-j\beta_i \ell}$ . The signal flow graph in Fig. 4 is extremely simple, since along the transmission line there is no cross coupling between different modes.

Figure 5 shows a MTL section with 3 conductors above the ground plane. At  $z=0$ , a source is coupled to the MTL, inducing the waves traveling toward the  $+z$  and  $-z$  directions. The amplitudes of the  $i$ th mode produced by the source are  $a_{is}$  and  $b_{is}$ . The direction of propagation of these waves is indicated by a wavy arrow. The wave traveling in  $+z$  direction arrives at  $z=\ell_4$  shifted in phase for  $e^{-j\beta_i \ell_4}$ . There, a three-port network terminates the MTL. The impedance matrix of this network is  $\underline{Z}_4$ .

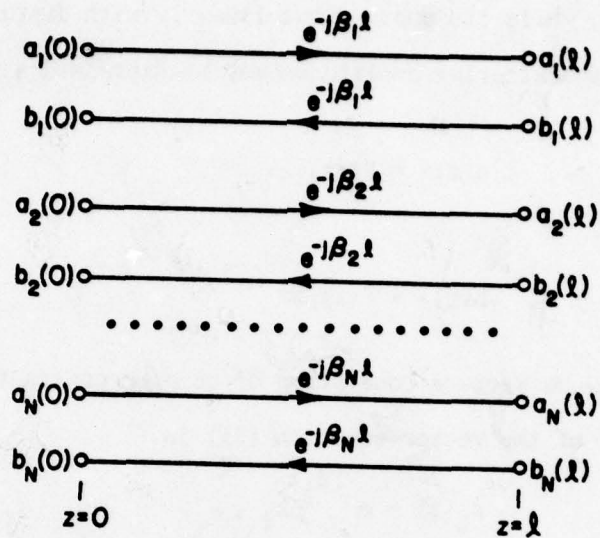
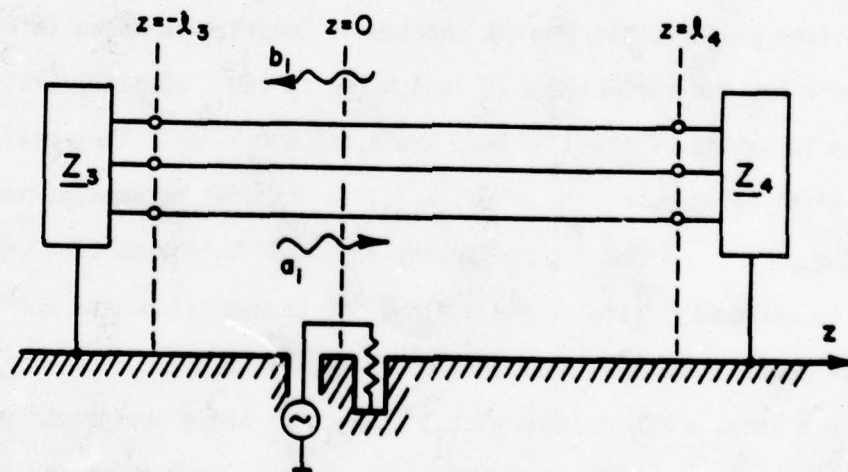


Fig. 4. Signal Flow graph of a MTL section.

Fig. 5. Terminated MTL with a source of outgoing waves located at  $z = 0$ .

The amount of reflection on the MTL can be computed from  $\underline{Z}_4$  as follows.

At  $z=0$ , the total amplitude  $a_i$  of the  $i$ th mode traveling in the positive  $z$  direction consists of two parts: the source part  $a_{is}$  and the part which arrives reflected from the left-hand termination at  $z=-\ell_3$ . The total amplitudes of all waves at  $z=0$  are arranged in vector  $|a\rangle$ . Then, the vector of all waves arriving at  $z=\ell_4$  is

$$|a(\ell_4)\rangle = \underline{E}^*(\ell_4) |a\rangle \quad (26a)$$

From (21), this is furthermore equal to

$$|a(\ell_4)\rangle = \frac{1}{2}(\underline{M}_I^+ |V(\ell_4)\rangle + \underline{M}_V^+ |I(\ell_4)\rangle). \quad (27)$$

From (22), the reflected mode vector at the end of line is

$$|b(\ell_4)\rangle = \frac{1}{2}(\underline{M}_I^+ |V(\ell_4)\rangle - \underline{M}_V^+ |I(\ell_4)\rangle). \quad (28)$$

The currents and voltages at the load network terminals are related through  $\underline{Z}_4$

$$|V(\ell_4)\rangle = \underline{Z}_4 |I(\ell_4)\rangle. \quad (29)$$

By eliminating  $|V(\ell_4)\rangle$  and  $|I(\ell_4)\rangle$  from the last three equations one obtains

$$|b(\ell_4)\rangle = \underline{S}_4 |a(\ell_4)\rangle \quad (30)$$

where the reflection matrix at port 4 is

$$\underline{S}_4 = (\underline{M}_I^+ \underline{Z}_{L4} \underline{M}_I - \underline{U}) (\underline{M}_I^+ \underline{Z}_{L4} \underline{M}_I + \underline{U})^{-1} \quad (31)$$

When the load impedance matrix is equal to the characteristic impedance  $\underline{Z}_L = \underline{Z}_0$ , one has a reflectionless termination, as can be verified by (C-46) and (C-50). Otherwise,  $\underline{S}_4$  is a matrix which has usually non-vanishing off-diagonal elements. This means that a single incoming mode  $a_i$  produces a multitude of reflected modes  $b_j$  ( $j=1,2,3$ , etc.). Thus, energy transfers from any one mode into all other modes.

This fact is illustrated in the signal-flow diagram on Fig. 6. On top of the figure,  $a_{1s}$  represents the amount of energy coupled from an external source to mode 1 traveling in +z direction. The total wave amplitude  $a_1$  at the origin, consists of  $a_{1s}$  plus the wave which was reflected from the termination at  $z=-\ell_3$ :

$$a_1 = a_{1s} + a_1(-\ell_3)e^{-j\beta\ell_3}.$$

This wave arrives at port 4 as

$$a_1(\ell_4) = a_1 e^{-j\beta_1\ell_4}.$$

A portion of this wave goes back as a reflected wave of the mode 1

$$S_{4,11}a_1(\ell_4)$$

where  $S_{4,11}$  is the coefficient (1,1) of the matrix  $\underline{S}_4$ .

Another portion of the wave  $a_1(\ell_4)$  goes to the enhancement of the reflected mode 2

$$S_{4,21}a_1(\ell_4)$$

and so on, as shown in Fig. 6. For example, the total reflected wave of the mode 2 is

$$b_2(\ell_4) = S_{4,21}a_1(\ell_4) + S_{4,22}a_2(\ell_4) + S_{4,23}a_3(\ell_4).$$

Similar situation occurs at port 3, where the load network  $\underline{Z}_{L3}$  is attached. There, the reflected wave is

$$|a(-\ell_3)\rangle = \underline{S}_3 |b(-\ell_3)\rangle, \quad (32)$$

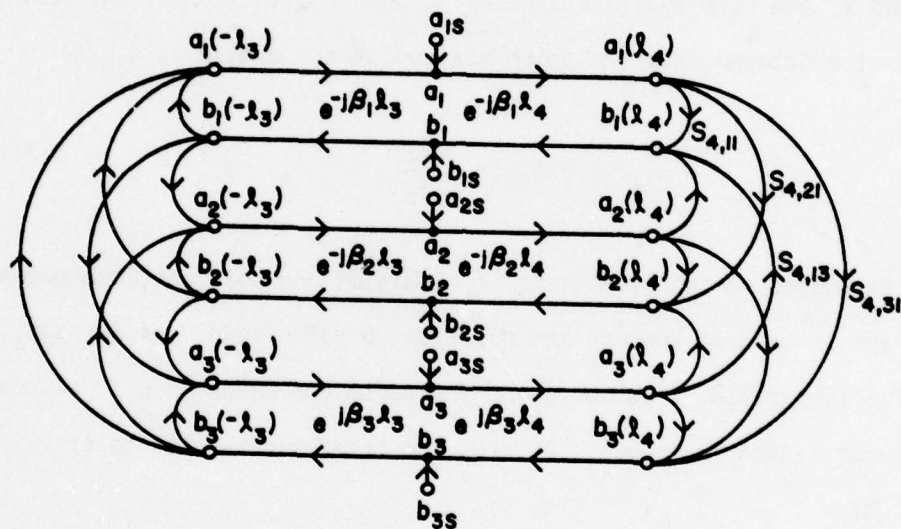


Fig. 6. Signal flow graph of the MTL from Fig. 5.

with

$$\underline{S}_3 = (\underline{M}_I^+ \underline{Z}_{L3} \underline{M}_I - \underline{U}) (\underline{M}_I^+ \underline{Z}_{L3} \underline{M}_I + \underline{U})^{-1} \quad (33)$$

The above discussion was based entirely on the frequency-domain considerations, where each mode was a steady-state sinusoidal function of time. Assuming the quasi-TEM waves are non-dispersive, an arbitrary waveform is transmitted by each mode without a distortion. Therefore, for mode  $i$ , the wave  $a_{i4}(t)$  traveling in the  $+z$  direction at the port 4 is just a delayed waveform which started at the origin as  $a_{i0}(t)$

$$a_{i4}(t) = a_{i0}(t - \frac{\ell_4}{v_i}) \quad (34)$$

Since the waves are now functions of both time and position, the second subscript is used to specify the position 0 for origin, 4 for  $z=\ell_4$  etc.

The time-table of the outgoing and reflected waves on a 3 conductor line is presented in Fig. 7. At  $z=0$ , the three waves start to travel to the right

$$a_{10}(t), a_{20}(t), a_{30}(t)$$

and similarly the three waves start to travel to the left,

$$b_{10}(t), b_{20}(t), b_{30}(t)$$

Each wave travels with its mode velocity  $v_i$ . At  $t=t_1$ , the first wave arrives at port 4,

$$t_1 = \frac{\ell_4}{v_1}$$

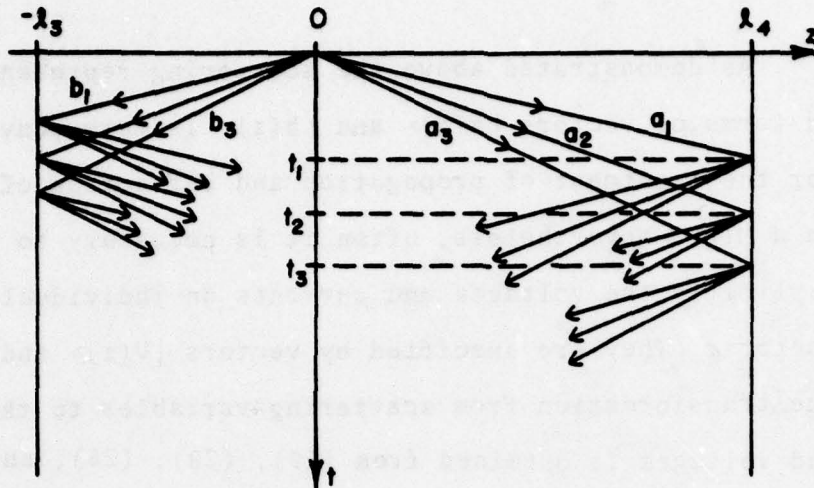


Fig. 7. Time-table representation of multiple reflections on the terminated MTL.

Its shape is a shifted shape of the wave which started from the origin, according to (34). This wave produces three reflected waves, which then travel with their corresponding velocities back in the negative  $z$  direction. When the load network contains inductances and capacitances, the shape of the reflected waves will be different from the incoming waveshape. For simplicity, consider the case when the load network is purely resistive. In that case, the reflected waves will be of the same shape as the incoming waves. The amount of reflection is specified by (30) and (31), where  $Z_{L4}$  is a purely resistive network, thus  $S_4$  has also purely real elements. The reflections from the left-hand termination are handled in an analogous manner.

As demonstrated above, the scattering representation in terms of vectors  $|a(z)\rangle$  and  $|b(z)\rangle$  is very convenient for the treatment of propagation and reflection of waves on a MTL. Nevertheless, often it is necessary to compute explicitly the voltages and currents on individual conductors. They are specified by vectors  $|V(z)\rangle$  and  $|I(z)\rangle$ . The transformation from scattering variables to the currents and voltages is obtained from (19), (20), (25), and (26) as follows

$$|V(z)\rangle = \underline{M}_V(|a(z)\rangle + |b(z)\rangle), \quad (35)$$

$$|I(z)\rangle = \underline{M}_I(|a(z)\rangle - |b(z)\rangle). \quad (36)$$

The inverse transformation is obtained from (21), (22), (25), and (26):

$$|a(z)\rangle = \frac{1}{2} (\underline{M}_I^+ |V(z)\rangle + \underline{M}_V^+ |I(z)\rangle), \quad (37)$$

$$|b(z)\rangle = \frac{1}{2} (\underline{M}_I^+ |V(z)\rangle - \underline{M}_V^+ |I(z)\rangle). \quad (38)$$

Note that the components of scattering vectors  $|a(z)\rangle$  and  $|b(z)\rangle$  correspond to the individual normal modes, while the components of the voltage and current vectors  $|V(z)\rangle$  and  $|I(z)\rangle$  correspond to the individual conductors. As an example,  $a_i$  is the complex amplitude of the  $i$ th mode. On the other hand,  $V_i$  is the voltage of the  $i$ th conductor with respect to ground.

Fig. 8.(a) shows a section of MTL of the length  $\ell$ . The voltages  $V_i(z)$  are specified between each conductor and the ground, where the conductor side is considered as positive. The currents  $I_i(z)$  on the individual conductors are specified positive when flowing in (+z) direction. This apparently trivial fact is pointed out because by using this convention, the current at  $z=\ell$  points out of the MTL section, which is not customary in the network theory. However, the present convention is found to be more natural for the matrix manipulations which follow. The consequence of this convention is that the total power

$$P = \frac{1}{2} \operatorname{Re} \langle V | I \rangle$$

is not always pointed into the network, as customary in network theory, but here  $P$  represents the power flow in the positive  $z$  direction. Thus, at  $z=0$ ,  $P$  is into the MTL, at  $z=\ell$ ,  $P$  is out of the MTL.

The use of  $|a\rangle$  and  $|b\rangle$  variables in place of  $|V\rangle$  and  $|I\rangle$  variables is indicated in Fig. 8. (b). At each end of the MTL there is a transforming network  $N_T$ , which transforms the variables according to (35)-(38). At  $z=0$ , the left-hand terminals of  $N_T$  are the actual MTL conductors. Here, the variables are  $|V(0)\rangle$  and  $|I(0)\rangle$ . The other side of the  $N_T$  network has the mode variables  $|a(0)\rangle$  and  $|b(0)\rangle$ . Each mode is represented by a fictitious single transmission line, shielded from all the other lines. Each single transmission line passes the wave through by simply adding the phase shift  $(-\beta_i \ell)$  as follows

$$a_i(\ell) = a_i(0)e^{-j\beta_i \ell}$$

At the other end of the MTL, at  $z=\ell$ , variables  $|a(\ell)\rangle$  and  $|b(\ell)\rangle$  are transformed back to variables  $|a(0)\rangle$  and  $|b(0)\rangle$  in another identical transforming network  $N_T$ .

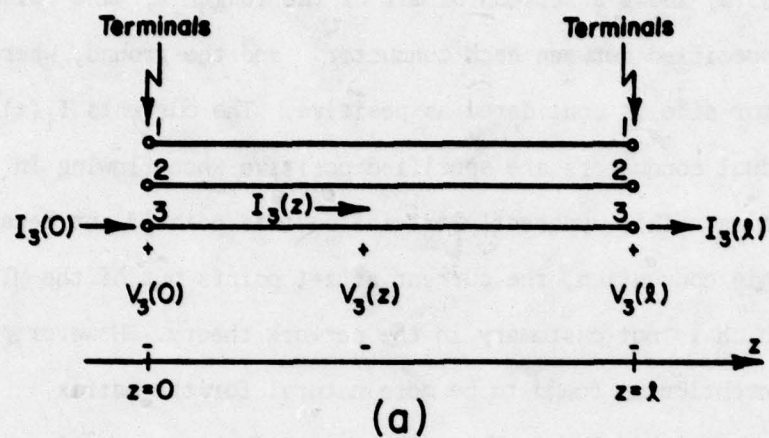
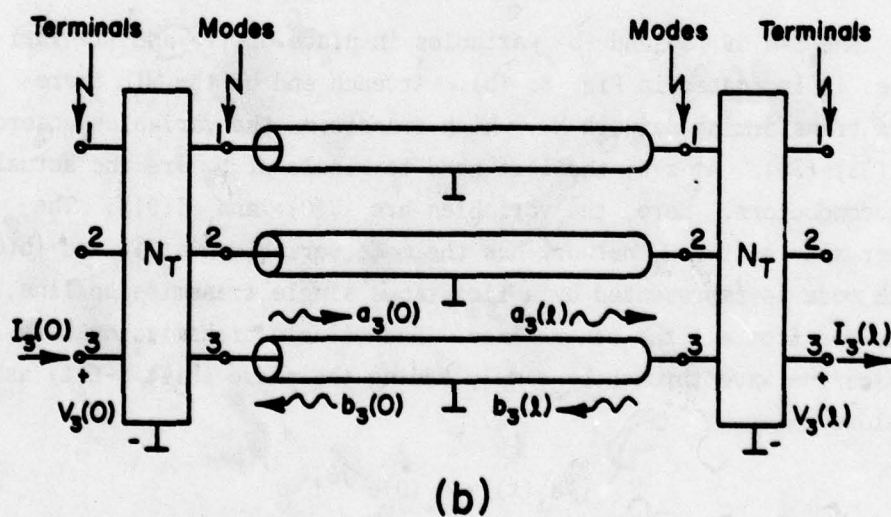
Fig. 8(a). MTL section of length  $l$ .

Fig. 8(b). Equivalent circuit for normal modes.

## SECTION III

## EQUIVALENT SOURCES FOR APERTURE EXCITATION

Each normal mode is described by its scattering amplitude  $a_i$  (waves traveling in  $+z$  direction) or  $b_i$  (waves traveling in  $-z$  direction). The detailed distribution of the electric and magnetic field, for the  $i$ th mode traveling in  $+z$  direction, is

$$\vec{E}_i(x, y, z) = a_i e^{-j\beta_i z} \vec{e}_i(x, y) \quad (39)$$

$$\vec{H}_i(x, y, z) = a_i e^{-j\beta_i z} \vec{h}_i(x, y) \quad (40)$$

$\vec{e}_i$  and  $\vec{h}_i$  are the normalized modal field distributions over the cross section of the MTL. The total power transmitted by the  $i$ th mode traveling in  $+z$  direction is obtained by integrating the Poynting vector over the cross section:

$$P_i^+ = \frac{1}{2} \operatorname{Re} \iint_{\text{cross section}} [\vec{E}_i(x, y) \times \vec{H}_i^*(x, y)] \cdot d\vec{s}$$

For normalized modal field distributions

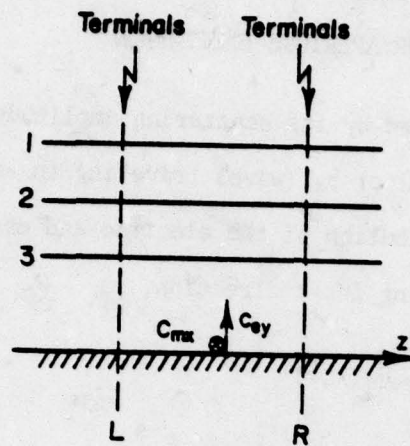
$$\iint_{\text{cross section}} [\vec{e}_i(x, y) \times \vec{h}_j^*(x, y)] \cdot d\vec{s} = \delta_{ij} \quad (41)$$

and the power transmitted by the  $i$ th mode is

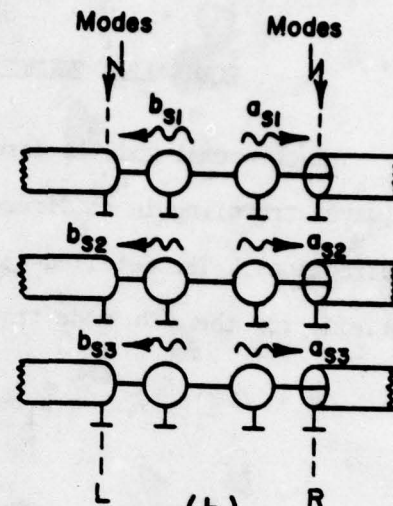
$$P_i^+ = \frac{1}{2} |a_i|^2$$

in accordance with circuit theory.

Fig. 9. (a) shows the junction representing an aperture on a MTL. The aperture is excited by an external field from below the ground plane.



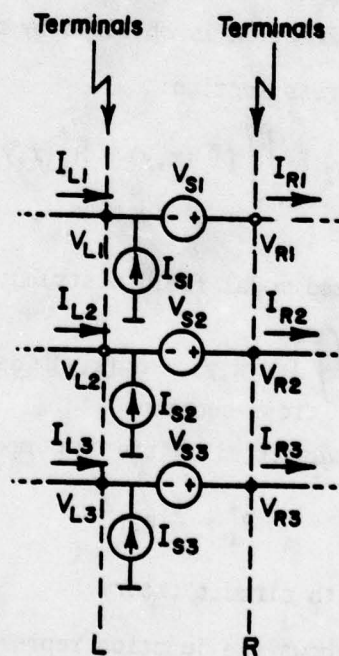
(a)



(b)

Fig. 9(a). A junction with an aperture.

Fig. 9(b). Normal-mode sources.



(c)

Fig. 9(c). Voltage and current sources.

This excitation is replaced by an equivalent pair of dipoles  $c_{mx}$  and  $c_{ey}$ . In what follows, an equivalent circuit will be established for the junction between the two infinitely close planes, denoted by L and R (letters stand for "left" and "right").

According to (13), the dipole pair  $c_{mx}$  and  $c_{ey}$  excites the  $i$ th mode traveling in  $+z$  direction as follows

$$a_{si} = \frac{1}{2} [c_{mx} h_{xi}(x_0, 0) - c_{ey} e_{yi}(x_0, 0)] \quad (42)$$

As indicated previously, a convention in the present report is that the waves traveling in  $+z$  direction are denoted by  $a_i$ , while the waves traveling in  $-z$  direction are denoted by  $b_i$ . Therefore, (42) gives a source of the traveling mode in  $+z$  direction, and is denoted by  $a_{si}$ . A traveling wave source is a three-terminal device, as explained in Appendix B.

Another word about the notation in (42):  $h_{xi}(x_0, 0)$  is the  $x$ -component of the magnetic-field modal distribution of the  $i$ th mode evaluated at the point  $x=x_0$  and  $y=0$ . Similarly  $e_{yi}(x_0, 0)$  is the  $y$ -component of the normalized electric modal field.

For the traveling-wave source of the  $i$ th mode propagating in  $-z$  direction, the following is obtained from (9):

$$b_{si} = \frac{1}{2} [-c_{mx} h_{xi}(x_0, 0) - c_{ey} e_{yi}(x_0, 0)] \quad (43)$$

Fig. 9.(b) shows the modal sources between the left and right reference planes. This equivalent circuit is appropriate for an analysis in terms of scattering coefficients. The equivalent circuit in terms

of voltages and currents can now be obtained by a simple matrix manipulation. First, define the vectors containing the scattering sources as follows:

$$|a_s\rangle = \begin{pmatrix} a_{s1} \\ \vdots \\ a_{sN} \end{pmatrix} \quad |b_s\rangle = \begin{pmatrix} b_{s1} \\ \vdots \\ b_{sN} \end{pmatrix} \quad (44)$$

The traveling wave vector,  $|a_R\rangle$  traveling in  $+z$  direction out of the right-hand reference plane is a sum of the source vector  $|a_s\rangle$  and the wave vector  $|a_L\rangle$  incoming from the left upon the left-hand reference plane:

$$|a_R\rangle = |a_L\rangle + |a_s\rangle \quad (45)$$

Similarly, the waves traveling in the  $-z$  direction are related as

$$|b_L\rangle = |b_R\rangle + |b_s\rangle \quad (46)$$

The voltage and current variables of the source junction are shown in Fig. 9.(c). The voltages and currents at the left-hand plane are defined by  $|V_L\rangle$  and  $|I_L\rangle$ , while the right-hand variables are  $|V_R\rangle$  and  $|I_R\rangle$ . The current sources from Fig. 9.(c). constitute vector  $|I_s\rangle$  while the voltage sources make  $|V_s\rangle$ . The Kirchhoff laws require

$$|V_L\rangle + |V_s\rangle = |V_R\rangle \quad (47)$$

and

$$|I_L\rangle + |I_s\rangle = |I_R\rangle \quad (48)$$

To change from scattering representation to voltage representation, use (35)

$$|V_s\rangle = |V_R\rangle - |V_L\rangle = M_V(|a_R\rangle - |a_L\rangle + |b_R\rangle - |b_L\rangle)$$

By virtue of (45) and (46):

$$|V_s\rangle = \underline{M}_V(|a_s\rangle - |b_s\rangle) \quad (50)$$

The components of  $|a_s\rangle$  and  $|b_s\rangle$  are given by (28) and (29). The difference term is

$$a_{si} - b_{si} = c_{mx} h_{xi}(x_0, 0) \quad (51)$$

and it depends only on the magnetic dipole excitation. Thus, the voltage sources in Fig. 9(c) are to be computed as follows:

$$|V_s\rangle = \underline{M}_V \begin{pmatrix} c_{mx} h_{x1}(x_0, 0) \\ \dots\dots\dots \\ c_{mx} h_{xN}(x_0, 0) \end{pmatrix} \quad (52)$$

The current sources are similarly found as follows

$$|I_s\rangle = \underline{M}_I(|a_s\rangle + |b_s\rangle) \quad (53)$$

The sum term depends entirely on the electric dipole moment

$$a_{si} + b_{si} = c_{ey} e_{yi}(x_0, 0) \quad (54)$$

so that the formula for computation of the current sources becomes

$$|I_s\rangle = \underline{M}_I \begin{pmatrix} c_{ey} e_{y1}(x_0, 0) \\ \dots\dots\dots \\ c_{ey} e_{yN}(x_0, 0) \end{pmatrix} \quad (55)$$

In the above derivation, the energy storage at the junction was not taken into account. The circuits from Fig. 9.(b) and (c) are thus the zeroth-order equivalents, such as the zeroth order equivalent of a single transmission line from reference [13].

#### SECTION IV

##### EXAMPLES OF VOLTAGE WAVEFORMS

The voltages induced on a 2-conductor transmission line filled with inhomogeneous dielectric will now be computed in order to illustrate the use of the theory developed thus far. The system is shown in Fig. 10. A small circular aperture of diameter  $d = 2$  cm is located at  $z = 0$ . The two-conductor transmission line is located between  $z = -\ell_3 = -7$  m and  $z = \ell_4 = 5$  m.

The cross section of the transmission line is shown in Fig. 11: it consists of two strip conductors of width  $w$ , placed between the three layers of dielectrics denoted  $\epsilon_1$ ,  $\epsilon_2$ , and  $\epsilon_3$ . The dielectric thicknesses are denoted by  $h_1$ ,  $h_2$ , and  $h_3$ . This parallel-plate model of the transmission line is selected because of its simplicity, and it will be used to illustrate the procedure of computing voltages induced by an EMP wave. The electrostatic field within the transmission line from Fig. 11 may be produced in two independent ways. In the excitation A, a potential  $V_a$  is applied to conductor a, while conductor b and the shield are held at zero potential. Then, the fields in the three regions are

$$\vec{E}_{1A} = \vec{a}_y \frac{V_a}{h_1} ; \quad \vec{E}_{2A} = \vec{0} ; \quad \vec{E}_{3A} = -\vec{a}_y \frac{V_a}{h_2} .$$

In the excitation B, a potential  $V_b$  is applied to conductor b, while conductor a and the shield are held at zero potential. The corresponding fields are

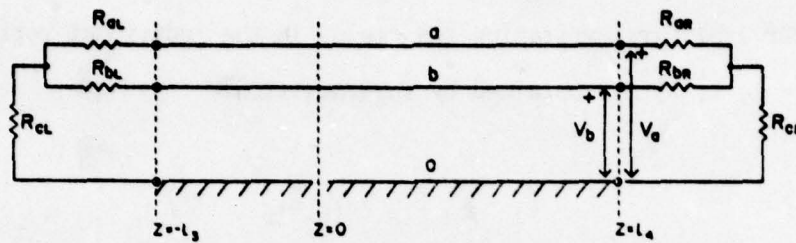


Fig. 10. Terminated 2-conductor transmission line with an aperture.

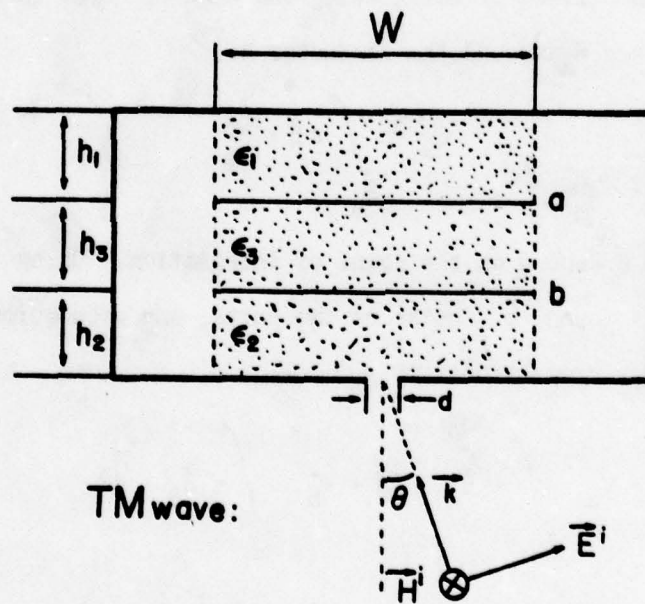


Fig. 11. Parallel-plate 2-conductor transmission line.

$$\vec{E}_{1B} = \vec{0} ; \vec{E}_{2B} = -\vec{a}_y \frac{V_b}{h_2} ; \vec{E}_{3B} = \vec{a}_y \frac{V_b}{h_3} .$$

Under arbitrary excitation the fields in the individual regions ( $i = 1, 2, 3$ ) are obtained by superposition:

$$\vec{E}_i = V_a \vec{E}_{ia} + V_b \vec{E}_{ib} \quad (56)$$

In order to compute the coefficients of electric induction matrix, one must find the charge per unit length of the conductor a. This is accomplished by integrating the electric flux through the closed surface  $S_a$  around the conductor a:

$$Q_a = \int_{S_a} \epsilon \vec{E} \cdot d\vec{S}$$

where  $\epsilon$  and  $\vec{E}$  depend on the point of integration. Using (56), the charge  $Q_a$  is found to consist of two parts, one proportional to  $V_a$  and the other proportional to  $V_b$ .

$$Q_a = V_a \int_{S_a} \epsilon \vec{E}_A \cdot d\vec{S} + V_b \int_{S_a} \epsilon \vec{E}_B \cdot d\vec{S}$$

$$Q_a = V_a K_{aa} + V_b K_{ab} \quad (57)$$

The constants of proportionality are called induction coefficients, denoted  $K_{aa}$  and  $K_{ab}$ . They depend only on the geometry of the system. For example,  $K_{aa}$  is computed as follows:

$$K_{aa} = \epsilon_1 \int_{x=-w/2}^{w/2} \vec{E}_{1A} \cdot \vec{a}_y dx - \epsilon_3 \int_{x=-w/2}^{w/2} \vec{E}_{3A} \cdot \vec{a}_y dx$$

$$K_{aa} = w \left( \frac{\epsilon_1}{h_1} + \frac{\epsilon_3}{h_3} \right) \quad (58)$$

Similarly, the other induction coefficients are found as follows:

$$K_{ab} = K_{ba} = -w \frac{\epsilon_3}{h_3} \quad (59)$$

$$K_{bb} = w \left( \frac{\epsilon_3}{h_3} + \frac{\epsilon_2}{h_2} \right) \quad (60)$$

These coefficients form induction coefficient matrix  $\underline{K}$

$$\underline{K} = \begin{pmatrix} K_{aa} & K_{ab} \\ K_{ab} & K_{bb} \end{pmatrix} \quad (61)$$

As an example of a symmetric system, the following dimensions have been selected:

$$h_1 = 2 \text{ cm}, h_2 = 2 \text{ cm}, h_3 = 1 \text{ cm}, w = 10 \text{ cm}, \epsilon_{1r} = 1.0,$$

$$\epsilon_{2r} = 1.0, \epsilon_{3r} = 2.0, d = 2 \text{ cm}.$$

The corresponding matrix  $\underline{K}$  is

$$\underline{K} = \epsilon_0 \begin{pmatrix} 25 & -20 \\ -20 & 25 \end{pmatrix}$$

The induction coefficient matrix with only air as dielectric will be denoted  $\underline{K}'$ :

$$\underline{K}' = \epsilon_0 \begin{pmatrix} 15 & -10 \\ -10 & 15 \end{pmatrix}$$

By using matrices  $\underline{K}$  and  $\underline{K}'$  one can find the modal velocities, voltage and current eigenvectors, and the impedance matrix by the procedure described in Appendix C. The inverse of the induction matrix  $\underline{L}$  is directly proportional to  $\underline{K}'$  as follows

$$\underline{L}^{-1} = c^2 \underline{K}' \quad (62)$$

where  $c$  is the velocity of the light in vacuum. Next, the eigenvectors and eigenvalues of  $\underline{L}^{-1}$  are found, and an auxiliary matrix  $\underline{B}$  is formed according to (C-15). When the eigenvalues of  $\underline{B}$  are computed, the modal velocities  $v_i$  are found as their inverse square roots, according to (C-16). The eigenvectors of  $\underline{B}$  are then used to form the modal matrices  $\underline{M}_V$  and  $\underline{M}_I$ , according to (C-42) and (C-43):

$$\underline{M}_V = \begin{pmatrix} \phi_{a1} & \phi_{a2} \\ \phi_{b1} & \phi_{b2} \end{pmatrix} = \begin{pmatrix} -6.136 & -2.369 \\ -6.136 & 2.369 \end{pmatrix} \quad (63)$$

$$\underline{M}_I = \begin{pmatrix} \psi_{a1} & \psi_{a2} \\ \psi_{b1} & \psi_{b2} \end{pmatrix} = \begin{pmatrix} -0.081489 & -0.21106 \\ -0.081489 & 0.21106 \end{pmatrix} \quad (64)$$

Subscripts a and b denote the conductors, and subscripts 1 and 2 denote the modes.

Next, modal functions  $e_y$  and  $h_x$  will be evaluated. The aperture is placed at the center of the bottom shield conductor, as shown in Fig. 11. By definition, the electric field of the  $n$ th mode traveling in positive  $z$  direction is

$$\vec{E}_n(x, y, z) = a_n \vec{e}_n(x, y) e^{-j\beta_n z} \quad (65)$$

By selecting  $a_n = 1$ , the electric field at  $z = 0$  becomes

$$\vec{E}_n(x, y, 0) = \vec{e}_n(x, y) \quad (66)$$

When  $a_n = 1$  and  $b_n = 0$ , the voltage vector is obtained from (35) as follows

$$|V_n\rangle = |\phi_n\rangle = \begin{pmatrix} \phi_{an} \\ \phi_{bn} \end{pmatrix} \quad (67)$$

Thus, in order to find the modal function  $\vec{e}_n$  of the mode  $n$  (here,  $n = 1$  or  $2$ ), the potentials on the two conductors must be selected equal to  $\phi_{an}$  and  $\phi_{bn}$  as shown in Fig. 12. Then the modal function is equal to the electric field, according to (66). Since the field has only the  $y$  component, the result is

$$e_{yn} = \phi_{an} E_{y2A} + \phi_{bn} E_{y2B} = -\frac{\phi_{bn}}{h_3} \quad (68)$$

The modal function  $\vec{h}_n(x, y)$  is equal to the magnetic field  $\vec{H}_n(x, y, 0)$  inside the transmission line, when conductor a carries a current  $I_a = \psi_{an}$

and conductor b carries current  $I_b = \psi_{bn}$ . The situation is shown in Fig. 13. The currents are assumed to be uniformly distributed over the conductor surfaces. An elementary computation gives the following value for the magnetic field modal function:

$$h_{xn} = \frac{\psi_{an} h_1 + \psi_{bn} (h_1 + h_3)}{w(h_1 + h_2 + h_3)} \quad (69)$$

In the example treated here, a time domain response will be evaluated, while most of the theory presented until now has been formulated in the frequency domain. In order to use formulas (8) and (9) for a general time variation, they are rewritten as follows:

$$c_{mx} = -\mu \alpha_m \frac{\partial}{\partial t} \left( H_{xs}^{ext} - H_{xs}^{int} \right) \quad (70)$$

$$c_{ey} = \epsilon \alpha_e \frac{\partial}{\partial t} \left( E_{ys}^{ext} - E_{ys}^{int} \right) \quad (71)$$

The polarizabilities  $\alpha_m$  and  $\alpha_e$  are given by (10).

The incident wave orientation is specified by angles  $\alpha$  and  $\theta$  as shown in Fig. 3. Then for a TM polarization, the field components of importance are

$$E_{ys}^{ext} = 2E_0 F(t) \sin \theta, \quad H_{xs}^{ext} = -\frac{2E_0}{\eta} F(t) \sin \alpha \quad (72)$$

An arbitrary time variation of the incident plane wave is described by function  $F(t)$ . For EMP wave, a simple function is selected as follows

$$F(t) = e^{-\alpha_1 t} - e^{-\beta_1 t} \quad (73)$$

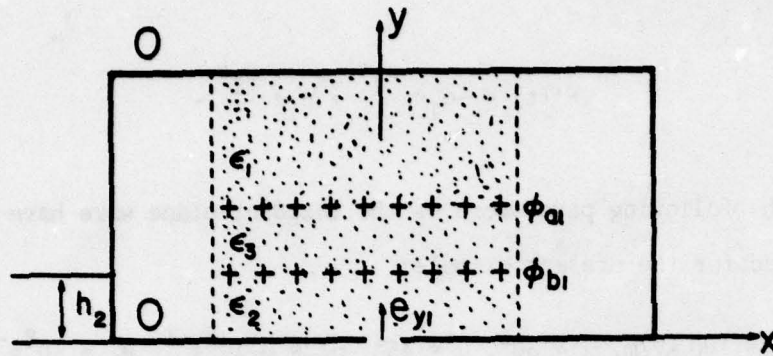


Fig. 12. Evaluation of the electric field on the line from Fig. 11.

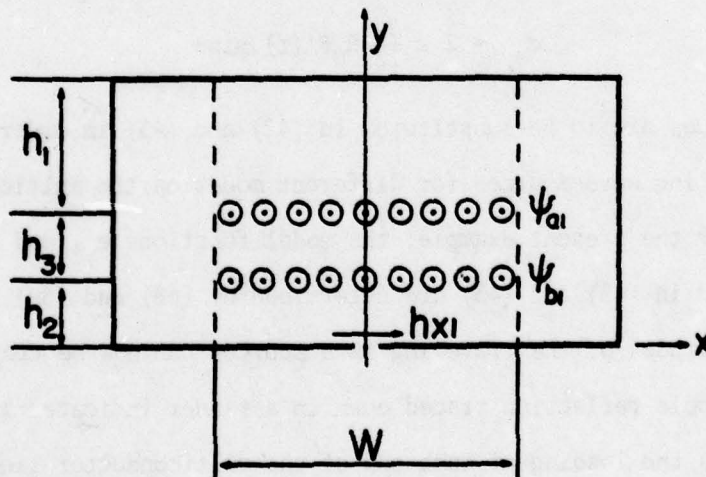


Fig. 13. Evaluation of the magnetic field on the line from Fig. 11.

having the following derivative

$$F'(t) = -\alpha_1 e^{-\alpha_1 t} + \beta_1 e^{-\beta_1 t} \quad (74)$$

The following parameters of the incident plane wave have been selected for the present example:

$$E_0 = 100 \text{ kV/m}, \alpha = 30^\circ, \theta = 45^\circ, \alpha_1 = 3.10^6 \text{ s}^{-1}, \beta_1 = 10^8 \text{ s}^{-1}.$$

The electric and magnetic current moments are now computed by (70) and (71):

$$c_{mx} = 2 \frac{\mu}{\eta} \frac{d^3}{6} E_0 F'(t) \sin \alpha \quad (75)$$

$$c_{ey} = 2 \epsilon \frac{d^3}{12} E_0 F'(t) \sin \theta \quad (76)$$

These values are to be substituted in (42) and (43) in order to compute the traveling wave sources for different modes on the multiconductor line. For the present example, the modal functions  $e_{yi}$  and  $h_{xi}$  which are needed in (42) and (43) are determined by (68) and (69). The initial amplitudes of the traveling wave sources can now be computed and the multipole reflection traced down in a manner indicated in Fig. 7. As long as the loading at each end of the multiconductor line consists of pure resistances, such as in Fig. 10, the wave shape remains unchanged after each reflection, and is specified by the function  $F'(t)$  from (74).

In the first example to be computed, the following loading resistances have been selected:

$$R_{aL} = R_{aR} = 1k\Omega, R_{bL} = R_{bR} = 100\Omega, R_{cL} = R_{cR} = 1\Omega$$

The load impedance matrix of a T network is then obtained as

$$Z_{L11} = R_{aL} + R_{cL} = 1.001k\Omega$$

$$Z_{L12} = R_{cL} = 1\Omega$$

$$Z_{L22} = R_{bL} + R_{cL} = 1.001k\Omega$$

The corresponding scattering matrix is obtained from (33)

$$\underline{S}_3 = \begin{pmatrix} 0.43488 & 0.17495 \\ 0.17495 & 0.90584 \end{pmatrix}$$

Since the load resistances on the right-hand side are the same as on the left-hand side,  $\underline{S}_4 = \underline{S}_3$ . For each incident wave  $a_i$  at the port 4, the reflected waves are computed by

$$b_j = S_{ji} a_i \quad \text{for } j = 1, 2$$

Then, the voltages are obtained from (35)

$$|V\rangle = \underline{M}_V (|a\rangle + |b\rangle)$$

The velocities of the two waves are  $v_1 = 3 \cdot 10^8$  m/s and  $v_2 = 2.236 \cdot 10^8$  m/s. Fig. 14 shows the voltages on the right-hand end of the transmission line.  $V_1$  is the voltage on the conductor a, while  $V_2$  is the voltage on the conductor b. First pulse arrives at  $t_1 = \ell_4/v_1 = 16.6$  ns. Note that this is even mode, since the polarity of the pulse is the same on both conductors. Shortly afterwards, at  $t_2 = \ell_4/v_2 = 22.4$  ns, the odd mode arrives producing a positive pulse of  $V_1$  and a negative pulse of  $V_2$ . The next arrival is the group of four waves which are reflected from the left-hand end of the line, and the process is continued through multiple reflections bouncing back and forth on the line.

At each of the bounces, some of the energy is lost in resistances terminating the line, so the process gradually dies off as seen in Figure 14. If one end of the line is terminated in a resistance matrix equal to the characteristic impedance matrix  $\underline{Z}_0$ , there are no reflections from that end. In the next example, we terminate the right-hand end of the MTL by a matched impedance. The necessary resistances are obtained from  $\underline{Z}_0$  as follows. First  $\underline{Z}_0$  is computed by (C50)

$$\underline{Z}_0 = \begin{pmatrix} 43.260 & 32.036 \\ 32.036 & 43.260 \end{pmatrix}$$

Then, the resistances of the T-network are obtained as

$$R_{aR} = Z_{011} - Z_{012} = 11.224\Omega$$

$$R_{bR} = Z_{022} - Z_{012} = 11.224\Omega$$

$$R_{cR} = Z_{012} = 32.036\Omega$$

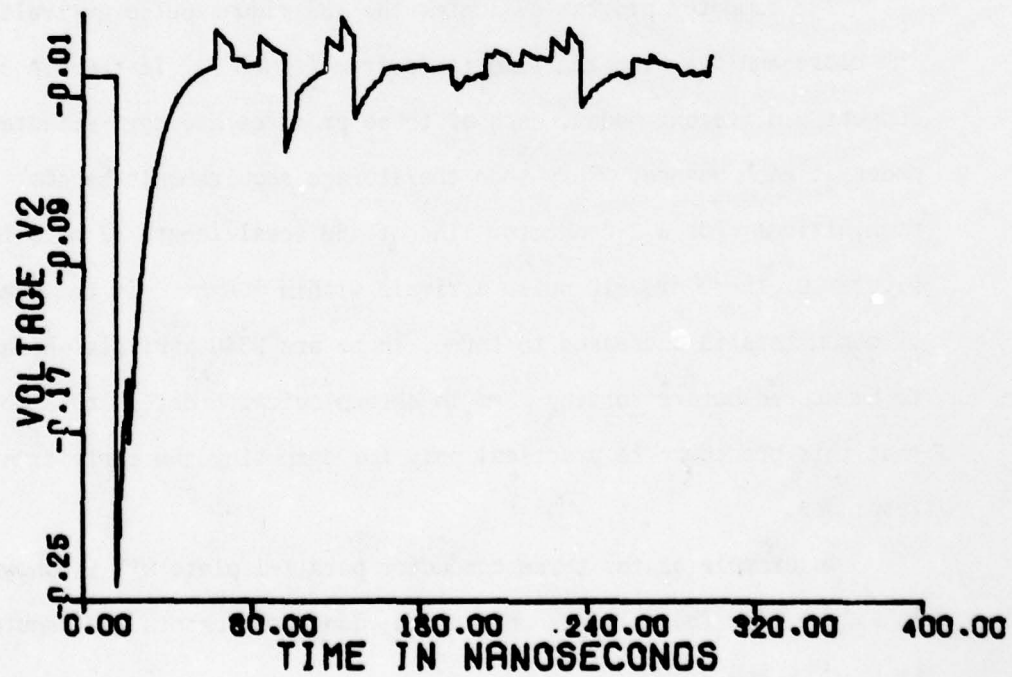
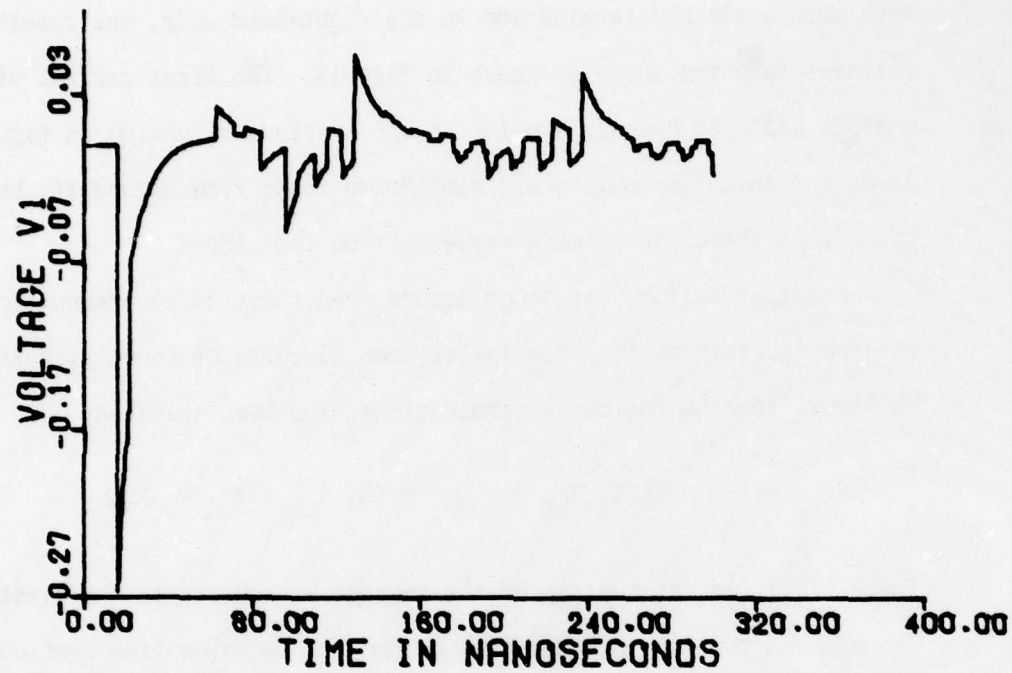


Fig. 14. Voltage waveforms on a 2-conductor line: moderate mismatch.

With such a matched termination on the right-hand side, the resulting voltages take the shape as shown in Fig. 15. The first arrival of the odd and even mode is similar to the previous situation in Figure 14. Also, the next four pulses are similar to those from Figure 14, but after that there are no more waves left on the line.

Another extreme situation occurs when there is no attenuation, because the terminations consist of open-circuits or short circuits. In Figure 16, the following terminations have been selected

$$R_{aL} = R_{aR} = 1k\Omega, \quad R_{bL} = R_{bR} = 0.1\Omega, \quad R_{cL} = R_{cR} = 0.01\Omega$$

There is little attenuation of the voltage waveshapes in the first 300 ns, and the multiple bouncing on the transmission line continues for a long time.

The computer program evaluates the individual pulse arrivals in the close analogy with the time-table from Figure 7. If the MTL can support  $N$  different modes, each of those produces  $N$  other reflected modes at each bounce. Very soon the storage requirements become prohibitive. For a 2-conductor line of the total length 12 m as in Figure 10, there are 510 pulse arrivals within 300 ns. If the number of conductors is increased to three, there are 9840 arrivals which are to be stored before sorting them in chronological order. It is obvious that this procedure is practical only for computing the early time responses.

An example of the three conductor parallel-plate MTL is shown in Figure 17. The voltages on the individual conductors are denoted by  $V_1$ ,  $V_2$ , and  $V_3$ .

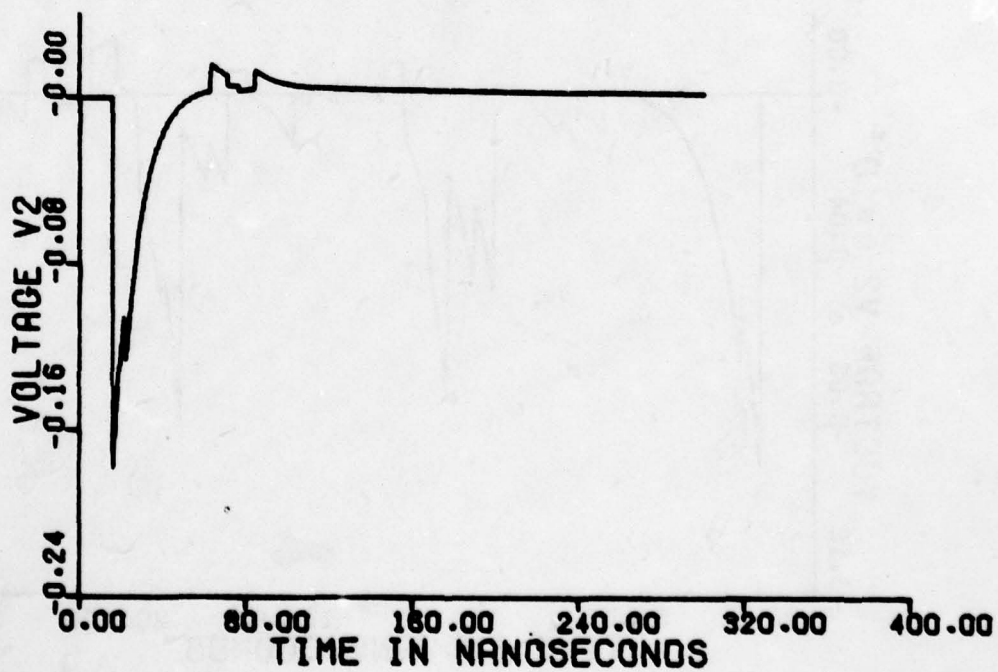
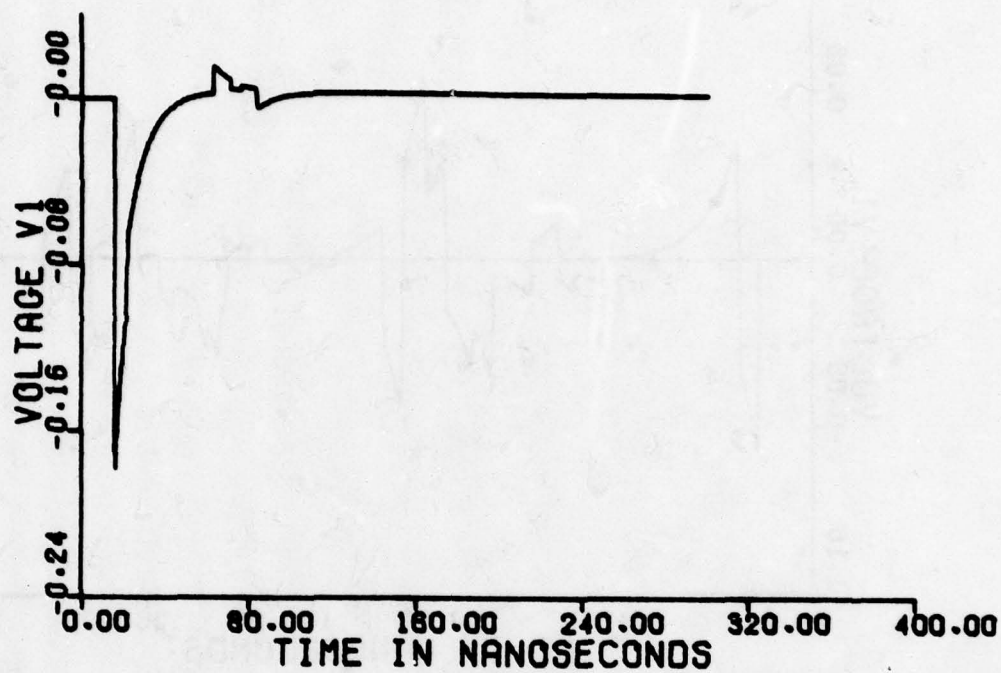


Fig. 15. Voltage waveforms on a 2-conductor line: matched load at left-hand terminals.

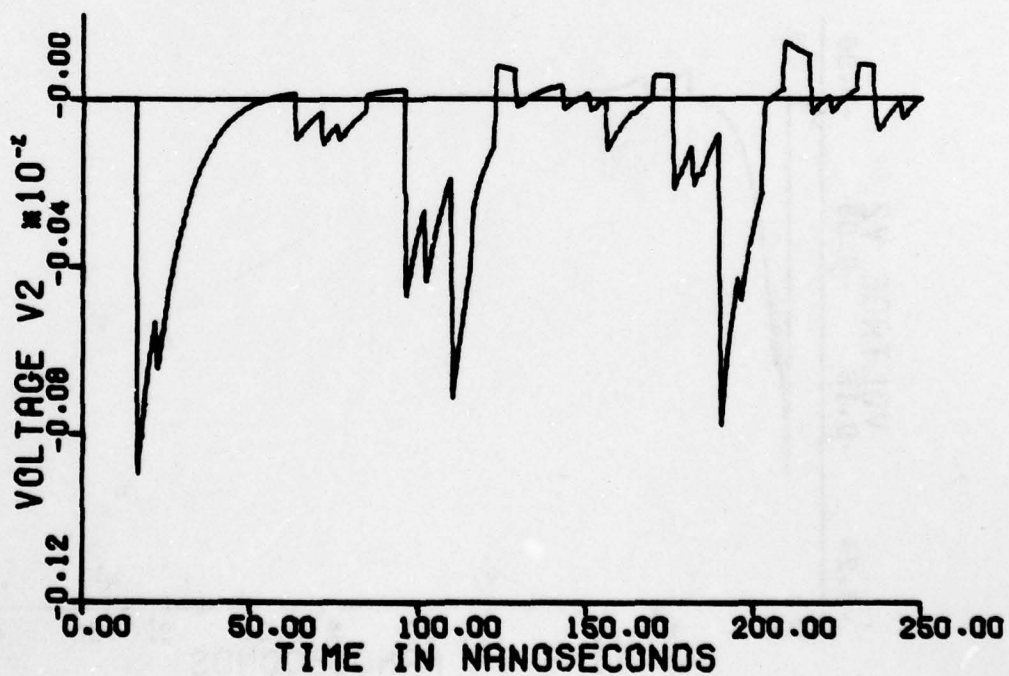
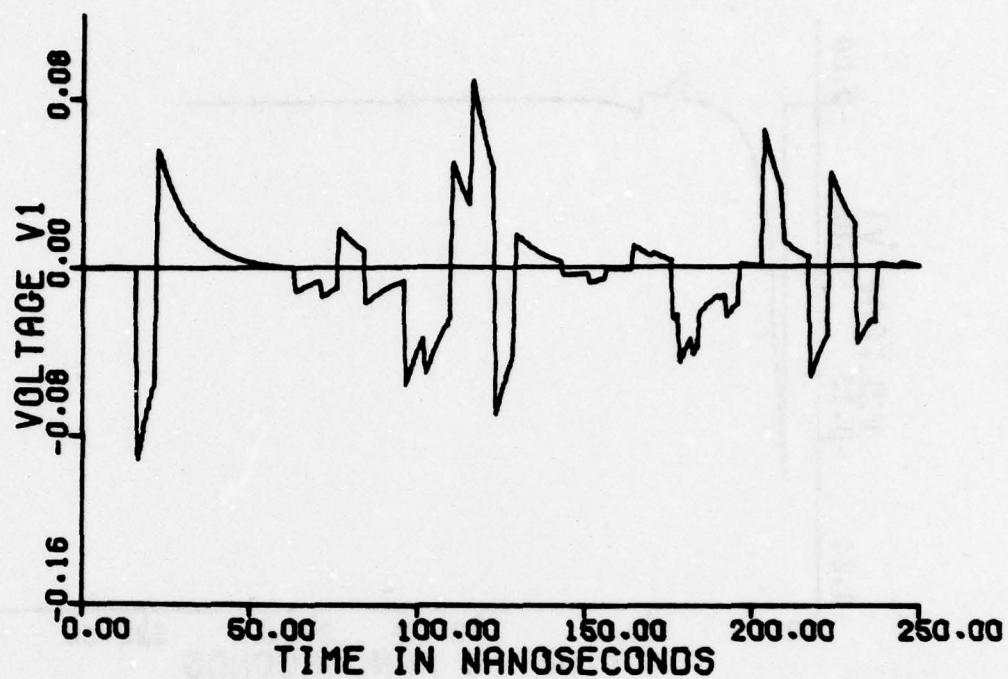


Fig. 16. Voltage waveforms on a 2-conductor line: large mismatch at both ends.

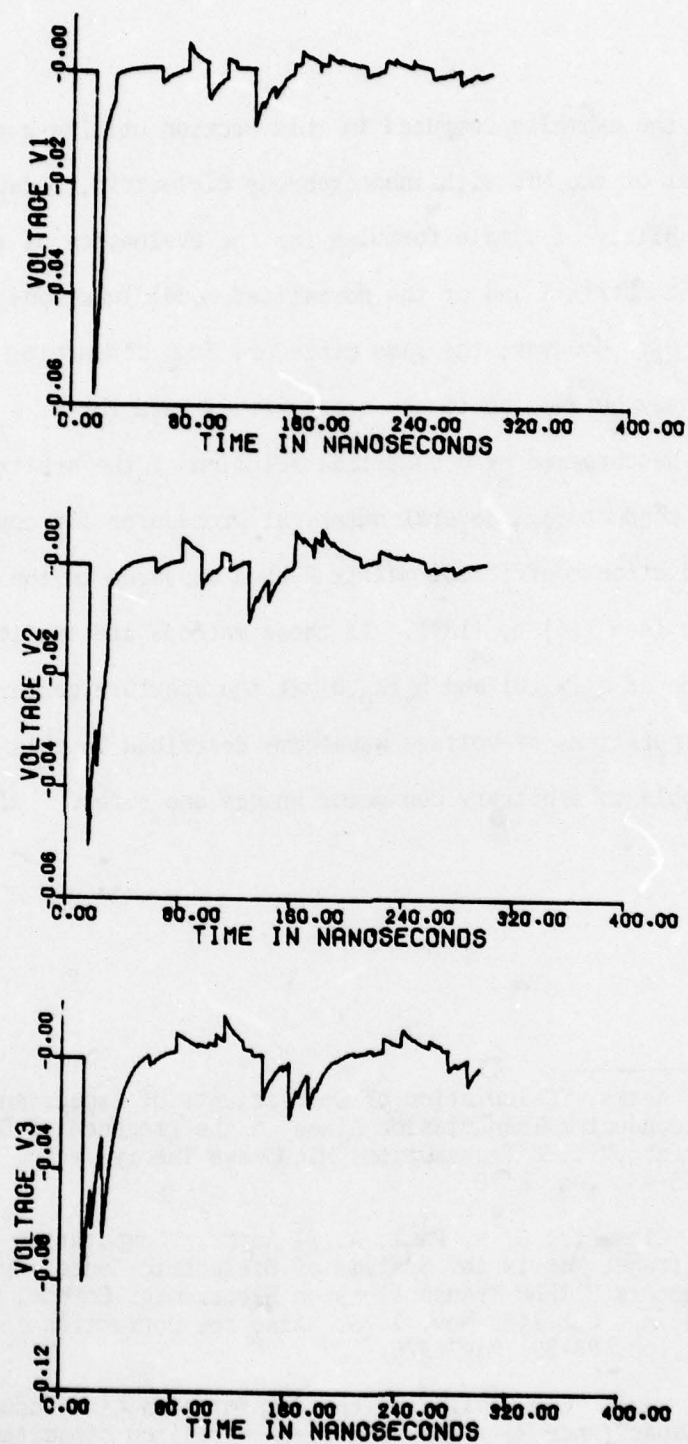


Fig. 17. Voltage waveforms on a 3-conductor line: moderate mismatch.

All the examples computed in this Section utilize a parallel-plate model of the MTL with inhomogeneous dielectric, because of the availability of simple formulas for the evaluation of induction coefficient matrix  $\underline{K}$  and of the normalized modal functions  $e_y(x_0, 0)$  and  $h_x(x_0, 0)$ . However, the same procedure for computing the voltage waveforms may be applied to any other set of data for  $\underline{K}$ ,  $e_y$  and  $h_x$  which may be obtained by a numerical solution of the arbitrary shapes of conductors. Several numerical procedures for computation of the induction coefficient matrix  $\underline{K}$  have appeared in the recent literature (see [16] to [18]). If these methods are supplemented by computation of  $e_y(x_0, 0)$  and  $h_x(x_0, 0)$  at the aperture center, the rest of the computations of voltage waveforms described in this Section is applicable to arbitrary conductor shapes and sizes.

- 
16. W. T. Weeks, "Calculation of Coefficients of Capacitance of Multiconductor Transmission Lines in the Presence of Dielectric Interface," IEEE Transactions Microwave Theory Techn. Vol. MTT-18, pp. 35-43, Jan. 1970.
  17. J. C. Clements, C. R. Paul, A. T. Adams, "Computation of the Capacitance Matrix for Systems of Dielectric-Coated Cylindrical Conductors," IEEE Transactions on Electromag. Compat. Vol. EMC-17, No. 4, pp. 238-248, Nov. 1975. Also see Correction in EMC-18 No. 2, pp. 88-89, May 1976.
  18. C. R. Paul, "Computation of the Transmission Line Inductance and Capacitance Matrices from the Generalized Capacitance Matrix," IEEE Transactions Electromag. Compat., Vol. EMC-18, No. 4, pp. 175-183, Nov. 1976.

## SECTION V

## FIRST-ORDER EQUIVALENT CIRCUIT OF THE SMALL APERTURE

In Fig. 13, a set of incident waves coming from the left is described by  $|a_L\rangle$ . The aperture region is located between two planes denoted L and R. There is no incident wave coming from the right,  $|b_R\rangle = 0$ . The waves  $|a_L\rangle$  excite the pair of dipoles  $c_{ey}$  and  $c_{mx}$ . The excitation field produced by the  $j$ th incident mode is

$$H_{xsj}^{int} = a_{Lj} h_{xj}(x_0, 0) \quad (77)$$

$$E_{ysj}^{int} = a_{Lj} e_{yj}(x_0, 0) \quad (78)$$

This is an internal field, according to Fig. 2. From (8) and (9), the dipole moments produced by the  $j$ th mode are

$$c_{mxj} = j\omega\mu\alpha_m h_{xj}(x_0, 0) a_{Lj} \quad (79)$$

$$c_{eyj} = -j\omega\epsilon\alpha_e e_{yj}(x_0, 0) a_{Lj} \quad (80)$$

Summed over all the incident modes:

$$c_{mx} = j\omega\mu\alpha_m \sum_{j=1}^N h_{xj} a_{Lj} \quad (81)$$

$$c_{ey} = -j\omega\epsilon\alpha_e \sum_{j=1}^N e_{yj} a_{Lj} \quad (82)$$

where argument  $(x_0, 0)$  has been omitted for brevity.

These dipoles produce the outgoing waves. Their  $i$ th component is, according to (13) and (14):

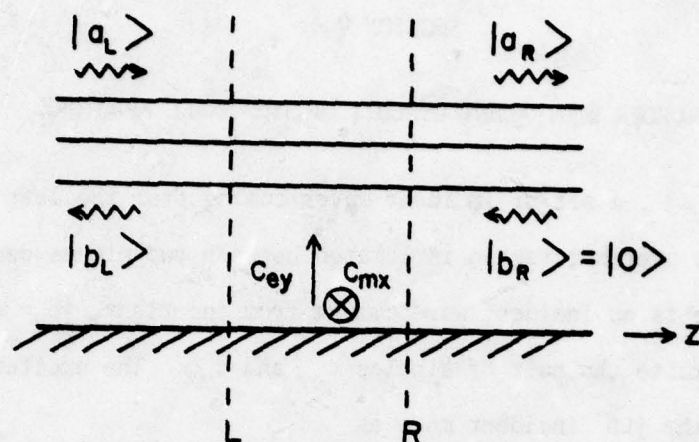


Fig. 18. Aperture junction with sources.

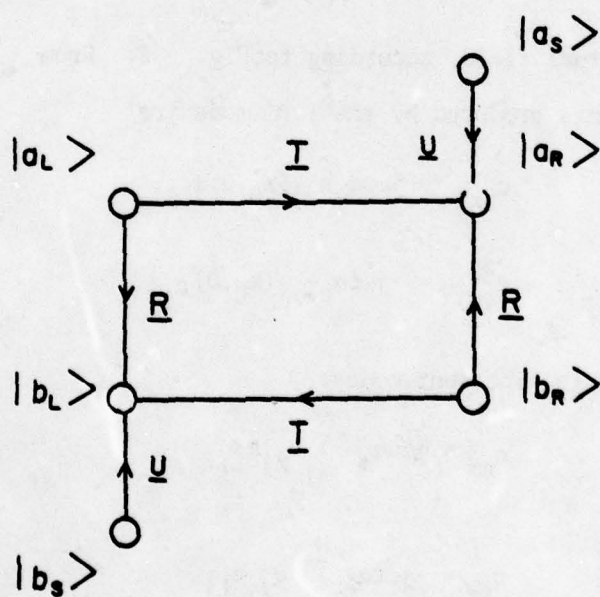


Fig. 19. Signal flow graph of the aperture junction with sources.

$$a_{Ri} = \frac{1}{2}[-c_{mx}h_{xi}(x_0,0) - c_{ey}e_{yi}(x_0,0)] + a_{Li} \quad (83)$$

$$b_{Li} = \frac{1}{2}[c_{mx}h_{xi}(x_0,0) - c_{ey}e_{yi}(x_0,0)] \quad (84)$$

In what follows, argument  $(x_0,0)$  will be omitted for brevity. In (83) the  $i$ th mode outgoing wave at the right-hand plane in Fig. 18 consists of the (unattenuated) incident wave  $a_{Li}$  and the wave originated by the dipole. Using (81) and (82)

$$a_{Ri} = a_{Li} + \frac{1}{2}[-j\omega\mu\alpha_m h_{xi} \sum_{j=1}^N h_{xj} a_{Lj} + j\omega\epsilon\mu\alpha_e \sum_{j=1}^N e_{yj} a_{Lj}] \quad (85)$$

$$b_{Li} = \frac{1}{2}[j\omega\mu\alpha_m h_{xi} \sum_{j=1}^N h_{xj} a_{Lj} + j\omega\epsilon\mu\alpha_e \sum_{j=1}^N e_{yj} a_{Lj}] \quad (86)$$

This can be written as

$$|a_R\rangle = (\underline{U} - j \underline{H} + j \underline{E}) |a_L\rangle \quad (87)$$

$$|b_L\rangle = (j \underline{H} + j \underline{E}) |a_L\rangle \quad (88)$$

where the real, symmetric matrices  $\underline{H}$  and  $\underline{E}$  are defined by

$$[\underline{H}]_{ij} = \frac{1}{2}\omega\mu\alpha_m h_{xi} h_{xj} \quad (89)$$

$$[\underline{E}]_{ij} = \frac{1}{2}\omega\epsilon\alpha_e e_{yi} e_{yj} \quad (90)$$

Thus, the scattering matrix of the aperture junction in partitioned form is

$$\begin{pmatrix} |b_L\rangle \\ |a_R\rangle \end{pmatrix} = \begin{pmatrix} \underline{I} & \underline{T} \\ \underline{T} & \underline{I} \end{pmatrix} \begin{pmatrix} |a_L\rangle \\ |b_R\rangle \end{pmatrix} \quad (91)$$

where

$$\underline{\Gamma} = j \underline{H} + j \underline{E} \quad (92)$$

$$\underline{T} = \underline{U} - j \underline{H} + j \underline{E} \quad (93)$$

The signal flow graph, [16], is in Fig. 19. Also shown are sources  $|a_S\rangle$  and  $|b_S\rangle$  from the zeroth-order equivalent circuit. Figure 19 is a complete first-order equivalent circuit for scattering representation. The corresponding immittance representation will be derived next.

Fig. 20 shows a small parallel perturbation on a MTL. The perturbation is described by

$$|V_L\rangle = |V_R\rangle \quad (94)$$

and

$$|I_2\rangle = \underline{Y} |V_L\rangle \quad (95)$$

Kirchhoff current law requires

$$|I_L\rangle = |I_2\rangle + |I_R\rangle \quad (96)$$

Change variables  $|V\rangle$  and  $|I\rangle$  into  $|a\rangle$  and  $|b\rangle$  according to (35) and (36). Then, (94) and (96) become:

$$\underline{M}_V(|a_L\rangle + |b_L\rangle) = \underline{M}_V(|a_R\rangle + |b_R\rangle) \quad (94a)$$

$$\underline{M}_I(|a_L\rangle - |b_L\rangle) = \underline{Y} \underline{M}_V(|a_L\rangle + |b_L\rangle) + \underline{M}_I(|a_R\rangle - |b_R\rangle) \quad (95a)$$

Multiply the first equation from the left by  $\underline{M}_V^{-1}$  and the second equation by  $\underline{M}_I^{-1}$ . Use (C-46) and (C-47) to obtain

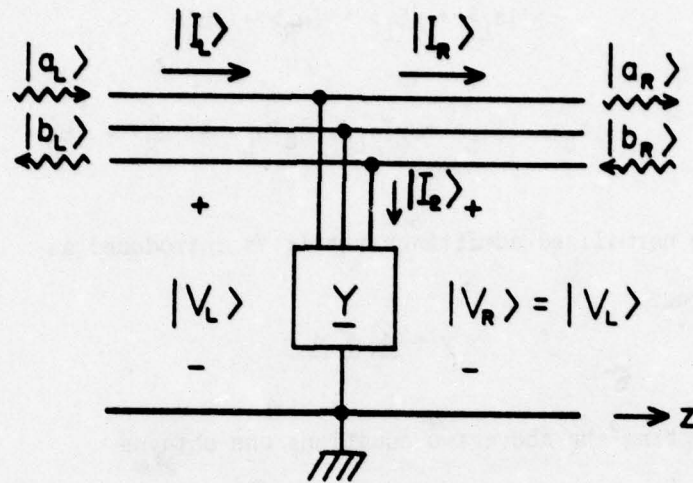


Fig. 20. Small parallel admittance perturbation on MTL.

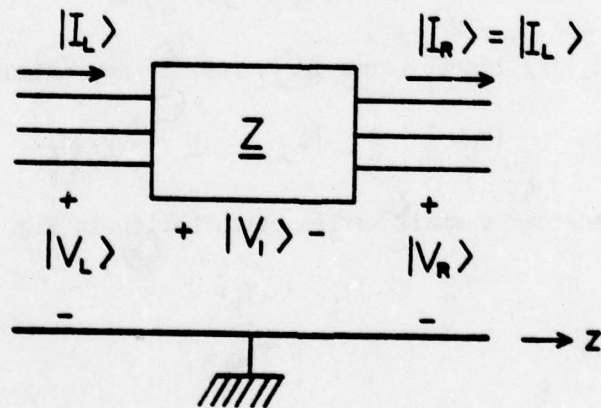


Fig. 21. Small series impedance perturbation on MTL.

$$|a_L\rangle + |b_L\rangle = |a_R\rangle + |b_R\rangle \quad (94b)$$

$$|a_L\rangle - |b_L\rangle = \underline{\gamma}|a_L\rangle + \underline{\gamma}|b_L\rangle + |a_R\rangle - |b_R\rangle \quad (95b)$$

where the normalized admittance matrix is introduced as

$$\underline{\gamma} = \underline{M}_V^{-1} \underline{Y} \underline{M}_V \quad (97)$$

By subtracting the above two equations one obtains

$$|b_L\rangle = -(2\underline{U} + \underline{\gamma})^{-1} \underline{\gamma} |a_L\rangle + 2(2\underline{U} + \underline{\gamma})^{-1} |b_R\rangle \quad (98)$$

When the normalized admittance matrix is "small", [19], it is possible to use the first two terms from Neumann's series:

$$(2\underline{U} + \underline{\gamma})^{-1} \approx \frac{1}{2}(\underline{U} - \frac{1}{2}\underline{\gamma})$$

Retaining only the linear terms in  $\underline{\gamma}$ , (98) is approximately given by

$$|b_L\rangle \approx -\frac{1}{2}\underline{\gamma} |a_L\rangle + (\underline{U} + \frac{1}{2}\underline{\gamma}) |b_R\rangle \quad (99)$$

Next, consider a small series perturbation in Fig. 21, described by

$$|I_L\rangle = |I_R\rangle \quad (100)$$

$$|V_L\rangle = \underline{Z}|I_L\rangle \quad (101)$$

and

$$|V_L\rangle = |V_L\rangle + |V_R\rangle \quad (102)$$

Expressed by scattering variables

$$\underline{M}_I(|a_L\rangle - |b_L\rangle) = \underline{M}_I(|a_R\rangle - |b_R\rangle) \quad (100a)$$

$$\underline{M}_V(|a_L\rangle + |b_L\rangle) = \underline{Z} \underline{M}_I(|a_L\rangle - |b_L\rangle) + \underline{M}_V(|a_R\rangle + |b_R\rangle) \quad (101a)$$

Introduce the normalized impedance matrix

$$\underline{z} = \underline{M}_I^{-1} \underline{Z} \underline{M}_I \quad (103)$$

Using the same approximations as in (99) one obtains

$$|b_L\rangle = \frac{1}{2} \underline{z} |a_L\rangle + (\underline{U} - \frac{1}{2} \underline{z}) |b_R\rangle \quad (104)$$

Now add both series and parallel perturbations as in Fig. 22. The small reflections are simply added as follows

$$|b_L\rangle = \frac{1}{2}(\underline{z} - \underline{y}) |a_L\rangle + (\underline{U} - \frac{1}{2} \underline{z} - \frac{1}{2} \underline{y}) |b_R\rangle \quad (105)$$

Invoking reciprocity and symmetry of the junction

$$\begin{pmatrix} |b_L\rangle \\ |a_R\rangle \end{pmatrix} = \begin{pmatrix} \frac{1}{2} \underline{z} - \frac{1}{2} \underline{y} & \underline{U} - \frac{1}{2} \underline{z} - \frac{1}{2} \underline{y} \\ \underline{U} - \frac{1}{2} \underline{z} - \frac{1}{2} \underline{y} & \frac{1}{2} \underline{z} - \frac{1}{2} \underline{y} \end{pmatrix} \begin{pmatrix} |a_L\rangle \\ |b_R\rangle \end{pmatrix} \quad (106)$$

Comparing (106) with (91), one concludes

$$\begin{aligned} j\underline{H} + j\underline{E} &= \frac{1}{2}(\underline{z} - \underline{y}) \\ -j\underline{H} + j\underline{E} &= -\frac{1}{2}(\underline{z} + \underline{y}) \end{aligned}$$

Solving for  $\underline{z}$  and  $\underline{y}$ :

$$\underline{z} = j2\underline{H} \quad (107)$$

$$\underline{y} = -j2\underline{E} \quad (108)$$

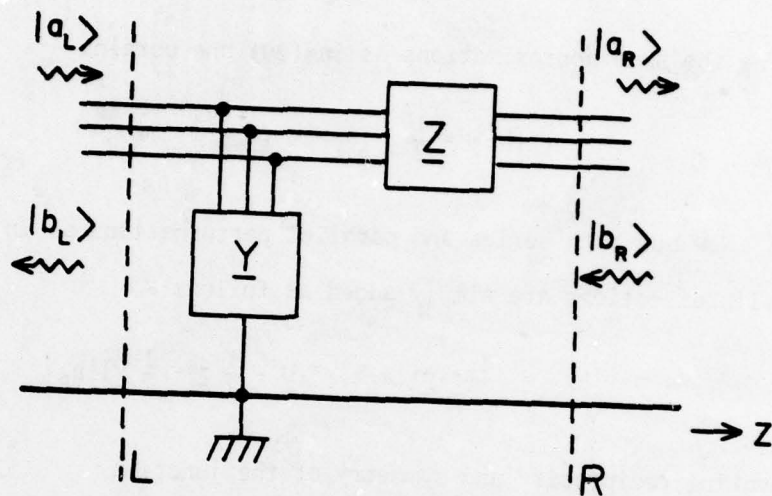


Fig. 22. MTL with both series and parallel perturbations.

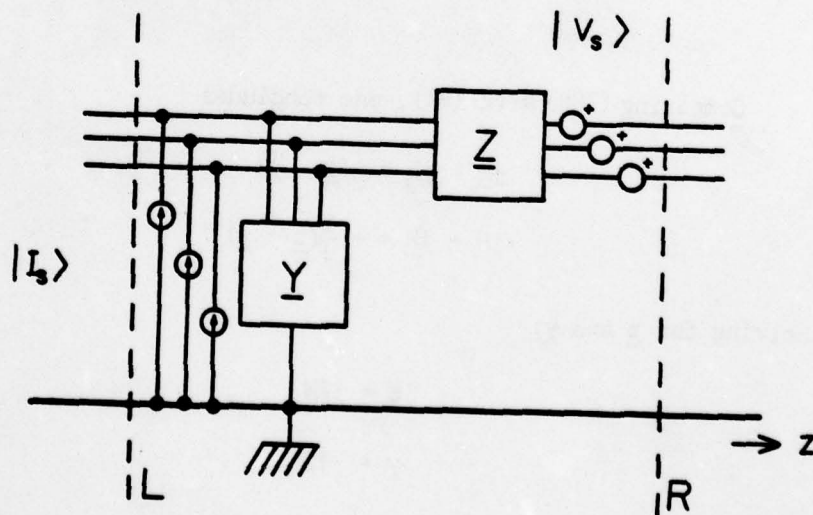


Fig. 23. Equivalent circuit of the aperture junction with sources.

From (89) and (90) it can be seen that all the elements of  $\underline{H}$  and of  $\underline{E}$  are real and proportional to frequency  $\omega$ . Thus, the elements of  $\underline{z}$  are represented by self and mutual normalized inductances

$$\underline{z} = j\omega \underline{\ell} \quad (109)$$

where:

$$\ell_{ij} = \mu \alpha_m h_{xi}(x_0, 0) h_{xj}(x_0, 0) \quad (110)$$

These inductances may be positive or negative, depending on the signs of  $h_{xi}$  and  $h_{xj}$ .

Analogously, the normalized admittance matrix consists of self and coupling capacitances:

$$\underline{y} = -j \omega \underline{c} \quad (111)$$

where the elements of  $\underline{c}$  are

$$c_{ij} = \epsilon \alpha_e e_{yi}(x_0, 0) e_{yj}(x_0, 0) \quad (112)$$

The negative sign signifies that the capacitance is negative if the product  $e_{yi}e_{yj}$  comes out to be positive. A note of explanation is necessary on the meaning of the coupling capacitance  $c_{ij}$  (when  $i \neq j$ ). Such a circuit element does not exist in lumped-circuit theory. It signifies that the current at the port  $i$  is proportional to the rate of change of voltage at the port  $j$ , the constant of proportionality being defined as a coupling capacitance.

Finally, to obtain the actual impedance matrix  $\underline{Z}$ , (103) has to be denormalized as follows

$$\underline{Z} = \underline{M}_V \underline{z} \underline{M}_V^\dagger = j\omega \underline{M}_V \underline{\ell} \underline{M}_V^\dagger \quad (113)$$

AD-A074 265

AIR FORCE WEAPONS LAB KIRTLAND AFB NM  
ELECTROMAGNETIC PULSE INTERACTION NOTES-EMP 3-39.(U)  
JUL 79 C E BAUM

F/G 20/14

UNCLASSIFIED

AFWL-TR-79-402

SBIE-AD-E200 363

NL

2 OF 5

AD  
A074265





Similarly, the denormalized admittance matrix is

$$\underline{Y} = \underline{M}_I \underline{Y} \underline{M}_I^\dagger = -j\omega \underline{M}_I \underline{C} \underline{M}_I^\dagger \quad (114)$$

Note that all the matrices on the right-hand sides of (113) and (114) are real, thus the equivalent circuit is easy to interpret.

When also the voltage- and current sources from (52) and (55) are included in the circuit, the complete first-order equivalent circuit takes the form shown in Fig. 23.

This representation is valid below the first resonant frequency of the aperture. As shown in reference [20], the lowest resonance of a circular aperture of radius  $a$  appears at

$$k a = 1.841$$

Thus, the representation is valid for frequencies

$$f \ll \frac{87.9 \cdot 10^6}{a}$$

For an aperture of radius  $a = 10$  cm, the equivalent circuit is valid for  $f \ll 880$  MHz. The validity of the equivalent circuit could be further extended in the region close to the aperture resonance by the methods described in [21], which will not be pursued here.

The circuit diagram of matrix  $\underline{Z}$  for a 3-conductor system is shown in Fig. 24a. The self inductances are denoted by  $L_{11}$ ,  $L_{22}$ , and  $L_{23}$ , and

[20] R. E. Collin, Foundations for Microwave Engineering, New York: McGraw-Hill, 1966, p. 111.

[21] G. L. Matthaei, L. Young, E. M. T. Jones, Microwave Filters, Impedance-Matching Networks, and Coupling Structures, New York: McGraw-Hill, 1964, p. 242.

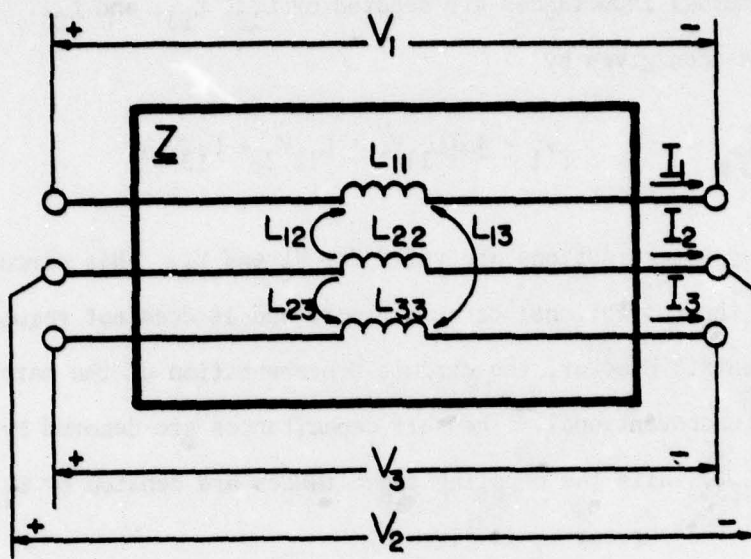


Fig. 24(a). Impedance perturbation circuit.

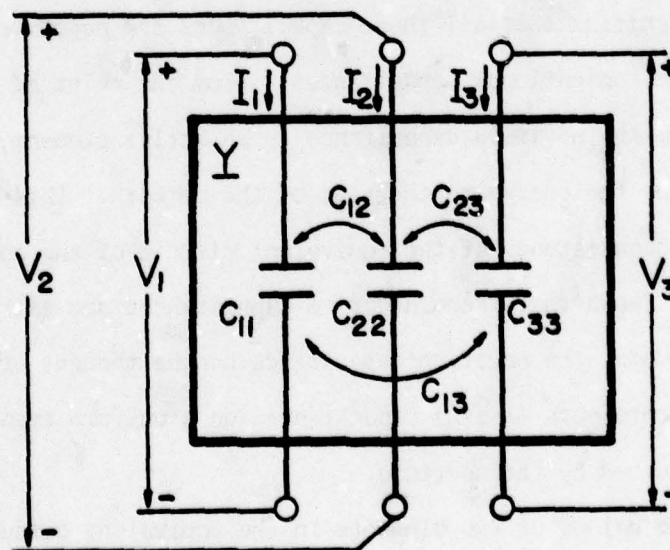


Fig. 24(b). Admittance perturbation circuit.

the mutual inductances are denoted by  $L_{12}$ ,  $L_{13}$ , and  $L_{23}$ . The voltage  $V_1$  is then given by

$$V_1 = j\omega(L_{11}V_1 + L_{12}V_2 + L_{13}V_3)$$

Analogous expressions are valid for  $V_2$  and  $V_3$ . This circuit is familiar from the conventional circuit theory and it does not require further comments. However, the circuit representation of the matrix  $\underline{Y}$  is somewhat unconventional. The self capacitances are denoted by  $C_{11}$ ,  $C_{22}$ , and  $C_{23}$ , while the coupling capacitances are denoted by  $C_{12}$ ,  $C_{23}$ , and  $C_{13}$ . The current  $I_1$  is given by

$$I_1 = -j\omega(C_{11}V_1 + C_{12}V_2 + C_{13}V_3)$$

and similar expressions may be written for  $I_2$  and  $I_3$ . The negative sign signifies that all these capacitances are negative, as compared with the conventional capacitances. From the point of view of energy balance, the negative capacitance is an active element, capable of supplying the energy to the rest of the network. This may be considered as an inconsistency of the equivalent circuit of the aperture, but it will be shown that these negative capacitances are extremely small. Furthermore, the negative capacitance can be thought of as the element which represents missing capacitances on a uniform transmission line which is perturbed by the aperture.

The values of the elements in the equivalent circuit from Fig. 24 will be next computed for a 2-conductor parallel-plate MTL described in Section IV. For a circular aperture of diameter  $d = 2$  cm the electric modal functions are computed from (68)

$$e_{y1}(x_0, 0) = - \frac{-6.1358}{1.10^{-2}} = 613.58$$

$$e_{y2}(x_0, 0) = \frac{2.3690}{1.10^{-2}} = -236.90$$

The values of the magnetic modal functions at the position of the aperture are found from (69)

$$h_{x1}(x_0, 0) = -0.81491 \quad h_{x2}(x_0, 0) = 0.42212$$

From (110) and (10) the normalized inductances are obtained as

$$\ell_{11} = 1.1127 \cdot 10^{-12}, \ell_{22} = 2.9855 \cdot 10^{-13}, \ell_{12} = -5.7636 \cdot 10^{-13}$$

For the frequency 1 GHz, the normalized reactances are

$$\omega \ell_{11} = 6.9913 \cdot 10^{-3}, \omega \ell_{22} = 1.8758 \cdot 10^{-3}, \omega \ell_{12} = -3.6214 \cdot 10^{-3}$$

Similarly the normalized susceptances in parallel with the MTL are found from (112) and (10)

$$\omega c_{11} = 1.3963 \cdot 10^{-2}, \omega c_{12} = -5.3909 \cdot 10^{-3}, \omega c_{22} = 2.0814 \cdot 10^{-3}$$

Therefore, even at the highest frequency of interest for EMP calculations, the normalized reactances and susceptances are small numbers. Thus it is expected that they do not cause appreciable reflections when a wave is propagating along the MTL.

Consider that an incident wave  $|a_L\rangle$  is coming from the left toward the equivalent circuit of the aperture in Fig. 22. Assuming that the right-hand side of the equivalent circuit is terminated in an infinitely long MTL, it is of interest to find  $|b_L\rangle$  in terms of  $|a_L\rangle$ . Since for an infinitely long MTL the vector  $|b_R\rangle$  vanishes, the equation (106) gives

$$|b_L\rangle = \underline{\Gamma}(\underline{z}-\underline{y}) |a_L\rangle \quad (114a)$$

Therefore, the reflections due to the presence of the equivalent circuit on a uniform MTL are determined by reflection matrix  $\underline{\Gamma}$

$$\underline{\Gamma} = \underline{\Gamma}(\underline{z}-\underline{y}) = \frac{j}{2} \begin{pmatrix} \omega l_{11} + \omega c_{11} & \omega l_{12} + \omega c_{12} \\ \omega l_{12} + \omega c_{12} & \omega l_{22} + \omega c_{22} \end{pmatrix} \quad (114b)$$

For the case under consideration, the reflection matrix is

$$\underline{\Gamma} = j \begin{pmatrix} 1.0478 \cdot 10^{-2} & -9.0123 \cdot 10^{-3} \\ -9.0123 \cdot 10^{-3} & 3.9572 \cdot 10^{-3} \end{pmatrix} \quad (114c)$$

It can be seen that the reflected amplitude of the first mode is only 1.05% of the incident amplitude for the same mode. The other reflections are even smaller than 1%. At lower frequencies all coefficients of the reflection matrix are proportionally reduced. This fact justifies the procedure from Section IV of computing the voltage waveforms by entirely neglecting the presence of inductances and capacitances in the equivalent circuit.

It is of interest to investigate the equivalent circuit of the aperture on a single-conductor transmission line. The geometry of the problem is such as specified by Fig. 3. A round wire of radius  $r$  is placed in parallel with the ground plane, so that the center of the wire is elevated above the ground plane for distance  $d$ . The circular aperture of radius  $a$  is located at  $x = x_0$ ,  $y = 0$ ,  $z = 0$ .

When  $N = 1$ , it follows from formulas in Appendix C that matrices  $\underline{M}_I$  and  $\underline{M}_V$  reduce to simple scalars:

$$M_I = \sqrt[4]{\frac{C'}{L'}} \quad , \quad M_V = \sqrt[4]{\frac{L'}{C'}} \quad (114d)$$

where  $C'$  and  $L'$  are the distributed capacitance and inductance of the single-wire transmission line. When the subscripts  $i$  and  $j$  are omitted, the normalized inductance from (110) becomes

$$l = \mu \alpha_m h_x^2(x_0, 0) \quad (114e)$$

and the normalized negative capacitance from (112) becomes

$$c = \epsilon \alpha_e e_y^2(x_0, 0) \quad (114f)$$

The normalized modal functions  $h_x$  and  $e_y$  for the TEM mode of a single wire above the ground plane have been derived in [13] as follows

- 
- [13] D. Kajfez, "Excitation of a Terminated TEM Transmission Line Through a Small Aperture," Interaction Note 215, July 1974.

$$h_x = \frac{h}{\pi \sqrt{Z_0} (x_0^2 + h^2)} \quad (114g)$$

$$e_y = - \frac{\eta h}{\pi \sqrt{Z_0} (x_0^2 + h^2)} \quad (114h)$$

where  $h$  denotes the reduced height of the wire:

$$h = \sqrt{d^2 - r^2} \quad (114i)$$

In order to obtain the actual values of the equivalent inductance and capacitance, the values are to be denormalized according to (113) and (114):

$$Z = j\omega L = j\omega M_V^2 z \quad (114j)$$

$$Y = -j\omega C = -j\omega M_I^2 y \quad (114k)$$

The values of  $L$  and  $C$  are, therefore

$$L = \mu \alpha_e \frac{h^2}{\pi^2 (x_0^2 + h^2)^2} \quad (115)$$

$$C = \epsilon \alpha_e \frac{\eta^2 h^2}{Z_0^2 (x_0^2 + h^2)^2} \quad (116)$$

where

$$Z_0 = 60 \cosh^{-1} \left( \frac{d}{r} \right) \quad (116a)$$

The similar formulas have been derived by Lee and Yang [22]. Their formulas (20.a) reduce to (115) and (116) in the case of a thin wire ( $r \ll d$ ,  $h \approx d$ ). For thick wires it is believed that (115) and (116) are more accurate, because the exact TEM modal functions have been used in the derivation.

---

[22] K. S. H. Lee, F. C. Yang, "A Wire Passing by a Circular Aperture in an Infinite Ground Plane," Interaction Note 317, February 1977.

## SECTION VI

## INTERACTION BETWEEN AN APERTURE AND A SINGLE WIRE

In this section we examine the validity of the assumption that the dipole moments in the aperture can be determined from the plane wave exciting the aperture ignoring the presence of the MTL. This assumption has been used to derive the model for aperture coupling to the lines in the preceding sections. For simplicity, we treat only a single wire line over a ground plane. It is possible, in principle, to extend the analysis to treat a MTL backscattering into the aperture by superimposing the backscatter from the individual lines, accounting for the mutual interaction of the various conductors. The general situation is too difficult to treat here, however. As an additional simplification, we assume the conducting line is bare.

Referring to Figs. 2 and 3, in addition to the plane wave fields  $\vec{E}_s^{\text{ext}}$  and  $\vec{H}_s^{\text{ext}}$  exciting the aperture, we must now consider aperture fields  $\vec{E}_s^{\text{int}}$  and  $\vec{H}_s^{\text{int}}$  which are the fields reradiated from the transmission line. These fields are linearly related to the dipole moments in the aperture and we show in the following that they can be written as

$$H_{xs}^{\text{int}} = t_m c_{mx} \quad (117)$$

$$E_{ys}^{\text{int}} = t_e c_{ey} \quad (118)$$

where  $t_m(t_e)$  is the  $x(y)$  component of the short circuit magnetic (electric) field at the aperture reradiated from the line due to the appropriately directed unit magnetic (electric) current moment in the aperture. In the absence of any other sources in the interior region, Equations (8) and (9) in combination with (117) and (118) become

$$c_{mx} = \frac{-j\omega\alpha_m H_{xs}^{\text{ext}}}{(1-j\omega\alpha_m t_m)} \quad (119)$$

$$c_{ey} = \frac{j\omega\epsilon\alpha_e E_{ys}^{ext}}{1+j\omega\epsilon\alpha_e t_e} \quad (120)$$

It is easily seen that the coupling from the line to the aperture can thus be neglected if it can be shown that

$$\omega\mu\alpha_m t_m \ll 1 \quad (121)$$

$$\omega\epsilon\alpha_e t_e \ll 1 \quad (122)$$

In the following we determine  $t_e$  and  $t_m$ , the aperture fields scattered from the wires due to unit electric and magnetic dipoles in the aperture.

Beginning with the dipole sources  $\vec{c}_e$  and  $\vec{c}_m$  (see, e. g., Fig. 1(b)), and a single wire in the internal region, the ground plane is removed so that the dipole and wires are imaged as in Fig. 25. Note that imaging merely doubles the current moments of the dipole sources. Transverse polar coordinates  $\vec{\rho} = (\rho, \phi)$  and  $\vec{\rho}_i = (\rho_i, \phi_i)$  measured from the wire axis and the image wire axis, respectively, are also introduced in Fig. 25. The vector  $\vec{\rho}_0$  establishes the location of the aperture with respect to the wire axis.

The fields due to the dipoles in the absence of the conductors may be determined from free space magnetic and electric vector potentials given by

$$A_{ey} = \frac{\mu c_{ey} e^{-jk|\vec{r}-x_0\vec{a}_x|}}{2\pi|\vec{r}-\vec{\rho}_0|} \quad (123)$$

$$F_{mx} = \frac{\epsilon c_{mx} e^{-jk|\vec{r}-x_0\vec{a}_x|}}{2\pi|\vec{r}-\vec{\rho}_0|} \quad (124)$$

respectively, where

$$\vec{r} = x\vec{a}_x + y\vec{a}_y + z\vec{a}_z$$

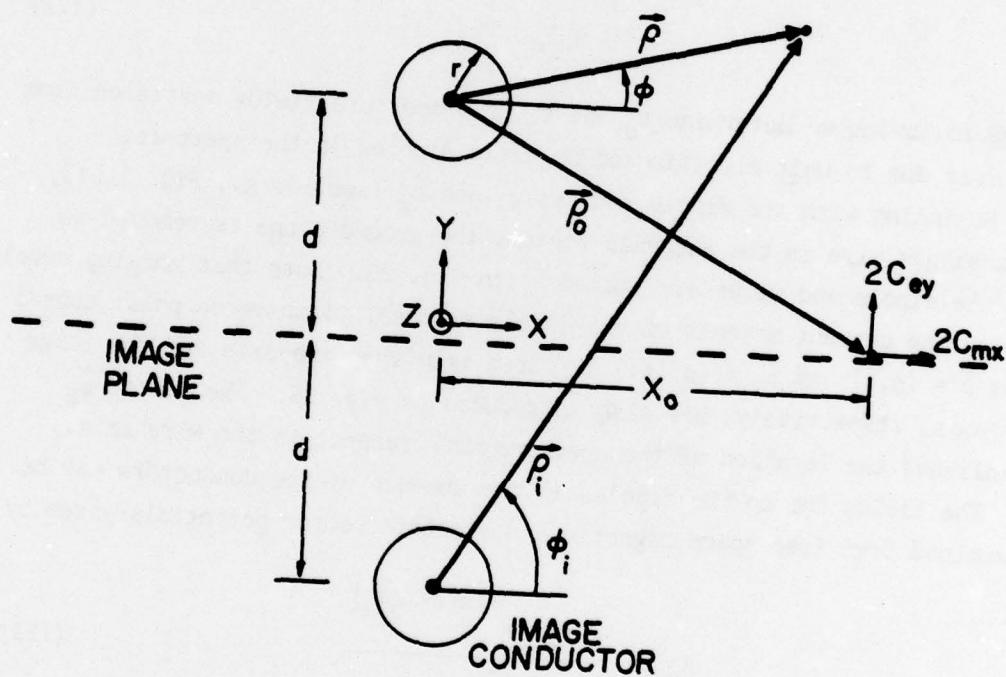


Fig. 25. Geometry of wire over a ground screen with equivalent dipole moments representing an aperture.

The currents on the wire and its image are assumed to be entirely  $z$ -directed but in opposite directions. Hence they determine a magnetic vector potential  $A_z$  which can in turn be used to determine all field quantities. Boundary conditions require the  $z$ -component of electric field to vanish at the surface of the upper wire in Fig. 25. However, it must vanish everywhere interior to the wire as well and if we restrict our observation to the wire axis,  $\vec{\rho} = \vec{0}$ , only the total or average current  $I(z)$  from the upper wire contributes to the vector potential there. This choice of the observation point thus averages out of the problem any circumferential variation in the current on the upper wire; the circumferentially varying currents on the image wire do, however, contribute to the vector potential at  $\vec{\rho} = \vec{0}$ . But if the wire is thin and sufficiently far from the ground plane in terms of the wire radius, i.e., if

$$kr \ll 1, \quad (125)$$

$$r \ll d, \quad (126)$$

then the image wire may essentially be replaced by a line source along the image wire axis which carries a current  $I(z)$  directed opposite to that of the upper wire. In other words, under conditions (125) and (126), if the image wire is replaced by multipole line sources located at  $\vec{\rho}_i = \vec{0}$ , the contributions of the dipole, quadrupole and higher order multipole terms can be neglected compared to that of the monopole current filament  $I(z)$ . Thus the magnetic vector potential along the upper wire axis due to the wire and image current is approximately

$$A_z \Big|_{\vec{\rho}=\vec{0}} = \frac{\mu}{4\pi} \int_{-\infty}^{\infty} I(z') \left[ \frac{e^{-jk\sqrt{r^2+(z-z')^2}}}{\sqrt{r^2+(z-z')^2}} - \frac{e^{-jk\sqrt{4d^2+(z-z')^2}}}{\sqrt{4d^2+(z-z')^2}} \right] dz'. \quad (127)$$

Along the axis of the upper wire  $E_z$  must vanish, that is

$$\vec{a}_z \cdot \left[ \frac{1}{j\omega\mu\epsilon} (k^2 + \nabla\nabla \cdot) (\vec{a}_y A_{ey} + \vec{a}_z A_z) - \frac{1}{\epsilon} \nabla \times (\vec{a}_x F_{mx}) \right] \Big|_{\vec{\rho} = \vec{0}} = 0 \quad (128)$$

or writing out the desired components,

$$\frac{1}{j\omega\mu\epsilon} \left( \frac{\partial^2}{\partial z^2} + k^2 \right) A_z \Big|_{\vec{\rho} = \vec{0}} = - \frac{1}{j\omega\mu\epsilon} \frac{\partial^2 A_{ey}}{\partial z \partial y} \Big|_{\vec{\rho} = \vec{0}} - \frac{1}{\epsilon} \frac{\partial F_{mx}}{\partial y} \Big|_{\vec{\rho} = \vec{0}} \quad (129)$$

Equation (129) with (123), (124), and (127), is an integro-differential equation for the current  $I(z)$  induced on the transmission line by current moments  $c_{ey}$  and  $c_{mx}$  in the aperture. In order to determine the current we introduce the Fourier transform pair

$$\psi(z) = \frac{1}{\sqrt{2\pi}} \int_{-\infty}^{\infty} \tilde{\psi}(k_z) e^{-jk_z z} dk_z \quad (130)$$

$$\tilde{\psi}(k_z) = \frac{1}{\sqrt{2\pi}} \int_{-\infty}^{\infty} \psi(z) e^{+jk_z z} dz \quad (131)$$

where the tilde indicates Fourier transformed quantities. Writing the current in (127) as an inverse transform and making use of the identity

$$\frac{e^{-jk\sqrt{\rho^2 + (z-z')^2}}}{\sqrt{\rho^2 + (z-z')^2}} = \frac{1}{2j} \int_{-\infty}^{\infty} H_0^{(2)}(k_\rho \rho) e^{-jk_z(z-z')} dk_z \quad (132)$$

where  $k_\rho = \sqrt{k^2 - k_z^2}$ ,  $\text{Re } k_\rho > 0$ ,  $\text{Im } k_\rho < 0$ , (127) becomes

$$A_z \Big|_{\vec{\rho}=\vec{0}} = \frac{\mu}{4j(2\pi)^{3/2}} \int_{-\infty}^{\infty} \int_{-\infty}^{\infty} \int_{-\infty}^{\infty} \tilde{I}(k_z) [H_0^{(2)}(k_\rho r) - H_0^{(2)}(2k_\rho d)] e^{-j(k_z - k'_z)z'} \\ \times e^{-jk'_z z} dk_z dk'_z dz' \quad (133)$$

Noting that

$$\int_{-\infty}^{\infty} e^{-j(k_z - k'_z)z'} dz' = 2\pi \delta(k_z - k'_z) \quad (134)$$

(133) simplifies to the transform representation

$$A_z \Big|_{\vec{\rho}=\vec{0}} = \frac{\mu}{4j\sqrt{2\pi}} \int_{-\infty}^{\infty} \tilde{I}(k_z) [H_0^{(2)}(k_\rho r) - H_0^{(2)}(2k_\rho d)] e^{-jk_z z} dk_z \quad (135)$$

Similarly, we express the right hand side of (129) in transform representation:

$$\frac{\partial^2 A_{ey}}{\partial z \partial y} \Big|_{\vec{\rho}=\vec{0}} = \frac{\partial^2}{\partial z \partial y} \left[ \frac{\mu c_{ey} e^{-jk|\vec{r}-\vec{\rho}_0|}}{2\pi |\vec{r}-\vec{\rho}_0|} \right]_{\vec{\rho}=\vec{0}} \\ = \frac{\mu c_{ey}}{4j\pi} \frac{\partial^2}{\partial z \partial y} \int_{-\infty}^{\infty} H_0^{(2)}(k_\rho |\vec{r}-\vec{\rho}_0|) e^{-jk_z z} dk_z \Big|_{\vec{\rho}=\vec{0}} \\ = \frac{\mu c_{ey} d}{4\pi \sqrt{x_0^2 + d^2}} \int_{-\infty}^{\infty} k_z k_\rho H_1^{(2)}(k_\rho \sqrt{x_0^2 + d^2}) e^{-jk_z z} dk_z \quad (136)$$

and

$$\begin{aligned}
 \left. \frac{\partial F_{mx}}{\partial y} \right|_{\vec{\rho}=\vec{0}} &= \frac{\partial}{\partial y} \left[ \frac{\epsilon c_{mx} e^{-jk|\vec{r}-\vec{\rho}_0|}}{2\pi|\vec{r}-\vec{\rho}_0|} \right]_{\vec{\rho}=\vec{0}} \\
 &= \frac{\epsilon c_{mx}}{4j\pi} \frac{\partial}{\partial y} \int_{-\infty}^{\infty} H_0^{(2)}(k_\rho |\vec{\rho}-\vec{\rho}_0|) e^{-jk_z z} dk_z \Big|_{\vec{\rho}=\vec{0}} \\
 &= \frac{j\epsilon c_{mx} d}{4\pi\sqrt{x_0^2+d^2}} \int_{-\infty}^{\infty} k_\rho H_1^{(2)}\left(k_\rho \sqrt{x_0^2+d^2}\right) e^{-jk_z z} dk_z
 \end{aligned} \tag{137}$$

Substituting (135), (136) and (137) into (129) and taking the Fourier inverse of the resulting equation yields finally the transform of the current,

$$\begin{aligned}
 \tilde{I}(k_z) &= \frac{j\sqrt{2/\pi} d}{k_\rho \sqrt{x_0^2+d^2}} \frac{H_1^{(2)}\left(k_\rho \sqrt{x_0^2+d^2}\right)}{H_0^{(2)}(k_\rho r) - H_0^{(2)}(2k_\rho d)} \left( \frac{k c_{mx}}{\eta} - k_z c_{ey} \right) \\
 &= \tilde{I}_m(k_z) + \tilde{I}_e(k_z)
 \end{aligned} \tag{138}$$

where  $\tilde{I}_m(k_z)$  and  $\tilde{I}_e(k_z)$  are identified as the partial currents arising from the corresponding source terms  $c_{mx}$  and  $c_{ey}$ , respectively. Note that  $\tilde{I}_m$  is an even function whereas  $\tilde{I}_e$  is an odd function of the variable  $k_z$ .

The total line current can be obtained by taking the Fourier inverse of (138). Our interest, however, is in obtaining the fields that the wire and image currents scatter into the aperture and these can be found most easily from the vector potential expressed in terms of the current transform. The vector potential at an arbitrary point is obtained by again treating both the line and its image as current filaments at  $\vec{\rho}=\vec{0}$  and  $\vec{\rho}_i=\vec{0}$ , respectively:

$$\begin{aligned}
 A_z &= \frac{\mu}{4\pi} \int_{-\infty}^{\infty} I(z') \left[ \frac{e^{-jk|\vec{\rho}+\vec{a}_z(z-z')|}}{|\vec{\rho}+\vec{a}_z(z-z')|} - \frac{e^{-jk|\vec{\rho}_i+\vec{a}_z(z-z')|}}{|\vec{\rho}_i+\vec{a}_z(z-z')|} \right] dz' \\
 &= \frac{\mu}{4j\sqrt{2\pi}} \int_{-\infty}^{\infty} \tilde{I}(k_z) [H_0^{(2)}(k_\rho|\vec{\rho}|) - H_0^{(2)}(k_\rho|\vec{\rho}_i|)] e^{-jk_z z} dk_z
 \end{aligned} \tag{139}$$

where, again, (132) and (134) have been used. The desired field quantities in the aperture are

$$\begin{aligned}
 E_{ys}^{int} &= \frac{1}{j\omega\epsilon} \frac{\partial^2 A_z}{\partial y \partial z} \bigg|_{x=x_0, y=z=0} \\
 &= \frac{jd}{2\sqrt{2\pi\omega\epsilon}\sqrt{x_0^2+d^2}} \int_{-\infty}^{\infty} \tilde{I}(k_z) k_z k_\rho H_1^{(2)}(k_\rho\sqrt{x_0^2+d^2}) dk_z \\
 &= \frac{jd}{2\sqrt{2\pi\omega\epsilon}\sqrt{x_0^2+d^2}} \int_{-\infty}^{\infty} \tilde{I}_e(k_z) k_z k_\rho H_1^{(2)}(k_\rho\sqrt{x_0^2+d^2}) dk_z \\
 &= \frac{c_{ey}\eta}{2\pi k} \left( \frac{d^2}{x_0^2+d^2} \right) \int_{-\infty}^{\infty} \frac{k_z^2 [H_1^{(2)}(k_\rho\sqrt{x_0^2+d^2})]^2}{H_0^{(2)}(k_\rho r) - H_0^{(2)}(2k_\rho d)} dk = t_e c_{ey}
 \end{aligned} \tag{140}$$

and

$$\begin{aligned}
 H_{xs}^{int} &= \frac{1}{u} \frac{\partial A_z}{\partial y} \bigg|_{\substack{x=x_0 \\ y=z=0}} \\
 &= \frac{d}{2j\sqrt{2\pi} \sqrt{x_0^2+d^2}} \int_{-\infty}^{\infty} \tilde{I}(k_z) k_\rho H_1^{(2)}(k_\rho \sqrt{x_0^2+d^2}) dk_z \\
 &= \frac{d}{2j\sqrt{2\pi} \sqrt{x_0^2+d^2}} \int_{-\infty}^{\infty} \tilde{I}_m(k_z) k_\rho H_1^{(2)}(k_\rho \sqrt{x_0^2+d^2}) dk_z \\
 &= \frac{c_{mx} k}{2\pi\eta} \left( \frac{d^2}{x_0^2+d^2} \right) \int_{-\infty}^{\infty} \frac{[H_1^{(2)}(k_\rho \sqrt{x_0^2+d^2})]^2 dk_z}{H_0^{(2)}(k_\rho r) - H_0^{(2)}(2k_\rho d)} \\
 &= t_m c_{mx}
 \end{aligned} \tag{141}$$

where we have used the even and odd properties of  $\tilde{I}_m$  and  $\tilde{I}_e$  to appropriately simplify the integrals (140) and (141).

Returning to the examination of conditions (121) and (122), we first note that the four parameters  $k$ ,  $x_0$ ,  $d$ , and  $r$  in the integrals can be reduced to three parameters if all distances are measured in terms of wavelengths. Thus, we examine

$$\omega \mu \alpha_m t_m = \frac{(SF)_m (kl)^3 (kd)^2 \tilde{t}_m(k\alpha_0, kd, kr)}{(k\alpha_0)^2 + (kd)^2} \tag{142}$$

$$\omega \epsilon_0 \epsilon_e t_e = \frac{(SF)_e (k\ell)^3 (kd)^2 \tilde{t}_e(kx_0, kd, kr)}{(kx_0)^2 + (kd)^2} \quad (143)$$

where we have introduced the aperture shape factors defined as

$$(SF)_m = \frac{\alpha_m}{\ell^3} \quad (144)$$

$$(SF)_e = \frac{\alpha_e}{\ell^3} \quad (145)$$

where  $\alpha_m$  and  $\alpha_e$  are the aperture polarizabilities and  $\ell$  is the largest aperture dimension. The shape factors have been determined for a variety of aperture shapes by numerical and experimental means [11-12] and are typically somewhat smaller than unity. The normalized functions  $\tilde{t}_m$  and  $\tilde{t}_e$  are defined as

$$\begin{aligned} \tilde{t}_m(kx_0, kd, kr) &= \frac{n(x_0^2 + d^2)}{k^2 d^2} t_m \\ &= \frac{1}{2\pi} \int_{-\infty}^{\infty} \frac{H_1^{(2)} \sqrt{(1-\alpha^2) [(kx_0)^2 + (kd)^2]}^2 d\alpha}{H_0^{(2)} \sqrt{1-\alpha^2} kr - H_0^{(2)} \sqrt{1-\alpha^2} kd} \end{aligned} \quad (146)$$

- 
- [11] S.B. Cohn, "Determination of Aperture Parameters by Electrolytic-Tank Measurements", Proc. I.R.E., Vol. 39, pp. 1416-1421, November 1951.
- [12] S.B. Cohn, "The Electric Polarizability of Apertures of Arbitrary Shape," Proc. I.R.E., Vol. 40, pp. 1069-1071, September 1952.

$$\begin{aligned} \tilde{t}_0(kx_0, kd, kr) &= \frac{x_0^2 + d^2}{k^2 d^2 \eta} t_e \\ &= \frac{1}{2\pi} \int_{-\infty}^{\infty} \frac{\alpha^2 \left[ H_1^{(2)} \left( \sqrt{(1-\alpha^2) [(kx_0)^2 + (kd)^2]} \right) \right]^2}{H^{(2)} \left( \frac{\sqrt{1-\alpha^2}}{kr} \right) - H_0^{(2)} \left( \frac{\sqrt{1-\alpha^2}}{kd} \right)} d\alpha \end{aligned} \quad (147)$$

Since our assumption that the aperture may be replaced by current moments  $\tilde{c}_e$  and  $\tilde{c}_m$  requires that the aperture be small, say less than a tenth of a wavelength, then  $(k\ell)^3 < .25$  and since

$$(SF)_{e,m} < 1 \quad (148)$$

$$\frac{kd^2}{(kx_0)^2 + (kd)^2} \leq 1 \quad (149)$$

we need only demonstrate that

$$|\tilde{t}_m| \ll 1 \quad (150)$$

$$|\tilde{t}_e| \ll 1 \quad (151)$$

to show that the wire does not sufficiently excite the aperture that its effect needs to be accounted for in computing the aperture dipole moments.

The integrals (146) and (147) are numerically evaluated by (1) noting the symmetry of the integrals about  $\alpha = 0$ ; (2) integrating numerically using Gauss-Legendre integration on the interval  $0 \leq \alpha \leq 2$ , with a singularity of the form  $1/(\alpha-1)$  removed; (3) adding a contribution from the branch point at  $\alpha = 1$ ; and (4) integrating numerically on the interval  $2 \leq \alpha \leq \infty$  using

Gauss-Laguerre integration which assumes an exponentially decaying integrand. The appropriate rate of exponential decay in the integrand can be determined from the large argument approximations to the Hankel functions appearing in (146) and (147).

From the numerical calculations, Figs. 26-33 show that over a wide range of parameters  $kx_0$ ,  $kd$ , and  $kr$ , Eqs. (150) and (151) are indeed satisfied. However, when the wire is directly above and close to the aperture ( $kx_0 = 0$  and  $kd$  small), (150) and (151) are not satisfied. If the wire is close to the aperture, however, the aperture must be small in order for the dipole moment representation to remain valid. Calculations by Lee and Yang, [22], indicate that the dipole moment representation of a circular aperture (without considering backscattering from the wire) is accurate to about 10% only if  $2kl \leq kd$  and it seems reasonable that this upper bound on the maximum aperture dimension would hold for other aperture shapes as well. Using this as an upper bound on  $kl$  and noting that  $\tilde{t}_m$  and  $\tilde{t}_e$  are largest when  $kx_0 \neq 0$ , it is sufficient to show that

$$\left(\frac{kd}{2}\right)^3 \left| \tilde{t}_m(0, kd, kr) \right| \ll 1 \quad (152)$$

$$\left(\frac{kd}{2}\right)^3 \left| \tilde{t}_e(0, kd, kr) \right| \ll 1 \quad (153)$$

in order to exclude consideration of wire-to-aperture coupling. These quantities are plotted in Figs. 34-35. The figures show that the effect of the wire on the aperture dipole moment is negligible whenever the representation of the aperture by dipole moments is valid.

This completes the task set for this section, but it is interesting and instructive to return to the current transform (138) and use it to find the current on the line by inverse transforming:

---

[22] K. S. H. Lee, F. C. Yang, "A Wire Passing by a Circular Aperture in an Infinite Ground Plane," Interaction Note 317, February 1977.

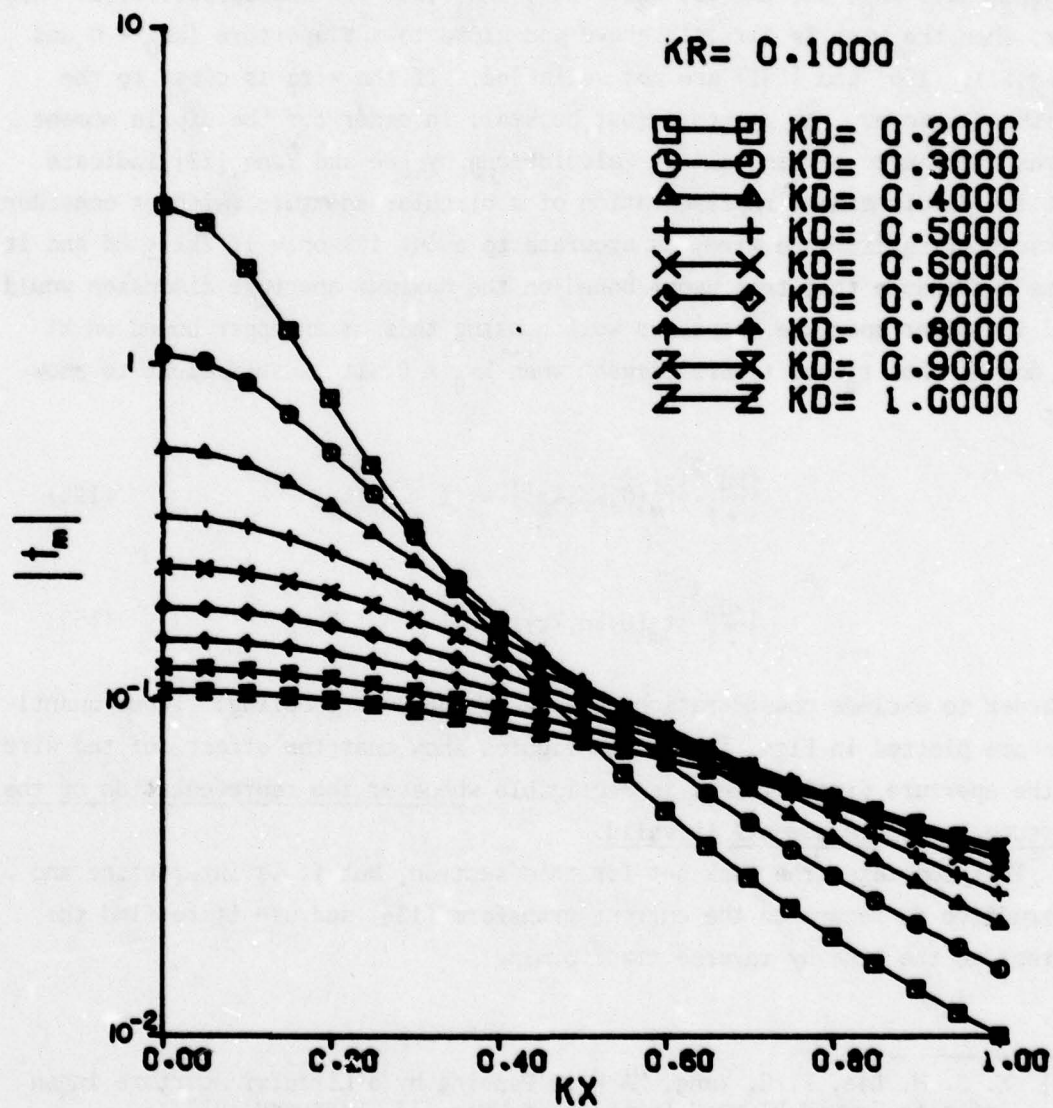


Fig. 26. Magnitude of  $t_m$  for a wire of radius  $kr = 0.1$ .

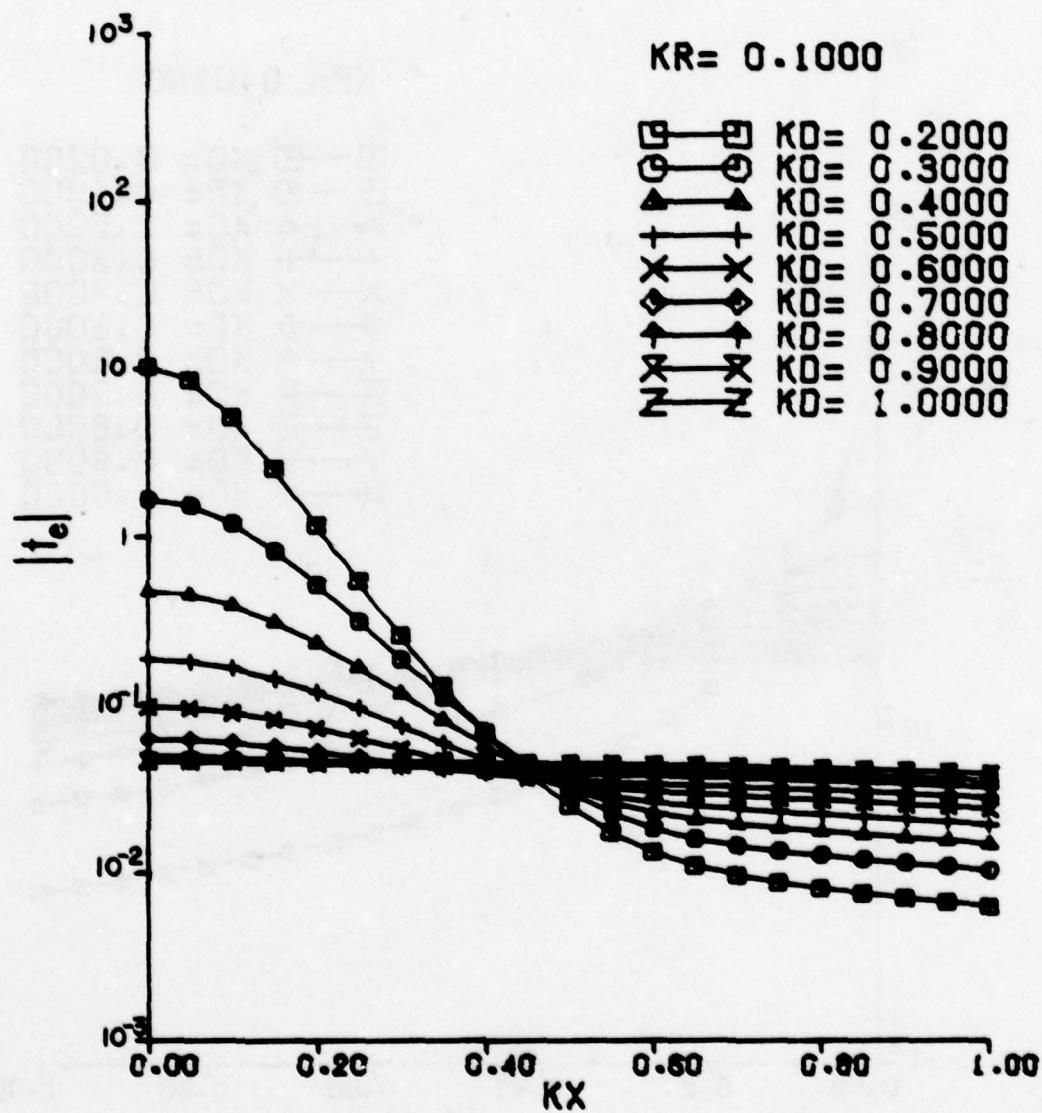


Fig. 27. Magnitude of  $t_e$  for a wire of radius  $kr = 0.1$ .

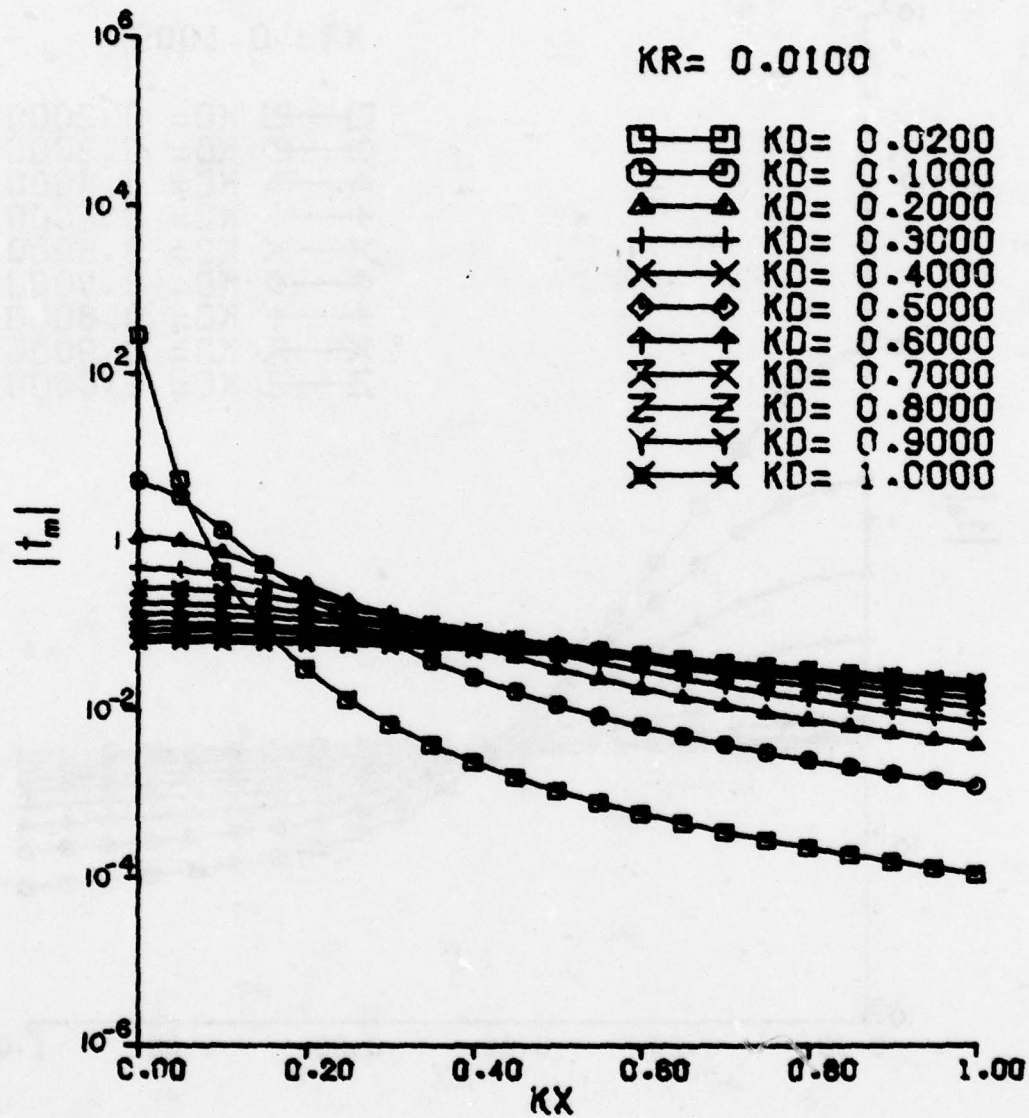


Fig. 28. Magnitude of  $t_m$  for a wire of radius  $kr = 0.01$ .

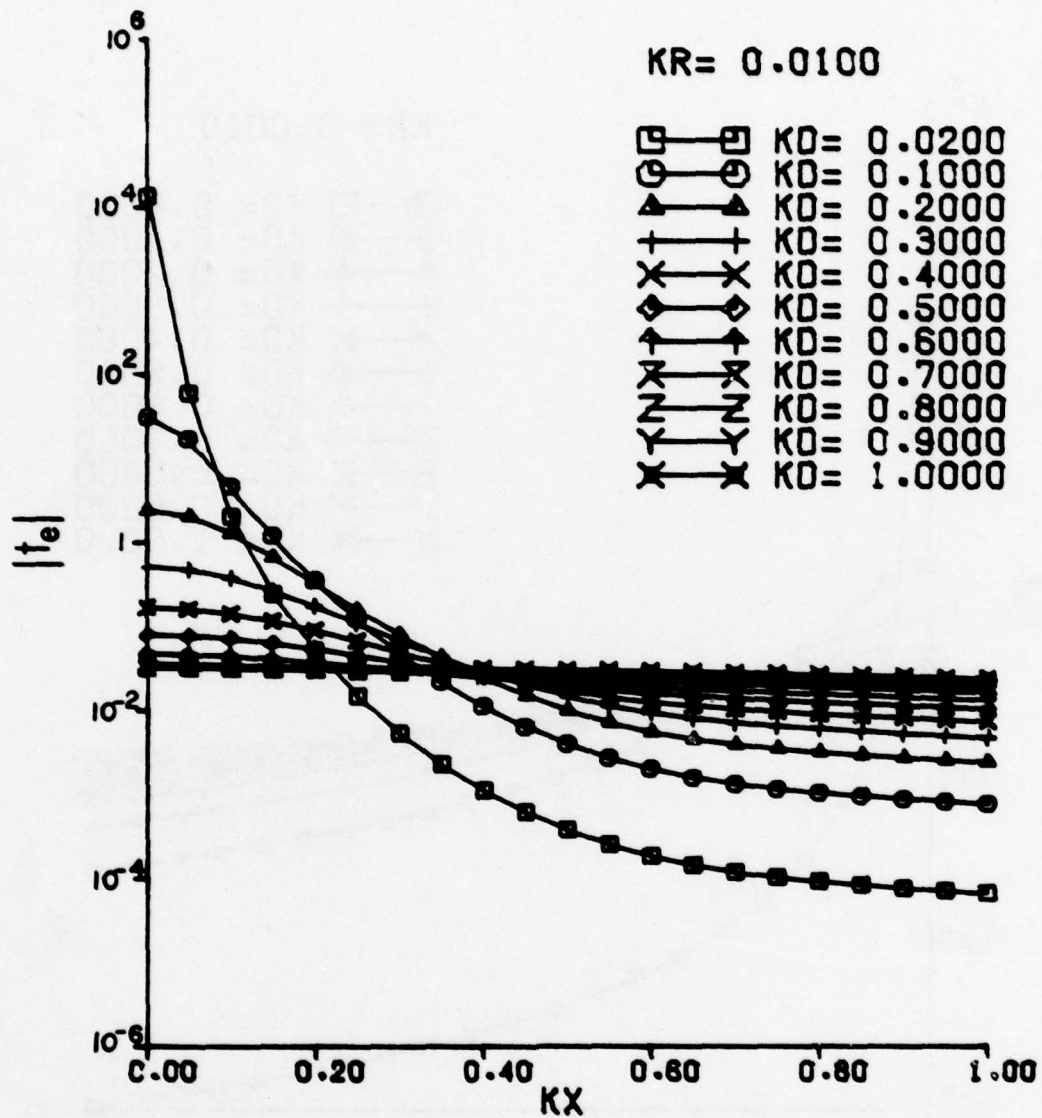


Fig. 29. Magnitude of  $t_e$  for a wire of radius  $kr = 0.01$ .

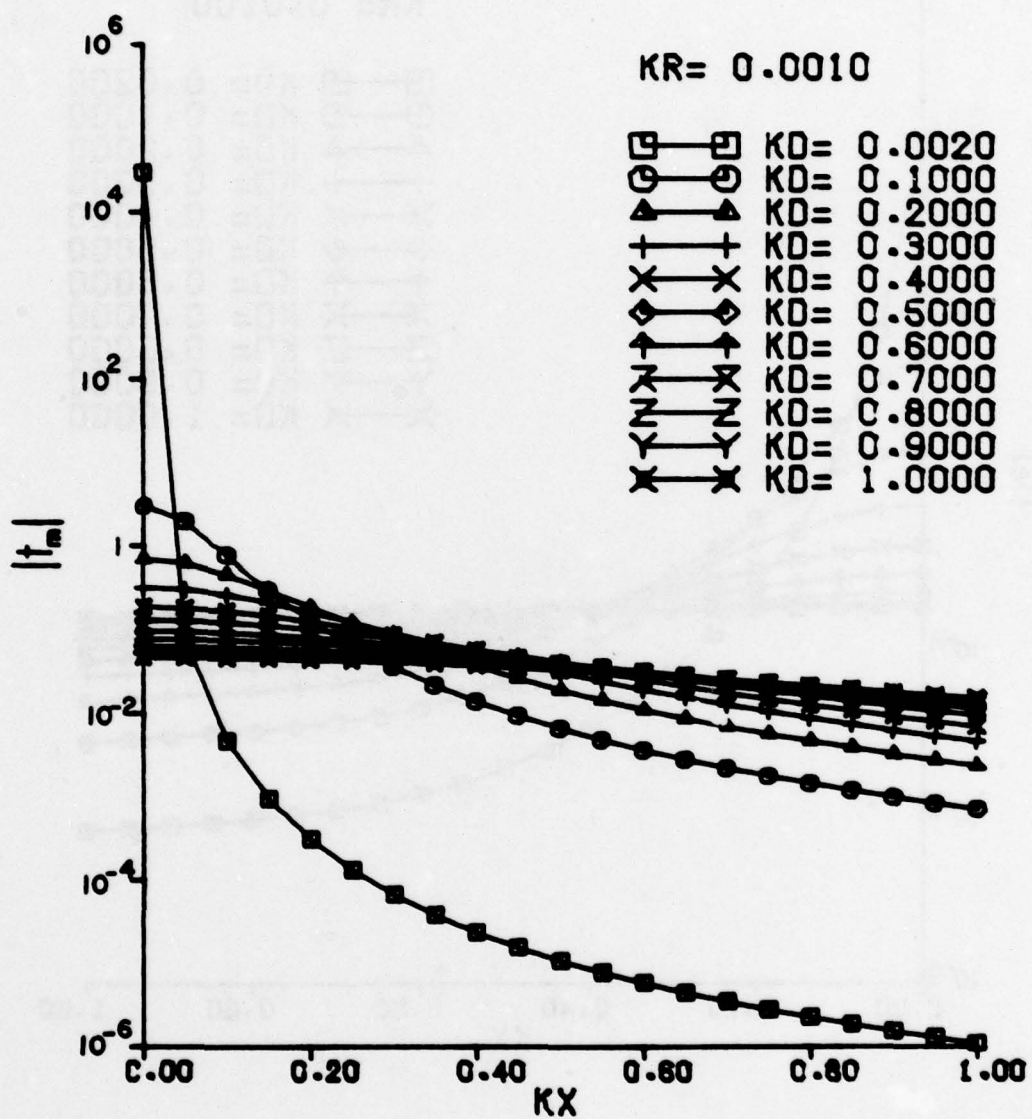


Fig. 30. Magnitude of  $t_m$  for a wire of radius  $kr = 0.001$ .

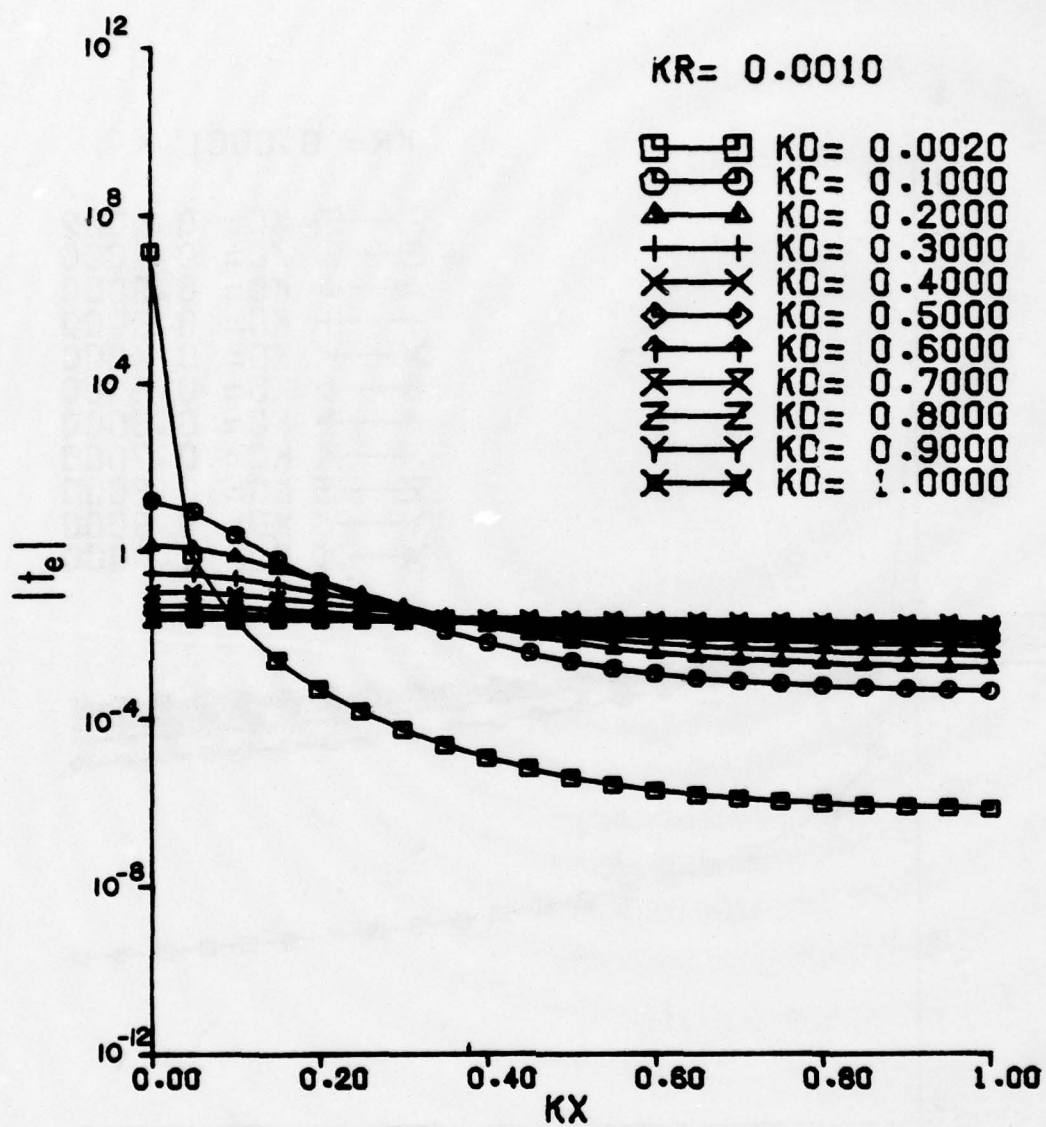


Fig. 31. Magnitude of  $t_e$  for a wire of radius  $kr = 0.001$ .

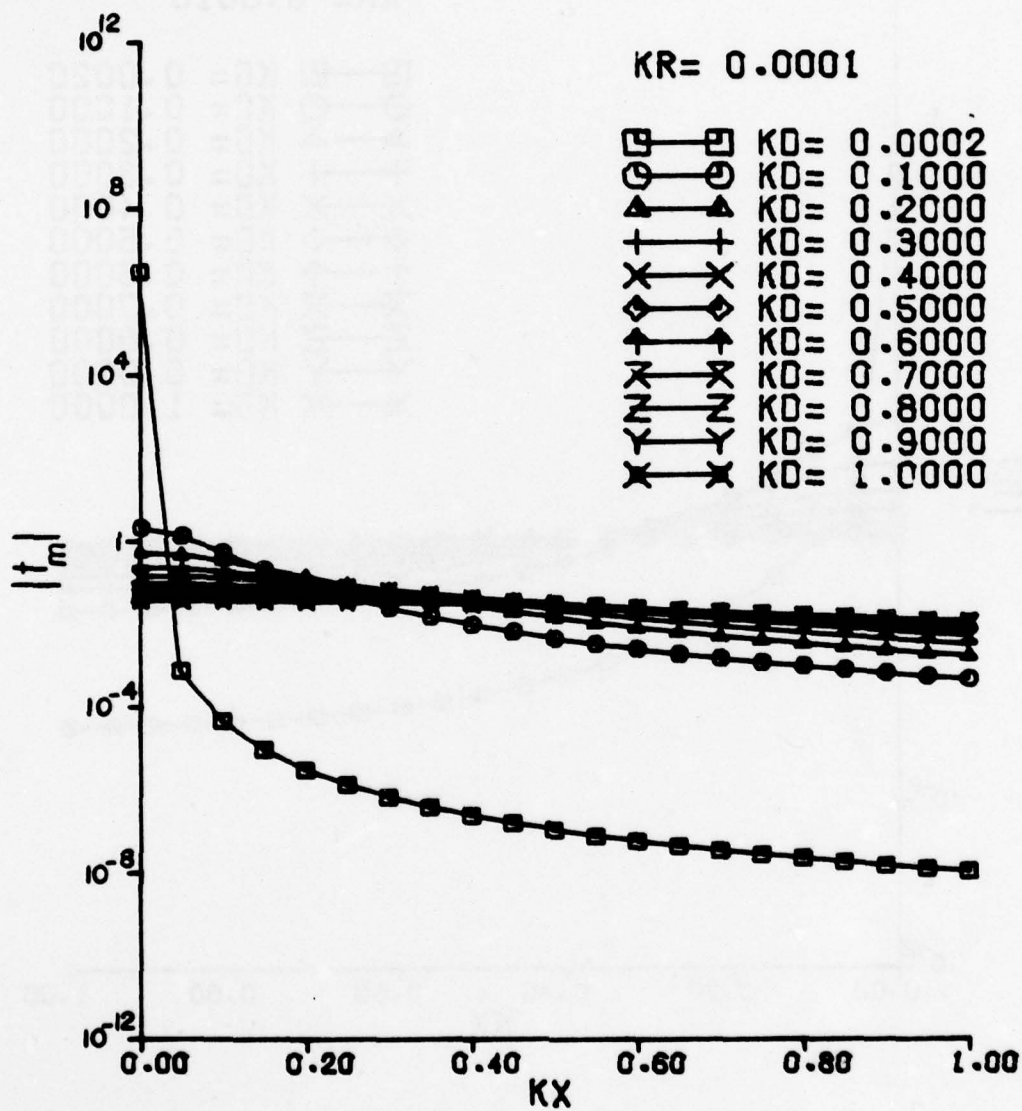


Fig. 32. Magnitude of  $t_m$  for a wire of radius  $kr = 0.0001$ .

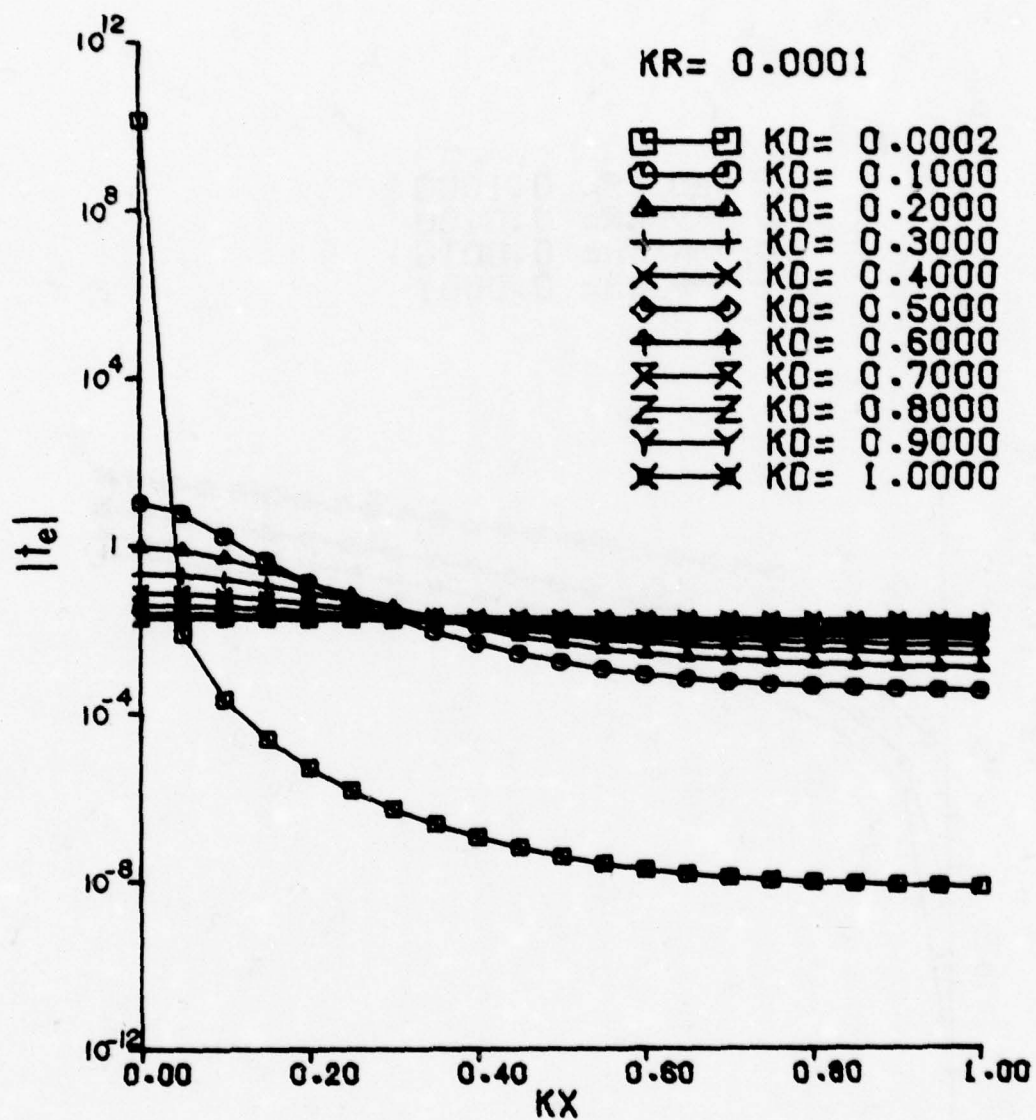


Fig. 33. Magnitude of  $t_e$  for a wire of radius  $kr = 0.0001$ .

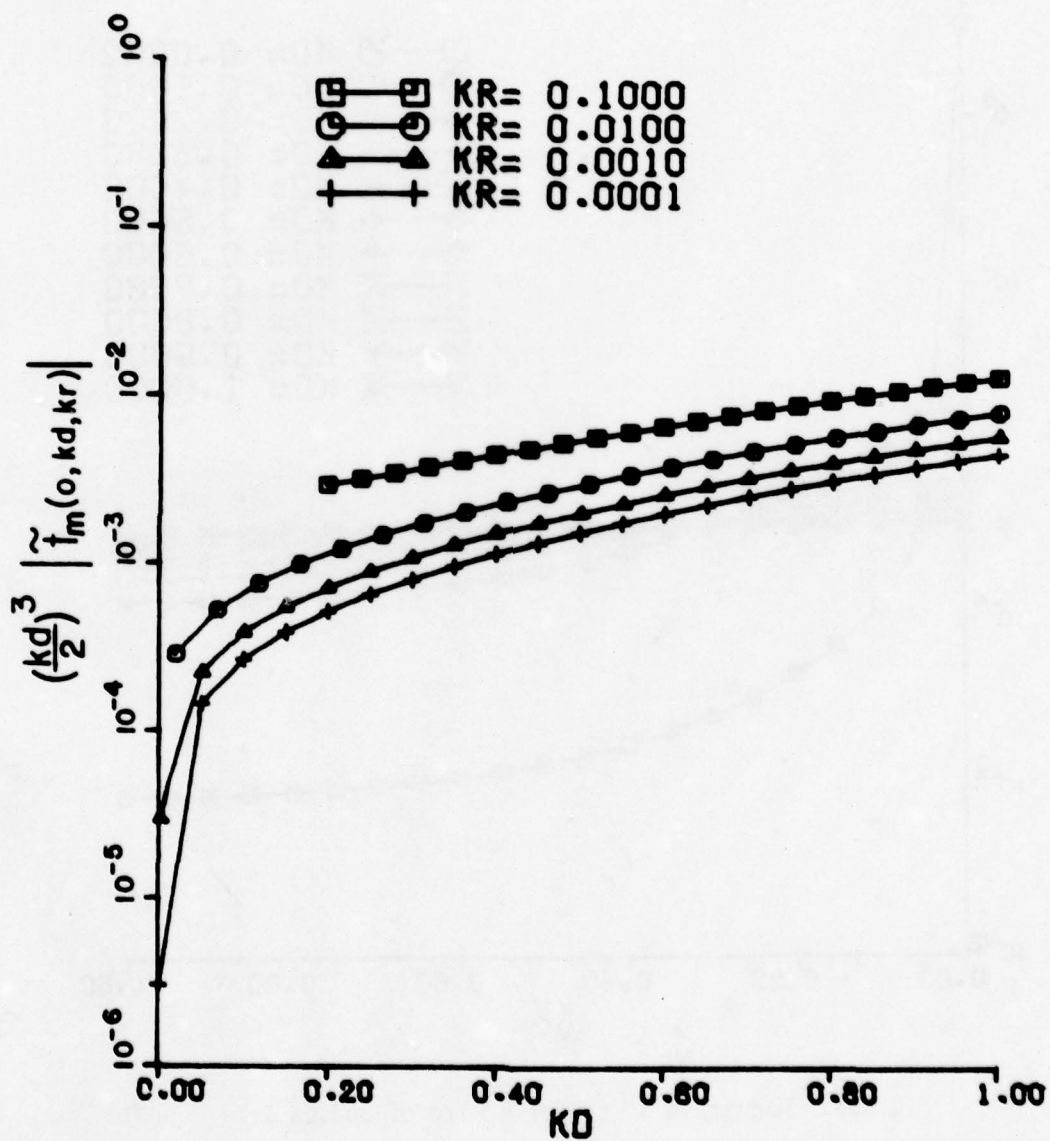


Fig. 34. Magnitude of  $(kd/2)^3 \tilde{t}_m(0, kd, kr)$ .

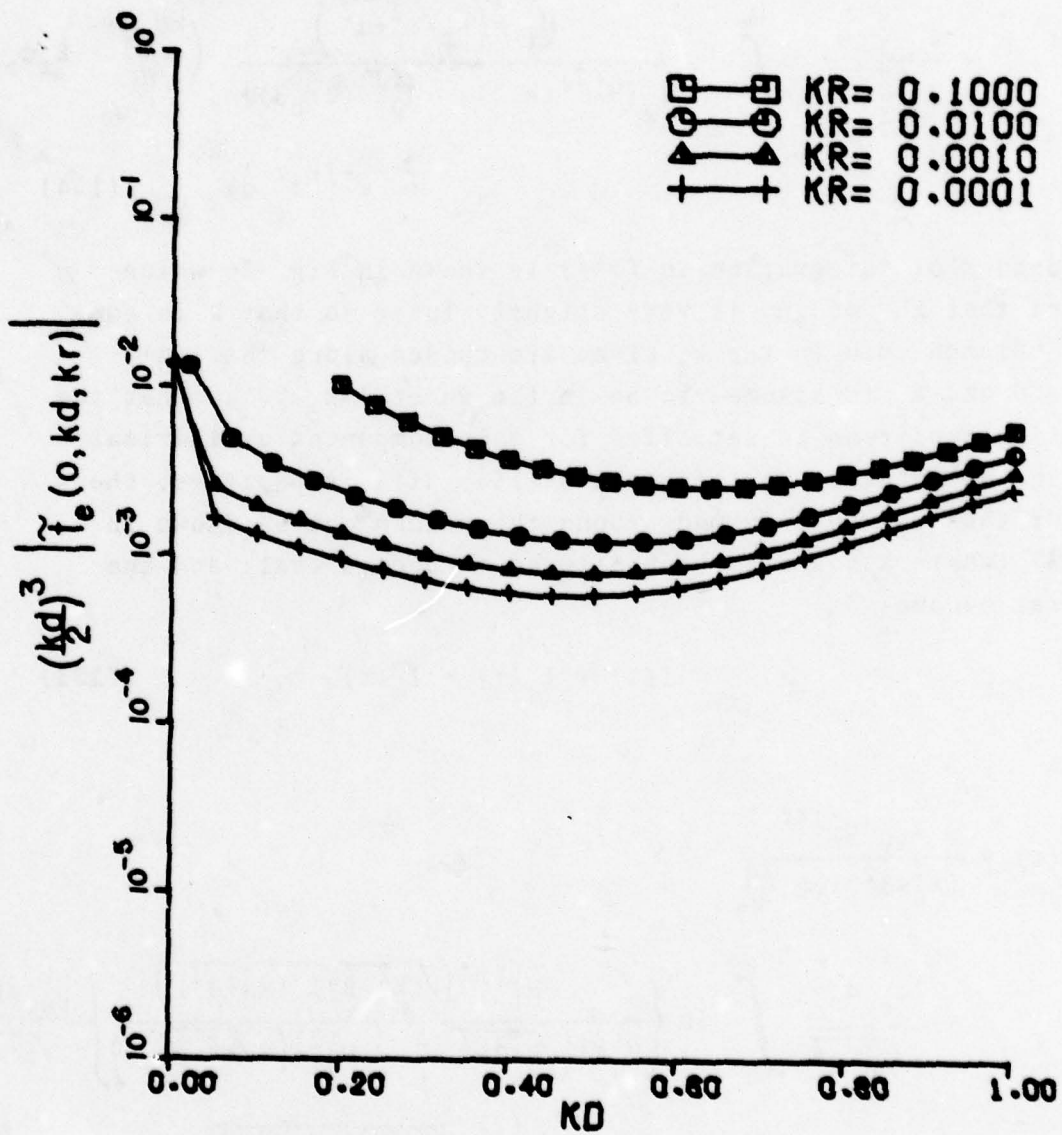


Fig. 35. Magnitude of  $(kd/2)^3 \tilde{t}_e(0, kd, kr)$ .

$$\begin{aligned}
 I(z) &= \frac{1}{\sqrt{2\pi}} \int_{-\infty}^{\infty} \tilde{I}(k_z) e^{-jk_z z} dk_z \\
 &= \frac{jd}{\pi \sqrt{x_0^2 + d^2}} \int_{-\infty}^{\infty} \frac{H_1^{(2)}(k_\rho \sqrt{x_0^2 + d^2})}{k_\rho [H_0^{(2)}(k_\rho r) - H_0^{(2)}(2k_\rho d)]} \left( \frac{kc_{mx}}{n} - k_z c_{ey} \right) \\
 &\quad \times e^{-jk_z z} dk_z \quad (154)
 \end{aligned}$$

The contour of integration in (154) is shown in Fig. 36 which assumes that the medium is very slightly lossy so that  $k$  is complex. Branch cuts in the  $k_z$  plane are chosen along the loci  $\text{Im} k_\rho = 0$  and  $k_z$  is assumed to be in the sheet  $\text{Im} k_\rho < 0$  so that the radiation condition is satisfied for each component cylindrical wave in the integral representation (154). If  $z$  is positive, the contour then may be deformed around the branch cut as shown in Fig. 37 (where  $k$  has also been allowed to become real) and the integral becomes

$$I(z) = I_e(z) + I_m(z) \quad (155)$$

where

$$\begin{aligned}
 I_e(z) &= \frac{c_{ey} d e^{-jkz}}{(x_0^2 + d^2) \log \frac{2d}{a}} \\
 &+ \frac{2c_{ey} d}{\pi \sqrt{x_0^2 + d^2}} \int_0^k \text{Im} \left\{ \frac{H_1^{(2)}(\sqrt{(k^2 - \beta^2)(x_0^2 + d^2)})}{H_0^{(2)}(\sqrt{k^2 - \beta^2} r) - H_0^{(2)}(2\sqrt{k^2 - \beta^2} d)} \right\} \frac{\beta e^{-j\beta z} d\beta}{\sqrt{k^2 - \beta^2}} \\
 &+ \frac{2c_{ey} d}{\pi \sqrt{x_0^2 + d^2}} \int_0^\infty \text{Im} \left\{ \frac{H_1^{(2)}(\sqrt{(k^2 + \alpha^2)(x_0^2 + d^2)})}{H_0^{(2)}(\sqrt{k^2 + \alpha^2} r) - H_0^{(2)}(2\sqrt{k^2 + \alpha^2} d)} \right\} \frac{\alpha e^{-\alpha z} d\alpha}{\sqrt{k^2 + \alpha^2}} \\
 &= -I_e(-z), \quad z > 0 \quad (156)
 \end{aligned}$$

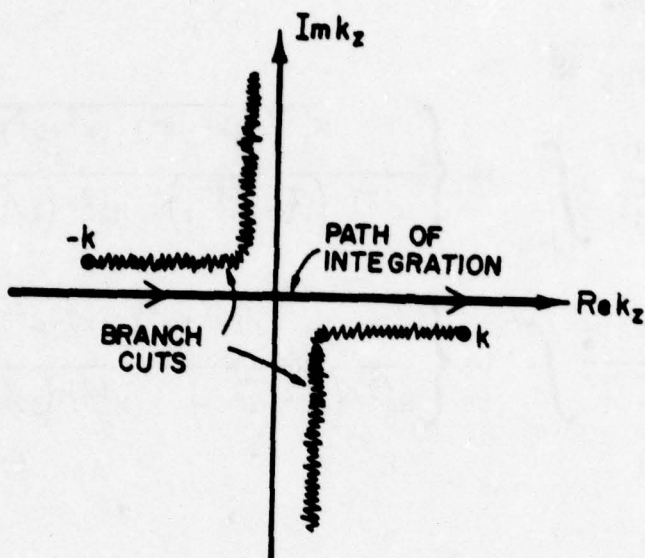


Fig. 36. Branch cuts and contour of integration in the  $k_z$  plane.

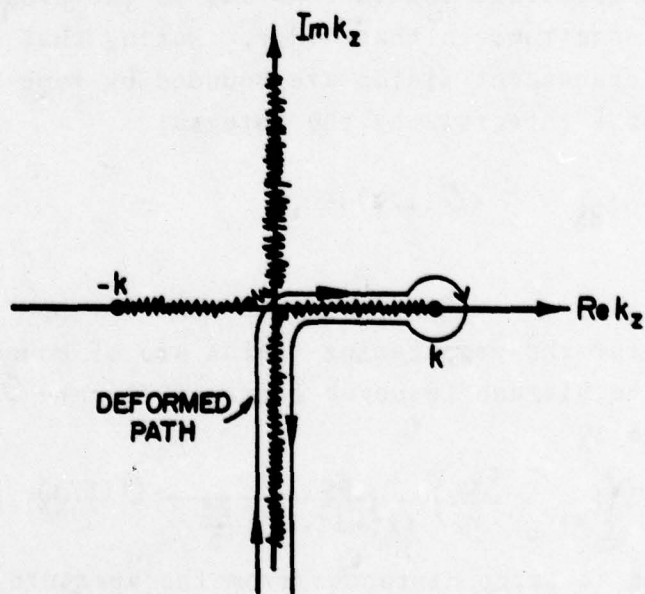


Fig. 37. Deformation of the contour around the branch cut.

$$\begin{aligned}
I_m(z) = & \frac{-c_{mx} de^{-jkz}}{\eta(x_0^2 + d^2) \log \frac{2d}{a}} \\
& - \frac{2c_{mx} kd}{\eta \pi \sqrt{x_0^2 + d^2}} \int_0^k \operatorname{Im} \left\{ \frac{H_1^{(2)} \sqrt{(k^2 - \beta^2)} (x_0^2 + d^2)}{H_0^{(2)} (\sqrt{k^2 - \beta^2} r) - H_0^{(2)} (2\sqrt{k^2 - \beta^2} d)} \right\} \frac{e^{-j\beta z} d\beta}{\sqrt{k^2 - \beta^2}} \\
& - j \frac{2c_{mx} kd}{\eta \pi \sqrt{x_0^2 + d^2}} \int_0^\infty \operatorname{Im} \left\{ \frac{H_1^{(2)} \sqrt{(k^2 + \alpha^2)} (x_0^2 + d^2)}{H_0^{(2)} (\sqrt{k^2 + \alpha^2} r) - H_0^{(2)} (2\sqrt{k^2 + \alpha^2} d)} \right\} \frac{e^{-\alpha z} d\alpha}{\sqrt{k^2 + \alpha^2}} \\
= & I_m(-z), \quad z > 0
\end{aligned} \tag{157}$$

The first two terms on the right hand side of (156) and (157) represent the TEM modes excited by the electric and magnetic dipoles, respectively, and arise from the branch point contribution from the deformed path in Fig. 37. The remaining two integrals in each expression represent the current due to the propagating and the evanescent spectrum, in that order. Noting that the integrands for the evanescent fields are bounded by some number  $C$ , we can bound those integrals by the integral

$$\int_0^\infty C e^{-\alpha z} d\alpha = \frac{C}{z} = \mathcal{O}(1/z). \tag{158}$$

The integrands for the propagating fields are of bounded variation and hence, by the Riemann-Lesbegue lemma, [23], are  $\mathcal{O}(1/z)$  as well. Hence, for large  $z$ ,

$$I(z) \sim \left( c_{ey} - \frac{c_{mx}}{\eta} \right) \frac{de^{-jkz}}{(x_0^2 + d^2) \log \frac{2d}{a}} + \mathcal{O}(1/z) \tag{159}$$

which shows that at large distances from the aperture, only the TEM wave is significant.

[23] E. T. Whittaker, G. N. Watson, A Course of Modern Analysis, New York: Cambridge Press, 1973, p. 172.

# APPENDIX A

## LUMPED ELEMENT TRAVELING WAVE SOURCE

In many network computations it is convenient to use scattering parameters, defined in (ref. A1), (ref. A2)

$$a_k = \frac{1}{2\sqrt{R_{0k}}} (V_k + Z_{0k} I_k) \quad (A1)$$

$$b_k = \frac{1}{2\sqrt{R_{0k}}} (V_k - Z_{0k}^* I_k) \quad (A2)$$

In the above,  $V_k$  and  $I_k$  are the actual (not normalized) voltage and current at port  $k$  of an  $N$ -port, while  $Z_{0k} = R_{0k} + jX_{0k}$  is the normalization impedance at port  $k$ . The asterisk denotes a complex-conjugate number. When scattering representation of networks is used, it is convenient to replace the voltage and current sources with corresponding traveling-wave sources. It seems that no convenient circuit elements have been found for that purpose. Penfield and Rafuse (ref. A3) have used a symbol reminiscent of a voltage source in combination with a directional coupler, such as in Figure A1. However, this symbol represents a pure traveling-wave source only in the limiting case when the coupling tends to zero and the voltage source tends to infinity. For any finite value of the coupling, a fraction of the energy from the main guide will be unavoidably absorbed in the matched termination.

- 
- A1. D. C. Youla, "On Scattering Matrices Normalized to Complex Port Numbers," Proc. I.R.E. Vol. 49, p. 1221, July 1961.
  - A2. M. T. Carlin, A. B. Giordano, Network Theory, an Introduction to Reciprocal and Nonreciprocal Circuits, Englewood Cliffs: Prentice Hall, 1964, pp. 326 and 144.
  - A3. P. Penfield, Jr., R. P. Rafuse, Varactor Applications, Cambridge: M.I.T. Press, 1962, p. 26.

A convenient source of the traveling-wave to be proposed here is a combination of the voltage source and the current source such as shown in Figure A2(a). To verify this, write the Kirchhoff laws for this circuit:

$$I_1 + I_2 + I_s = 0 \quad (A3)$$

$$V_1 - V_2 + V_s = 0 \quad (A4)$$

Take the normalization impedance for the port 1 to be  $Z_{01}$  and for the port 2 to be  $Z_{02}$ . Then using (A1) and (A2) obtain the following:

$$\begin{bmatrix} b_1 \\ b_2 \end{bmatrix} = \begin{bmatrix} \frac{Z_{02} - Z_{01}^*}{Z_{02} + Z_{01}} \sqrt{\frac{R_{01}}{R_{02}}} & \frac{Z_{02} + Z_{01}^*}{Z_{02} + Z_{01}} \\ \sqrt{\frac{R_{01}}{R_{02}}} & \frac{Z_{01} + Z_{01}^*}{Z_{01} + Z_{02}} \frac{Z_{01} - Z_{02}^*}{Z_{01} + Z_{02}} \end{bmatrix} \begin{bmatrix} a_1 \\ a_2 \end{bmatrix} + \begin{bmatrix} \sqrt{R_{02}} \frac{Z_{01} I_s - V_s}{Z_{01} + Z_{02}} \\ \sqrt{R_{01}} \frac{Z_{02} I_s + V_s}{Z_{01} + Z_{02}} \end{bmatrix} \quad (A5)$$

A convenient choice of the normalization impedance, is as follows:

$$Z_{01} = Z_{02}^* = Z_0 = R_0 + jX_0 \quad (A6)$$

When such a choice is made the diagonal terms in (A5) become zero and the two port in Figure A2a becomes an allpass:

$$\begin{bmatrix} b_1 \\ b_2 \end{bmatrix} = \begin{bmatrix} 0 & 1 \\ 1 & 0 \end{bmatrix} \begin{bmatrix} a_1 \\ a_2 \end{bmatrix} + \frac{1}{2\sqrt{R_0}} \begin{bmatrix} Z_0 I_s - V_s \\ Z_0^* I_s + V_s \end{bmatrix} \quad (A7)$$

Furthermore, the source of the outgoing wave at port 1 can be made equal to zero by choosing

$$I_s = \frac{V_s}{Z_0} \quad (A8)$$

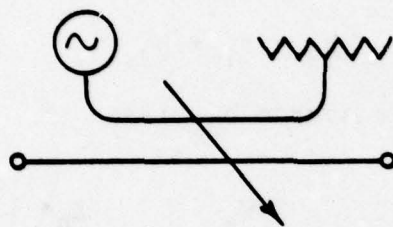
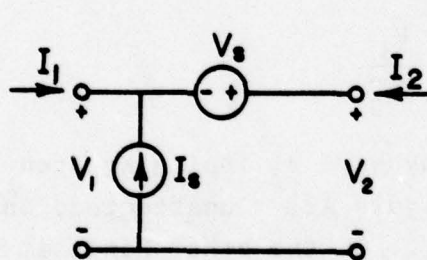
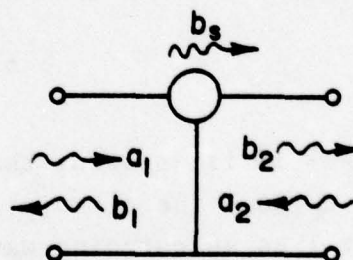


Fig. A1. Conventional symbol for traveling-wave source.



(a)



(b)

Fig. A2(a). Combination of voltage and current sources.

Fig. A2(b). Proposed symbol for traveling-wave source.

Therefore, under constraints (A6) and (A8), the circuit in Figure A2(a) becomes a true source of an outgoing wave emerging from port 2. Matrix equation (A5) reduces to

$$b_1 = a_2 \quad (A9)$$

$$b_2 = a_1 + b_{2s} \quad (A10)$$

where the outgoing-wave source  $b_{2s}$  is

$$b_{2s} = \frac{V_s}{2\sqrt{R_0}} \left( 1 + \frac{Z_0^*}{Z_0} \right) \quad (A11)$$

Very often, one chooses a real normalization:

$$Z_{01} = Z_{02} = R_0 \quad (A12)$$

so that the corresponding outgoing-wave source becomes

$$b_{2s} = \frac{V_s}{\sqrt{R_0}} \quad (A13)$$

From (A9) it is apparent that any wave  $a_2$  impinging upon port 2, passes through the circuit in Figure A2a unaffected, and emerges at port 1 as an outgoing wave  $b_1$ . On the other hand, it follows from (A10) that wave  $a_1$ , incident at port 1, passes unaffected through the circuit and emerges at port 2. In addition to  $a_1$ , a source wave  $b_{2s}$  also emerges at port 2. This source wave is independent of  $b_1$  or  $b_2$ . Hence, it has been shown that a source of a traveling wave is a twoport consisting of a voltage source and a current source such as in Figure A2a. These two sources must be related by (A8) and the normalization impedances must be selected according to (A6) for the complex normalization, or according to (A12) for the real normalization.

To simplify the circuit diagrams, the traveling-wave source between ports 1 and 2 could be represented by a single symbol such as in Figure A2b. Note that the symbol represents a two port which is a three-terminal device. The value of the source  $b_{2s}$  is given by (A11) for complex normalization and by (A13) for real normalization.

## APPENDIX B

## MATRIX ALGEBRA IN DIRAC'S NOTATION

The presented material is an abridgement from (ref. B1) and (ref. B2). A column vector in an N-dimensional space is denoted by

$$|x\rangle = \begin{pmatrix} x_1 \\ x_2 \\ \vdots \\ x_N \end{pmatrix}$$

A square matrix in an N-dimensional space is denoted by

$$\underline{A} = \begin{pmatrix} a_{11} & a_{12} & \cdots & a_{1N} \\ a_{21} & a_{22} & \cdots & a_{2N} \\ \vdots & \vdots & & \vdots \\ a_{N1} & a_{N2} & & a_{NN} \end{pmatrix}$$

Matrix  $\underline{A}$  is an operator. When it operates on vector  $|x\rangle$ , the result is a new vector  $|v\rangle$

$$|v\rangle = \underline{A}|x\rangle \quad (\text{B1})$$

Using the rule for matrix multiplication, one finds that the kth component of the vector  $|v\rangle$  is

$$v_k = \sum_{j=1}^N A_{kj} x_j \quad (\text{B2})$$

B1. B. Friedman, Principles and Techniques of Applied Mathematics, New York: Wiley, 1956, pp. 1-33.

B2. A. Messiah, Quantum Mechanics, Vol I, Amsterdam: North Holland, 1965, pp. 162-179.

The transpose conjugate of column vector  $|x\rangle$  is denoted by  $\langle x|$ , and it represents a row vector as follows

$$\langle x| = (x_1^* \ x_2^* \ \cdots \ x_N^*) , \quad (B3)$$

where  $*$  denotes a complex-conjugate value. The transpose conjugate of a square matrix  $\underline{A}$  is denoted  $\underline{A}^+$

$$\underline{A}^+ = \begin{pmatrix} a_{11}^* & \cdots & a_{N1}^* \\ a_{12}^* & \cdots & a_{N2}^* \\ \vdots & & \vdots \\ a_{1N}^* & \cdots & a_{NN}^* \end{pmatrix}$$

The transpose conjugate of a product of several matrices is obtained by reversing the order of multiplication and by taking the transpose conjugate of each individual matrix in the product:

$$(\underline{A} \ \underline{B} \ \underline{C})^+ = \underline{C}^+ \ \underline{B}^+ \ \underline{A}^+$$

The same rule applies if one of the matrices is a vector ( $=N \times 1$  matrix):

$$(\underline{A} \ \underline{B} \ |x\rangle)^+ = \langle x| \underline{A}^+ \ \underline{B}^+ \quad (B4)$$

The result of the above operation is a row vector. A matrix which is equal to its own transpose conjugate:

$$\underline{A}^+ = \underline{A}$$

is said to be Hermitian. Instead of  $N^2$  distinct elements, such a matrix contains only  $\frac{1}{2} N(N+1)$  distinct elements. The elements located symmetrically across the main diagonal are complex conjugates of each other. Also, the elements on the main diagonal are

all real.

Frequently, a product of a row vector and a column vector is to be computed as follows

$$\langle x|y \rangle = (x_1^* \ x_2^* \ \cdot \cdot \cdot \ x_N^*) \begin{pmatrix} y_1 \\ y_2 \\ \cdot \\ \cdot \\ y_N \end{pmatrix} = \sum_{j=1}^N x_j^* y_j \quad (B5)$$

The result of this operation is a scalar (= a complex number), and (B5) is called scalar product. The same two vectors  $|x\rangle$  and  $|y\rangle$  can be used to form a scalar product in the reverse order:

$$\langle y|x \rangle = (y_1^* \ y_2^* \ \cdot \cdot \cdot \ y_N^*) \begin{pmatrix} x_1 \\ x_2 \\ \cdot \\ \cdot \\ x_N \end{pmatrix} = \sum_{j=1}^N y_j^* x_j \ .$$

The result is equal to the complex conjugate of (B5). Thus,

$$\langle x|y \rangle = \langle y|x \rangle^* \ .$$

If one of the vectors in a scalar product has been obtained by the linear transformation such as in (B1) above, the scalar product takes the following form

$$\langle v|y \rangle = \langle x|\underline{A}^+|y \rangle \quad (B6)$$

Again, the result of this operation is a scalar. The right-hand side in (B6) may be interpreted as a scalar product of the row vector  $\langle x|\underline{A}^+$  with the column vector  $|y\rangle$ . Alternatively, (B6)

may be interpreted as a scalar product of the row vector  $\langle x|$  with the column vector  $\underline{A}^+|y\rangle$ . Computing the product in either way gives identical results, because a matrix multiplication is associative:

$$\underline{A} (\underline{B} \underline{C}) = (\underline{A} \underline{B}) \underline{C} .$$

When the order of multiplication in (B5) is such that a column vector multiplies a row vector:

$$|y\rangle\langle x| = \begin{pmatrix} y_1 \\ y_2 \\ \vdots \\ y_N \end{pmatrix} (x_1^* \ x_2^* \ \cdots \ x_N^*) ,$$

the result is a square matrix:

$$|y\rangle\langle x| = \begin{pmatrix} y_1 x_1^* & y_1 x_2^* & \cdots & y_1 x_N^* \\ \cdots & \cdots & \cdots & \cdots \\ y_N x_1^* & y_N x_2^* & \cdots & y_N x_N^* \end{pmatrix} \quad (B7)$$

This is a special class of a square matrix, defined by only  $2N$  distinct numbers ( $y_1$  through  $y_N$  and  $x_1$  through  $x_N$ ).

One of the advantages of writing the matrix equations in Dirac's notation is that the notation itself clearly indicates what type of the result one should expect. For example, the expressions like

$$\langle x|\underline{A}|x\rangle , \beta\langle c|x\rangle , \langle x|\underline{A}^+\underline{B}|y\rangle$$

represent scalars. Another class of expressions which looks like

$$\underline{A}|x\rangle, \quad |x\rangle\langle y|c\rangle, \quad \sum_{n=1}^N \alpha_n |x_n\rangle$$

represent vectors. Finally, the operations like

$$\underline{A} \underline{B} \underline{C}^+ \quad \text{or} \quad \underline{A}|x\rangle\langle b|\underline{B}|y\rangle\langle c|$$

will each result in a square matrix. For the sake of clarity, one should specify the following was assumed:

$B, \alpha_n \dots$  are scalars,

$|x_n\rangle, |x\rangle, |y\rangle, |b\rangle, |c\rangle \dots$  are vectors,

$\underline{A}, \underline{B}, \underline{C} \dots$  are square matrices.

## APPENDIX C

MULTICONDUCTOR-LINE FORMULATION BY SIMULTANEOUS  
DIAGONALIZATION OF TWO MATRICES

Multiconductor transmission line (abbrev. MTL) consists of  $N$  conductors and a reference, or a "ground" conductor. The voltages of each conductor with respect to reference are arranged in voltage vector  $|V\rangle$

$$|V\rangle = \begin{pmatrix} V_1 \\ \vdots \\ V_N \end{pmatrix}$$

and the currents are similarly arranged in current vector  $|I\rangle$ . The length coordinate of the MTL is  $z$ , while the cross section coordinates are  $x$  and  $y$ . The reference directions of the currents and voltages on any of the conductors are such that real, positive values of  $V_i$  and  $I_i$  result in a power flow in the positive  $z$  direction (see Fig. C1). On the lossless MTL, the sinusoidal steady-state voltages and currents are related through the following equations (see e.g. references [C1] through [C8])

$$\frac{d}{dz} |V\rangle = -j\omega \underline{L} |I\rangle \quad (C1)$$

$$\frac{d}{dz} |I\rangle = -j\omega \underline{K} |V\rangle \quad (C2)$$

$\underline{L}$  is the inductance matrix, and  $\underline{K}$  is the electric induction coefficient matrix. Often a symbol  $\underline{C}$  is used to denote the induction coefficient matrix. Unfortunately, some recent publications associate the erroneous term "capacitance matrix" with the symbol  $\underline{C}$  (see [C8] and [C9]), although the proper term should be "electric induction coefficient matrix" [C10]. To avoid the possible confusion, symbol  $\underline{K}$  has been used here.

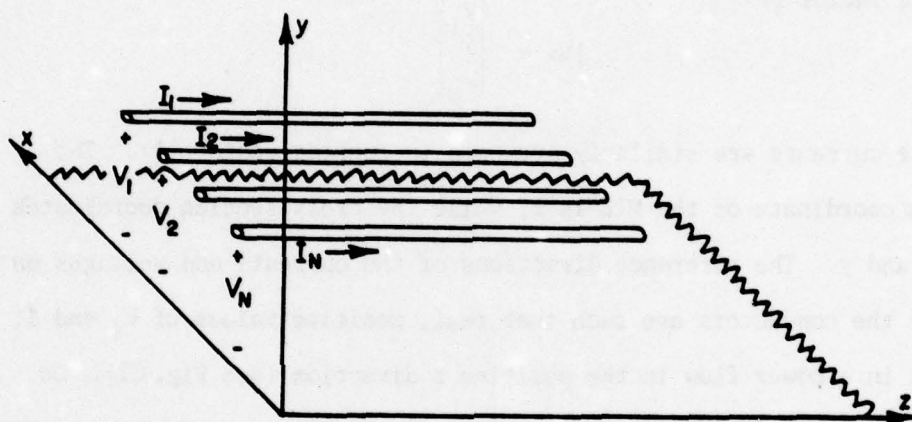


Fig. C1. Voltages and currents on MTL.

Only the lossless lines without magnetic materials and with isotropic dielectrics will be considered here. When the dielectric is homogeneous, the well-known TEM propagation occurs, in which all the waves propagate with the velocity of light. Such MTL are commonly treated in terms of impedance parameters [C11], [C8], image parameters scattering matrix parameters [C13], and chain parameters [C14].

When the dielectric between conductors is not homogeneous, the waves on MTL are HEM, [C15], i.e. both the electric and the magnetic vectors acquire a longitudinal component. However, the dominant HEM modes do not have a cutoff frequency, and at very low frequencies, their longitudinal field components are negligibly small. For this reason these dominant HEM waves are called "quasi-TEM" waves, which are the subject of the present report.

The formulation of voltages and currents on MTL in terms of voltage and current eigenvectors, as introduced by Anemiyi [C6] and Marx [C7], is well suited to the treatment of transients as well as steady state waveforms. Their analysis starts from the decoupled equations, which are obtained from (C1) and (C2):

$$\frac{d^2}{dz^2} |V\rangle = -\omega^2 \underline{L} \underline{K} |V\rangle \quad (C3)$$

$$\frac{d^2}{dz^2} |I\rangle = -\omega^2 \underline{K} \underline{L} |I\rangle \quad (C4)$$

In the present report, the eigenvector formulation of Anemiyi and Marx will be extended by using a simultaneous diagonalization of two matrices, [C8], [C16], [C17]. For this purpose, it is convenient to rewrite (C3) and (C4) as follows:

$$\underline{L}^{-1} \frac{d^2}{dz^2} |V\rangle = -\omega^2 \underline{K} |V\rangle \quad (C5)$$

$$\underline{K}^{-1} \frac{d^2}{dz^2} |I\rangle = -\omega^2 \underline{L} |I\rangle \quad (C6)$$

The method of simultaneous diagonalization of two real, symmetric matrices, [C16], presents a convenient way of solving these two equations. The method can be applied only when one of the two matrices is positive definite. Since both  $\underline{L}$  and  $\underline{K}$  matrices represent the stored energy of a passive multiconductor network, they are both positive definite and thus qualify.

The first step in the method is to find the eigenvectors  $|x_i\rangle$  and eigenvalues  $\lambda_i$  of the matrix  $\underline{L}^{-1}$ :

$$\underline{L}^{-1} |x_i\rangle = \lambda_i |x_i\rangle \quad (C7)$$

The corresponding eigenvalue equation is

$$\det(\underline{L}^{-1} - \lambda \underline{U}) = 0 \quad (C8)$$

where  $\underline{U}$  is the identity matrix. It is convenient to make eigenvectors orthonormal:

$$\langle x_i | x_j \rangle = \delta_{ij} \text{ (Kroneker delta)} \quad (C9)$$

Next, a square matrix  $\underline{G}$  is formed, having eigenvectors  $|x_i\rangle$  for its columns

$$\underline{G} = (|x_1\rangle, \dots, |x_N\rangle) \quad (C10)$$

$\underline{G}$  is an orthogonal real matrix which diagonalizes  $\underline{L}^{-1}$  as follows

$$\underline{G}^+ \underline{L}^{-1} \underline{G} = \begin{pmatrix} \lambda_1 & & 0 \\ & \dots & \\ 0 & & \lambda_N \end{pmatrix} = \underline{\Lambda} \quad (C11)$$

where superscript + denotes a transpose conjugate. Since  $\underline{L}^{-1}$  is positive definite,  $\lambda_i$ 's are positive real. Therefore, it is meaningful to define a square-root matrix  $\underline{\Lambda}^{1/2}$

$$\underline{\Lambda}^{1/2} = \begin{pmatrix} \sqrt{\lambda_1} & & 0 \\ & \ddots & \\ 0 & & \sqrt{\lambda_N} \end{pmatrix} \quad (C12)$$

such that

$$\underline{\Lambda}^{-1/2} \underline{\Lambda} \underline{\Lambda}^{-1/2} = \underline{U}$$

with  $\underline{U}$  being an identity matrix.

Next, a new variable,  $|y\rangle$ , is defined in terms of  $|V\rangle$  :

$$|V\rangle = \underline{G} \underline{\Lambda}^{-1/2} |y\rangle \quad (C13)$$

When this change of variables is introduced in (C5), the following equation is obtained

$$\frac{d^2}{dz^2} |y\rangle = -\omega^2 \underline{B} |y\rangle \quad (C14)$$

where  $\underline{B}$  is a symmetric real matrix

$$\underline{B} = \underline{\Lambda}^{-1/2} \underline{G}^+ \underline{K} \underline{G} \underline{\Lambda}^{-1/2} \quad (C15)$$

where (C11) has been used to eliminate matrix  $\underline{L}$ .

Thus,  $\underline{B}$  can be diagonalized by an orthogonal transformation matrix, which will be here denoted by  $\underline{Q}$ . The eigenvalues of  $\underline{B}$  are all real positive. It comes out that they have a dimension of inverse velocity squared:

$$\underline{B} |t_i\rangle = \frac{1}{v_i^2} |t_i\rangle \quad (C16)$$

where  $|t_i\rangle$  are eigenvectors of  $\underline{B}$ . Transformation matrix  $\underline{Q}$  consists of

orthonormal eigenvectors  $|t_i\rangle$  as its columns:

$$Q = (|t_1\rangle \dots |t_N\rangle) \quad (C17)$$

$Q$  diagonalizes  $B$  as follows

$$Q^* B Q = \begin{pmatrix} \frac{1}{v_1^2} & & 0 \\ & \ddots & \\ 0 & & \frac{1}{v_N^2} \end{pmatrix} \quad (C18)$$

(C14) can be thus diagonalized by the following change of variables

$$|y\rangle = Q |\xi\rangle \quad (C19)$$

Using (C19) in (C14) one obtains the diagonal equation

$$\frac{d^2}{dz^2} |\xi\rangle = - \begin{pmatrix} \beta_1^2 & & 0 \\ & \ddots & \\ 0 & & \beta_N^2 \end{pmatrix} |\xi\rangle \quad (C20)$$

where

$$\beta_i^2 = \frac{\omega^2}{v_i^2} \quad \text{for } i = 1, 2, \dots, N \quad (C21)$$

(C20) is a decoupled system of differential equations

$$\frac{d^2}{dz^2} \xi_i = -\beta_i^2 \xi_i \quad \text{for } i = 1, 2, \dots, N \quad (C22)$$

which has exponential solutions

$$\xi_i = \xi_i^+ e^{-j\beta_i z} + \xi_i^- e^{j\beta_i z} \quad (C23)$$

These are the normal modes (or fundamental modes) of the multiconductor transmission line, each of them propagating with its own propagation constant  $\beta_i$  in the positive or negative  $z$  direction. The total vector

$|\xi\rangle$  is then

$$|\xi\rangle = \sum_{i=1}^N (\xi_i^+ e^{-j\beta_i z} + \xi_i^- e^{j\beta_i z}) |u_i\rangle \quad (C24)$$

where  $|u_i\rangle$  denotes a unit column vector having all zero components except the  $i$ th:

$$|u_i\rangle = \begin{pmatrix} 0 \\ 0 \\ \vdots \\ 1 \\ \vdots \\ 0 \end{pmatrix} \leftarrow i\text{th row} \quad (C25)$$

Vector  $|\xi\rangle$  thus represents the state of the multiconductor transmission line in terms of individual modes, the component  $\xi_i$  describes the magnitude of the  $i$ th mode at some position  $z$  along the line. Each mode has in turn certain magnitude of voltage and current on each of the conductors of the multiconductor transmission line. The voltages on individual conductors can now be determined by transforming the coordinates  $|\xi\rangle$  back into  $|V\rangle$ , where the transformation is specified by (C13) and (C19)

$$|V\rangle = \underline{G} \underline{\Lambda}^{-1/2} Q |\xi\rangle \quad (C26)$$

The voltages on individual conductors are now

$$|V\rangle = \sum_{i=1}^N (\xi_i^+ e^{-j\beta_i z} + \xi_i^- e^{j\beta_i z}) \underline{G} \underline{\Lambda}^{-1/2} |t_i\rangle \quad (C27)$$

In the above (C17) was used to write  $Q|u_i\rangle = |t_i\rangle$ . The current vector may now be obtained from  $|V\rangle$  by using (C1):

$$|I\rangle = \sum_{i=1}^N \frac{\beta_i}{\omega} (\xi_i^+ e^{-j\beta_i z} - \xi_i^- e^{j\beta_i z}) \underline{L}^{-1} \underline{G} \underline{\Lambda}^{-1/2} |t_i\rangle \quad (C28)$$

The power carried along the multiconductor transmission line is

$$P = \frac{1}{2} \operatorname{Re} \langle V | I \rangle \quad (\text{C29})$$

where  $\langle V |$  denotes a transpose conjugate of  $|V\rangle$ , and  $\operatorname{Re}$  denotes the real part. For simplicity, consider only the waves propagating in positive  $z$  direction ( $\xi_i^- = 0$  for all  $i$ ). Then, (C29) gives the following simple expression for the power transmitted in the positive  $z$  direction:

$$P^+ = \frac{1}{2} \sum_{i=1}^N \frac{1}{v_i} |\xi_i^+|^2 \quad (\text{C30})$$

The  $i$ th mode carries the power  $\frac{1}{2} |\xi_i^+|^2 / v_i$ . In analogy with the two-wire transmission lines (which e.g. consist of a single conductor and a shield), the forward-wave scattering amplitude of the  $i$ th mode will be denoted by  $a_i$ , and the reverse-wave amplitude with  $b_i$ :

$$a_i = \frac{\xi_i^+}{\sqrt{v_i}}, \quad b_i = \frac{\xi_i^-}{\sqrt{v_i}} \quad (\text{C31})$$

so that the forward-traveling wave carries the power  $\frac{1}{2} |a_i|^2$ , and the reverse-traveling wave the power  $\frac{1}{2} |b_i|^2$ . In terms of scattering amplitudes, (C27) becomes

$$|V\rangle = \sum_{i=1}^N (a_i e^{-j\beta_i z} + b_i e^{j\beta_i z}) |\phi_i\rangle \quad (\text{C32})$$

where the voltage eigenvector  $|\phi_i\rangle$  is defined as

$$|\phi_i\rangle = \sqrt{v_i} \underline{G} \underline{\Lambda}^{-1/2} |t_i\rangle \quad (\text{C33})$$

The current vector  $|I\rangle$  from (C28) may be expressed in terms of the same voltage eigenvectors  $|\phi_i\rangle$  as follows:

$$|I\rangle = \sum_{i=1}^N (a_i e^{-j\beta_i z} - b_i e^{j\beta_i z}) \frac{1}{v_i} \underline{L}^{-1} |\phi_i\rangle \quad (C34)$$

Alternately, one can introduce the current eigenvectors  $|\psi_i\rangle$  as follows:

$$|\psi_i\rangle = \frac{1}{v_i} \underline{L}^{-1} |\phi_i\rangle \quad (C35)$$

and represent the current vector as

$$|I\rangle = \sum_{i=1}^N (a_i e^{-j\beta_i z} - b_i e^{j\beta_i z}) |\psi_i\rangle \quad (C36)$$

If (C36) is substituted in (C2), an alternative expression for  $|V\rangle$  is obtained

$$|V\rangle = \sum_{i=1}^N (a_i e^{-j\beta_i z} + b_i e^{j\beta_i z}) \frac{1}{v_i} \underline{K}^{-1} |\psi_i\rangle \quad (C36a)$$

Comparison with (C32) yields

$$|\phi_i\rangle = \frac{1}{v_i} \underline{K}^{-1} |\psi_i\rangle \quad (C37)$$

Normalized voltage eigenvectors  $|\phi_i\rangle$ , defined by (C33), are also eigenvectors of the matrix  $\underline{L} \underline{K}$

$$\underline{L} \underline{K} |\phi_i\rangle = \frac{1}{v_i} \underline{L} |\phi_i\rangle \quad (C38)$$

what can be verified by using (C33) and (C16). Similarly,  $|\psi_j\rangle$  is the eigenvector of the matrix  $\underline{K} \underline{L}$

$$\underline{K} \underline{L} |\psi_j\rangle = \frac{1}{v_j} \underline{K} |\psi_j\rangle \quad (C39)$$

Voltage and current eigenvectors form the bi-orthonormal set

$$\langle \phi_i | \psi_j \rangle = \delta_{ij} \quad (C40)$$

From (C37) and (C11) the explicit expression for current eigenvector is obtained

$$|\psi_i\rangle = \frac{1}{\sqrt{V_i}} \underline{G} \underline{\Lambda}^{1/2} |t_i\rangle \quad (C41)$$

Following the notation from [C6] and [C7], define  $\underline{M}_V$  as a matrix which contains the voltage eigenvectors as its columns:

$$\underline{M}_V = (|\phi_1\rangle \dots |\phi_N\rangle) \quad (C42)$$

Similarly  $\underline{M}_I$  is a matrix containing all the current eigenvectors

$$\underline{M}_I = (|\psi_1\rangle \dots |\psi_N\rangle) \quad (C43)$$

An arbitrary forward traveling wave is, from (C32)

$$|V_f\rangle = \sum_{i=1}^N a_i e^{-j\beta_i z} |\phi_i\rangle \quad (C44)$$

Take the scalar product from the left with  $\langle\psi_j|$

$$\langle\psi_j|V_f\rangle = \sum_{i=1}^N a_i e^{-j\beta_i z} \langle\psi_j|\phi_i\rangle = a_j e^{-j\beta_j z}$$

Thus, the expansion (C44) can be also written as

$$|V_f\rangle = \sum_{i=1}^N \langle\psi_i|V_f\rangle |\phi_i\rangle$$

Since the bracket is a scalar, one can place it behind  $|\phi_i\rangle$

$$|V_f\rangle = \sum_{i=1}^N |\phi_i\rangle \langle\psi_i|V_f\rangle \quad (C45)$$

The above is true for arbitrary  $|V_f\rangle$ , thus the following identity is obtained

$$\sum_{i=1}^N |\phi_i\rangle \langle\psi_i| = \underline{U}$$

which can also be written as

$$\underline{M}_I \underline{M}_V^* = \underline{U} \quad (C46)$$

Similarly, one obtains

$$\underline{M}_V \underline{M}_I^* = \underline{U} \quad (C47)$$

When the propagation is assumed to be in the forward  $z$  direction, as in (C44), the current vector for an arbitrary forward-traveling mixture of modes is

$$|I_f\rangle = \sum_{i=1}^N a_i e^{-j\beta_i z} |\psi_i\rangle \quad (C48)$$

By multiplying from the left with  $\langle \phi_j |$  one obtains

$$a_j e^{-j\beta_j z} = \langle \phi_j | I_f \rangle$$

Comparison of this equation and (C45) yields

$$|V_f\rangle = \sum_{i=1}^N \langle \phi_i | I_f \rangle |\phi_i\rangle$$

Again, the bracket is a scalar, thus it may postmultiply  $|\phi_i\rangle$  :

$$|V_f\rangle = \sum_{i=1}^N |\phi_i\rangle \langle \phi_i | I_f \rangle = \underline{Z}_0 |I_f\rangle$$

The matrix relating  $|V_f\rangle$  and  $|I_f\rangle$  is the characteristic impedance matrix

$\underline{Z}_0$ :

$$\underline{Z}_0 = \sum_{i=1}^N |\phi_i\rangle \langle \phi_i| = |\phi_1\rangle \langle \phi_1| + \dots + |\phi_N\rangle \langle \phi_N| \quad (C49)$$

This can be written as

$$\underline{Z}_0 = \underline{M}_V \underline{M}_V^* = \underline{M}_V \underline{M}_I^{-1} \quad (C50)$$

where also (C46) has been used. Similarly one finds the characteristic admittance matrix as

$$\underline{Y}_0 = \underline{Z}_0^{-1} = \underline{M}_I \underline{M}_I^+ = \underline{M}_I \underline{M}_V^{-1} \quad (C51)$$

Multiplying (C49) from the right by  $|\psi_j\rangle$  and using the biorthogonality property (C40) one obtains

$$|\phi_j\rangle = \underline{Z}_0 |\psi_j\rangle \quad (C52)$$

which has the inverse

$$|\psi_j\rangle = \underline{Y}_0 |\phi_j\rangle \quad (C53)$$

Characteristic impedance and admittance matrices can be also related through matrices  $\underline{L}$  and  $\underline{K}$ . The relationship can be obtained by substituting (C35) into (C42) and (C43)

$$\underline{M}_V = \underline{L} \underline{M}_I \underline{v} \quad (C54)$$

where the diagonal velocity matrix is defined as

$$\underline{v} = \text{diag} (v_1, v_2, \dots, v_N) \quad (C55)$$

When (C37) is substituted into (C42) and (C43) it follows

$$\underline{M}_I = \underline{K} \underline{M}_V \underline{v} \quad (C56)$$

If these equations are now substituted in (C51) the following relation is obtained

$$\underline{Y}_0 \underline{L} = \underline{K} \underline{Z}_0 \quad (C57)$$

For each mode  $i$ , there is a fixed ratio of the voltage and current on conductor  $j$ . This ratio is also called a characteristic impedance of the conductor  $j$  for the mode  $i$ , denoted  $Z_{0i}^j$ , [C18]. These characteristic impedances

(scalars) are not to be confused with the elements of the characteristic admittance matrix  $\underline{Z}_0$ . If the coordinates of the eigenvectors are denoted by superscripts, such as

$$|\phi_i\rangle = \begin{pmatrix} \phi_i^1 \\ \vdots \\ \phi_i^N \\ \phi_i^N \end{pmatrix} ; \quad |\psi_i\rangle = \begin{pmatrix} \psi_i^1 \\ \vdots \\ \psi_i^N \\ \psi_i^N \end{pmatrix}$$

then, for the mode  $i$ , the characteristic impedance of the  $j$ th conductor is

$$Z_{0i}^j = \frac{\phi_i^j}{\psi_i^j} = \frac{\langle u_j | \underline{Z}_0 | \psi_i \rangle}{\langle u_j | \psi_i \rangle} \quad (C58)$$

## REFERENCES

- [1] H.A. Bethe, "Theory of Diffraction by Small Holes", Phys. Rev., Vol. 66, pp. 163-182, October 1944.
- [2] S.A. Schelkunoff, Electromagnetic Waves, Princeton: Van Nostrand, 1943, p. 129.
- [3] R.F. Harrington, Time-Harmonic Electromagnetic Fields, New York: McGraw-Hill, 1961, p. 78.
- [4] W.L. Weeks, Electromagnetic Theory for Engineering Applications, New York: Wiley, 1964, p. 310.
- [5] G.L. Matthaei, L. Young, E.M.T. Jones, Microwave Filters, Impedance-Matching Networks and Coupling Structures, New York: McGraw-Hill, 1964, pp. 229-243.
- [6] C.E. Baum, K.S.H. Lee, "Application of Modal Analysis to Braided-Shield Cables", Interaction Note 132, January 1973.
- [7] C.E. Baum, "Some Characteristics of Electric and Magnetic Dipole Antennas for Radiating Transient Pulses", Sensor and Simulation Note 125, January 1971, p. 16.
- [8] S.A. Schelkunoff, Electromagnetic Waves, Princeton: Van Nostrand, 1943, p. 162.
- [9] R.F. Harrington, Time-Harmonic Electromagnetic Fields, New York: McGraw-Hill, 1961, p. 100.
- [10] W.L. Weeks, Electromagnetic Theory for Engineering Applications, New York: Wiley, 1964, p. 565.
- [11] S.B. Cohn, "Determination of Aperture Parameters by Electrolytic-Tank Measurements", Proc. I.R.E., Vol 39, pp. 1416-1421 November 1951.
- [12] S.B. Cohn, "The Electric Polarizability of Apertures of Arbitrary Shape", Proc. I.R.E., Vol. 40, pp. 1069-1071, September 1952.
- [13] D. Kajfez, "Excitation of a Terminated TEM Transmission Line through a Small Aperture," Interaction Note 215, July 1974.
- [14] R.E. Collin, Foundations for Microwave Engineering, New York: McGraw-Hill, 1966, p. 146.

- [15] M.T. Carlin, A.B. Giordano, Network Theory, an Introduction to Reciprocal and Nonreciprocal Circuits, Englewood Cliffs: Prentice Hall, 1964.
- [16] W.T. Weeks, "Calculation of Coefficients of Capacitance of Multi-conductor Transmission Lines in the Presence of Dielectric Interface," IEEE Transactions on Microwave Theory Techn., Vol. MTT-18, pp. 35-43, Jan. 1970.
- [17] J.C. Clements, C.R. Paul, A.T. Adams, "Computation of the Capacitance Matrix for Systems of Dielectric-Coated Cylindrical Conductors," IEEE Transactions on Electromag. Compat., Vol. EMC-17, No. 4, pp. 238-248, November 1975. Also see Correction in EMC-18, No. 2, pp. 88-89, May 1976.
- [18] C.R. Paul, "Computation of the Transmission Line Inductance and Capacitance Matrices from the Generalized Capacitance Matrix," IEEE Transactions Electromag. Compat., Vol. EMC-18, No. 4, pp. 175-183, November 1976.
- [19] B. Friedman, Principles and Techniques of Applied Mathematics, New York: Wiley, 1956, p. 34.
- [20] R.E. Collin, Foundations for Microwave Engineering, New York: McGraw-Hill, 1966, p. 111.
- [21] G.L. Matthaei, L. Young, E.M.T. Jones, Microwave Filters, Impedance-Matching Networks, and Coupling Structures, New York: McGraw-Hill, 1964, p. 242.
- [22] K.S.H. Lee, F. C. Yang, "A Wire Passing by a Circular Aperture in an Infinite Ground Plane," Interaction Note 317, February 1977.
- [23] E.T. Whittaker, G.N. Watson, A Course of Modern Analysis, New York: Cambridge Press, 1973, p. 172.
- [A1] D. C. Youla, "On Scattering Matrices Normalized to Complex Port Numbers," Proc. I.R.E., Vol 49, p. 1221, July 1961.
- [A2] M. T. Carlin, A. B. Giordano, Network Theory, an Introduction to Reciprocal and Nonreciprocal Circuits, Englewood Cliffs: Prentice Hall, 1964, pp. 326 and 144.
- [A3] P. Penfield, Jr., R. P. Rafuse, Varactor Applications, Cambridge: M.I.T. Press, 1962, p. 26.
- [B1] B. Friedman, Principles and Techniques of Applied Mathematics, New York: Wiley, 1956, pp. 1-33.

- [B2] A. Messiah, Quantum Mechanics, Vol. I, Amsterdam: North Holland, 1965, pp. 162-179.
- [C1] J.R. Carson, R.S. Hoyt, "Propagation of Periodic Currents Over a System of Parallel Wires", Bell Syst. Tech. Jour., Vol. 6, pp. 495-545, July 1927.
- [C2] L.A. Pipes, "Matrix Theory of Multiconductor Transmission Lines", Phil. Mag., Vol. 24, pp. 97-113, July 1937.
- [C3] L.V. Bewley, Traveling Waves on Transmission Systems, New York: Dover, 1963.
- [C4] S.A. Schelkunoff, "Generalized Telegraphist's Equations for Waveguides", Bell Syst. Tech. Jour., Vol. 31, pp. 784-801, July 1952.
- [C5] S. Frankel, Cable and Multiconductor Transmission Line Analysis, Springfield, VA: Nat'l Tech. Info. Service, AD-A000848, June 1974.
- [C6] H. Amemiya, "Time-domain Analysis of Multiple Parallel Transmission Lines", RCA Rev., Vol. 28, pp. 241-276, June 1967.
- [C7] K.D. Marx, "Propagation Modes, Equivalent Circuits, and Characteristic Termination For Multiconductor Transmission Lines with Inhomogeneous Dielectrics", IEEE Trans. Microwave Theory Tech., Vol. MTT-21, pp. 456-457, July 1973.
- [C8] C.R. Paul, "Efficient Numerical Computation of the Frequency Response of Cables Illuminated by an Electromagnetic Field", IEEE Trans. Microw. Theory Tech., Vol. MTT-22, pp. 454-457, April 1974.
- [C9] R.A. Speciale, "Even- and Odd-Mode Waves for Nonsymmetrical Coupled Lines in Nonhomogeneous Media", IEEE Trans. Microw. Theory Tech., Vol. MTT-23, pp. 897-908, November 1975.
- [C10] S. Ramo, J.R. Whinnery, T. Van Duzer, Fields and Waves in Communication Electronics, New York: Wiley, 1965, p. 314.
- [C11] A. Matsumoto (ed.), Microwave Filters and Circuits, New York: Acad. Press, 1970, Ch. 8.
- [C12] T. Nishide, A. Matsumoto, "Multiport Image Parameter Theory", Monogr. No. 18, Research Institute of Applied Electricity, Hokkaido Univ., 1970.
- [C13] D. Kajfez, "Multiconductor Transmission Lines", Interaction Note 151, June 1972.
- [C14] C.R. Paul, "Useful Matrix Chain Parameters Identities of Multiconductor Transmission Lines", IEEE Trans. Microw. Theory Tech., Vol. MTT-23, pp. 756-760, Sep. 1975.

- [C15] IRE Standards on Antennas and Waveguides: Definitions of Terms, 1953, Proc. I.R.E., pp. 1721-1728, December 1953.
- [C16] B. Friedman, Principles and Techniques of Applied Mathematics, New York: John Wiley, 1956, pp. 107-110.
- [C17] D. Kajfez, "Distributed Circuit Approach to the Curved Multi-conductor Transmission Lines", Jour. Mississippi Acad. Sci., Vol. 13, pp. 75-83, 1967.
- [C18] G.L. Matthaei, L. Young, E.M.T. Jones, Microwave Filters, Impedance-Matching Networks, and Coupling Structures, New York: McGraw-Hill, 1964, p. 193.

NOTE 348

ON THE ELECTROMAGNETIC FIELD EXCITATION OF  
UNSHIELDED MULTICONDUCTOR CABLES

by

Clayborne D. Taylor  
J. Philip Castillo

January 1978

ON THE ELECTROMAGNETIC FIELD EXCITATION OF  
UNSHIELDED MULTICONDUCTOR CABLES

ABSTRACT

Unshielded multiconductor cables are considered to be illuminated by electromagnetic plane wave fields. A study of the currents, that are induced in the terminations, is made using quasistatic circuit theory, transmission line theory and wire antenna theory. Questions of accuracy, ranges of validity and general trends are addressed.

## INTRODUCTION

In the construction of facilities with many interconnecting electrical systems, unshielded multiconductor cables are used extensively. Generally the routing and branching of the cables are selected for convenience with no definite pattern intended. However under the illumination of intense electromagnetic fields deleterious voltages and/or currents may be induced in the cable terminations.

The response of multiconductor cables to an electromagnetic illumination may be determined by using multiconductor transmission line theory.<sup>1,2</sup> But this technique requires that the relative orientation of the wires within the cable remain fixed over the cable run or at least maintain some identifiable weave pattern. However, the typical cable bundle is not intended to be a multiconductor transmission line, and generally the relative orientation of wires varies considerably and without pattern. Because of this difficulty, the cable bundle is often treated as a single wire with some equivalent radius and then transmission line theory is used to obtain the so-called "core current" or common mode current among the cable wires.<sup>3</sup>

This paper considers a few simple cable configurations and determines the response under different load conditions while examining the common mode currents as related to the differential mode currents. To obtain the results three separate solution techniques are employed. Firstly, standard coupled circuit analysis is used with Faraday's law--the quasistatic formulation. Secondly, transmission line theory is used and thirdly, wire antenna theory is utilized to determine the wire

currents. Inasmuch as transmission line theory neglects reradiation from the wire configuration, a comparison of the aforementioned three results gives an indication of the accuracy and range of validity of the transmission line formulation.

## ANALYSIS

1. Single Wire Cable Over a Ground Plane

The first configuration to be considered is a finite length wire parallel to a perfectly conducting ground plane. Extending from  $z = 0$  to  $z = l$  the wire is terminated with respect to the ground in the impedances  $Z_0$  at  $z = 0$  and  $Z_1$  at  $z = l$  (see figure 1). The wire together with its electromagnetic image forms a two wire transmission line provided that the wire height  $h$  satisfies,  $h \ll l$  and  $h \ll \lambda$ . From transmission line theory the currents induced in the terminations are<sup>4\*</sup>

$$I_0 = \frac{1}{D} \int_0^l K(z) [Z_c \cosh \gamma(z-l) - 2Z_1 \sinh \gamma(z-l)] dz - \frac{2Z_c}{D} \int_0^h [E_x^{inc}(x,l) + E_x^{ref}(x,l)] dx + 2 \frac{Z_c \cosh \gamma l + 2Z_1 \sinh \gamma l}{D} \int_0^h [E_x^{inc}(x,0) + E_x^{ref}(x,0)] dx \quad \dots (1)$$

$$I_1 = \frac{1}{D} \int_0^l K(z) [Z_c \cosh \gamma z + 2Z_0 \sinh \gamma z] dz + \frac{2Z_c}{D} \int_0^h [E_x^{inc}(x,0) + E_x^{ref}(x,0)] dx - 2 \frac{Z_c \cosh \gamma l + 2Z_0 \sinh \gamma l}{D} \int_0^h [E_x^{inc}(x,l) + E_x^{ref}(x,l)] dx \quad \dots (2)$$

where

$$K(z) = [E_z^{inc}(x,z) + E_z^{ref}(x,z)]_{x=-h}^{x=h} \quad (3)$$

$$D = 2Z_c(Z_0 + Z_1) \cosh \gamma l + (Z_c^2 + 4Z_0Z_1) \sinh \gamma l \quad (4)$$

\*Some modification of Smith's formulas are made to fit the situation being considered here.

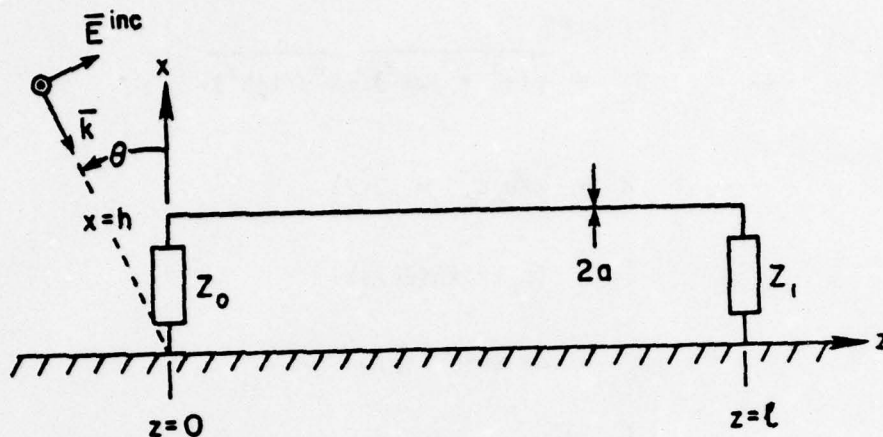


Figure 1: Finite Length Wire Parallel to a Ground Plane and Terminated in Impedances  $Z_0$  and  $Z_1$  with Plane Wave Illumination.

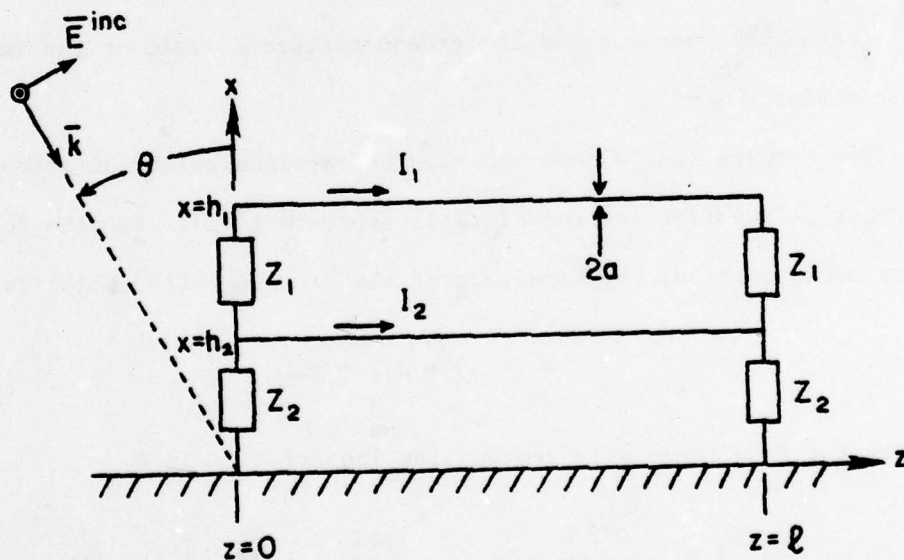


Figure 2: Two Wire Transmission Line Oriented Parallel to a Ground Plane with Plane Wave Illumination.

$$\gamma^2 = jk^2(z^i + j\omega l^e)/\omega l^e \quad (5)$$

$$Z_c = \sqrt{(z^i + j\omega l^e)(\omega l^e)/(jk^2)} \quad (6)$$

$$k = \omega \sqrt{\mu_0 \epsilon_0} = 2\pi/\lambda$$

$$l^e = (\mu_0/\pi) \ln(2h/a)$$

$$\mu_0 = 4\pi \times 10^{-7} \text{ H/m}$$

$z^i$  is the distributed series resistance  
of the two wire line ( $\Omega/\text{m}$ )

Here  $E_x^{\text{inc}}$  and  $E_z^{\text{inc}}$  are components of the incident field and  $E_x^{\text{ref}}$  and  $E_z^{\text{ref}}$  are the components of the ground reflected field or the image source field.

The termination current can also be obtained by circuit theory and Faraday's Induction law (quasistatic approximation). For the foregoing wire configuration, the impedance of the circuit (with image) is

$$Z = 2(Z_0 + Z_1) + j\omega L \quad (7)$$

where the inductance of a rectangular loop of wire is<sup>5</sup>

$$L = \frac{\mu_0}{\pi} \left[ l \ln \frac{4hl}{a(l+d)} + 2h \ln \frac{4hl}{a(2h+d)} + 2d - \frac{7}{4} (l+2h) \right] \quad (8)$$

$$d = \sqrt{(2h)^2 + l^2}$$

The induced voltage in the circuit is

$$e_i = -j\omega(2B_y^{\text{inc}})(2hl)$$

Hence the currents in the terminations are

$$I_o = I_1 = \frac{e_1}{Z} = -j\omega \frac{4hl B_y^{inc}}{2(Z_o + Z_1) + j\omega L} \quad (9)$$

The foregoing circuit theory is expected to be accurate whenever  $h, l \ll \lambda$ , and the transmission line theory result is expected to be accurate when  $l \gg h$  and  $h \ll \lambda$ . However neither accounts for reradiation from the wire structure. Since reradiation should be most important when the structure resonates and the terminations are shorted, these conditions will be considered explicitly to ascertain the accuracy of the transmission line theory result.

For convenience the illumination on the configuration is considered to be plane wave with the plane of incidence coincident with the plane of the loop and with the incident magnetic field perpendicular to the plane of incidence. When the terminations are also shorted,  $Z_o = Z_1 = 0$ , then (1) and (2) yield

$$I_o = \frac{4E_o h}{Z_c} \quad (10)$$

$$I_1 = \frac{4E_o h}{Z_c} e^{-jkl \sin \theta} \quad (11)$$

where  $\theta$  is the angle of incidence and  $E_o$  is the amplitude of the incident plane wave. It is readily noted that (10) and (11) do not exhibit a resonant effect. It may also be noted that if  $l \gg h$  and  $h \gg a$  then (8) yields

$$L \approx l^e l$$

and correspondingly (9) agrees exactly with (10).

## 2. Two Wire Cable Over a Ground Plane

The second configuration to be considered consists of two parallel wires oriented over a ground plane so that the plane of the wires is normal to the ground. As before the wires are considered to be finite length extending from  $z = 0$  to  $z = l$  with terminations as shown in figure 2.

Together with their electromagnetic images the two wires form a 4 wire configuration, and the current that is induced on the wires by an electromagnetic field may be obtained by using the formulation that was developed by Paul<sup>2</sup> for multiconductor lines. Of course the inherent approximations are those of standard transmission line theory. It is convenient to use the wire currents that are obtained to define differential mode and common mode currents,

$$I_D(z) = I_1(z) - I_2(z) \quad (12)$$

and

$$I_C(z) = I_1(z) + I_2(z) \quad (13)$$

respectively. The common mode current (sometimes referred to as the bulk cable current) can be easily measured without disturbing the cable configuration. Moreover a knowledge of the common mode and differential mode current provides insight into the nature of the cable response. Also the common mode current can be used to obtain an approximation for the individual wire currents.<sup>3</sup>

The wire currents can also be determined by using circuit theory as presented in the previous section. Beginning with the equivalent circuit shown in figure 3, the circuit equations for the wire currents are

$$e_1 = [4(Z_1 + Z_2) + j\omega L_1]I_1 + [4Z_2 + j\omega M]I_2 \quad (14)$$

$$e_2 = [4Z_2 + j\omega M]I_1 + [4Z_2 + j\omega L_2]I_2 \quad (15)$$

where

$$e_1 = -j\omega(2B_y^{\text{inc}})(2h_1\ell) \quad (16)$$

$$e_2 = -j\omega(2B_y^{\text{inc}})(2h_2\ell) \quad (17)$$

Here  $L_1$  and  $L_2$  can be obtained using (8) by letting  $h = h_1$  and  $h = h_2$ , respectively. Provided  $\ell^2 \gg h_1^2 \gg a^2$  the expression for the mutual inductance becomes

$$M = \frac{\mu_0}{\pi} \left\{ \ell \ln \frac{h_1 + h_2}{h_1 - h_2} + (h_1 + h_2) \left[ \ln \frac{2(h_1 + h_2)}{a} - 2 \right] - (h_1 - h_2) \left[ \ln \frac{2(h_1 - h_2)}{a} - 2 \right] \right\} \quad (18)$$

Solving (14) and (15) for  $I_C$  and  $I_D$  yields

$$I_C = \frac{4Z_1 e_2 + j\omega[e_1(L_2 - M) + e_2(L_1 - M)]}{[4(Z_1 + Z_2) + j\omega L_1][4Z_2 + j\omega L_2] - [4Z_2 + j\omega M]^2} \quad (19)$$

$$I_D = \frac{e_1[8Z_2 + j\omega(L_2 + M)] - e_2[8Z_2 + 4Z_1 + j\omega(L_1 + M)]}{[4(Z_1 + Z_2) + j\omega L_1][4Z_2 + j\omega L_2] - [4Z_2 + j\omega M]^2} \quad (20)$$

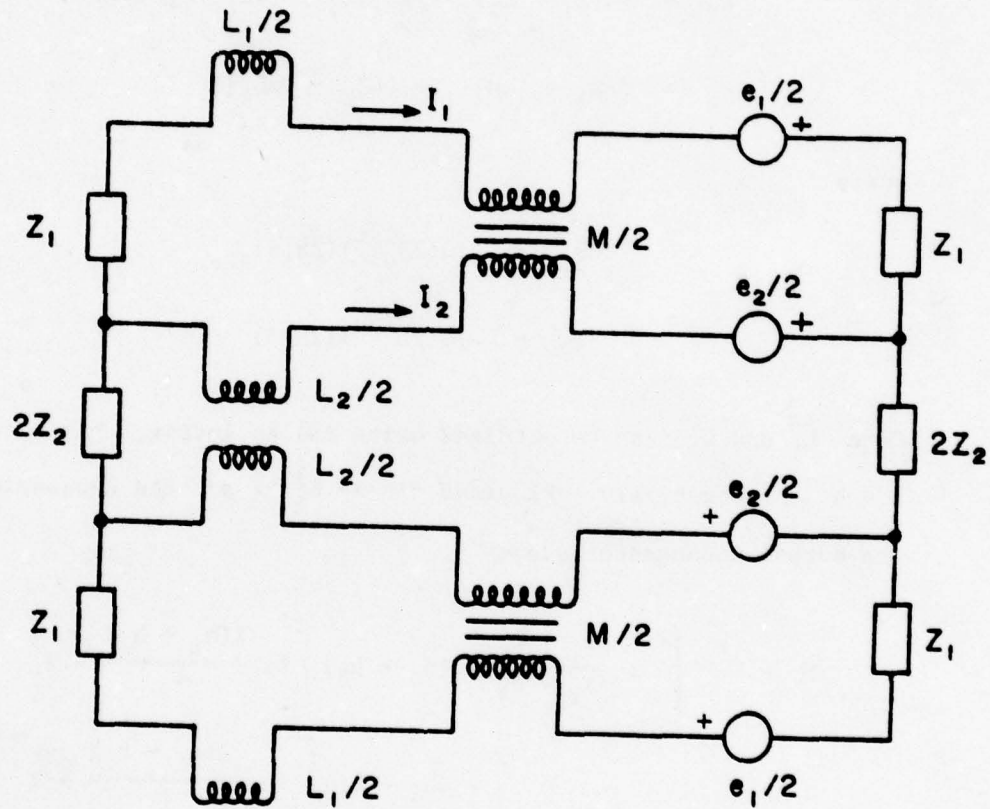


Figure 3: Equivalent Circuit for the Quasistatic Analysis of the Cable Configuration of Figure 2.

Of course the circuit theory result is valid only for low frequency excitation, i.e., when  $h_1, h_2, \ell \ll \lambda$ . The transmission line result is expected to be valid for  $h_1 \ll \lambda$  and  $\ell \gg h_1$ . Normally these conditions are satisfied for typical multiconductor cables and frequencies of interest.

Another termination configuration for a two wire cable is shown in figure 4. If  $\Delta \ll \ell$  the mutual and self inductances are virtually the same as the corresponding inductances that are obtained for the cable configuration shown in figure 2. However, the circuit equations are different. They are

$$e_1 = (4Z_1 + j\omega L_1)I_1 + j\omega MI_2$$

$$e_2 = j\omega MI_1 + (4Z_2 + j\omega L_2)I_2$$

Solving these equations yields

$$I_1 = \frac{e_1(4Z_2 + j\omega L_2) - e_2(j\omega M)}{(4Z_1 + j\omega L_1)(4Z_2 + j\omega L_2) + (\omega M)^2} \quad (21)$$

$$I_2 = \frac{-e_1(j\omega M) + e_2(4Z_1 + j\omega L_1)}{(4Z_1 + j\omega L_1)(4Z_2 + j\omega L_2) + (\omega M)^2} \quad (22)$$

From the foregoing equations for the wire currents certain general observations are possible. It is noted that if

$$|4Z_1|^2 \gg (\omega L_1 - \frac{e_1}{e_2} \omega M)^2$$

and

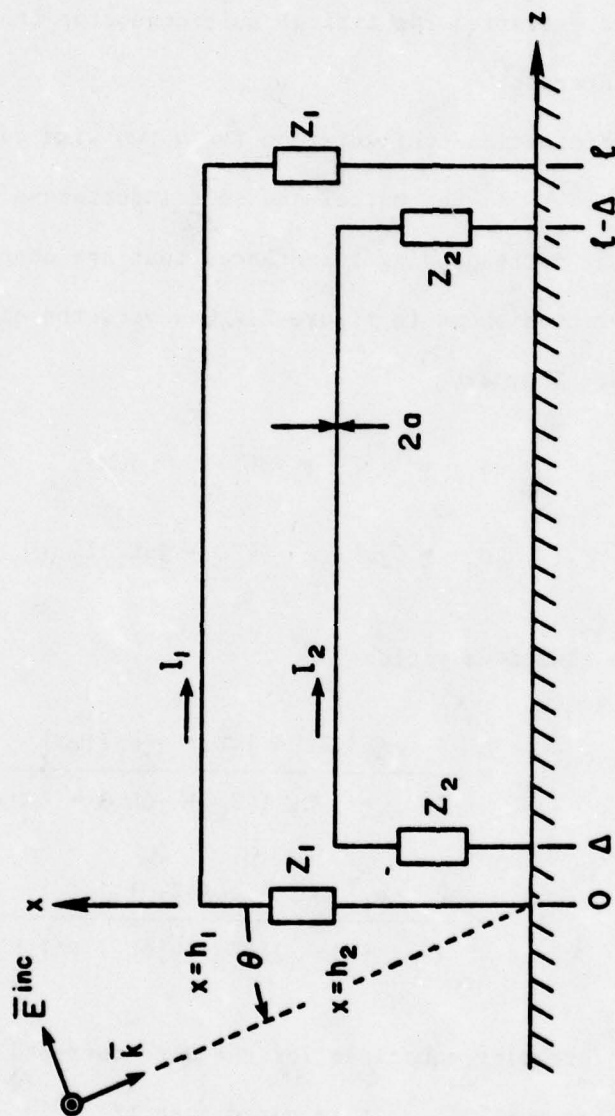


Figure 4: Two Wire Transmission Line Oriented Parallel to a Ground Plane with Plane Wave Illumination.

$$|4Z_2|^2 \gg (\omega L_2 - \frac{e_2}{e_1} \omega M)^2$$

then

$$\left| \frac{I_1}{I_2} \right|^2 = \frac{h_1}{h_2} \left| \frac{Z_2}{Z_1} \right| \quad (23)$$

This simple result should be valid over a wide range of parameters and frequencies.

### 3. Wire Antenna Theory

The Numerical Electromagnetic Code, NEC-(1,2)A<sup>6</sup> was used to obtain the response of the wire problems treated in this paper. The computer code is based on the electric-field-integral equation (EFIE) for thin wire structures. Assuming that: (a) transverse currents are small relative to axial currents, (b) the variation of axial current is uniform around the periphery of the conductors, (c) the total current can be approximated by a current filament on the wire axis and (d) the electric field boundary condition is enforced in the axial direction only, the EFIE for the thin wire becomes

$$-\hat{s} \cdot E^{inc}(\vec{r}) = \frac{-j}{4\pi k} \int_L I(s') \left[ k^2 \hat{s} \cdot \hat{s}' - \frac{\partial^2}{\partial s \partial s'} \right] g(\vec{r}, \vec{r}') ds' \quad (24)$$

where  $E^{inc}(\vec{r})$  is the incident electric field,

$I(s)$  is the induced axial current ,

$$g(\vec{r}, \vec{r}') = \exp\left[-jk |\vec{r} - \vec{r}'| \right] / |\vec{r} - \vec{r}'| ,$$

$$k = \omega \sqrt{\mu_0 \epsilon_0}$$

$$\eta = \sqrt{\mu_0/\epsilon_0} ,$$

$\hat{s}$  is the unit vector tangent to the wire at  $\vec{r}$  ,  
 $s$  and  $s'$  are the distances along the wire at  $\vec{r}$ , and  $\vec{r}'$ ,  
 respectively.

Equation (24) is solved by using the method of moments. For the geometry shown in Figures 1, 2, 4, the horizontal wires were divided into 51 segments each and the vertical wires into single segments. In applying the method of moments convenient basis functions and weight functions must be selected. The NEC-(1,2)A code employs basis functions for the axial current of the form

$$I_j(s) = A_j + B_j \sin[k(s-s_j)] + C_j \cos[k(s-s_j)] \quad (25)$$

where A, B, and C are constants to be determined. The weight functions selected are a set of delta functions:

$$W_1(\vec{r}) = \delta(\vec{r} - \vec{r}_1) . \quad (26)$$

The sample point,  $\vec{r}_1$ , is taken at the center of each segment. At a junction of two or more wires of the same radius the conditions of current and charge continuity are imposed. The NEC-(1,2)A code allows the calculation of currents or charge at any segment of a wire. Impedance loading at any segment is also allowed. The perfectly conducting ground plane is included in the model via the method of images.

The results of NEC-(1,2)A are expected to be valid for

$$\Delta/a \geq 4$$

EMP 3-39

348-15

and

$$(ka)^2 \ll 1 ,$$

where  $\Lambda$  is the length of a segment. The radii for the wires making up the transmission lines were all equal.

## NUMERICAL RESULTS

The application of the various formulations that are presented in the foregoing provides information not only for the cable configurations but also provides a means of determining the accuracy of the results obtained from the formulations. For example, the single wire cable configuration of figure 1 provides a test of the predictions that are obtained using transmission line approximations. Considering the cable to be electrically shorted at both ends, data are obtained from transmission line theory and wire antenna theory and presented in figure 5. There is very good agreement over most of the frequency range with the exceptions of the neighborhoods of the loop resonances at  $f = 7.5$  MHz and  $f = 15$  MHz. Note that the results from transmission line theory failed to exhibit the resonances for the structure. This result is explained in the appendix. Also it should be mentioned that the wire antenna results that are shown in figure 5 do not necessarily include the peak current values that occur.

The aforementioned single wire cable was also considered to be illuminated with  $\theta = 0^\circ$ . As seen from (10) the magnitudes of the transmission line currents are independent of  $\theta$ . The wire antenna results differ from the transmission line current only in the neighborhood of the  $f = 7.5$  resonance. Since the excitation of the cable for  $\theta = 0^\circ$  is symmetric about  $z = \ell/2$  and the resonant current mode at  $f = 7.5$  MHz is antisymmetric about  $z = \ell/2$ , this resonant current mode is not excited.<sup>7</sup>

For pulse excitation the response can be obtained by using frequency domain results (such as those considered) and Fourier frequency

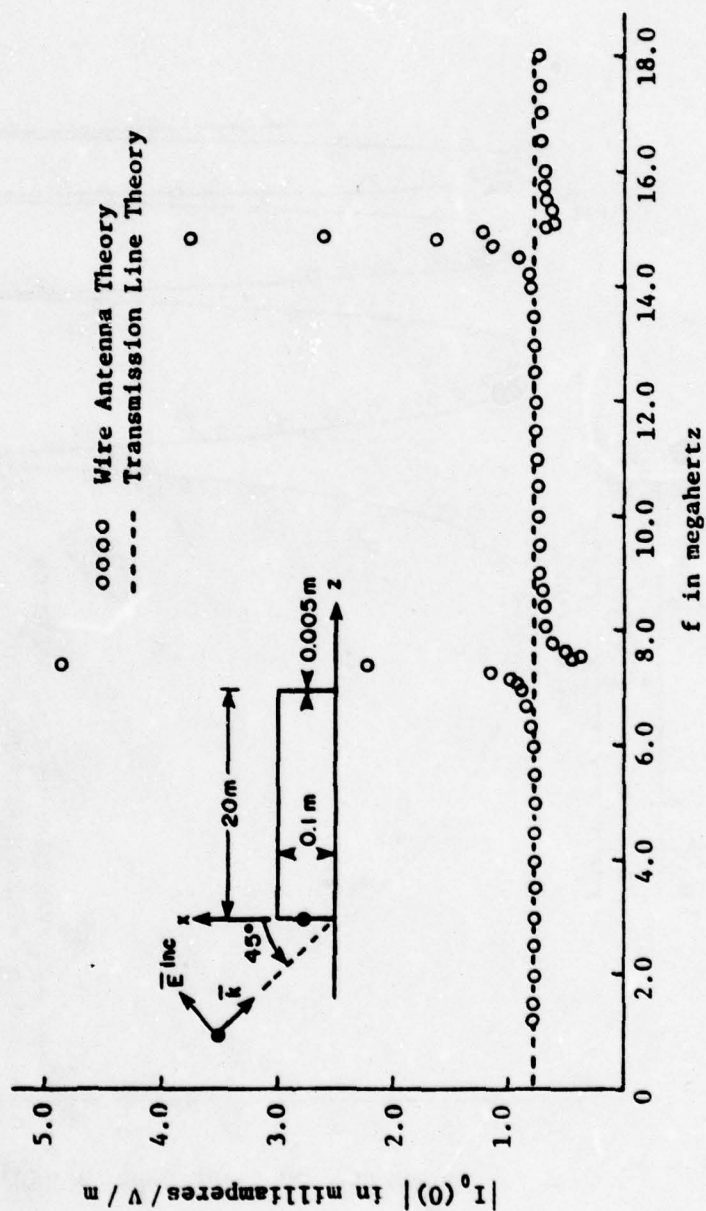


Figure 5: Termination Current for a Rectangular Loop Oriented Normal to a Perfect Ground Plane and Illuminated by a Plane Electromagnetic Wave.

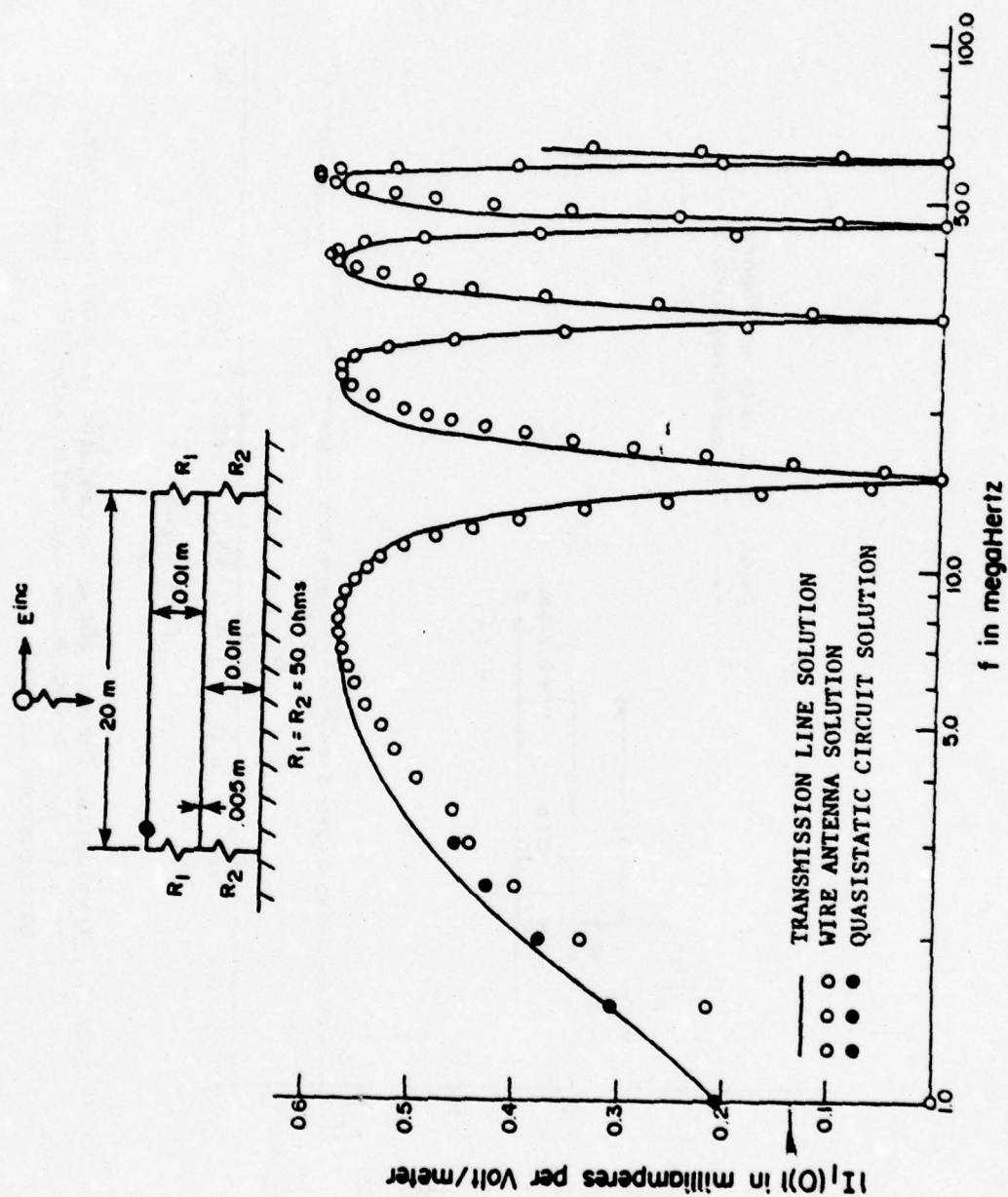


Figure 6: Two-Wire Transmission Line Oriented Parallel to a Perfect Ground Plane and Illuminated by a Plane Electromagnetic Wave.

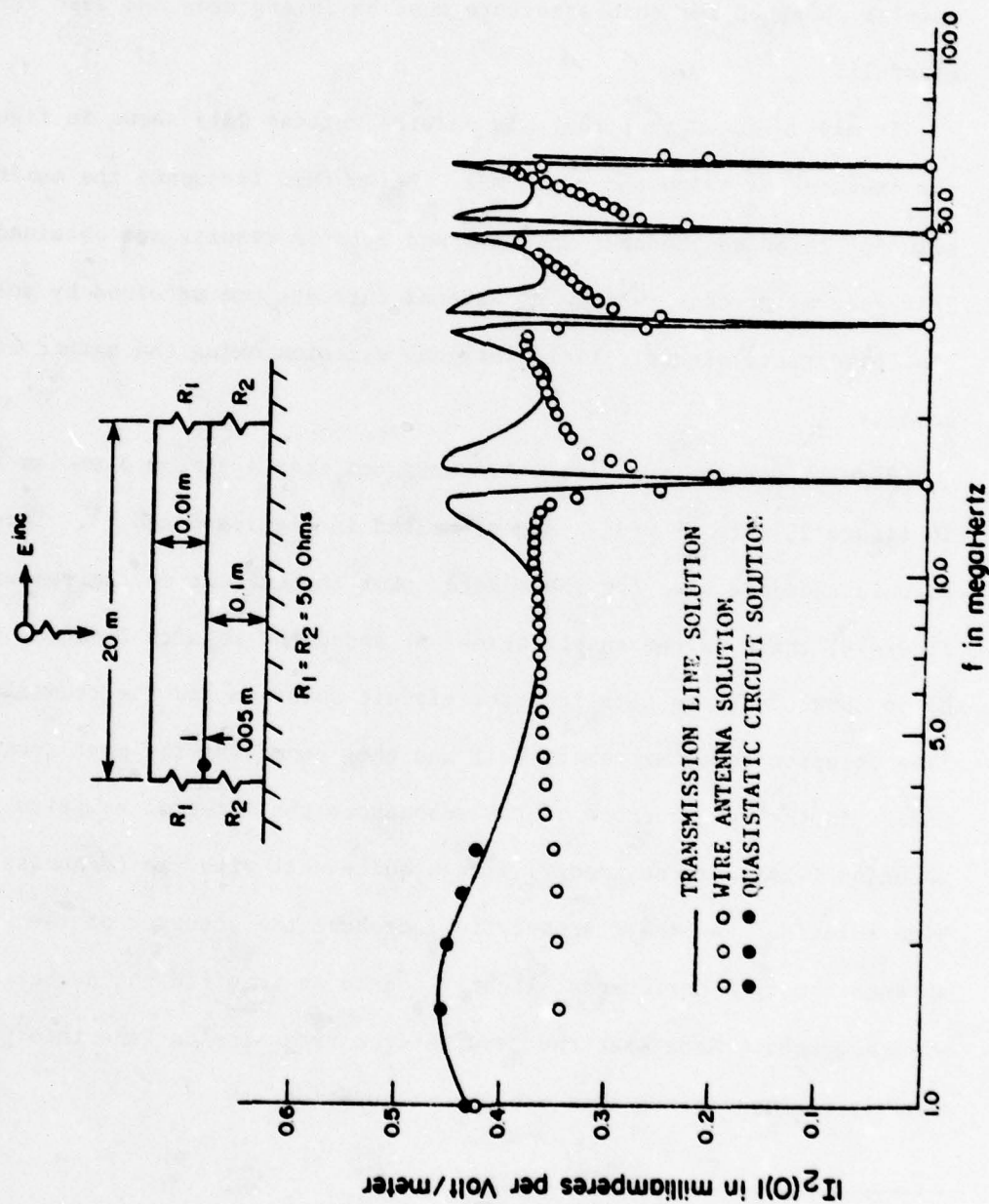


Figure 7: Two-Wire Transmission Line Oriented Parallel to a Perfect Ground Plane and Illuminated by a Plane Electromagnetic Wave.

superposition. Hence the differences between the wire antenna results and the transmission line results for the shorted single wire cable would affect the time domain results. Accordingly the transmission line results obtained for this structure must be interpreted and used very carefully.

It may be noted that there is no wire antenna data shown in figure 5 for frequencies below about 1.5 MHz. Below this frequency the numerical solution technique becomes unstable and erratic results are obtained. This generally occurs when wire antenna currents are obtained by solving the appropriate electric field integral equation using the method of moments.

Results for the two wire cable oriented over a ground plane as shown in figure 2, with  $\theta = 0^\circ$ , are presented in figures 6 and 7\*. Three formulations are used for these data. For the current on the top wire, figure 6, there is reasonable agreement among the results from the three. Up to about 3 MHz results from the circuit solution and the transmission line solution agree extremely well and they represent the most accurate data. In the neighborhood of the resonances the integral equation solution (wire antenna theory) agrees quite well with the transmission line solution. As the frequency is increased the accuracy of the wire antenna theory deteriorates slightly due to an insufficient number of wire segments. Note that the results from transmission line theory does exhibit resonances for this cable configuration.

---

\*The transmission line theory data were provided by Dr. C. R. Paul from a computer code described in reference 8.

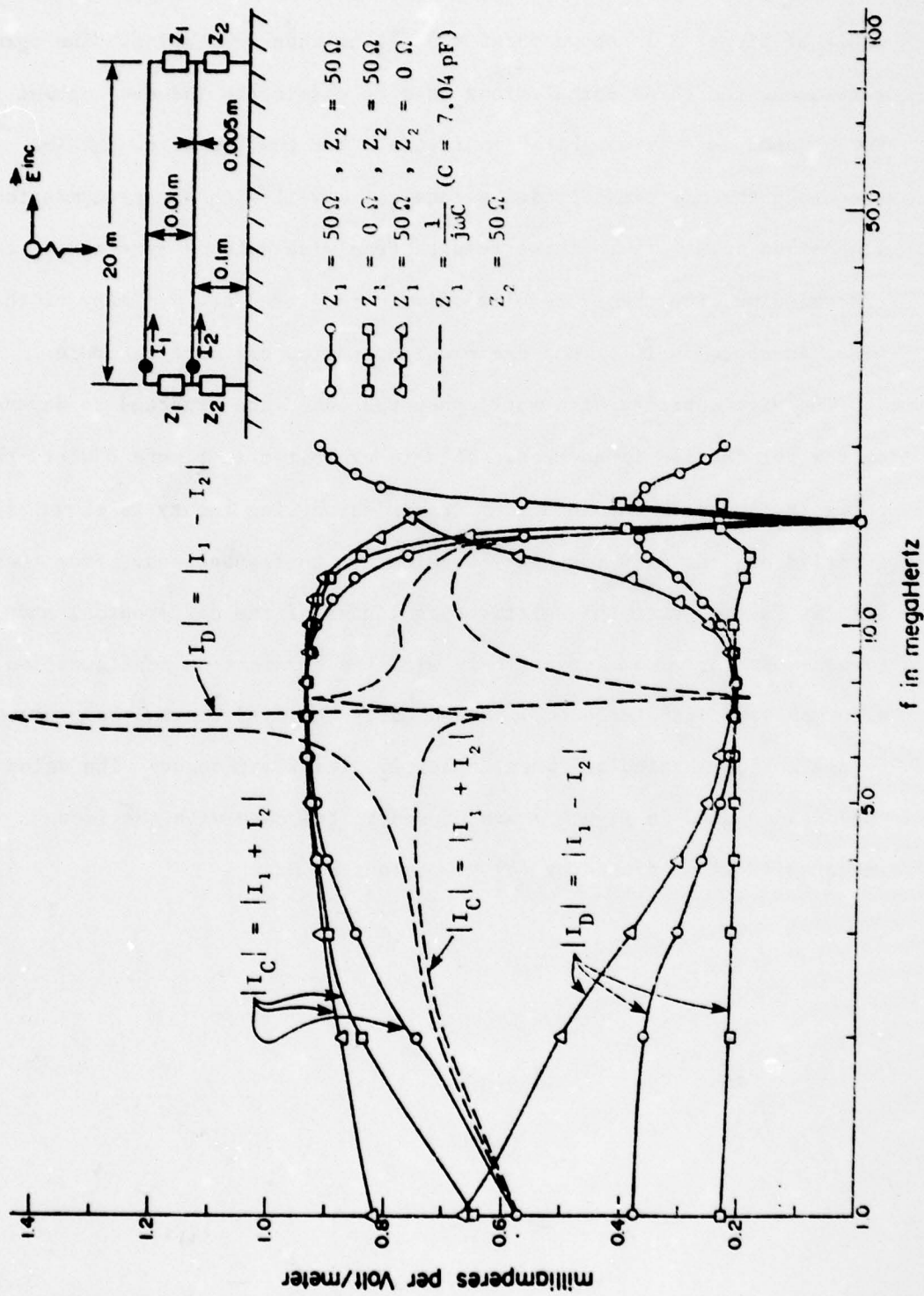


Figure 8. Two-Wire Transmission Line Oriented Parallel to a Perfect Ground Plane and Illuminated by a Plane Electromagnetic Wave.

In figure 7 the current induced in the lower wire of the two wire cable of figure 2 is shown for  $\theta = 0^\circ$  plane wave excitation. The agreement among the three formulations used to obtain the induced current is not as good as that exhibited in figure 6 for the top wire. At low frequency the circuit solution agrees quite well with the transmission line solution. Note that the results from wire antenna agrees with the transmission line theory results only in the immediate vicinity of the wire resonances. It is not clear which results are more accurate.

The wire currents of a multiconductor cable are expected to depend on the termination impedances. This is exhibited in figure 8 where the currents  $I_C$  and  $I_D$  obtained from transmission line theory is shown as a function of frequency for a few termination configurations. From these data it is seen that the relative magnitudes of the differential and common mode currents vary not only with the termination configuration but also may vary with frequency. And clearly the differential mode cannot be neglected, particularly when capacitive loads may occur. The value of capacitance used in figure 8 was chosen to resonate with the loop inductance, as predicted by (8), at about 7 MHz.

## CONCLUSIONS

A few simple multiconductor cable configurations are considered to determine the accuracy of various formulations and to examine the relative importance of the common mode and differential mode currents induced by plane wave illumination. Three independent theoretical formulations are used to study the induced cable currents with several general observations resulting.

1. Transmission line theory does not predict resonances in the current induced at the terminations of a transmission line that is shorted at both ends and illuminated by a plane wave electromagnetic field. With the exception of the shorted transmission line, the transmission line theory result agreed reasonably well with the wire antenna result.

2. The application of wire antenna theory to multiwire cables encounters difficulty in the low frequency regime due to numerical instability and in the high frequency regime due to convergence problems.

3. The relative importance of the common mode and the differential mode depends upon the terminations and may be a function of frequency.

4. In general the differential mode currents induced on a multiconductor cable by electromagnetic illumination cannot be neglected in comparison with the common mode currents.

## REFERENCES

1. S. A. Schelkunoff, Electromagnetic Waves, (D. Van Nostrand: New York, 1943) Chapter 7, Section 25.
2. C. R. Paul, "Frequency Response of Multiconductor Transmission Lines Illuminated by an Electromagnetic Field," IEEE Trans. Electromag. Compat., Vol. EMC-18, No. 4, pp. 183-190, November 1976.
3. A. A. Smith, Jr., Coupling of External Electromagnetic Fields to Transmission Lines, (Wiley Interscience: New York, 1977) p. 7.
4. A. A. Smith, Jr., "A More Convenient Form of the Equations for the Response of a Transmission Line Excited by Nonuniform Fields," IEEE Trans. Electromag. Compat., Vol. EMC-15, No. 3, pp. 151-152, August 1973.
5. W. R. Smythe and C. Yeh, "Electricity and Magnetism-Formulas," American Institute of Physics Handbook, (edited by D. E. Gray). (McGraw-Hill: New York, 1972) Chapter 5, Section 5b.
6. G. J. Burke and A. J. Poggio, "NEC-(1,2)A Program Description, Part I: Theory, Part II: Code and Part III: Users Guide," Interaction Note to be published.
7. S. Ramo, J. R. Whinnery and T. Van Duzer, Fields and Waves in Communication Electronics, (John Wiley: New York, 1975) p. 58.
8. C. R. Paul, "Applications of Multiconductor Transmission Line Theory to the Prediction of Cable Coupling, Vol. VI, A Digital Computer Program for Determining Terminal Currents Induced in a Multiconductor Transmission Line by an Incident Electromagnetic Field," Technical Report, RADC-TR-76-101, Rome Air Development Center, Griffis AFB, NM, (To be Published).

## APPENDIX

Contrary to normal expectations the transmission line theory predictions for the single wire parallel to the ground did not exhibit resonances in the termination currents. Which brings up two important questions, (1) Why are resonances not predicted by the analysis? and (2) Do resonances actually occur? This appendix is written to respond to these questions.

First consider the situation where  $Z_1 = 0$  and  $Z_0 \neq 0$  (see figure 1). Accordingly (1) yields, for a lossless line,

$$I_0 = \frac{j 4 h Z_c E_0 \sin k \ell}{D} \quad (A1)$$

where

$$D = j Z_c^2 \left[ \sin k \ell - j 2 \frac{Z_0}{Z_c} \cos k \ell \right] \quad (A2)$$

The zeros of  $I_0$  in the complex  $s$ -plane are those values of  $s = j\omega = jkc$  for which

$$\sin k \ell = 0 \quad (A3)$$

Hence the zeros are

$$s_z = j n \pi \frac{c}{\ell} \quad n = 1, 2, 3, \dots \quad (A4)$$

Note that the zeros are independent of  $Z_0$ .

The poles of  $I_0$  in the complex  $s$ -plane are those values of  $s$  for which  $D = 0$ . These are for  $Z_0 = \delta Z_c$ , where  $\delta^2 \ll 1$ ,

$$s_p = [-2\delta + j m \pi] \frac{c}{\ell} \quad m = 1, 2, 3, \dots \quad (A5)$$

The resonant frequencies are therefore

$$\omega_{\text{res}} = |s_p|$$

Hence, if  $Z_0 \neq 0$ , transmission line theory predicts resonances. However if  $\delta \rightarrow 0$  then the poles coalesce with the zeros and the resonances thereby are canceled. The result is frequency independent as exhibited in figure 5. It should be pointed out that the zeros of the wire currents are position dependent. That is, resonances are predicted by transmission line theory at other points along the wire when  $Z_0 = Z_1 = 0$ .

The first question posed at the outset has been answered. In answer to the second question regarding the existence of resonances on an actual structure, one must conclude that actual resonances do occur just as is predicted by the wire antenna theory analysis, since the poles for the actual configuration can never lie on the  $j\omega$  axis of the complex  $s$ -plane and thereby be canceled by the zeros.

NOTE 349

A COUPLING MODEL FOR A PAIR OF  
SKEWED TRANSMISSION LINES

by

David V. Giri  
Steve K. Chang  
Fred M. Tesche

12 September 1978

A COUPLING MODEL FOR A PAIR OF  
SKEWED TRANSMISSION LINES

ABSTRACT

A coupling model in the form of an equivalent circuit is developed for a pair of skewed transmission lines. The inductive coupling is evaluated in closed form and the capacitances are obtained from the solution of a pair of coupled integral equations for the excess charge distributions along the transmission lines. The coupled integral equations for the excess charges are solved by an approximate analytical method and also by employing the method of moments. The two solutions are seen to be in excellent agreement. The excess charge distributions are then used in a parametric study of the capacitances in the coupling model. The results are presented in graphical form.

## CONTENTS

<u>Section</u>	<u>Page</u>
I. Introduction and Problem Definition	349-3
II. Mutual Inductance	349-9
A. Discussion of Results	349-16
III. Capacitive Coupling	349-23
A. Approximate Analytical Solution	349-31
B. Numerical Solution	349-37
C. Discussion of Results	349-41
IV. Conclusions	349-49
Appendix A. Transmission Line Coupling for the Special Case of $\theta = 0$	349-50
References	349-52

## I. Introduction and Problem Definition

This report addresses a rather specific problem in the area of multiconductor transmission theory. Specifically, we desire to obtain an equivalent circuit in the vicinity of the junction region of two skewed transmission lines, so that the coupling of energy from one line to another can be estimated. It is noted that the term "junction" does not refer to lines in physical contact, but rather the position of smallest separation between the lines. The geometry of the problem is shown in Figure 1.1. It consists of a two-wire transmission line of characteristic impedance  $Z_{c2}$  passing over another two-wire transmission line of characteristic impedance  $Z_{c1}$ . The wires 1 and 2 in Figure 1.1 are both parallel to a perfectly conducting ground plane and are located at heights of  $h_1$  and  $h_2$  respectively. The wires are assumed to be of the same radius, although this is not essential. Figure 1.2 shows an equivalent geometry with the image conductors; the relevant distances between source and observation points are also indicated. As illustrated in this figure, the two lines are modelled by closed rectangular loops by introducing the vertical segments at both ends.

The objective is to compute the elements of a coupling model in the form of an equivalent circuit. In general, for arbitrary values of  $\theta$  in the range of  $[0 < \theta \leq (\pi/2)]$ , one would expect inductive and capacitive coupling between the transmission lines. The special case of  $\theta = 0$  is precluded here because of the distributed nature of the coupling which cannot be treated with localized lumped elements. Appendix A includes

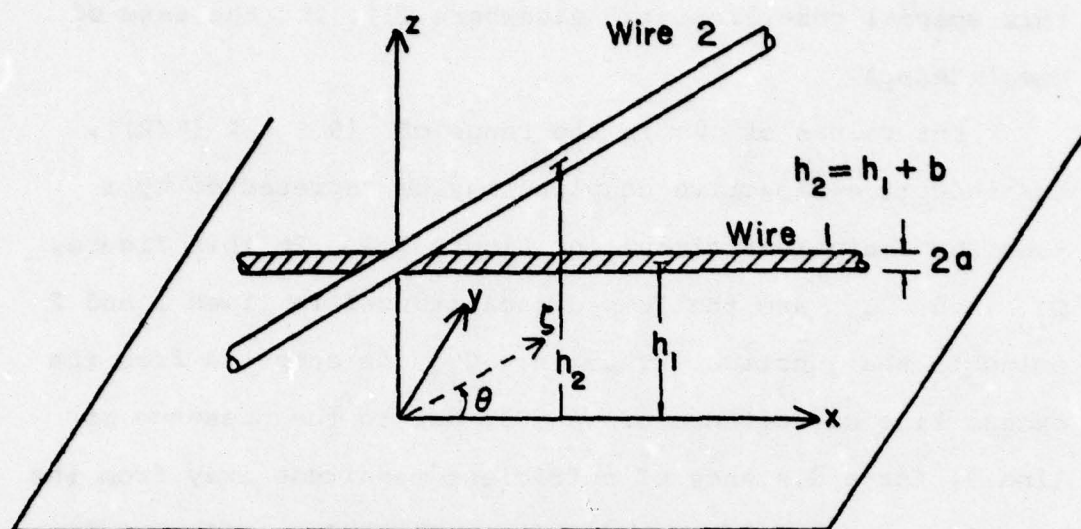


Figure 1.1. Two skewed wires of the same radius above an image plane.

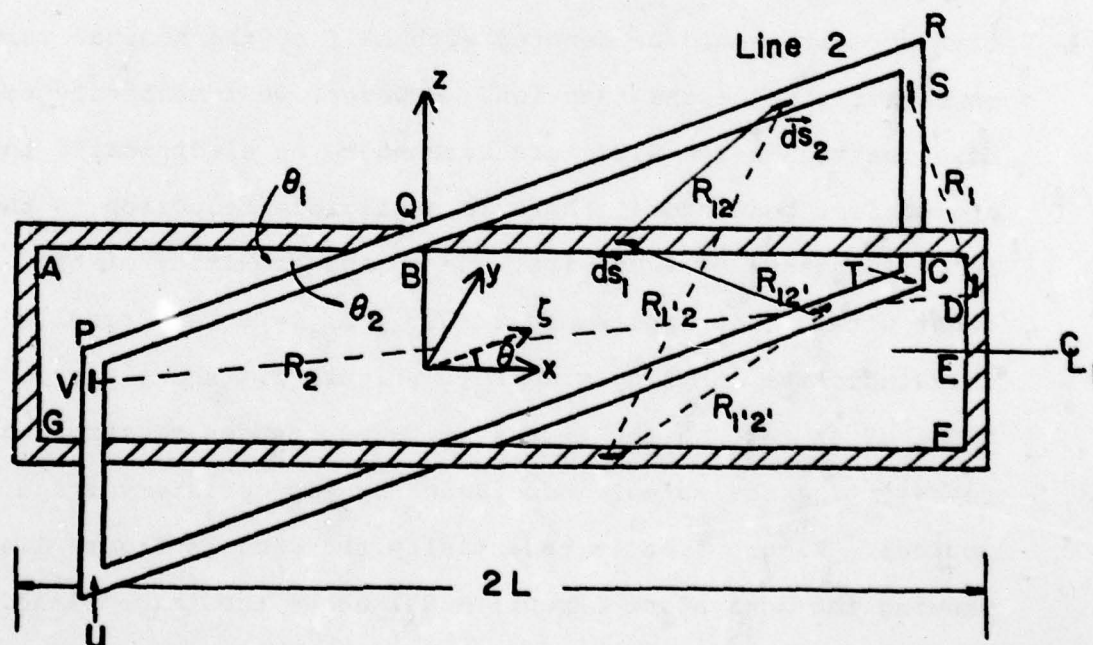


Figure 1.2. Equivalent pair of skewed two-wire transmission lines of length  $2L$ .

this special case, reported elsewhere [1], for the sake of completeness.

For values of  $\theta$  in the range of  $[0 < \theta \leq (\pi/2)]$ , the inductive-capactive coupling may be represented by a junction equivalent circuit of Figure 1.3. In this figure,  $C_{1j}$  and  $C_{2j}$  are the lumped capacitances in lines 1 and 2 owing to the junction. That is,  $C_{1j}$  is computed from the excess line capacitance of line 1, due to the presence of line 2, for a distance of sufficient magnitude away from the junction on both sides.  $C_{mj}$  is the lumped mutual capacitance. The inductive coupling is shown in the form of a transformer comprised of self inductances  $L_{1j}$  and  $L_{2j}$ , as well as a mutual inductance  $L_{mj}$ . To display the symmetry, the inductive circuit should be denoted with half of the nominal values on either side of the junction. However, we immediately recognize that since the wires are assumed to be electrically thin and perfect conductors, there is negligible reduction in the self-inductance of each wire, due to the proximity of the other wire. This implies that  $L_{1j} = L_{2j} = 0$  and results in only inductive coupling via  $L_{mj}$ . Figure 1.4 shows the coupling model after setting the excess self-inductances to zero and representing the mutual inductances by appropriate voltage sources. Figure 1.5a is essentially the same as Figure 1.4, showing the equivalent circuit model above the image plane. In Figure 1.5b, we show the symmetric form of the coupling model and the potentials on all the four lines with respect to the image plane which is chosen as the reference potential.

Note:

The inductive circuit is shown on one side of the junction for convenience only.

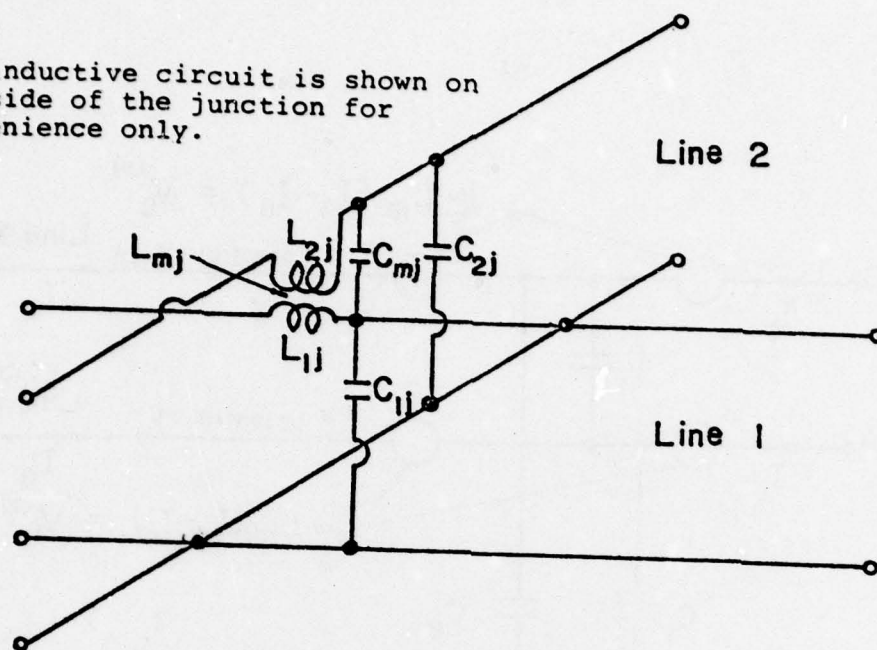


Figure 1.3. A generalized coupling model for the junction of two skewed transmission lines.

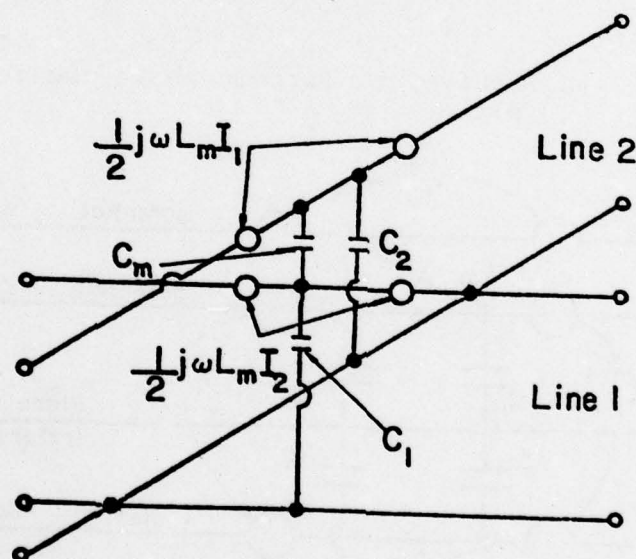


Figure 1.4. Coupling model showing the mutual inductance as voltage sources; (note that the subscript  $j$ , denoting the junction has been dropped).

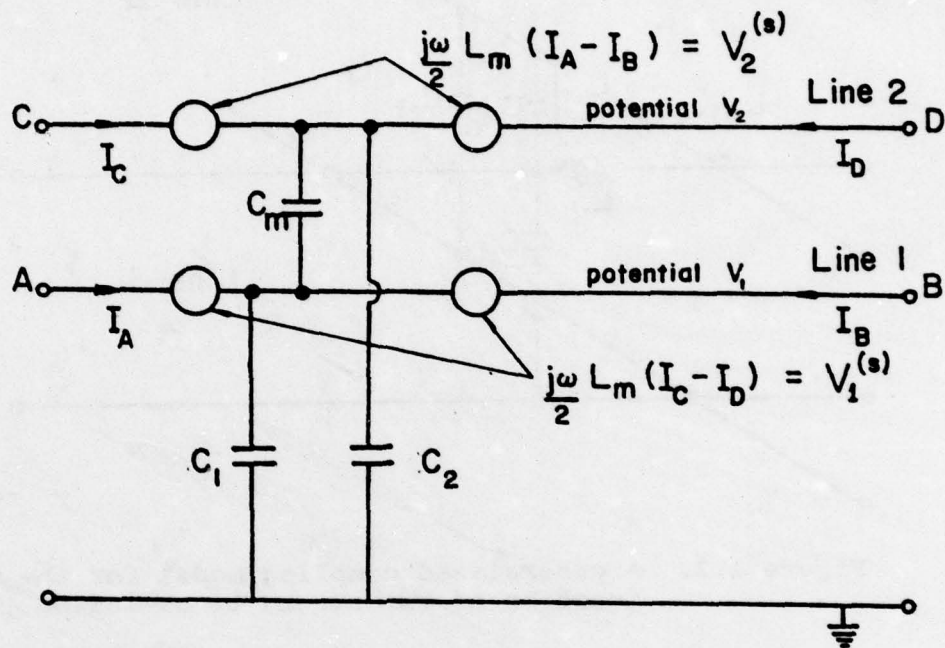


Figure 1.5a. Equivalent circuit above the image plane.

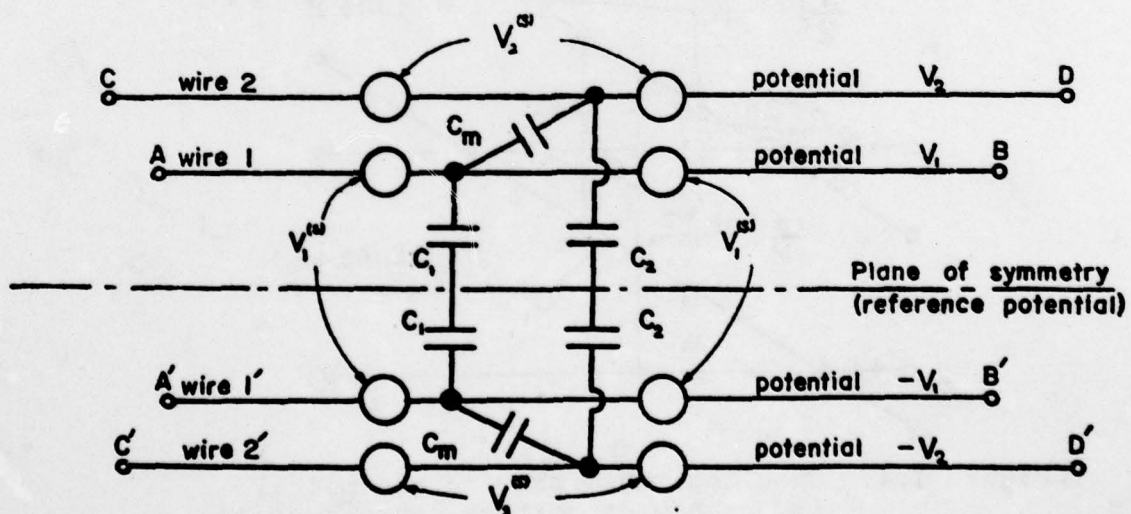


Figure 1.5b. Symmetrical form of the above circuit.

The problem at hand then, is to determine the elements  $L_m$ ,  $C_1$ ,  $C_2$  and  $C_m$ . For ease of data presentation, we define a set of normalized lumped parameters as follows.

$$\begin{aligned}
 L_m^{(n1)} &= L_m / (h_1 L'_1) \\
 C_1^{(n1)} &= C_1 / (h_1 C'_1) \\
 C_2^{(n2)} &= C_2 / (h_2 C'_2) \\
 C_m^{(n1)} &= C_m / (h_1 C'_1)
 \end{aligned}
 \tag{1.1}$$

The superscript  $n1$  in the above equation indicates normalization with respect to the line constants of line 1 and likewise for  $n2$ . Some preliminary information concerning the two isolated transmission lines is given below in Table 1. Note that the image plane is chosen as the reference potential.

TABLE I. PRELIMINARY INFORMATION ABOUT THE TWO ISOLATED TRANSMISSION LINES.

Parameter	Line 1	Line 2
radius	$a \quad (a \ll h_1)$	$a \quad (a \ll h_2)$
separation	$2h_1$	$2h_2$
inductance/ unit length	$L'_1$ $\approx \frac{\mu_0}{2\pi} \ln(2h_1/a)$	$L'_2$ $\approx \frac{\mu_0}{2\pi} \ln(2h_2/a)$
capacitance/unit length	$C'_1$ $\approx 2\pi\epsilon_0 / \ln(2h_1/a)$	$C'_2$ $\approx 2\pi\epsilon_0 / \ln(2h_2/a)$
characteristic impedance	$\sqrt{L'_1/C'_1}$ $= 60 \ln(2h_1/a)$	$\sqrt{L'_2/C'_2}$ $\approx 60 \ln(2h_2/a)$

AD-A074 265

AIR FORCE WEAPONS LAB KIRTLAND AFB NM  
ELECTROMAGNETIC PULSE INTERACTION NOTES-EMP 3-39.(U)  
JUL 79 C E BAUM

F/G 20/14

UNCLASSIFIED

AFWL-TR-79-402

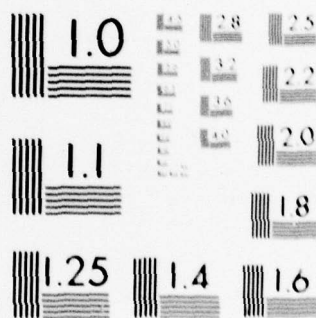
SBIE-AD-E200 363

NL

3 OF 5

AD  
A074265





MICROCOPY RESOLUTION TEST CHART  
NATIONAL BUREAU OF STANDARDS-1963-A

## 11. Mutual Inductance

In this section, we evaluate the mutual inductance element  $L_m$  between the two skewed transmission lines of Figure 1.2. It is believed that more insight into the problem is gained by looking at the skewed transmission lines of finite length  $2L$  and later let  $L$  tend to infinity. The assumptions made in the following analysis are listed below.

$$L \gg h_{>} \quad (\text{long lines}) \quad (2.1a)$$

$$(h_{>} - h_{<}) \gg a \quad (\text{sufficiently apart}) \quad (2.1b)$$

$$0 < \theta < (\pi/2), \text{ but } \theta \neq 0 \quad (\text{no distributed interaction}) \quad (2.1c)$$

$$\begin{aligned} (\partial/\partial\theta_1) (\text{charge distribution}) &\equiv 0 \quad (\text{thin wire approximation}) \\ (\partial/\partial\theta_2) (\text{charge distribution}) &\equiv 0 \quad (\text{or rotational symmetry}) \end{aligned} \quad (2.1d)$$

where  $h_{<}$  and  $h_{>}$  are respectively smaller and larger of  $h_1$  and  $h_2$ . With the above assumptions, one can write the mutual inductance as [2],

$$L_m \approx \left[ \frac{\mu_0}{4\pi} \oint_{C_1} \vec{ds}_1 \cdot \oint_{C_2} \frac{1}{R_{12}} \vec{ds}_2 \right] \quad (2.2)$$

where

$\mu_0$  = free space permeability =  $4\pi \times 10^{-7}$  (H/m), and  $C_1$  and  $C_2$  represent the closed (assumed) loops formed by the two transmission lines. With reference to Figure 1.2, we can formally write

$$L_m \approx \frac{\mu_0}{4\pi} \oint_{\substack{(ABCD) \\ (EFGA)}} \vec{ds}_1 \cdot \oint_{\substack{(PQRS) \\ (TUVF)}} \vec{ds}_2 \left(\frac{1}{R}\right)$$

Taking advantage of symmetry, we have

$$L_m \approx \frac{\mu_0}{\pi} \int_{BCDE} \vec{ds}_1 \cdot \int_{\substack{PQRS \\ TUVF}} \vec{ds}_2 \left(\frac{1}{R}\right) \quad (2.3)$$

Since there is no inductive interaction between the sections of transmission lines that are orthogonal, equation (2.3) simplifies to

$$L_m \approx \frac{\mu_0}{\pi} \left[ \cos(\theta) \int_0^L dx \int_{-L}^L \left( \frac{1}{R_{12}} - \frac{1}{R_{12'}} \right) d\xi + \int_0^{h_1} dz_1 \int_{-h_2}^{h_2} \left( \frac{1}{R_1} - \frac{1}{R_2} \right) dz_2 \right] \quad (2.4a)$$

$$= \frac{\mu_0}{\pi} [\cos(\theta) I_1(\theta) + I_2(\theta)] \quad (2.4b)$$

In view of the assumptions of equation (2.1), the R's in the above equation may be approximated by

$$R_{12} \approx [x^2 + \xi^2 - 2x\xi \cos(\theta) + (h_2 - h_1)^2]^{1/2} \quad (2.5a)$$

$$R_{12'} \approx [x^2 + \xi^2 - 2x\xi \cos(\theta) + (h_2 + h_1)^2]^{1/2} \quad (2.5b)$$

$$R_1 \approx [(z_2 - z_1)^2 + 4L^2 \sin^2(\theta/2)]^{1/2} \quad (2.5c)$$

$$R_2 \approx [(z_2 - z_1)^2 + 4L^2 \cos^2(\theta/2)]^{1/2} \quad (2.5d)$$

We will now proceed to evaluate the two integrals  $I_1(\theta)$  and  $I_2(\theta)$  separately. Setting

$$\alpha = |(h_2 - h_1)| \text{ and } \beta = (h_2 + h_1) \quad (2.6)$$

$I_1(\theta)$  is given by

$$\begin{aligned} I_1(\theta) &= \int_0^L dx \int_{-L}^L \left( \frac{1}{\sqrt{x^2 + \xi^2 - 2x\xi \cos(\theta) + \alpha^2}} - \frac{1}{\sqrt{x^2 + \xi^2 - 2x\xi \cos(\theta) + \beta^2}} \right) d\xi \\ &= \int_0^L dx \left[ \int_0^L \left( \frac{1}{\sqrt{x^2 + \xi^2 - 2x\xi \cos(\theta) + \alpha^2}} - \frac{1}{\sqrt{x^2 + \xi^2 - 2x\xi \cos(\theta) + \beta^2}} \right) d\xi \right. \\ &\quad \left. + \int_0^L \left( \frac{1}{\sqrt{x^2 + \xi^2 + 2x\xi \cos(\theta) + \alpha^2}} - \frac{1}{\sqrt{x^2 + \xi^2 + 2x\xi \cos(\theta) + \beta^2}} \right) d\xi \right] \\ &= \int_0^L dx \left[ I_{11}(x, \theta) + I_{11}(x, \pi - \theta) \right] \quad (2.7) \end{aligned}$$

where

$$\begin{aligned} I_{11}(x, \theta) &= \int_0^L d\xi \left( \frac{1}{\sqrt{(x^2 + \alpha^2) + [-2x \cos(\theta)]\xi + \xi^2}} \right. \\ &\quad \left. - \frac{1}{\sqrt{(x^2 + \beta^2) + [-2x \cos(\theta)]\xi + \xi^2}} \right) \quad (2.8) \end{aligned}$$

This integral may be performed using the result 2.261 of reference [3],

$$\begin{aligned}
I_{11}(x, \theta) &= \ln \left\{ \frac{\sqrt{x^2 + \alpha^2 - 2xL \cos(\theta) + L^2} + L - [x \cos(\theta)]}{\sqrt{x^2 + \beta^2 - 2xL \cos(\theta) + L^2} + L - [x \cos(\theta)]} \right\} \\
&+ \ln \left\{ \frac{\sqrt{x^2 + \beta^2} - x \cos(\theta)}{\sqrt{x^2 + \alpha^2} - x \cos(\theta)} \right\} \\
&= \ln \left\{ \frac{\sqrt{x^2 + \beta^2} - x \cos(\theta)}{\sqrt{x^2 + \alpha^2} - x \cos(\theta)} \right\} + I_n(x, \theta)
\end{aligned} \tag{2.9}$$

where  $I_n(\theta)$  is the first term on the right side of equation (2.9). Therefore,

$$I_{11}(x, \pi - \theta) = \ln \left\{ \frac{\sqrt{x^2 + \beta^2} + x \cos(\theta)}{\sqrt{x^2 + \alpha^2} + x \cos(\theta)} \right\} + I_n(x, \pi - \theta) \tag{2.10}$$

Substituting the above two equations into equation (2.7), we obtain,

$$\begin{aligned}
I_1(\theta) &= \left[ \int_0^L dx \ln \left\{ \frac{x^2 + \beta^2 \operatorname{cosec}^2(\theta)}{x^2 + \alpha^2 \operatorname{cosec}^2(\theta)} \right\} \right] + \int_0^L I_n(x, \theta) dx \\
&+ \int_0^L I_n(x, \pi - \theta) dx
\end{aligned} \tag{2.11}$$

Using the result 2.733.1 of reference [3],

$$\begin{aligned}
I_1(\theta) &= L \ln \left\{ \frac{L^2 + \beta^2 \operatorname{cosec}^2(\theta)}{L^2 + \alpha^2 \operatorname{cosec}^2(\theta)} \right\} + \left[ \frac{2\beta}{\sin(\theta)} \arctan \left| \frac{L \sin(\theta)}{\beta} \right| \right] \\
&- \left[ \frac{2\alpha}{\sin(\theta)} \arctan \left| \frac{L \sin(\theta)}{\alpha} \right| \right] \\
&+ [i_n(\theta) + i_n(\pi - \theta)]
\end{aligned} \tag{2.12}$$

where  $i_n(\theta)$  is an integral to be evaluated numerically and is given by

$$i_n(\theta) = \int_0^L I_n(x, \theta) dx$$

$$= \int_0^L \ln \left\{ \frac{\sqrt{x^2 + \alpha^2 - 2xL \cos(\theta) + L^2} + L - [x \cos(\theta)]}{\sqrt{x^2 + \beta^2 - 2xL \cos(\theta) + L^2} + L - [x \cos(\theta)]} \right\} dx \quad (2.13)$$

It may be shown that, when the lengths of the transmission lines are large compared to the heights,  $i_n(\theta)$  does not contribute significantly to the result in equation (2.12). We still have the second term of equation (2.4a) to compute, which accounts for the interaction between the vertical end wires and it is given by

$$I_2(\theta) = \int_0^{h_1} dz_1 \int_{-h_2}^{h_2} dz_2 \left( \frac{1}{\sqrt{(z_2 - z_1)^2 + A_1^2}} - \frac{1}{\sqrt{(z_2 - z_1)^2 + A_2^2}} \right) \quad (2.14a)$$

where

$$A_1 = 2L \sin(\theta/2); \quad A_2 = 2L \cos(\theta/2) \quad (2.14b)$$

Consider the first term on the right side of the above,

$$\text{Integral} = \int_0^{h_1} dz_1 \int_{-h_2}^{h_2} dz_2 \left( \frac{1}{\sqrt{(z_2 - z_1)^2 + A_1^2}} \right) \quad (2.15)$$

Using (2.261.2 of Ref. [3]), we can evaluate this integral to be

$$\begin{aligned}
&= \int_0^{h_1} dz_1 \left[ \operatorname{arcsinh} \left\{ \frac{h_2 - z_1}{A_1} \right\} + \operatorname{arcsinh} \left\{ \frac{h_2 + z_1}{A_1} \right\} \right] \\
&= A_1 \left[ \int_{(h_2/A_1)}^{(\beta/A_1)} \operatorname{arcsinh} (y) dy - \int_{(h_2/A_1)}^{(\alpha/A_1)} \operatorname{arcsinh} (y) dy \right] \\
&= A_1 \left[ \int_{(\alpha/A_1)}^{(\beta/A_1)} \operatorname{arcsinh} (y) dy \right]
\end{aligned}$$

using (2.741.2. of [3]), we get

$$= \left[ \beta \operatorname{arcsinh} (\beta/A_1) - \alpha \operatorname{arcsinh} (\alpha/A_1) - \sqrt{\beta^2 + A_1^2} + \sqrt{\alpha^2 + A_1^2} \right] \quad (2.16)$$

Therefore

$$\begin{aligned}
I_2(\theta) &= \beta \left[ \operatorname{arcsinh} (\beta/A_1) - \operatorname{arcsinh} (\beta/A_2) \right] \\
&\quad - \alpha \left[ \operatorname{arcsinh} (\alpha/A_1) - \operatorname{arcsinh} (\alpha/A_2) \right] \\
&\quad - \left[ \sqrt{\beta^2 + A_1^2} - \sqrt{\beta^2 + A_2^2} \right] \\
&\quad + \left[ \sqrt{\alpha^2 + A_1^2} - \sqrt{\alpha^2 + A_2^2} \right] \quad (2.17)
\end{aligned}$$

Substituting our results for  $I_1(\theta)$  and  $I_2(\theta)$  from equations (2.12) and (2.17) respectively into equation (2.4b), we finally obtain for the mutual inductance

$$\begin{aligned}
L_m = \frac{\mu_0}{\pi} & \left[ L \ln \left\{ \frac{1 + \frac{\beta^2}{L^2} \csc^2(\theta)}{1 + \frac{\alpha^2}{L^2} \csc^2(\theta)} \right\} \cos(\theta) + \left\{ i_n(\theta) + i_n(\pi-\theta) \right\} \cos(\theta) \right. \\
& + \left\{ \frac{2\beta}{\sin(\theta)} \arctan\left(\frac{L \sin \theta}{\beta}\right) - \frac{2\alpha}{\sin(\theta)} \arctan\left(\frac{L \sin \theta}{\alpha}\right) \right\} \cos(\theta) \\
& + \beta \left\{ \operatorname{arcsinh}(\beta/A_1) - \operatorname{arcsinh}(\beta/A_2) \right\} \\
& - \alpha \left\{ \operatorname{arcsinh}(\alpha/A_1) - \operatorname{arcsinh}(\alpha/A_2) \right\} \\
& - \left\{ \sqrt{\beta^2 + A_1^2} - \sqrt{\beta^2 + A_2^2} \right\} \\
& + \left. \left\{ \sqrt{\alpha^2 + A_1^2} - \sqrt{\alpha^2 + A_2^2} \right\} \right]
\end{aligned}
\tag{2.18}$$

We recall that in the above expression, the various quantities are

$L$  = half length of the transmission lines

$\theta$  = skew angle

$\beta = (h_1 + h_2)$  ;  $\alpha = |h_2 - h_1|$

$A_1 = 2L \sin(\theta/2)$  ;  $A_2 = 2L \cos(\theta/2)$

$\mu_0$  = free space permeability

and  $i_n(\theta)$ , given in equation (2.13), is an integral which can be evaluated numerically, however small its contribution may be.

### A. Discussion of Results

Equation (2.18) is the mutual inductance of two skewed transmission lines each of length  $2L$ . It is interesting to note that for finite values of heights  $h_1$  and  $h_2$  and the skew angle in the range of  $0 < \theta < (\pi/2)$ , and letting the length of the transmission lines tend to infinity, the mutual inductance becomes

$$\begin{aligned} \lim_{L \rightarrow \infty} L_m &= \mu_0 (\beta - \alpha) \cot(\theta) \\ &= \mu_0 [(h_2 + h_1) - |h_2 - h_1|] \cot(\theta) \\ &= 2\mu_0 h_c \cot(\theta) \end{aligned} \quad (2.19)$$

with  $h_c$  being the smaller of  $(h_1$  and  $h_2)$ .

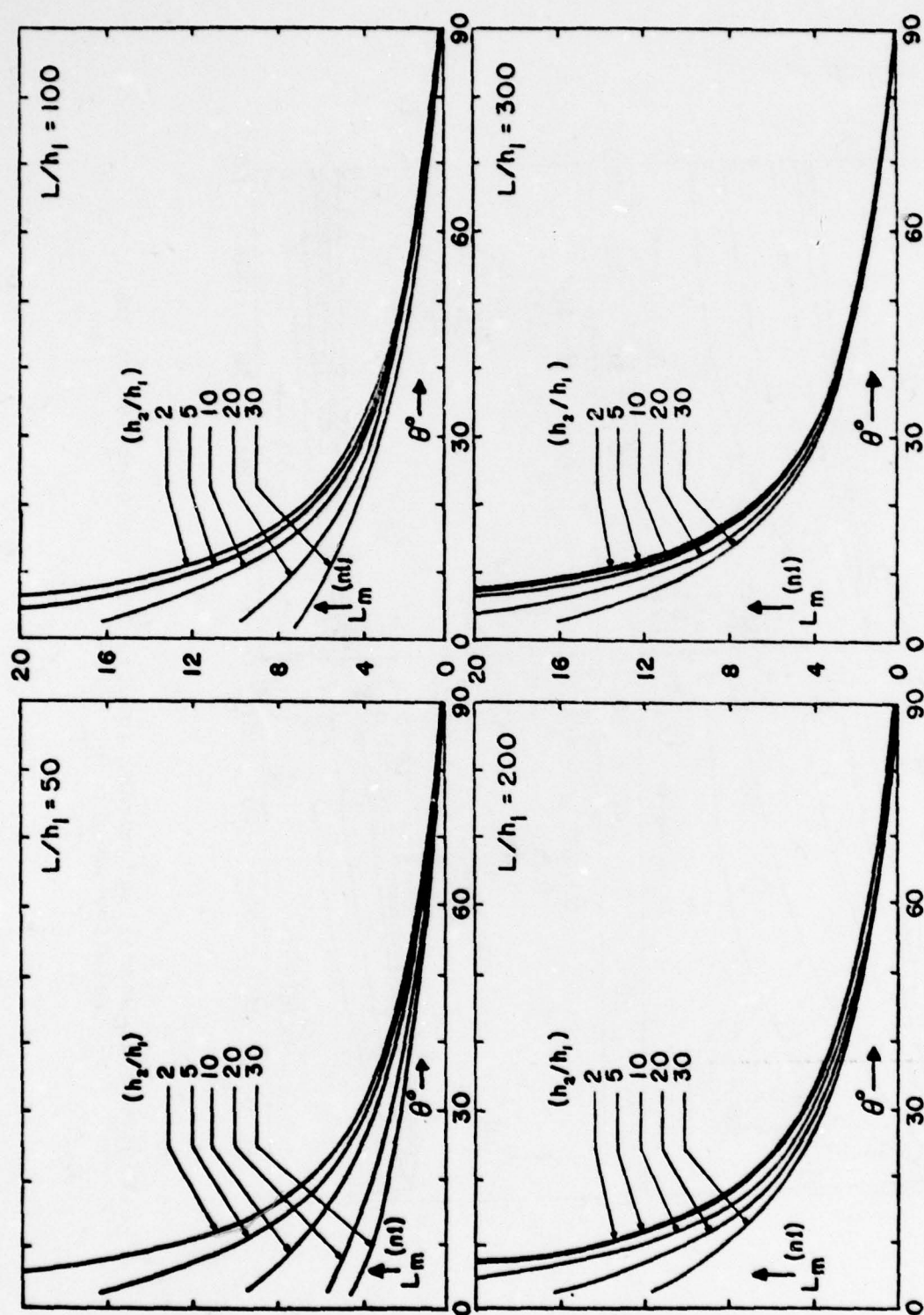
This result has been independently verified by starting the problem with infinitely long lines. It suggests that if the transmission lines are infinitely long, the mutual inductance is a property of only the transmission line with smaller spacing.

However, under the assumptions outlined in equation (2.1), equation (2.18) accurately gives the value of the mutual inductance and is parametrically displayed in Figures 2.1, 2.2, and 2.3. The quantity plotted is the normalized mutual inductance  $L_m^{(nl)}$  of equation (1.1) given by

$$\begin{aligned}
 L_m^{(nl)} &= L_m / [h_1 L_1'] \quad (\text{dimensionless}) \\
 &= L_m / \left[ h_1 \left( \frac{\mu_0}{2\pi} \right) \ln \left( \frac{2h_1}{a} \right) \right] \quad (2.20)
 \end{aligned}$$

All linear dimensions are normalized with respect to  $h_1$  by choosing  $h_1 = 1$ . The radius  $a$  is chosen to be .01347 so that  $\ln(2h_1/a) = 5$  and it occurs only in the normalization procedure. With this choice of normalization,  $L_m^{(nl)}$  is a function of three variables,  $\theta$ ,  $h_2$  and  $L$ . In Figures 2.1, 2.2, and 2.3,  $L_m^{(nl)}$  is shown plotted as a function of these three variables respectively. In computing  $L_m^{(nl)}$  from equation (2.20), the "exact" expression of  $L_m$  given by equation (2.18) is used which includes the contribution from the end wires as well. The two integrals appearing in equation (2.18) have smooth integrands and a simple Simpson's rule of integration was found to be adequate.

As a function of the skew angle  $\theta$ , the mutual inductance in Figure 2.1 goes to zero at  $\theta = (\pi/2)$ , as one would expect. In this figure, one can see the insensitivity of the mutual inductance with respect to  $h_2$  even for small  $\theta$  as the lengths of the transmission line increase. For all the four cases of varying  $L$ , it is seen that for  $\theta = 0$ , the mutual inductance displays a singularity corresponding to the transmission line or distributed type of interaction.

Figure 2.1 Normalized mutual inductance as a function of the skew angle  $\theta$

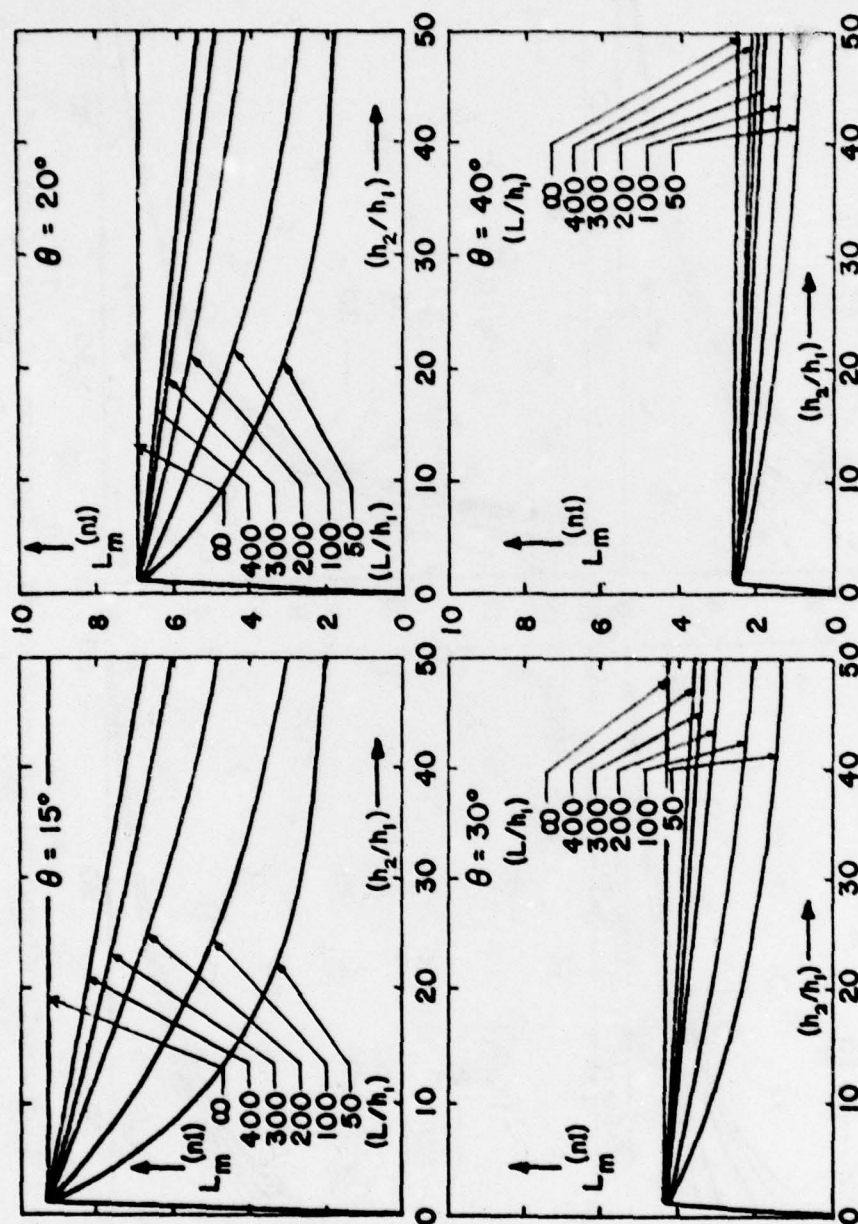


Figure 2.2 Normalized mutual inductance as a function of the relative height  $(h_2/h_1)$ .

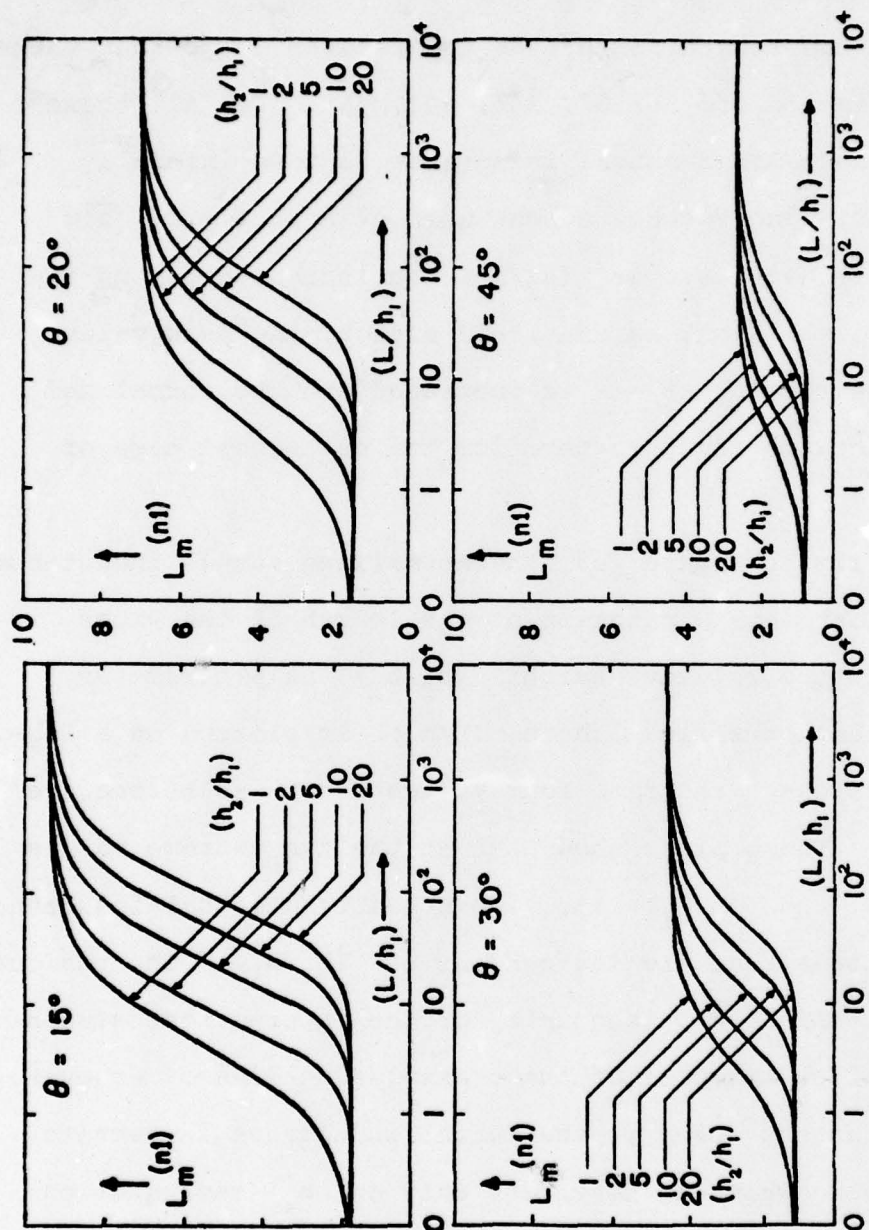


Figure 2.3 Normalized mutual inductance as a function of normalized line length  $(L/h_1)$ .

In Figure 2.2, the normalized mutual inductance is plotted as a function of  $(h_2/h_1)$ , for a fixed skew angle  $\theta$  and with the length  $(L/h_1)$  as a parameter. The four values of  $\theta$  considered are  $= 15^\circ, 20^\circ, 30^\circ, 45^\circ$ . For all these cases, the normalized mutual inductance is zero initially  $[(h_2/h_1) = 0]$  and reaches a peak when  $[(h_2/h_1) = 1]$  and monotonically decreases as  $(h_2/h_1)$  is increased beyond the value of unity. Also, as one would expect, the peak value itself is decreasing as  $\theta$  is increased and the normalized mutual inductance tends to zero for the orthogonal case of  $\theta = 90^\circ$ .

Finally in Figure 2.3, the normalized mutual inductance is shown plotted as a function of the length of the wires  $(L/h_1)$  with the relative height  $(h_2/h_1)$  as a parameter. Note that the normalized length  $(L/h_1)$  is plotted on a logarithmic scale and the same four values of  $\theta$  as before are considered. These plots show that at the two extreme values  $[(L/h_1) \rightarrow 0 \text{ and } (L/h_1) \gg 1]$ , the normalized mutual inductance tends to values that are independent of  $(h_2/h_1)$ . The residual value when  $(L/h_1) = 0$  accounts for the interaction between the vertical end members of the transmission lines. However, for large lengths  $L \gg h_1$ , the mutual inductance is seen to obtain a value which is dependent only on  $h_1$  (see equation 2.19). We reach an interesting conclusion that, if the

transmission lines are infinitely long, the mutual inductance is a property of only the transmission line with the smaller wire separation.

### III. Capacitive Coupling

The physical mechanism that justifies the use of a capacitive coupling model of Figure 1.5 may be described as follows. When the two lines are present by themselves and unperturbed by the other, the total charge per unit length on the two wires are constants given by  $Q'_{10}$  and  $Q'_{20}$  ([4]). The effect of the proximity of one wire on the other results in a redistribution of charge in the vicinity of the junction so that the total charges per unit lengths  $Q'_1(x, \theta)$  and  $Q'_2(\zeta, \theta)$  now become position dependent according as

$$\begin{aligned} Q'_1(x, \theta) &= Q'_{10} + q'_1(x, \theta) \\ Q'_2(\zeta, \theta) &= Q'_{20} + q'_2(\zeta, \theta) \end{aligned} \quad (3.1)$$

where the excess total charges per unit length  $q'_1(x, \theta)$  and  $q'_2(\zeta, \theta)$  permit us to derive a capacitive coupling model. Implicit in such a derivation is an assumption [4] that the excess charges which decay with distance away from the junction will have an integrated effect and can be represented by lumped parameters at the junction itself.

We also note here that for the case of  $\theta = 0$ , the total charges per unit length once again become independent of position, denoted by

$$\begin{aligned}
 Q'_1(x, 0) &\equiv Q'_{10} = (Q'_{10} + q'_{10}) \\
 Q'_2(\zeta, 0) &\equiv Q'_{20} = (Q'_{20} + q'_{20})
 \end{aligned}
 \tag{3.2}$$

where the excess charges for the case of  $\theta = 0$  also are constants according as

$$\begin{aligned}
 q'_1(x, 0) &\equiv q'_{10} \\
 q'_2(\zeta, 0) &\equiv q'_{20}
 \end{aligned}
 \tag{3.3}$$

The entire electrostatic system for all values of  $\theta$  is electrically neutral because the image wires carry exact amounts of opposite charges, i.e.,

$$\begin{aligned}
 [Q'_1(x, \theta) = -Q'_1(x, \theta)] & \quad ; \quad [Q'_2(\zeta, \theta) = -Q'_2(\zeta, \theta)] \\
 [q'_1(x, \theta) = -q'_1(x, \theta)] & \quad ; \quad [q'_2(\zeta, \theta) = -q'_2(\zeta, \theta)]
 \end{aligned}
 \tag{3.4}$$

Furthermore, by virtue of symmetry about the junction, all the charges are even functions in their respective variables, as shown below.

$$\begin{aligned}
 [Q'_1(x, \theta) = Q'_1(-x, \theta)] & \quad ; \quad [Q'_2(\zeta, \theta) = Q'_2(-\zeta, \theta)] \\
 [q'_1(x, \theta) = q'_1(-x, \theta)] & \quad ; \quad [q'_2(\zeta, \theta) = q'_2(-\zeta, \theta)]
 \end{aligned}
 \tag{3.5}$$

For  $\theta$  in the range of our interest  $[0 \leq \theta \leq (\pi/2)]$ , the coupled pair of integral equations for the potentials

$V_1$  and  $V_2$  in terms of the linear charge densities may be written down as,

$$V_1 = \frac{1}{4\pi\epsilon_0} \int_{-\infty}^{\infty} Q'_1(x', \theta) K_{11}(x, x') dx' + \frac{1}{4\pi\epsilon_0} \int_{-\infty}^{\infty} Q'_2(\zeta', \theta) K_{12}(x, \zeta') d\zeta' \quad (3.6a)$$

$$V_2 = \frac{1}{4\pi\epsilon_0} \int_{-\infty}^{\infty} Q'_1(x', \theta) K_{21}(\zeta, x', \theta) dx' + \frac{1}{4\pi\epsilon_0} \int_{-\infty}^{\infty} Q'_2(\zeta', \theta) K_{22}(\zeta, \zeta') d\zeta' \quad (3.6b)$$

where the kernels may be written down by inspection as,

$$K_{11}(x, x') = \left[ \frac{1}{r_{11}} - \frac{1}{r_{11}'} \right]; \quad K_{12}(x, \zeta', \theta) = \left[ \frac{1}{r_{12}} - \frac{1}{r_{12}'} \right] \quad (3.7a)$$

$$K_{21}(\zeta, x', \theta) = \left[ \frac{1}{r_{21}} - \frac{1}{r_{21}'} \right]; \quad K_{22}(\zeta, \zeta') = \left[ \frac{1}{r_{22}} - \frac{1}{r_{22}'} \right] \quad (3.7b)$$

with

$$r_{11} = [(x-x')^2 + a^2]^{1/2}; \quad r_{11}' = [(x-x')^2 + 4h_1^2]^{1/2} \quad (3.8a)$$

$$r_{12} = [x^2 + \zeta'^2 - 2x\zeta' \cos(\theta) + a^2]^{1/2} \\ = [\{\zeta' - x \cos(\theta)\}^2 + \{a^2 + x^2 \sin^2(\theta)\}]^{1/2} \quad (3.8b)$$

$$r_{12}' = [x^2 + \zeta'^2 - 2x\zeta' \cos(\theta) + \beta^2]^{1/2} \\ = [\{\zeta' - x \cos(\theta)\}^2 + \{\beta^2 + x^2 \sin^2(\theta)\}]^{1/2} \quad (3.8c)$$

$$r_{21} = [x'^2 + \zeta^2 - 2x'\zeta \cos(\theta) + a^2]^{1/2} \\ = [\{x' - \zeta \cos(\theta)\}^2 + \{a^2 + \zeta^2 \sin^2(\theta)\}]^{1/2} \quad (3.8d)$$

$$r_{21}' = [x'^2 + \zeta^2 - 2x'\zeta \cos(\theta) + \beta^2]^{1/2} \\ = [\{x' - \zeta \cos(\theta)\}^2 + \{\beta^2 + \zeta^2 \sin^2(\theta)\}]^{1/2} \quad (3.8e)$$

$$r_{22} = [(\zeta - \zeta')^2 + a^2]^{1/2}; \quad r_{22}' = [(\zeta - \zeta')^2 + 4h_2^2]^{1/2} \quad (3.8f)$$

$$\text{where recall that } a = |h_2 - h_1| \text{ and } \beta = (h_2 + h_1) \quad (3.8g)$$

Substituting for the total charges  $Q'_1(x, \theta)$  and  $Q'_2(\zeta, \theta)$  in equation (3.6) from equation (3.1), we have

$$V_1 = \left[ Q'_{10} \left\{ \frac{1}{4\pi\epsilon_0} \int_{-\infty}^{\infty} K_{11}(x, x') dx' \right\} + \frac{1}{4\pi\epsilon_0} \int_{-\infty}^{\infty} q'_1(x', \theta) K_{11}(x, x') dx' \right. \\ \left. + Q'_{20} \left\{ \frac{1}{4\pi\epsilon_0} \int_{-\infty}^{\infty} K_{12}(x, \zeta', \theta) d\zeta' \right\} + \frac{1}{4\pi\epsilon_0} \int_{-\infty}^{\infty} q'_2(\zeta', \theta) K_{12}(x, \zeta', \theta) d\zeta' \right] \quad (3.6a)$$

$$V_2 = \left[ Q'_{10} \left\{ \frac{1}{4\pi\epsilon_0} \int_{-\infty}^{\infty} K_{21}(\zeta, x', \theta) dx' \right\} + \frac{1}{4\pi\epsilon_0} \int_{-\infty}^{\infty} q'_1(x', \theta) K_{21}(\zeta, x', \theta) dx' \right. \\ \left. + Q'_{20} \left\{ \frac{1}{4\pi\epsilon_0} \int_{-\infty}^{\infty} K_{22}(\zeta, \zeta') d\zeta' \right\} + \frac{1}{4\pi\epsilon_0} \int_{-\infty}^{\infty} q'_2(\zeta', \theta) K_{22}(\zeta, \zeta') d\zeta' \right] \quad (3.6b)$$

The integrals of the kernel functions are somewhat tedious but can be performed to give

$$\left\{ \frac{1}{4\pi\epsilon_0} \int_{-\infty}^{\infty} K_{11}(x, x') dx' \right\} = \frac{1}{2\pi\epsilon_0} \ln \left( \frac{2h_1}{a} \right) \equiv S_{11} \quad (3.7a)$$

$$\left\{ \frac{1}{4\pi\epsilon_0} \int_{-\infty}^{\infty} K_{22}(\zeta, \zeta') d\zeta' \right\} = \frac{1}{2\pi\epsilon_0} \ln \left( \frac{2h_2}{a} \right) \equiv S_{22} \quad (3.7b)$$

$$\left\{ \frac{1}{4\pi\epsilon_0} \int_{-\infty}^{\infty} K_{12}(x, \zeta', \theta) d\zeta' \right\} = \frac{-1}{4\pi\epsilon_0} \ln \left\{ \frac{x^2 \sin^2(\theta) + a^2}{x^2 \sin^2(\theta) + \beta^2} \right\} \equiv \frac{-f(x, \theta)}{4\pi\epsilon_0} \quad (3.7c)$$

$$\left\{ \frac{1}{4\pi\epsilon_0} \int_{-\infty}^{\infty} K_{21}(\zeta, x', \theta) dx' \right\} = \frac{-1}{4\pi\epsilon_0} \ln \left\{ \frac{\zeta^2 \sin^2(\theta) + a^2}{\zeta^2 \sin^2(\theta) + \beta^2} \right\} \equiv \frac{-f(\zeta, \theta)}{4\pi\epsilon_0} \quad (3.7d)$$

Recognizing that  $Q'_{10} S_{11} = V_1$  and  $Q'_{20} S_{22} = V_2$  for the isolated lines, we arrive at the coupled pair of integral equations for the excess charges given by,

$$\int_{-\infty}^{\infty} q'_1(x', \theta) K_{11}(x, x') dx' + \int_{-\infty}^{\infty} q'_2(\zeta', \theta) K_{12}(x, \zeta', \theta) d\zeta' = C'_2 V_2 f(x, \theta) \quad (3.8a)$$

$$\int_{-\infty}^{\infty} q'_1(x', \theta) K_{21}(\zeta, x', \theta) dx' + \int_{-\infty}^{\infty} q'_2(\zeta', \theta) K_{22}(\zeta, \zeta') d\zeta' = C'_1 V_1 f(\zeta, \theta) \quad (3.8b)$$

In writing above, we have introduced the unperturbed line capacitances of the two transmission lines given by

$$C'_1 = \frac{Q'_{10} - (-Q'_{10})}{V_1 - (-V_1)} = \frac{Q'_{10}}{V_1} = \frac{2\pi\epsilon_0}{\ln(2h_1/a)} \equiv \frac{2\pi\epsilon_0}{\Omega_1} \quad (3.9a)$$

$$C'_2 = \frac{Q'_{20} - (-Q'_{20})}{V_2 - (-V_2)} = \frac{Q'_{20}}{V_2} = \frac{2\pi\epsilon_0}{\ln(2h_2/a)} \equiv \frac{2\pi\epsilon_0}{\Omega_2} \quad (3.9b)$$

and the two forcing functions can be written in a shorthand form as

$$f(\xi, \theta) \simeq \ln \left\{ \frac{\xi^2 \sin^2(\theta) + \alpha^2}{\xi^2 \sin^2(\theta) + \beta^2} \right\} \quad (3.10)$$

We can now define a capacitive coefficient matrix associated with the excess charges as

$$\begin{bmatrix} q'_1(x, \theta) \\ q'_2(\zeta, \theta) \end{bmatrix} = \begin{bmatrix} k_{11}(x, \theta) & k_{12}(x, \theta) \\ k_{21}(\zeta, \theta) & k_{22}(\zeta, \theta) \end{bmatrix} \begin{bmatrix} v_1 \\ v_2 \end{bmatrix} \quad (3.11)$$

so that

$$k_{11}(x, \theta) = \left. \frac{q'_1(x, \theta)}{v_1} \right|_{v_2 = 0} \quad (3.12a)$$

$$k_{12}(x, \theta) = \left. \frac{q'_1(x, \theta)}{v_2} \right|_{v_1 = 0} \quad (3.12b)$$

$$k_{21}(\zeta, \theta) = \left. \frac{q'_2(\zeta, \theta)}{v_1} \right|_{v_2 = 0} \quad (3.12c)$$

$$k_{22}(\zeta, \theta) = \left. \frac{q'_2(\zeta, \theta)}{v_2} \right|_{v_1 = 0} \quad (3.12d)$$

and the lumped self capacitances in the coupling model are given by,

$$\begin{aligned} C_1 &= \int_{-\infty}^{\infty} [k_{11}(x, \theta) + k_{12}(x, \theta)] dx \\ &= 2 \int_0^{\infty} [k_{11}(x, \theta) + k_{12}(x, \theta)] dx \quad (3.13a) \end{aligned}$$

$$\begin{aligned} C_2 &= \int_{-\infty}^{\infty} [k_{22}(\zeta, \theta) + k_{21}(\zeta, \theta)] d\zeta \\ &= 2 \int_0^{\infty} [k_{22}(\zeta, \theta) + k_{21}(\zeta, \theta)] d\zeta \quad (3.13b) \end{aligned}$$

$$\begin{aligned}
 C_m &= - \int_{-\infty}^{\infty} k_{12}(x, \theta) dx = -2 \int_0^{\infty} k_{12}(x, \theta) dx \\
 &= - \int_{-\infty}^{\infty} k_{21}(\zeta, \theta) d\zeta = -2 \int_0^{\infty} k_{12}(\zeta, \theta) d\zeta
 \end{aligned}
 \tag{3.13c}$$

We may now set up the integral equations for the excess capacitive coefficients of equation (3.12) by successively considering  $V_1 = 0$  and  $V_2 = 0$  in equation (3.8).

1. Setting  $V_1 = 0$  in equation (3.8) with  $V_2 \neq 0$ , but finite, leads to

$$\begin{aligned}
 \int_{-\infty}^{\infty} k_{12}(x', \theta) K_{11}(x, x') dx' + \int_{-\infty}^{\infty} k_{22}(\zeta', \theta) K_{12}(x, \zeta', \theta) d\zeta' \\
 = C'_2 f(x, \theta)
 \end{aligned}
 \tag{3.14a}$$

$$\int_{-\infty}^{\infty} k_{12}(x', \theta) K_{21}(\zeta, x', \theta) dx' + \int_{-\infty}^{\infty} k_{22}(\zeta', \theta) K_{22}(\zeta, \zeta') d\zeta' = 0
 \tag{3.14b}$$

2. Setting  $V_2 = 0$  in equation (3.8) with  $V_1 \neq 0$ , but finite, leads to

$$\int_{-\infty}^{\infty} k_{11}(x', \theta) K_{11}(x, x') dx' + \int_{-\infty}^{\infty} k_{21}(\zeta', \theta) K_{12}(x, \zeta', \theta) d\zeta' = 0
 \tag{3.15a}$$

$$\begin{aligned}
 \int_{-\infty}^{\infty} k_{11}(x', \theta) K_{21}(\zeta, x', \theta) dx' + \int_{-\infty}^{\infty} k_{21}(\zeta', \theta) K_{22}(\zeta, \zeta') d\zeta' \\
 = C'_1 f(\zeta, \theta)
 \end{aligned}
 \tag{3.15b}$$

The remainder of the procedure consists of solving coupled pairs of equations (3.14) and (3.15) for the excess capacitive coefficients and using them in equation (3.13) to get the lumped capacitances.

In concluding this formulation, it is observed that for the special case of  $\theta = 0$ , using equations (3.3) and (3.7) in (3.6), we obtain

$$V_1 = Q'_{10} S_{11} + q'_{10} S_{11} + Q'_{20} S_{12} + q'_{20} S_{12} \quad (3.16)$$

$$V_2 = Q'_{10} S_{21} + q'_{10} S_{21} + Q'_{20} S_{22} + q'_{20} S_{22}$$

or, using equation (3.2), (3.16) becomes

$$V_1 = Q_{10} S_{11} + Q_{20} S_{12} \quad (3.17)$$

$$V_2 = Q_{10} S_{21} + Q_{20} S_{22}$$

with

$$S_{11} = \frac{1}{2\pi\epsilon_0} \ln\left(\frac{2h_1}{a}\right); \quad S_{22} = \frac{1}{2\pi\epsilon_0} \ln\left(\frac{2h_2}{a}\right) \quad (3.18)$$

and

$$S_{12} = S_{21} = \frac{1}{2\pi\epsilon_0} \ln\left(\frac{\beta}{\alpha}\right) = \frac{1}{2\pi\epsilon_0} \ln\left(\frac{h_2 + h_1}{|h_2 - h_1|}\right)$$

These results for  $\theta = 0$ , are in complete agreement with the published results in the literature (see for example [1 or 5]).

## A. Approximate Analytical Solution

We now develop an approximate analytical solution for the coupled pairs of integral equations (3.14) and (3.15). Rewriting these equations in terms of dimensionless excess capacitive coefficients, we have

$$\int_{-\infty}^{\infty} f_{12}(x', \theta) K_{11}(x, x') dx' + \int_{-\infty}^{\infty} f_{22}(\zeta', \theta) K_{12}(x, \zeta', \theta) d\zeta' = f(x, \theta) \quad (3.19a)$$

$$\int_{-\infty}^{\infty} f_{12}(x', \theta) K_{21}(\zeta, x', \theta) dx' + \int_{-\infty}^{\infty} f_{22}(\zeta', \theta) K_{22}(\zeta, \zeta') d\zeta' = 0 \quad (3.19b)$$

and

$$\int_{-\infty}^{\infty} f_{11}(x', \theta) K_{11}(x, x') dx' + \int_{-\infty}^{\infty} f_{21}(\zeta', \theta) K_{12}(x, \zeta', \theta) d\zeta' = 0 \quad (3.20a)$$

$$\int_{-\infty}^{\infty} f_{11}(x', \theta) K_{21}(\zeta, x', \theta) dx' + \int_{-\infty}^{\infty} f_{21}(\zeta', \theta) K_{22}(\zeta, \zeta') d\zeta' = f(\zeta, \theta) \quad (3.20b)$$

where the unknown and normalized excess capacitive coefficients are defined by

$$\begin{aligned} f_{11}(x', \theta) &= k_{11}(x', \theta) / C_1' ; & f_{12}(x', \theta) &= k_{12}(x', \theta) / C_2' \\ f_{21}(\zeta', \theta) &= k_{21}(\zeta', \theta) / C_1' ; & f_{22}(\zeta', \theta) &= k_{22}(\zeta', \theta) / C_2' \end{aligned} \quad (3.21)$$

We now consider solving the coupled integral equation (3.19) and a similar method of solution will apply to equation (3.20) also. To begin with, we expand the excess charges per unit length  $q'_1(x', \theta)$  and  $q'_2(\zeta', \theta)$  in Taylor series about the points  $x$  and  $\zeta$  respectively. Then, the leading and the first correction terms are given by

$$\begin{aligned} q'_1(x', \theta) &= q'_1(x, \theta) + (x' - x) \frac{\partial q'_1}{\partial x}(x, \theta) + \dots \\ q'_2(\zeta', \theta) &= q'_2(\zeta, \theta) + (\zeta' - \zeta) \frac{\partial q'_2}{\partial \zeta}(\zeta, \theta) + \dots \end{aligned} \quad (3.22)$$

As a result, the unknown functions in equation (3.19) will have expansions given by

$$\begin{aligned} f_{12}(x', \theta) &= f_{12}(x, \theta) + (x' - x) \frac{\partial f_{12}}{\partial x}(x, \theta) + \dots \\ f_{22}(\zeta', \theta) &= f_{22}(\zeta, \theta) + (\zeta' - \zeta) \frac{\partial f_{22}}{\partial \zeta}(\zeta, \theta) + \dots \end{aligned} \quad (3.23)$$

Considering these expansions in the integrals involving the self kernels in equation (3.19), for instance,

$$\begin{aligned} \int_{-\infty}^{\infty} f_{12}(x', \theta) K_{11}(x, x') dx' &= A_{11} f_{12}(x, \theta) \\ &+ \frac{\partial f_{12}}{\partial x}(x, \theta) \int_{-\infty}^{\infty} (x' - x) K_{11}(x, x') dx' + \dots \end{aligned} \quad (3.24)$$

where, using equation (3.7a),  $A_{11}$  is a constant given by

$$A_{11} = 4\pi\epsilon_0 S_{11} = 2 \ln(2h_1/a) \quad (3.25)$$

King [2] has shown that all of the terms in equation (3.24) involving the derivatives of  $f_{12}(x, \theta)$  contribute insignificantly compared to the first term under the condition that the radiation from the transmission lines are negligible. As a consequence of this approximation which is well justified at low frequencies, the coupled integral equation (3.19) may be written approximately as

$$A_{11} f_{12}(x, \theta) + \int_{-\infty}^{\infty} f_{22}(\zeta', \theta) K_{12}(x, \zeta', \theta) d\zeta' = f(x, \theta) \quad (3.26a)$$

$$\int_{-\infty}^{\infty} f_{12}(x', \theta) K_{21}(\zeta, x', \theta) dx' + A_{22} f_{22}(\zeta, \theta) = 0 \quad (3.26b)$$

where it is recalled that

$$A_{11} = 2 \ln(2h_1/a) \quad \text{and} \quad A_{22} = 2 \ln(2h_2/a) \quad (3.27)$$

It is now observed that the above equation can be uncoupled by straightforward algebraic manipulations to obtain,

$$A_{11} f_{12}(x, \theta) - \frac{1}{A_{22}} \int_{-\infty}^{\infty} f_{12}(x', \theta) T(x, x', \theta) dx' = f(x, \theta) \quad (3.28)$$

$$A_{22} f_{22}(\zeta, \theta) - \frac{1}{A_{11}} \int_{-\infty}^{\infty} f_{22}(\zeta', \theta) T(\zeta, \zeta', \theta) d\zeta' = \frac{1}{A_{11}} t(\zeta, \theta) \quad (3.29)$$

where the various kernels and the forcing functions are given by

$$T(x, x', \theta) = \int_{-\infty}^{\infty} K_{12}(x, \zeta', \theta) K_{21}(\zeta', x', \theta) d\zeta' \quad (3.30a)$$

$$T(\zeta, \zeta', \theta) = \int_{-\infty}^{\infty} K_{12}(x', \zeta', \theta) K_{21}(\zeta, x', \theta) dx' \quad (3.30b)$$

$$f(x, \theta) = \ln \left\{ \frac{x^2 \sin^2(\theta) + \alpha^2}{x^2 \sin^2(\theta) + \beta^2} \right\} \quad (3.30c)$$

$$t(\zeta, \theta) = \int_{-\infty}^{\infty} T(\zeta, \zeta', \theta) d\zeta' = - \int_{-\infty}^{\infty} f(x', \theta) K_{21}(\zeta, x', \theta) dx' \quad (3.30d)$$

similarly,

$$t(x, \theta) = \int_{-\infty}^{\infty} T(x, x', \theta) dx' = - \int_{-\infty}^{\infty} f(\zeta', \theta) K_{12}(x, \zeta', \theta) d\zeta' \quad (3.30e)$$

Once again, using the same approximation as before i.e., essentially retaining the leading terms of the Taylor series expansions of  $f_{12}(x', \theta)$  about  $f_{12}(x, \theta)$ , and of,  $f_{22}(\zeta', \theta)$  about  $f_{22}(\zeta, \theta)$ , in equations (3.28) and (3.29), we have

$$A_{11} f_{12}(x, \theta) - f_{12}(x, \theta) \left\{ t(x, \theta) / A_{22} \right\} = f(x, \theta) \quad (3.31)$$

$$A_{22} f_{22}(\zeta, \theta) - f_{22}(\zeta, \theta) \left\{ t(\zeta, \theta) / A_{11} \right\} = \left\{ t(\zeta, \theta) / A_{11} \right\}$$

or, the approximate analytical solutions of the coupled pair of integral equation (3.19) are given by

$$f_{12}(x, \theta) \approx \left[ \frac{A_{22} f(x, \theta)}{A_{11} A_{22} - t(x, \theta)} \right] ; \quad f_{22}(\zeta, \theta) \approx \left[ \frac{t(\zeta, \theta)}{A_{11} A_{22} - t(\zeta, \theta)} \right] \quad (3.32)$$

This procedure of obtaining an approximate analytical solution can also be applied to the other coupled integral equation (3.20) resulting in similar expressions for  $f_{21}(\zeta, \theta)$  and  $f_{11}(x, \theta)$ . Collecting all the solutions and making use of equation (3.21), we may write the excess capacitive coefficients as

$$k_{11}(x, \theta) = C_1' f_{11}(x, \theta) = C_1' \left[ \frac{t(x, \theta)}{A_{11}A_{22} - t(x, \theta)} \right] \quad (3.33a)$$

$$k_{12}(x, \theta) = C_2' f_{12}(x, \theta) = C_2' \left[ \frac{A_{22} f(x, \theta)}{A_{11}A_{22} - t(x, \theta)} \right] \quad (3.33b)$$

$$k_{21}(\zeta, \theta) = C_1' f_{21}(\zeta, \theta) = C_1' \left[ \frac{A_{11} f(\zeta, \theta)}{A_{11}A_{22} - t(\zeta, \theta)} \right] \quad (3.33c)$$

$$k_{22}(\zeta, \theta) = C_2' f_{22}(\zeta, \theta) = C_2' \left[ \frac{t(\zeta, \theta)}{A_{11}A_{22} - t(\zeta, \theta)} \right] \quad (3.33d)$$

and therefore the normalized capacitances may be calculated using the above in equation (3.13) along with equation (1.1),

$$C_1^{(n1)} = \left( \frac{C_1}{h_1 C_1'} \right) = \int_{-\infty}^{\infty} \left[ \frac{t(x, \theta) + A_{11} f(x, \theta)}{A_{11}A_{22} - t(x, \theta)} \right] \frac{dx}{h_1} \quad (3.34a)$$

$$C_2^{(n2)} = \left( \frac{C_2}{h_2 C_2'} \right) = \int_{-\infty}^{\infty} \left[ \frac{t(\zeta, \theta) + A_{22} f(\zeta, \theta)}{A_{11}A_{22} - t(\zeta, \theta)} \right] \frac{d\zeta}{h_2} \quad (3.34b)$$

$$C_m^{(n1)} = \left( \frac{C_m}{h_1 C_1'} \right) = -A_{11} \int_{-\infty}^{\infty} \left[ \frac{f(\zeta, \theta)}{A_{11}A_{22} - t(\zeta, \theta)} \right] \frac{dx}{h_1} \quad (3.34c)$$

Equations (3.30) and (3.31) are adequate in evaluating the normalized excess capacitive coefficients ( $f_{11}$ ,  $f_{12}$ ,  $f_{21}$  and  $f_{22}$ ) and the normalized lumped capacitive elements of the equivalent circuit in Figure 1.5. In the following subsection, we describe and solve the coupled integral equation (3.16) or (3.17) by an alternate numerical method by casting the integral equations into a system of linear equations. The approximate analytical solution is compared with the numerical solution in Section III-C.

### B. Numerical Solution

The set of coupled integral equations (3.19) and (3.20) can also be solved by the method of moments. We may use the symmetry properties summarized below, to economize the calculations.

$$f_{11}(-x, \theta) = f_{11}(x, \theta) \quad (3.35a)$$

$$f_{12}(-x, \theta) = f_{12}(x, \theta) \quad (3.35b)$$

$$f_{21}(-\zeta, \theta) = f_{21}(\zeta, \theta) \quad (3.35c)$$

$$f_{22}(-\zeta, \theta) = f_{22}(\zeta, \theta) \quad (3.35d)$$

The infinite integrals of (3.19) and (3.20) become the following semi-infinite integrals by using the above symmetry relations.

$$\int_0^{\infty} f_{12}(x', \theta) G_{11}(x, x') dx' + \int_0^{\infty} f_{22}(\zeta', \theta) G_{12}(x, \zeta', \theta) d\zeta' = f(x, \theta) \quad (3.36a)$$

$$\int_0^{\infty} f_{12}(x', \theta) G_{21}(\zeta, x', \theta) dx' + \int_0^{\infty} f_{22}(\zeta', \theta) G_{22}(\zeta, \zeta') d\zeta' = 0 \quad (3.36b)$$

and

$$\int_0^{\infty} f_{11}(x', \theta) G_{11}(x, x') dx' + \int_0^{\infty} f_{21}(\zeta', \theta) G_{12}(x, \zeta', \theta) d\zeta' = 0 \quad (3.37a)$$

$$\int_0^{\infty} f_{11}(x', \theta) G_{21}(\zeta, x', \theta) dx' + \int_0^{\infty} f_{21}(\zeta', \theta) G_{22}(\zeta, \zeta') d\zeta' = f(\zeta, \theta) \quad (3.37b)$$

where the new kernels are

$$G_{11}(x, x') = K_{11}(x, x') + K_{11}(x, x') \quad (3.38a)$$

$$G_{12}(x, \zeta', \theta) = K_{12}(x, \zeta', \theta) + K_{12}(x, -\zeta', \theta) \quad (3.38b)$$

$$G_{21}(\zeta, x', \theta) = K_{21}(\zeta, x', \theta) + K_{21}(\zeta, -x', \theta) \quad (3.38c)$$

$$G_{22}(\zeta, \zeta') = K_{22}(\zeta, \zeta') + K_{22}(\zeta, -\zeta') \quad (3.38d)$$

In order to use the moment method, we divide  $x$  into  $x_i$ ,  $i = 0, 1, 2, \dots, N$ ; and  $\zeta$  into  $\zeta_i$ ,  $i = 0, 1, 2, \dots, N$ . The values  $x_i$  are taken to be equal to  $\zeta_i$  for convenience. The points  $x_N$  and  $\zeta_N$  are the truncation points for the moment method. It is expected that the charge density near the junction region of the wires changes fairly rapidly, and decays slowly to zero when  $x$  or  $\zeta$  is very large. Hence the two different mesh sizes are considered: from  $x_0$  to  $x_{N_1}$  the smaller meshes are used, and from  $x_{N_1}$  to  $x_N$ , we may use large meshes. The breaking point  $x_{N_1}$  was found to be very closely related to the right-hand-side vector  $f(x, \theta)$ .

For brevity, we shall consider equation (3.36). Let us assume

$$q_{12}^i = f_{12}(x_i, \theta) \quad \text{and} \quad q_{22}^i = f_{22}(\zeta_i, \theta) \quad (3.39)$$

Using the linear basis functions, we find that (3.36) can be evaluated by

$$\sum_{i=0}^N q_{12}^i I_{11}^{i,j} + \sum_{i=0}^N q_{22}^i I_{12}^{i,j} = f(x_j, \theta) \quad (3.40a)$$

$$\sum_{i=0}^N q_{12}^i I_{21}^{i,j} + \sum_{i=0}^N q_{22}^i I_{22}^{i,j} = 0 \quad (3.40b)$$

where

$$I_{uv}^{i,j} = \delta_{i0} \int_{x_{i-1}}^{x_i} \frac{x' - x_{i-1}}{x_i - x_{i-1}} G_{uv}(x_j, x') dx' \\ + \delta_{iN} \int_{x_i}^{x_{i+1}} \frac{x' - x_{i+1}}{x_i - x_{i+1}} G_{uv}(x_j, x') dx' ; \quad u = 1, 2; v = 1, 2 \quad (3.41)$$

$$\delta_{ik} = \begin{cases} 1 & \text{if } i = k \\ 0 & \text{if } i \neq k \end{cases}$$

Since  $x_i = \zeta_i$ , the variables  $x$  and  $\zeta$  are interchangeable in equation (3.41). The integrations of (3.41) can be evaluated analytically. By reviewing equation (3.38), (3.7), and (3.8), we find that all the integrations in (3.41) are of the following type:

$$\int_{u_1}^{u_2} \frac{r_3 x' + r_4}{[(x' - r_1)^2 + r_2]^{1/2}} dx' = r_3 \left[ \sqrt{u_2^2 - 2r_1 u_2 + r_1^2 + r_2} \right. \\ \left. - \sqrt{u_1^2 - 2r_1 u_1 + r_1^2 + r_2} \right] \\ + (r_4 + r_3 r_1) \left[ \operatorname{arcsinh} \left( \frac{u_2 - r_1}{\sqrt{r_2}} \right) - \operatorname{arcsinh} \left( \frac{u_1 - r_1}{\sqrt{r_2}} \right) \right] \quad (3.42)$$

A total number of  $(2N + 2)$  linear equations can be formulated from equation (3.40) by taking  $j = 0, 1, 2, \dots, N$ . The  $(2N + 2)$  unknowns,  $q_{12}^i$  and  $q_{22}^i$  can then be readily solved by matrix methods. The values of  $f_{21}(x_i, \theta)$  and  $f_{22}(\zeta_i, \theta)$  can also be solved in a similar manner.

The lumped capacitances can be obtained from equations (1.1), (3.13), and (3.18). They are

$$\begin{aligned} C_1^{(n1)} &= \frac{1}{h_1} \int_{-\infty}^{\infty} [f_{11}(x, \theta) + f_{12}(x, \theta)] dx \\ &= \frac{2}{h_1} \int_0^{\infty} [f_{11}(x, \theta) + f_{12}(x, \theta)] dx \end{aligned} \quad (3.43a)$$

$$\begin{aligned} C_2^{(n2)} &= \frac{1}{h_2} \int_{-\infty}^{\infty} [f_{22}(\zeta, \theta) + f_{21}(\zeta, \theta)] d\zeta \\ &= \frac{2}{h_2} \int_0^{\infty} [f_{22}(\zeta, \theta) + f_{21}(\zeta, \theta)] d\zeta \end{aligned} \quad (3.43b)$$

$$\begin{aligned} C_m^{(n1)} &= -\frac{1}{h_1} \int_{-\infty}^{\infty} f_{21}(\zeta, \theta) d\zeta \\ &= -\frac{2}{h_1} \int_0^{\infty} f_{21}(\zeta, \theta) d\zeta \end{aligned} \quad (3.43c)$$

This completes a brief description of the numerical method of solving the coupled integral equations. In the following subsection, we compare the approximate analytical solution with the numerical solution and present the capacitance data as well.

### C. Discussion of Results

In this section we present the results of a parametric study of the normalized excess charges and the normalized lumped capacitances in the equivalent circuit of Figure 1.5. It is recalled that, to obtain the normalized excess charges, one has to solve a set of coupled integral equations (3.19) and (3.20). Owing to a lack of experimental data on this problem, and also to ensure confidence in the solution, the coupled integral equations have been solved by two different methods. In Section III-A, an approximate analytical solution which leads to a closed integral form for the excess charges was presented. On the other hand, Section III-B described a numerical method of solving the same set of coupled integral equations.

In Figures 3.1 to 3.4, we compare the normalized excess charge distributions along the transmission lines, obtained by the two methods. This comparison is done graphically for the four representative cases;

- a)  $(h_2/h_1) = 1.5, \theta = 15^\circ$       b)  $(h_2/h_1) = 1.5, \theta = 90^\circ$   
c)  $(h_2/h_1) = 5, \theta = 15^\circ$       d)  $(h_2/h_1) = 5, \theta = 90^\circ$

The normalized excess charges are plotted as a function of normalized coordinates  $(x/h_1)$  and  $(z/h_1)$ , starting from the junction region and moving along the transmission lines. It is seen from the Figures 3.1 to 3.4, that for all the four cases, the agreement between the approximate

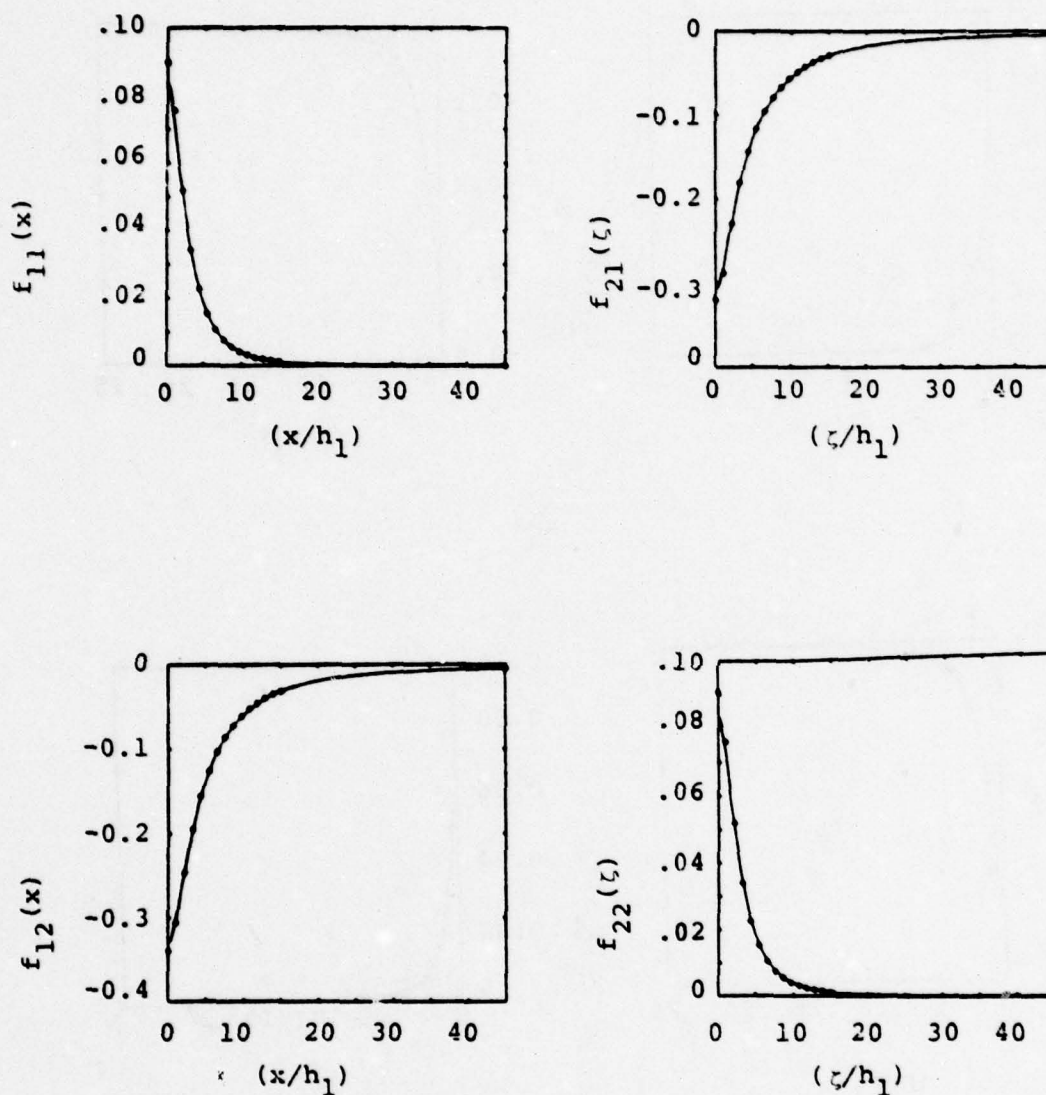


Figure 3.1. Normalized excess charge distributions along the two transmission lines;  $(h_2/h_1) = 1.5$ ,  $(a/h_1) = 0.01$ ,  $\theta = 15^\circ$ ; — approximate analytical solution, ..... numerical solution

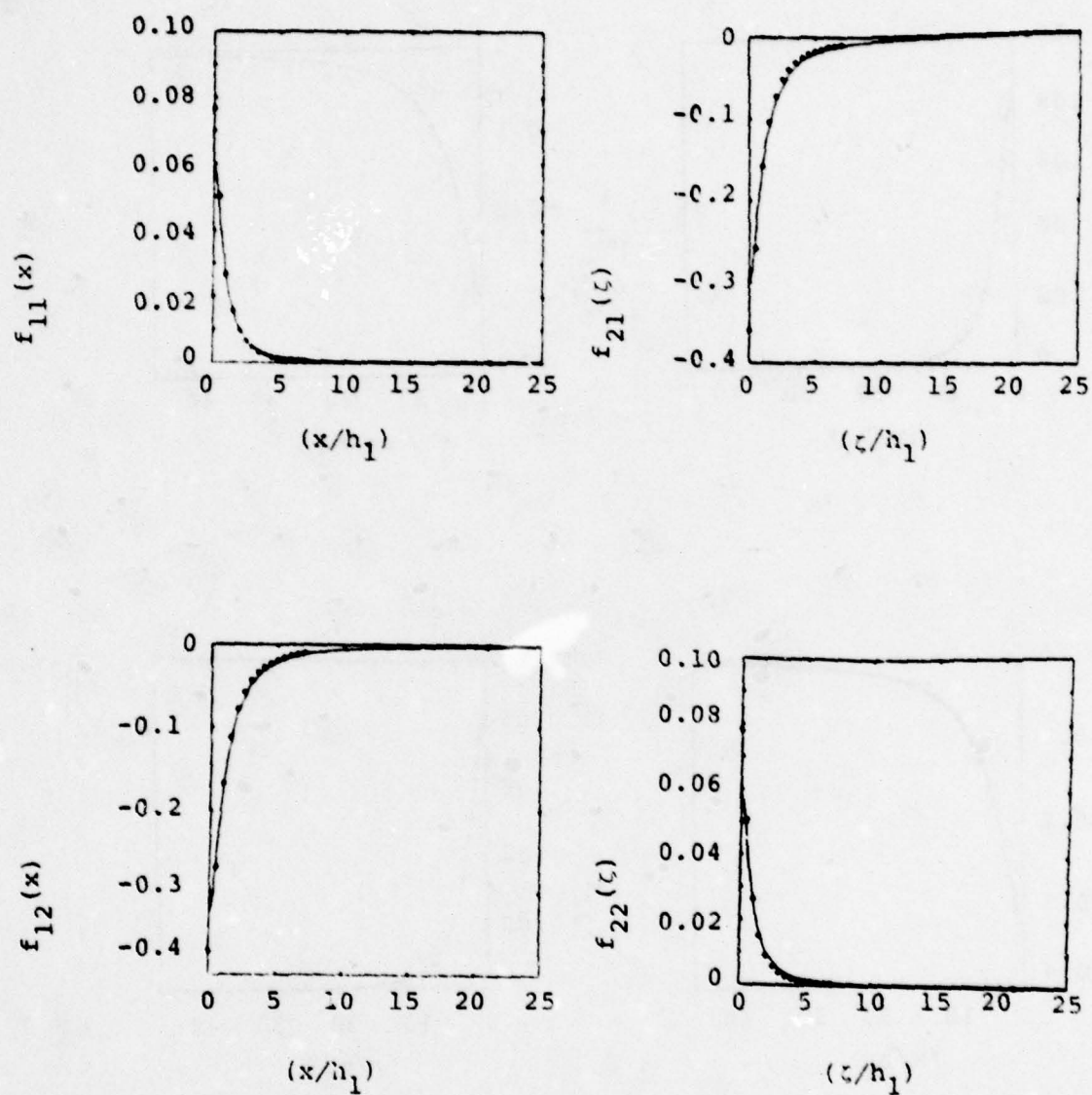


Figure 3.2. Normalized excess charge distributions along the two transmission lines;  $(h_2/h_1) = 1.5$ ,  $(a/h_1) = 0.01$ ,  $\theta = 90^\circ$ ; — approximate analytical solution, ..... numerical solution

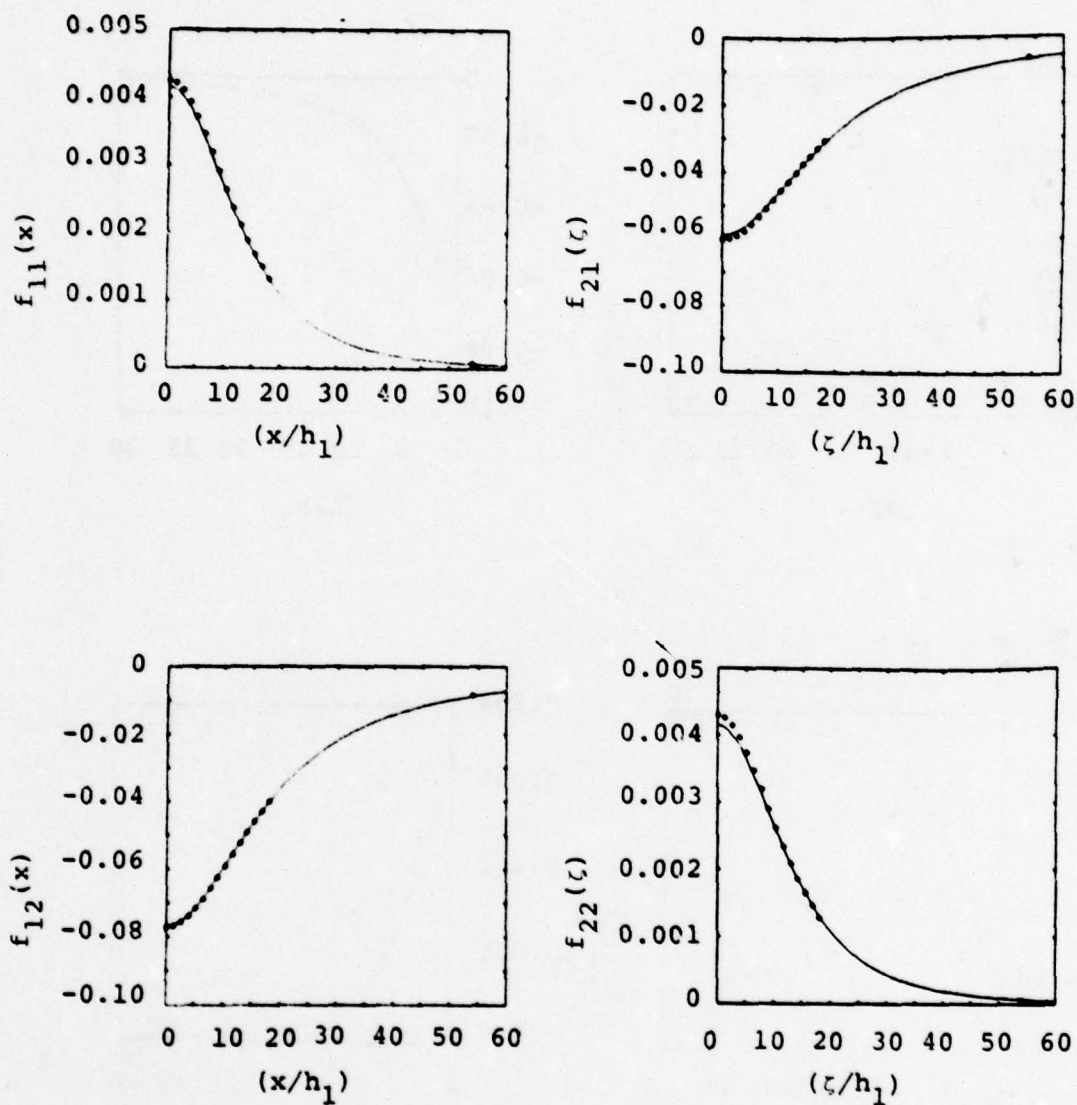


Figure 3.3. Normalized excess charge distributions along the two transmission lines;  $(h_2/h_1) = 5.0$ ,  $(a/h_1) = 0.01$ ,  $\theta = 15^\circ$  — approximate analytical solution, ..... numerical solution

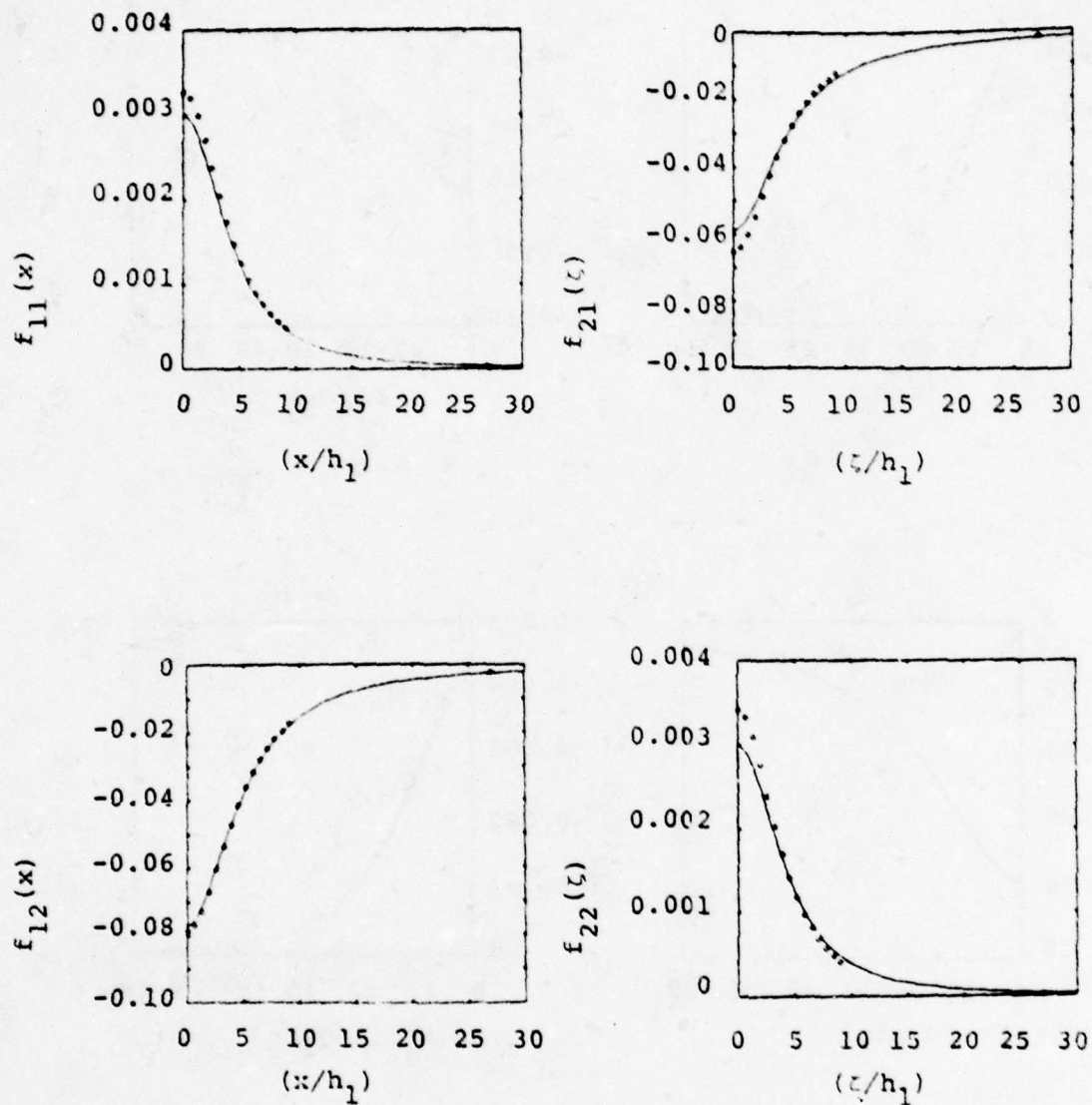


Figure 3.4. Normalized excess charge distributions along the two transmissions;  $(h_2/h_1) = 5.0$ ,  $(a/h_1) = 0.01$ ,  $\theta = 90^\circ$ ; — approximate analytical solution, ..... numerical solution

analytical and the numerical solution is excellent. Furthermore, as may be expected, the normalized excess charges have a peak at the junction and decay as one moves away from the junction.

The normalized excess charges computed from the approximate analytical solution can then be used in computing the normalized lumped capacitive elements via equation (3.34) or (3.43). The capacitance plots are parametrically displayed in Figures 3.5 and 3.6.

In Figure 3.5, the normalized lumped capacitances are plotted as a function of the skew angle which ranges from small angles to  $90^\circ$ . The case of  $\theta = 0^\circ$  is excluded here, because of the distributed interaction and has been considered elsewhere in this report. As expected, Figure 3.5 shows that as the height of the top line is increased, the self capacitance terms decrease.

Figure 3.6, graphically shows the normalized lumped capacitances as a function of the relative height  $(h_2/h_1)$  with the skew angle  $\theta$  as a parameter. Once again, we see the expected behavior as the skew angle or the relative height is varied.

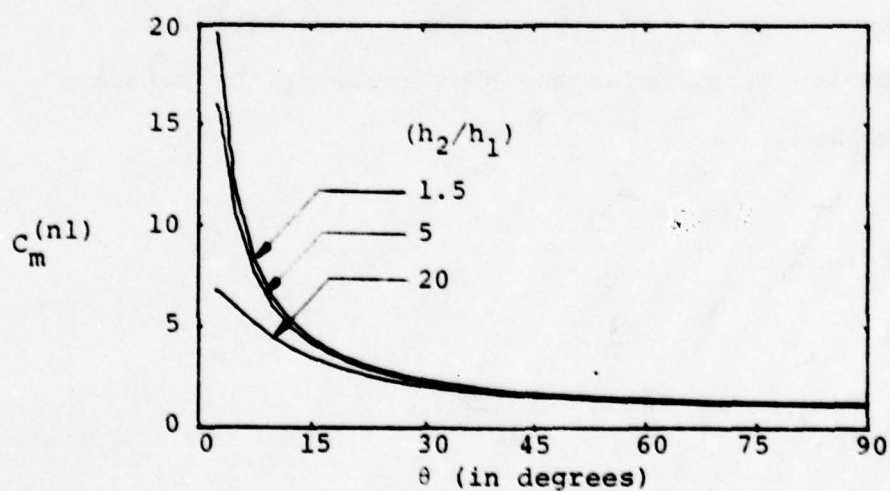
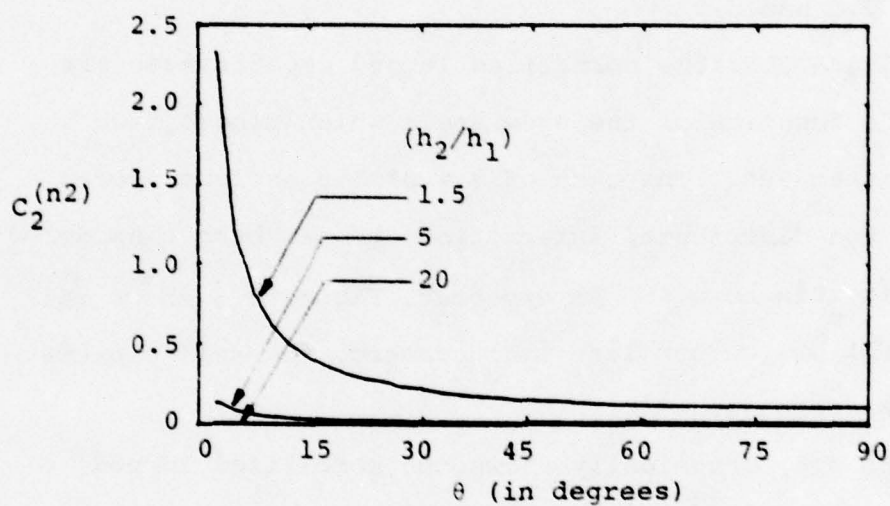
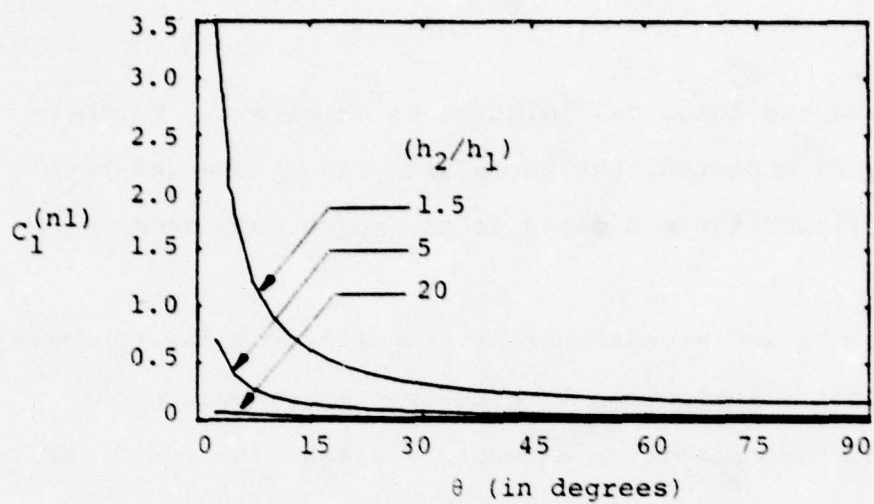


Figure 3.5 Normalized lumped capacitances as a function of skew angle.

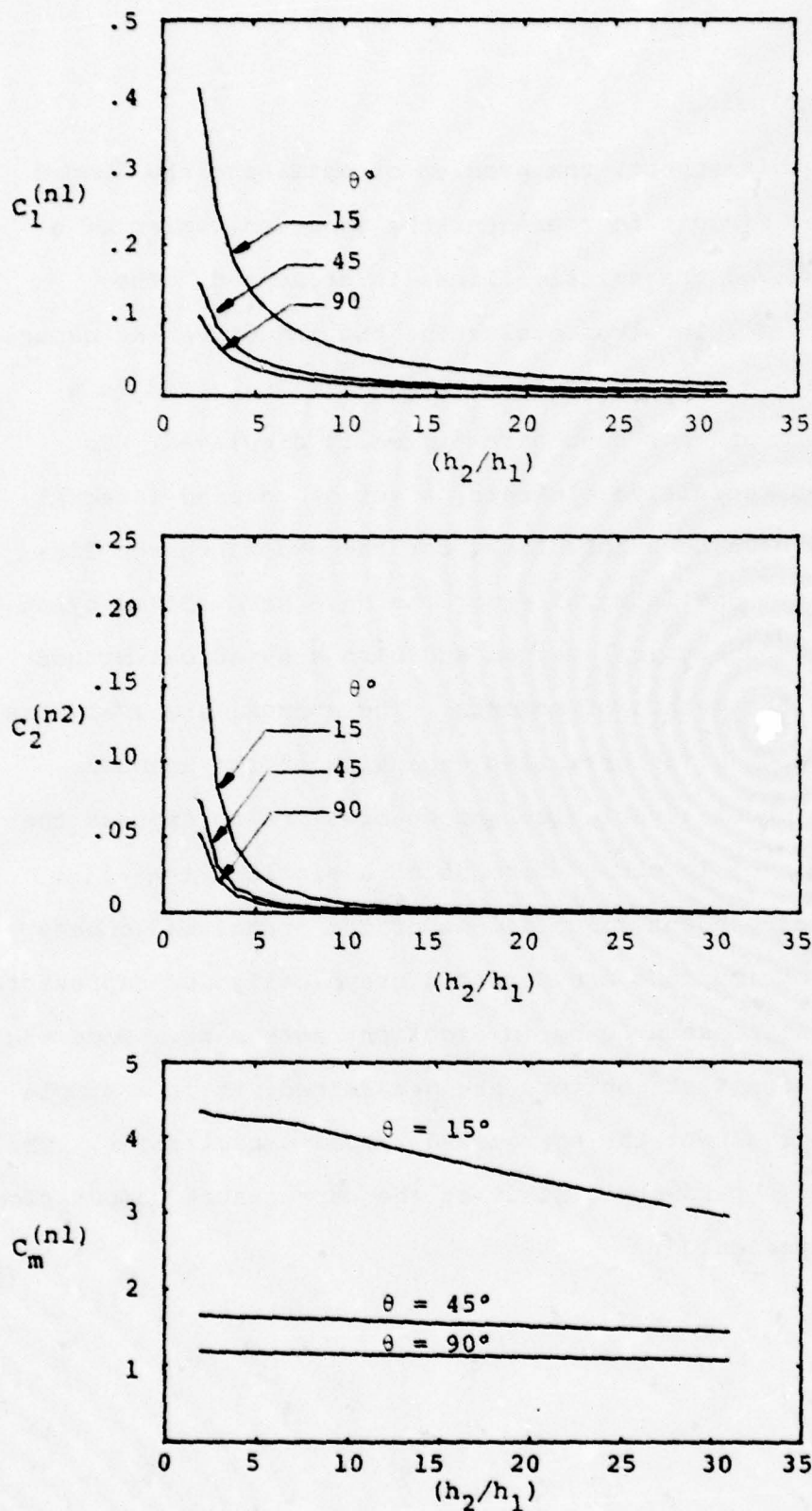


Figure 3.6 Normalized lumped capacitances as a function of relative height.

#### IV. Conclusions

In this report, the problem of obtaining the lumped equivalent circuit to represent the junction region of a pair of skewed transmission lines is presented. The coupling model involves evaluating the inductive and capacitive elements. The mutual inductance is evaluated in a closed form and has been parametrically displayed. To obtain the capacitive elements, a set of coupled integral equations have been formulated for the excess charge distributions. The integral equations have been solved by an approximate analytical method and also a numerical method employing the method of moments. The approximate analytical solution uses a Taylor series expansion of the unknown functions about a variable, and enables one to express the excess charges in closed form using a single integration. The two independent calculations of the normalized excess charge distributions are compared graphically for representative cases and seen to be in excellent agreement. Once the excess charge distributions are determined, it is a simple matter to evaluate the normalized lumped capacitances. The results of a parametric study of the capacitance computations are also presented.

## APPENDIX A

Transmission Line Coupling for the Special Case of  $\theta = 0$ 

In this appendix, we consider the special case of distributed interaction between the two transmission lines (see Figure 1.1) when the skew angle  $\theta$  is zero. In other words, the two wires are parallel to each other and are located at heights  $h_1$  and  $h_2$  above a perfectly conducting ground plane. In this case, one cannot derive a junction equivalent circuit because of the distributed interaction between the wires. Using the same notation as in Section III, the total charges per unit length  $Q'_{10}$  and  $Q'_{20}$  may be related to the potentials  $V_1$  and  $V_2$  on the two wires with respect to the ground plane, via the capacitance per unit length matrix  $[C']$  given by

$$\begin{bmatrix} Q'_{10} \\ Q'_{20} \end{bmatrix} = \begin{bmatrix} C'_{11} & C'_{12} \\ C'_{21} & C'_{22} \end{bmatrix} \begin{bmatrix} V_1 \\ V_2 \end{bmatrix} \quad (\text{A.1})$$

It was seen in Section III that the elements of the coefficients of elastance matrix  $[S']$  are given by

$$[S'_{n,m}] = [C'_{n,m}]^{-1} \quad (\text{A.2})$$

$$S'_{11} = \frac{1}{2\pi\epsilon_0} \ln\left(\frac{2h_1}{a}\right); \quad S'_{22} = \frac{1}{2\pi\epsilon_0} \ln\left(\frac{2h_2}{a}\right) \quad (\text{A.3})$$

$$S'_{12} = S'_{21} = \frac{1}{2\pi\epsilon_0} \ln\left(\frac{\beta}{\alpha}\right) = \frac{1}{2\pi\epsilon_0} \ln\left(\frac{h_2 + h_1}{|h_2 - h_1|}\right) \quad (\text{A.4})$$

These results are in complete agreement with the results reported in the literature [1]. The elements of the [C] matrix are then given by

$$C'_{11} = (S'_{22}/\Delta) ; \quad C'_{22} = (S'_{11}/\Delta) \quad (\text{A.5})$$

$$C'_{12} = C'_{21} = (-S'_{12}/\Delta) \quad (\text{A.6})$$

where

$\Delta \equiv$  determinant of the S matrix

$$= \left( \frac{1}{2\pi\epsilon_0} \right)^2 \left[ \ln\left(\frac{2h_1}{a}\right) \ln\left(\frac{2h_2}{a}\right) - \ln\left(\frac{\beta}{\alpha}\right) \ln\left(\frac{\beta}{\alpha}\right) \right] \quad (\text{A.7})$$

Furthermore, the inductance per unit length matrix is simply related to the [S'] matrix as

$$[L'_{n,m}] = \mu_0 \epsilon_0 [S'_{n,m}] \quad (\text{A.8})$$

so that,

$$L'_{11} = \left( \frac{\mu_0}{2\pi} \right) \ln\left(\frac{2h_1}{a}\right) ; \quad L'_{22} = \left( \frac{\mu_0}{2\pi} \right) \ln\left(\frac{2h_2}{a}\right) \quad (\text{A.9})$$

$$L'_{12} = L'_{21} = \left( \frac{\mu_0}{2\pi} \right) \ln\left(\frac{\beta}{\alpha}\right) \quad (\text{A.10})$$

We have included this special case of  $\theta = 0$  in this appendix mainly in the interest of completeness. These results are available in the literature and serve to check the consistency of our formulation in a limiting situation.

## References

1. C. R. Paul and A. E. Feather, "Computation of the Transmission Line Inductance and Capacitance Matrices from the Generalized Capacitance Matrix," IEEE Trans. Vol. EMC-18, No. 4, pp. 175-183, November 1976.
2. R. W. P. King, "Transmission Line Theory," Chapters I and V, Dover Publications, Inc., New York, 1965.
3. R. W. P. King, "Fundamental Electromagnetic Theory," Chapter VI, Dover Publications, Inc., New York, 1963.
4. I. S. Gradshteyn and I. M. Ryzhik, "Table of Integrals, Series, and Products," Academic Press, New York, 1965.

NOTE 350

ON THE ANALYSIS OF GENERAL MULTICONDUCTOR  
TRANSMISSION-LINE NETWORKS

by

Carl E. Baum  
Tom K. Liu  
Fred M. Tesche

November 1978

ON THE ANALYSIS OF GENERAL MULTICONDUCTOR  
TRANSMISSION-LINE NETWORKS

## ABSTRACT

Starting from the graph describing the topology of a transmission-line network in terms of junctions and tubes, this note addresses the formation of the overall network equation referred to as the BLT equation. The matrix equation of propagation on a tube consisting of a multiconductor transmission line with sources is formulated in terms of the combined voltage vector (a special combination of the voltage and current vectors) which reduces the differential equation to first order; this readily incorporates the combined voltage sources and boundary conditions into the solution of the tube propagation. Utilizing interconnection matrices (defined by the topology) which related waves on the tubes to junctions (tube ends) which the waves leave and enter, the scattering supermatrices for the junctions are converted into a scattering supermatrix for the waves on the transmission-line network. Appropriate supermatrices describing the delay on the tubes, the source terms on the tubes, and the identity are also defined. Together with combined voltage supervectors for waves and sources, the BLT equation is constructed in one of its possible forms. Various properties of the BLT equation and the associated supermatrices, or dimatrices (matrices of matrices) in this case, as well as the corresponding supervectors are developed.

## FOREWORD

This note has been planned for quite some time now. Some of the results were included in two papers [1.6,7] presented at the USNC/URSI Meeting in Amherst, Mass., October 1976. The basic concepts include the topology of the transmission-line network, the propagation on multiwire transmission lines, and supermatrix/supervector forms for representing the variables so as to produce the BLT equation. This note is then the first in perhaps a series concerning a general kind of approach to transmission-line network theory. It allows the consideration of the analytical properties of the network, besides the properties of the network components.

-----

"About halfway up is a cave,  
A gloomy cavern facing the West and Erebus,  
And beneath this cave, my gallant Odysseus, you  
Must steer your ship. It will be so high above you  
That not even the strongest man could reach it with an arrow  
Shot from the deck of his hollow ship below.  
In it lives Scylla, yelping terribly, with a voice  
That sounds no stronger than that of a puppy just born.  
But she herself is an evil monster that no one  
Would be glad to see, not though a god should meet her.  
She has twelve feet in all, horribly dangling,  
And six necks, tremendously long, on each of which  
Is a terrible head with teeth in triple tiers,  
Close set and chocked with black death. From her waist down  
The deep cave hides her, but her heads sway out from the awful  
Abyss, and with them, around the rock, she avidly  
Fishes for dolphin and dog-fish and what greater beast  
She may catch of the countless creatures that Amphitrite,  
Deeply moaning, feeds. Never yet have sailors  
Been able to boast that they got by her unscathed  
In their ship, for with each of her heads she snaps up a man  
From the dark-prowed ship."

---

From The Odyssey, Book XII, by Homer, translated by Ennis Rees,  
Modern Library, Random House, 1960, p. 198.

## TABLE OF CONTENTS

	Abstract	350-1
	Foreword	350-2
	Table of Contents	350-3
I.	Introduction	350-5
	References	350-7
II.	Topology	350-8
	A. Graphs	350-9
	B. Electrical Circuits	350-10
	C. Transmission Line Networks	350-16
	D. Equivalent Circuits of Junctions and Tubes	350-24
	E. Other Related Topics	350-28
	F. Topology Summary	350-29
	References	350-32
III.	Propagation on an N-Wire Transmission Line Tube	350-33
	A. Combined Voltage Equation	350-35
	B. Eigenmode Expansion	350-38
	C. Solution of Combined Voltage Equation	350-45
	D. Sign Convention of $q$	350-59
	E. Summary	350-59
	Tables 3.1-4	350-61
	References	350-64
IV.	Supermatrices and Supervectors	350-65
V.	Identity Supermatrix	350-69
VI.	Scattering Supermatrix	350-71
	A. Junction Scattering Supermatrix	350-71
	B. Reindexing of Elementary Matrices in the Collection of Junction Scattering Supermatrices	350-75
	C. Scattering Supermatrix	350-78

VII.	Definitions of Some Important Supermatrix and Supervector Quantities Based on Results for Waves on a Tube	80
A.	Common Equation for the Two Waves on a Tube	80
B.	Relation of Combined-Voltage Waves on Both Ends of a Tube	80
C.	Propagation Characteristic Supermatrix	84
D.	Source Supervector and Supermatrix Integral Operator	85
E.	Combined Voltage Supervector	87
VIII.	BLT Equation	88
IX.	Reconstruction of Voltages and Currents	90
X.	Some Forms of Solutions of BLT Equations	92
	References	99
XI	Conclusion	100
	Epilogue	101

## I. INTRODUCTION

Transmission-line theory has been with us for quite some time [1.1]. Its impact on communication technology should be obvious. However, its expression in one-dimensional scalar form for a single voltage-current pair has rather limited application to modern complex electronic systems. In the analysis of EMP interaction with electronic systems, transmission-line theory is commonplace [1.2]; however, its practical use is still in a rudimentary form, usually being applied in a one-dimensional scalar form as in the case of a coaxial cable or some simple approximation of a more complex system in one-dimensional scalar form [1.3].

Recent investigations have considered multiconductor transmission lines as an extension of transmission-line theory applicable to complex systems problems such as involved in EMP and EMC [1.4,5]. However, one should recognize that such models are still quite simplistic in the context of the total system response in typical cases. This note addresses the problem of networks of such multiconductor transmission lines.

Basic to the analysis of transmission-line networks is the network topology based on junctions and tubes, each tube being a representation of a multiconductor transmission line, and tube terminations (including connections to other tubes) occurring at junctions. So first we consider the network topology and the associated interconnection matrices which will be used to construct the network equation. This transmission-line network topology is compared to other kinds, such as those used for lumped-element networks and electromagnetic scatterers.

Next the equations describing a single tube or multiconductor transmission line are considered. The problem is reduced to a first-order matrix differential equation through the introduction of a combined voltage vector which is a special linear combination of the voltage and current vectors. This equation is readily solved for given boundary conditions at the tube ends and source vectors along the tube. The

propagation matrix is assumed diagonalizable and the resulting eigenmodes and eigenvalues are used to give representations of the various parameters describing the tube and its response.

The remainder of the note then integrates the result of a single tube with the scattering matrices of the junctions using the interconnectivity of the transmission-line network topology and its associated wave indexing. This forms the overall equation of the multiconductor transmission-line network, referred to as the BLT equation [1.6,7]. For this purpose it is useful to introduce the concept of supermatrices, or matrices of matrices, and corresponding supervectors. This separates the indices in a manner which associates different indices with different physical aspects of the multiconductor transmission-line network and its associated topology. In addition, the supermatrices correspond to a symmetric partitioning of matrices in a manner which makes them block sparse.

The supermatrices used in this note can also be referred to as dimatrices corresponding to a single level of partition resulting in two pairs of indices or subscripts to describe the *dimatrix* elements. This concept has already been generalized to higher order partitions and hence higher order supermatrices in applications concerning the topology of complex electromagnetic scatterers [1.8]. So when the reader has waded through the present tome he can cheerfully contemplate that more is to come (or he may need cheering up for the same reason).

## References

- 1.1 O. Heaviside, *Electromagnetic Theory*, New York: Dover, 1950 (from 3 vols., 1893, 1899, and 1912).
- 1.2 J.A. Cooper, D.E. Merewether, and R.L. Parker (eds.), "Electromagnetic Pulse Handbook for Missiles and Aircraft in Flight", EMP Interaction 1-1, Sept. 1972.
- 1.3 F.M. Tesche and T.K. Liu, "Selected Topics in Transmission-Line Theory for EMP Internal Interaction Problems", Interaction Note 318, March 1977.
- 1.4 S. Frankel, Multiconductor Transmission-Line Analysis, Artech House, 1977.
- 1.5 C. Paul, "On Uniform Multimode Transmission Lines", IEEE Trans. MTT, vol. MTT-21, Aug. 1973, pp. 556-558.
- 1.6 C.E. Baum, "Coupling into Coaxial Cables from Currents and Charges on the Exterior", USNC/URSI Meeting, Amherst, Massachusetts, Oct. 1976.
- 1.7 F.M. Tesche, "A General Multiconductor Transmission-Line Model", USNC/URSI Meeting, Amherst, Massachusetts, Oct. 1976.
- 1.8 C.E. Baum, "The Treatment of the Problem of Electromagnetic Interaction with Complex Systems", IEEE 1978 International Symposium on Electromagnetic Compatibility, Atlanta, Georgia, June 1978.

## II. TOPOLOGY

Network topology is a generic name given to the topological properties of a network. It is studied widely in lumped circuit theory to gain reliable knowledge concerning the number of independent equations in a circuit of arbitrary structural complexity [2.1]. For electromagnetic problems, a more general type of topology is required to describe the three-dimensional volumes and surfaces that are generally associated with the scatterers. Indeed, the scatterer topology has been introduced by Baum [2.2, 2.3], Tesche [2.4] and has found useful applications in considering practical shielding and grounding problems [2.5, 2.6].

For transmission-line networks, the topological description falls between that of lumped circuits and that of scatterers. Similar to a lumped circuit, there are well-defined material paths along which energy propagates, and there are positions in the transmission-line network where energy is distributed according to Kirchhoff's laws. Unlike a lumped circuit, energy may be coupled between the material paths, and the path characteristics (length, geometry, etc.) alter the ways energy propagates. Energy sources may also be induced along the lengths of the paths. These latter properties which are attributed to the distributed nature of transmission lines are more similar to those of scatterers. In fact, it is more appropriate to describe the transmission-line behavior as wave phenomena.

The specialized topological description of a transmission-line network has been called the transmission-line topology [2.3]. In the following, we first review the concept of circuit graphs and circuit topology. The transmission-line topology is then described. A brief outline of other related topologies is also included.

### A. Graphs

The basic elements of a graph are edges and vertices. They are termed differently in specific types of topology, and are summarized in Table 2.1 under Section 2F.

A graph is thus made up of a set of vertices which are interconnected by edges. It is structured to represent, in a simplified form, the electrical connections and/or signal flow paths of the network or system.

Often, for a complicated network, one cannot represent the network comprehensively by a single graph. Parts of the network are then represented by subgraphs. A subgraph fulfills all requirements of being a graph, but is limited to represent only part of the network. An example is that of a multiconductor transmission-line network where a network graph is used to show the transmission-line connections using tube and junction representations, but the detailed electrical connections within junctions are represented by separate subgraphs [2.6].

On the other hand, a network graph may be a subset to a graph which represents a larger system. The latter is called a supergraph. In the previous example, the transmission-line network graph is a supergraph of that of the junctions and tubes.

The concepts of supergraph, graph and subgraph define a hierarchical order of representing a system. However, the naming of super- and sub- are only relative when compared to a smaller or larger part of the network.

## B. Electrical Circuits

The most common network topological concepts have been applied to lumped circuits. The construction of the network graph and its associated development of cut sets and tie sets are assumed to be familiar to the reader. In transmission-line networks, often the junctions contain lumped elements, or the transmission-line discontinuities may be accurately modeled by lumped circuits at low frequencies [2.7 - 2.10]. Hence, in transmission-line network analysis, it is often necessary to include lumped circuit analysis. We summarize the essential points in the following.

The basic elements of a lumped circuit network graph are branches and nodes. A branch is a component part of a circuit characterized by two terminals to which connections can be made. A node is formed where two or more branches are connected. The graphic symbols for branches and nodes are respectively lines and dots. The nodes in a circuit are numbered and the  $n$ th node is denoted by  $N_n$ . The total number of nodes is  $N_N$ . The branch connecting nodes  $N_n$  and  $N_m$  is labeled  $B_{n,m}$ . Hence,  $B_{n,m}$  and  $B_{m,n}$  denote the same branch. The total number of branches is  $N_B$ . If between a node pair there is more than one branch, then by parallel combinations one can reduce this to a single branch.

As an example, a circuit graph is shown in Fig. 2.1a, representing a four node, five branch circuit. The branches are numbered by double subscripts using the rule outlined above.

It is useful to introduce three topology matrices which define the topological structure of a graph. They describe node-node (or node interconnection), node-branch and branch-branch (or branch interconnection) connections. These matrices contain somewhat redundant information and usually only one of them is sufficient to specify the associated graph. However, the last type (branch-branch) does not give unique node numbering.

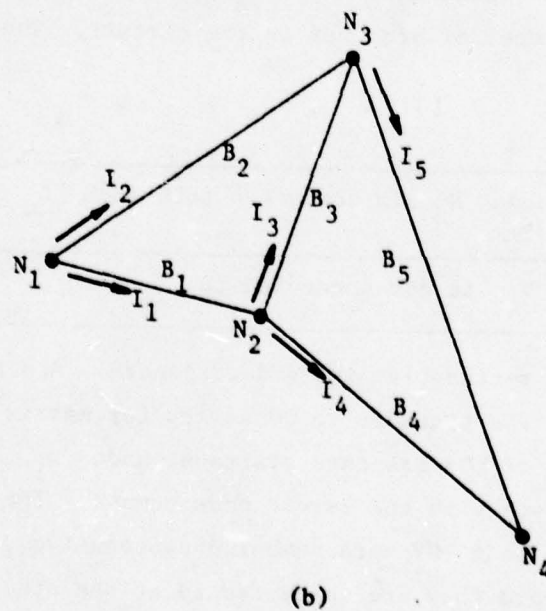
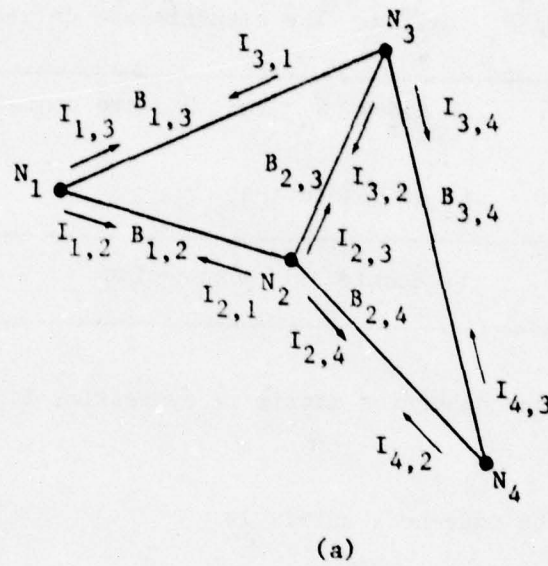


Fig. 2.1 A circuit graph with (a) double-subscripted branch numbers, (b) single-subscripted branch numbers.

For a circuit with  $N_N$  nodes, the node-node interconnection matrix  $(C_{n,m})_{N-N}$  is an  $N_N \times N_N$  matrix. The elements are defined by

$n \neq m$	$C_{n,m;N-N} = 1$ if nodes $N_n$ and $N_m$ are connected $= 0$ if no connection	(2.1)
$n = m$	$C_{n,n;N-N} = 1$ to denote self connection	

Note that the node-node interconnection matrix is symmetric, i.e.,

$$C_{n,m;N-N} = C_{m,n;N-N} \quad (2.2)$$

For example in Fig. 2.1, the node-node matrix is

$$(C_{n,m})_{N-N} = \begin{pmatrix} 1 & 1 & 1 & 0 \\ 1 & 1 & 1 & 1 \\ 1 & 1 & 1 & 1 \\ 0 & 1 & 1 & 1 \end{pmatrix} \quad (2.3)$$

Similarly, the node-branch matrix  $(C_{n,m})_{N-B}$  is  $N_N \times N_B$ , where  $N_B$  is the total number of branches in the circuit. The elements  $C_{n,m;N-B}$  are defined by

$C_{n,m;N-B} = 1$ if node $N_n$ is connected to branch $B_m$	(2.4)
$C_{n,m;N-B} = 0$ if $N_n$ is not connected to $B_m$	

This matrix is in general rectangular instead of square. A single-subscripted denotation of the branches is necessary for matrix manipulations. The numbering of the branches starts at node  $N_1$  for the branch going to the node with the lowest node number. The rest of the branches connected to node  $N_1$  are numbered consecutively with the increase of node numbers they are connected to at the other ends. The sequential numbering continues for branches connected to node  $N_2$ ,

again according to the increase of node numbers they are connected to at the other ends. Here, branches already assigned a branch number are not renumbered. This process repeats for all nodes.

The single-subscripted branch numbering for the graph in Fig. 2.1a is depicted in Fig. 2.1 b. The node-branch matrix is given by

$$(C_{n,m})_{N-B} = \begin{pmatrix} 1 & 1 & 0 & 0 & 0 \\ 1 & 0 & 1 & 1 & 0 \\ 0 & 1 & 1 & 0 & 1 \\ 0 & 0 & 0 & 1 & 1 \end{pmatrix} \quad (2.5)$$

The branch-branch interconnection matrix  $(C_{n,m})_{B-B}$  is an  $N_B \times N_B$  matrix describing branch-to-branch connections. The elements are defined by

$n \neq m$	$C_{n,m;B-B}$ = number of connections between the ends of branches $B_n$ and $B_m$  = 0 implies no connections  = 1 implies one end of each branch is connected
$n = m$	$C_{n,m;B-B} = 0$ excluding branches with both ends connected to the same node

(2.6)

Note that this matrix is symmetric, i.e.

$$C_{n,m;B-B} = C_{m,n;B-B} \quad (2.7)$$

The branch-branch matrix corresponding to the graph in Fig. 2.1b is

$$(C_{n,m})_{B-B} = \begin{pmatrix} 0 & 1 & 1 & 1 & 0 \\ 1 & 0 & 1 & 0 & 1 \\ 1 & 1 & 0 & 1 & 1 \\ 1 & 0 & 1 & 0 & 1 \\ 0 & 1 & 1 & 1 & 0 \end{pmatrix} \quad (2.8)$$

Note that the node-node matrix specifies the connections for a given set of nodes. The node-branch matrix specifies the connection for a given set of nodes and branches. Either of these two matrices can regenerate

the graph with the same node and branch numbering. This may be much more difficult for the branch-branch matrix. However, all the matrices are derived from the given network (graph) consisting of nodes and branches.

The Kirchhoff's laws can be written down comprehensively. One defines voltages  $\tilde{V}_n(s)$  at each node  $N_n$  and currents  $\tilde{I}_{n,m}(s)$  leaving  $N_n$  to  $N_m$  along the branch  $B_{n,m}$  with the condition

$$\sum_m \tilde{I}_{n,m} = 0, \quad \tilde{I}_{n,n} = 0 \quad (2.9)$$

The voltages and currents are related by

$$\tilde{V}_n - \tilde{V}_m = \tilde{Z}_{n,m} \tilde{I}_{n,m} - \tilde{v}_{n,m}^{(s)} \quad (2.10)$$

where  $\tilde{v}_{n,m}^{(s)}$  is a voltage source along branch  $B_{n,m}$  (and increases from  $n$  to  $m$ ) and  $\tilde{Z}_{n,m}$  is some impedance (assumed linear) on the same branch. In a degenerate case the branch current might be specified by a current source. For a closed loop,  $\tilde{V}_n - \tilde{V}_n \equiv 0$ , and (2.10) becomes

$$\begin{aligned} & \tilde{Z}_{n,m_1} \tilde{I}_{n,m_1} + \tilde{Z}_{m_1,m_2} \tilde{I}_{m_1,m_2} + \dots + \tilde{Z}_{m_l,n} \tilde{I}_{m_l,n} \\ & - (\tilde{v}_{n,m_1}^{(s)} + \tilde{v}_{m_1,m_2}^{(s)} + \dots + \tilde{v}_{m_l,n}^{(s)}) = 0 \end{aligned} \quad (2.11)$$

Appropriate applications of (2.9) and (2.11) to a given circuit yield the network equations. There are many forms of network equations which are derived according to the cut sets or tie sets chosen [2.1]. It is not intended to go into this subject here, but instead one form of the network equations for the example illustrated in Fig. 2.1 is given. Currents are labeled by single subscripts in the same way as the single-subscripted branch numbers. Application of (2.9) to  $N_1$ ,  $N_2$  and  $N_3$  yields

$$\begin{pmatrix} 1 & 1 & 0 & 0 & 0 \\ -1 & 0 & 1 & 1 & 0 \\ 0 & -1 & -1 & 0 & 1 \end{pmatrix} \begin{pmatrix} \tilde{I}_1 \\ \tilde{I}_2 \\ \tilde{I}_3 \\ \tilde{I}_4 \\ \tilde{I}_5 \end{pmatrix} = (0_n) \quad (2.12)$$

For the mesh containing branches  $B_1, B_2, B_3$  and the mesh containing  $B_3, B_4, B_5$ , (2.11) becomes

$$\begin{pmatrix} \tilde{Z}_{1,2} & -\tilde{Z}_{1,3} & \tilde{Z}_{2,3} & 0 & 0 \\ 0 & 0 & \tilde{Z}_{2,3} & -\tilde{Z}_{2,4} & \tilde{Z}_{3,4} \end{pmatrix} \cdot \begin{pmatrix} \tilde{I}_1 \\ \tilde{I}_2 \\ \tilde{I}_3 \\ \tilde{I}_4 \\ \tilde{I}_5 \end{pmatrix} = \begin{pmatrix} 1 & 1 & 1 & 0 & 0 \\ 0 & 0 & 1 & 1 & 1 \end{pmatrix} \cdot \begin{pmatrix} \tilde{V}_{1,2}^{(s)} \\ \tilde{V}_{1,3}^{(s)} \\ \tilde{V}_{2,3}^{(s)} \\ \tilde{V}_{2,4}^{(s)} \\ \tilde{V}_{3,4}^{(s)} \end{pmatrix} \quad (2.13)$$

For dimensional consistency, using an arbitrary impedance  $\tilde{Z}_{\text{ref}}$ , combination of (2.12) and (2.13) gives one form of the network equations, viz.,

$$\begin{pmatrix} \tilde{Z}_{\text{ref}} & \tilde{Z}_{\text{ref}} & 0 & 0 & 0 \\ -\tilde{Z}_{\text{ref}} & 0 & \tilde{Z}_{\text{ref}} & \tilde{Z}_{\text{ref}} & 0 \\ 0 & -\tilde{Z}_{\text{ref}} & -\tilde{Z}_{\text{ref}} & 0 & \tilde{Z}_{\text{ref}} \\ \tilde{Z}_{1,2} & -\tilde{Z}_{1,3} & \tilde{Z}_{2,3} & 0 & 0 \\ 0 & 0 & \tilde{Z}_{2,3} & -\tilde{Z}_{2,4} & \tilde{Z}_{3,4} \end{pmatrix} \cdot \begin{pmatrix} \tilde{I}_1 \\ \tilde{I}_2 \\ \tilde{I}_3 \\ \tilde{I}_4 \\ \tilde{I}_5 \end{pmatrix} = \begin{pmatrix} 0 & 0 & 0 & 0 & 0 \\ 0 & 0 & 0 & 0 & 0 \\ 0 & 0 & 0 & 0 & 0 \\ 1 & 1 & 1 & 0 & 0 \\ 0 & 0 & 1 & 1 & 1 \end{pmatrix} \cdot \begin{pmatrix} \tilde{V}_{1,2}^{(s)} \\ \tilde{V}_{1,3}^{(s)} \\ \tilde{V}_{2,3}^{(s)} \\ \tilde{V}_{2,4}^{(s)} \\ \tilde{V}_{3,4}^{(s)} \end{pmatrix} \quad (2.14)$$

The currents are readily obtained by inverting the  $5 \times 5$  matrix.

It is the purpose of this note to present similar network equations for transmission-line networks. These equations are complicated by the wave nature of the voltages and currents, and their dependence on positions and modal properties.

### C. Transmission-Line Networks

Concepts similar to those of circuit topology are developed for transmission-line networks to help summarize the network configurations, to define topology matrices and to set up network equations.

The basic elements of the transmission-line network graphs are tubes and junctions. A tube is a collection of wires characterized by two ends to which electrical connections can be made. A junction is where wires terminate. Usually a bundle of wires is considered as a tube which may be terminated by a circuit. Branching of a bundle of wires can be considered as a tube divided into a few tubes with the position of branching as a junction within which only direct electrical connections occur.

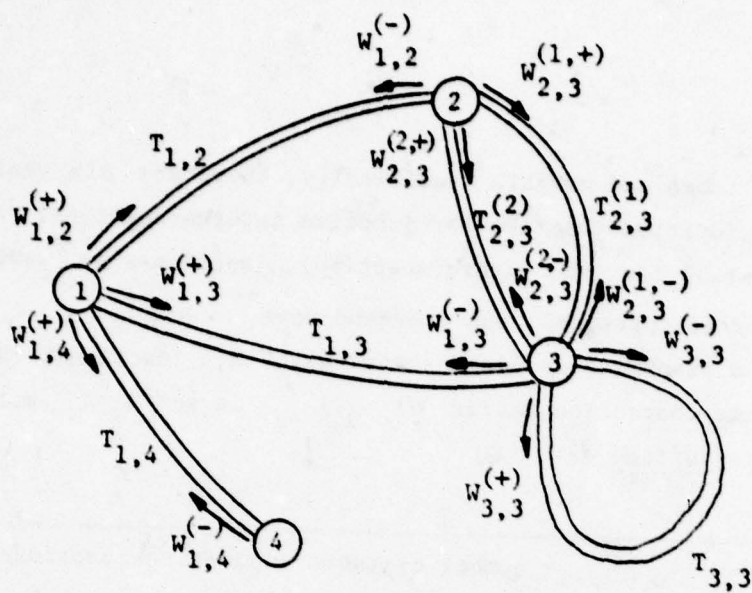
The graphic symbols for tubes and junctions are respectively "parallel" lines and circles. The  $v$ th junction is denoted as  $J_v$  for  $v = 1, \dots, N_J$  where  $N_J$  is the number of junctions in the network. For transmission-line networks, it is possible to have more than one tube between two junctions. The  $p$ th tube between junctions  $J_v$  and  $J_{v'}$  is labeled  $T_{v,v'}^{(p)}$ . If there is only one tube between  $J_v$  and  $J_{v'}$ , the simplified notation  $T_{v,v'} (= T_{v,v'}^{(1)})$  is often used.

Each tube can be characterized by two sets of waves: the forward traveling wave and the backward traveling wave. The waves on the  $p$ th tube between junctions  $J_v$  and  $J_{v'}$  are labeled  $W_{v,v'}^{(p,+)}$  and  $W_{v,v'}^{(p,-)}$ , where  $W_{v,v'}^{(p,+)}$  travels from  $J_v$  to  $J_{v'}$  and  $W_{v,v'}^{(p,-)}$  travels from  $J_{v'}$  to  $J_v$ . Thus,  $W_{v,v'}^{(p,+)} = W_{v',v}^{(p,-)}$ . There are thus two waves traveling in opposite directions on a given tube.

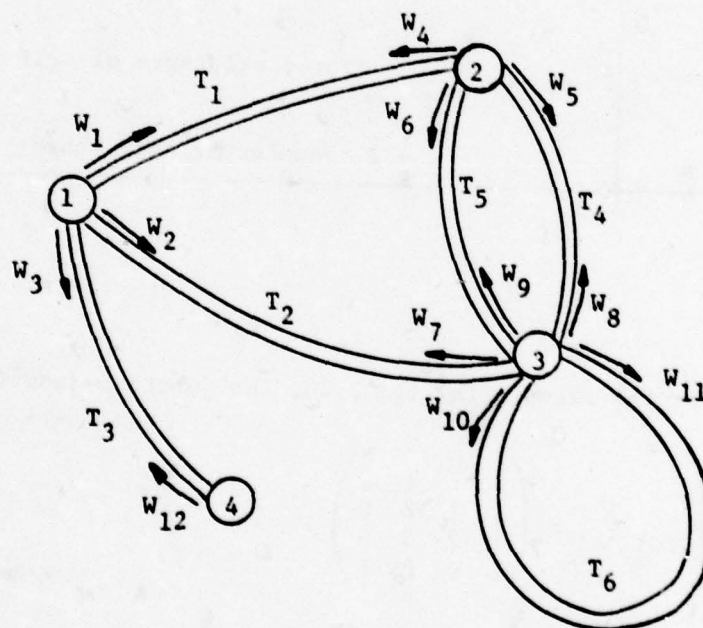
As an example, a transmission-line graph is shown in fig. 2.2a. There are four junctions and six tubes. The tubes and waves are numbered with double subscripts according to the rules outlined above. The parallel tubes and the self tube\* are unique for transmission-line networks as there are no corresponding elements for the circuits. Topology matrices similar to those used for lumped circuits can be defined here involving

---

\*A self tube is one that has both ends terminating in the same junction.



(a) Double-subscripted



(b) Single-subscripted

Fig. 2.2 A transmission line graph with (a) double-subscripted numbering and (b) single-subscripted numbering

junctions, tubes and waves. Specifically, there are six useful interconnection matrices: junction-junction (or junction interconnection), junction-tube, tube-tube (or tube interconnection), junction-wave, wave-wave (or wave interconnection), and tube-end-wave.

For a transmission-line network with  $N_J$  junctions, the junction-junction interconnection matrix  $(t_{v,v'})_{J-J}$  is an  $N_J \times N_J$  matrix. The elements are defined as:

$v \neq v'$	$t_{v,v';J-J}$ = number of tubes connecting junctions $J_v$ and $J_{v'}$ $t_{v,v';J-J} = 0$ implies no connection between the two junctions
$v = v'$	$t_{v,v;J-J} = 1$ denotes self connection (since a junction is always connected to itself) $t_{v,v;J-J} > 1$ denotes existence of self tubes $= 1 + 2 \times (\text{number of self tubes})$

(2.15)

For the example in Fig. 2.2a, the junction-junction matrix is

$$(t_{v,v'})_{J-J} = \begin{pmatrix} 1 & 1 & 1 & 1 \\ 1 & 1 & 2 & 0 \\ 1 & 2 & 3 & 0 \\ 1 & 0 & 0 & 1 \end{pmatrix} \quad (2.16)$$

Similarly, the junction-tube interconnection matrix  $(t_{v,n})_{J-T}$  has elements defined by

$$\begin{aligned}
 t_{v,n;J-T} &= 1 \quad \text{if junction } J_v \text{ is connected to tube } T_n \\
 &= 2 \quad \text{if junction } J_v \text{ is connected to self tube } T_n \\
 &= 0 \quad \text{if junction } J_v \text{ is not connected to tube } T_n \quad (2.17)
 \end{aligned}$$

The single-subscripted denotation of the tubes  $T_n$  is useful for matrix manipulations. The numbering system is similar to that for branches in the circuit topology. Consecutive numbering starts at the first tube linking junction  $J_1$  to the junction that has the lowest node number. (If there is a self tube at  $J_1$  this would be first.) The tube number increases for other parallel tubes going from  $J_1$  to the same junction until all these tubes are labeled. This process continues for tubes going to the junction with the next higher number until all junctions connected to  $J_1$  are exhausted. The procedure continues at  $J_2$  except for tubes which are already labeled: they are not repeated (i.e., tubes  $T_{1,2}^{(p)}$  are already labeled and are left out here). The process continues until all tubes are numbered.

One may note here that the tube labeling is not oriented, i.e.,  $T_{v,v'}^{(p)} = T_{v',v}^{(p)}$ .

For the example in Fig. 2.2b, the junction-tube matrix is:

$$(t_{v,n})_{J-T} = \begin{pmatrix} 1 & 1 & 1 & 0 & 0 & 0 \\ 1 & 0 & 0 & 1 & 1 & 0 \\ 0 & 1 & 0 & 1 & 1 & 2 \\ 0 & 0 & 1 & 0 & 0 & 0 \end{pmatrix} \quad (2.18)$$

The tube-tube interconnection matrix  $(t_{n,m})_{T-T}$  is defined in the following table:

$n \neq m$	$t_{n,m;T-T}$ = number of connections between the ends of tube $T_n$ and tube $T_m$  $= 0$ implies no connections  $= 1$ implies one end of each tube is connected  $= 2$ implies either (i) two parallel tubes or (ii) one is a self tube  $= 4$ implies both are self tubes
$n = m$	$t_{n,n;T-T} = 0$ for a simple tube (normal situation)  $= 2$ for a self tube

(2.19)

The  $(t_{n,m})_{T-T}$  matrix for the case of Fig. 2.2b is

$$(t_{n,m})_{T-T} = \begin{pmatrix} 0 & 1 & 1 & 1 & 1 & 0 \\ 1 & 0 & 1 & 1 & 1 & 2 \\ 1 & 1 & 0 & 0 & 0 & 0 \\ 1 & 1 & 0 & 0 & 2 & 2 \\ 1 & 1 & 0 & 2 & 0 & 2 \\ 0 & 2 & 0 & 2 & 2 & 2 \end{pmatrix} \quad (2.20)$$

Each tube is also characterized by two waves. The junction-wave matrix  $(t_{v,u})_{J-W}$  describes the waves that are incident or reflected from a junction. One defines

$$t_{v,u;J-W} = \begin{cases} 1 & \text{if wave } W_u \text{ is leaving junction } J_v \text{ (transmitted and/or reflected)} \\ 1 & \text{if wave } W_u \text{ is entering junction } J_v \text{ (incident)} \\ 0 & \text{if junction } J_v \text{ is not associated with wave } W_u \\ 2 & \text{if wave } W_u \text{ is on a self tube} \end{cases} \quad (2.21)$$

The single-subscripted denotation of a wave,  $W_u$ , is numbered similar to that of a tube. However, there are two waves on a tube, oriented to propagate in opposite directions. Thus, numbering starts at junction  $J_1$  for a wave leaving  $J_1$  on tube  $T_1$  until all tubes are exhausted. Numbering continues at junction  $J_2$  for all tubes (in ascending tube numbers), again for waves leaving  $J_2$ . This is repeated for all junctions. This results in different numbering as compared to the tubes. In fact, for  $N_T$  tubes, there are  $N_W$  waves given by

$$N_W = 2 N_T \quad (2.22)$$

The junction-wave matrix for the example in Fig. 2.2b is

$$(t_{v,u})_{J-W} = \begin{pmatrix} 1 & 1 & 1 & 1 & 0 & 0 & 1 & 0 & 0 & 0 & 0 & 1 \\ 1 & 0 & 0 & 1 & 1 & 1 & 0 & 1 & 1 & 0 & 0 & 0 \\ 0 & 1 & 0 & 0 & 1 & 1 & 1 & 1 & 1 & 2 & 2 & 0 \\ 0 & 0 & 1 & 0 & 0 & 0 & 0 & 0 & 0 & 0 & 0 & 1 \end{pmatrix} \quad (2.23)$$

The wave-wave matrix  $(W_{u,v})$  describes interconnection of waves (via junctions). Elements are defined by

$W_{u,v} = 1$  if wave  $W_v$  scatters into wave  $W_u$ , i.e., if  $W_v$  is connected to  $W_u$  via a junction into which  $W_v$  is incoming and  $W_u$  is outgoing.

$$W_{u,v} = \begin{cases} 1 & \text{for a self tube} \\ 0 & \text{otherwise (normal situation).} \end{cases} \quad (2.24)$$

For the example in Fig. 2.2b,  $(W_{u,v})$  is

$$(W_{u,v}) = \begin{pmatrix} 0 & 0 & 0 & 1 & 0 & 0 & 1 & 0 & 0 & 0 & 0 & 1 \\ 0 & 0 & 0 & 1 & 0 & 0 & 1 & 0 & 0 & 0 & 0 & 1 \\ 0 & 0 & 0 & 1 & 0 & 0 & 1 & 0 & 0 & 0 & 0 & 1 \\ 1 & 0 & 0 & 0 & 0 & 0 & 0 & 1 & 1 & 0 & 0 & 0 \\ 1 & 0 & 0 & 0 & 0 & 0 & 0 & 1 & 1 & 0 & 0 & 0 \\ 1 & 0 & 0 & 0 & 0 & 0 & 0 & 1 & 1 & 0 & 0 & 0 \\ 0 & 1 & 0 & 0 & 1 & 1 & 0 & 0 & 0 & 1 & 1 & 0 \\ 0 & 1 & 0 & 0 & 1 & 1 & 0 & 0 & 0 & 1 & 1 & 0 \\ 0 & 1 & 0 & 0 & 1 & 1 & 0 & 0 & 0 & 1 & 1 & 0 \\ 0 & 1 & 0 & 0 & 1 & 1 & 0 & 0 & 0 & 1 & 1 & 0 \\ 0 & 1 & 0 & 0 & 1 & 1 & 0 & 0 & 0 & 1 & 1 & 0 \\ 0 & 1 & 0 & 0 & 1 & 1 & 0 & 0 & 0 & 1 & 1 & 0 \\ 0 & 1 & 0 & 0 & 1 & 1 & 0 & 0 & 0 & 1 & 1 & 0 \\ 0 & 1 & 0 & 0 & 1 & 1 & 0 & 0 & 0 & 1 & 1 & 0 \\ 0 & 0 & 1 & 0 & 0 & 0 & 0 & 0 & 0 & 0 & 0 & 0 \end{pmatrix} \quad (2.25)$$

Another matrix of interest is the tube-end-wave interconnection matrix. We denote by the index  $r$  in  $J_{v;r}$  the tube ends reaching the junction  $J_v$ ; then, for a wave entering  $J_v$  via  $J_{v;r}$ , it is labeled as  $J_{v;r,-}$ , and for a wave leaving  $J_v$  via  $J_{v;r}$ , it is labeled  $J_{v;r,+}$ .

The tube-end-wave interconnection matrix  $(t_{r,u})_{v;E-W}$  is defined as follows:

$$t_{r,u;v;E-W} = \begin{cases} 0 & \text{if wave } W_u \text{ does not connect to } J_v \text{ via end } J_{v;r} \\ -1 & \text{if wave } W_u \text{ enters } J_v \text{ via } J_{v;r} \text{ (i.e., } J_{v;r,-}) \\ 1 & \text{if wave } W_u \text{ leaves } J_v \text{ via } J_{v;r} \text{ (i.e., } J_{v;r,+}) \end{cases} \quad (2.26)$$

Thus, for junction  $J_3$  of fig. 2.2b, a new illustration is depicted in fig. 2.3. Here the tube-end-wave interconnection matrix is

$$(t_{r,u})_{v;E-W} = \begin{pmatrix} 0 & -1 & 0 & 0 & 0 & 0 & 1 & 0 & 0 & 0 & 0 & 0 \\ 0 & 0 & 0 & 0 & -1 & 0 & 0 & 1 & 0 & 0 & 0 & 0 \\ 0 & 0 & 0 & 0 & 0 & -1 & 0 & 0 & 1 & 0 & 0 & 0 \\ 0 & 0 & 0 & 0 & 0 & 0 & 0 & 0 & 0 & -1 & 1 & 0 \\ 0 & 0 & 0 & 0 & 0 & 0 & 0 & 0 & 0 & -1 & 1 & 0 \end{pmatrix} \quad (2.27)$$

Note that the junction-wave interconnection matrix is formed by

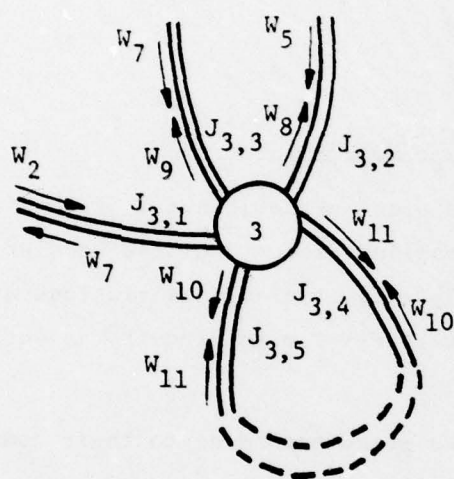


Fig. 2.3. Tube-end labeling for Junction  $J_3$ .

$$t_{v,u;J-W} = \sum_{r=1}^{r_v} |t_{r,u;v;E-W}| \quad (2.28)$$

where

$$\begin{aligned} r_v &\equiv \text{maximum value of } r \\ &= \text{number of tube ends at } J_v \\ || &\equiv \text{absolute value} \end{aligned} \quad (2.29)$$

#### D. Equivalent Circuits of Junctions and Tubes

Most junctions of interest either consist of physical lumped circuits or are transmission-line discontinuities modeled by lumped circuit elements [2.8-2.10]. Topological descriptions of a junction can thus be similar to those for a lumped circuit, as outlined in Section 2B.

Junctions can be classified according to their complexities. The simplest one involves only one tube terminated by an impedance network (including sources). This includes the special cases of open-circuited and short-circuited terminations. The voltage-current relation is given by

$$(\tilde{V}_n(s)) + (\tilde{V}_n^{(s)}(s)) = (\tilde{Z}_{n,m}(s)) \cdot [(\tilde{I}_n(s)) + (\tilde{I}_n^{(s)}(s))] \quad (2.30)$$

The dual relationship is

$$(\tilde{I}_n(s)) + (\tilde{I}_n^{(s)}(s)) = (\tilde{Y}_{n,m}(s)) \cdot [(\tilde{V}_n(s)) + (\tilde{V}_n^{(s)}(s))] \quad (2.31)$$

The configuration is depicted in fig. 2.4; note that current is taken positive into the junction.

For the short-circuited case

$$(\tilde{V}_n(s)) = (0_n) \quad (2.32)$$

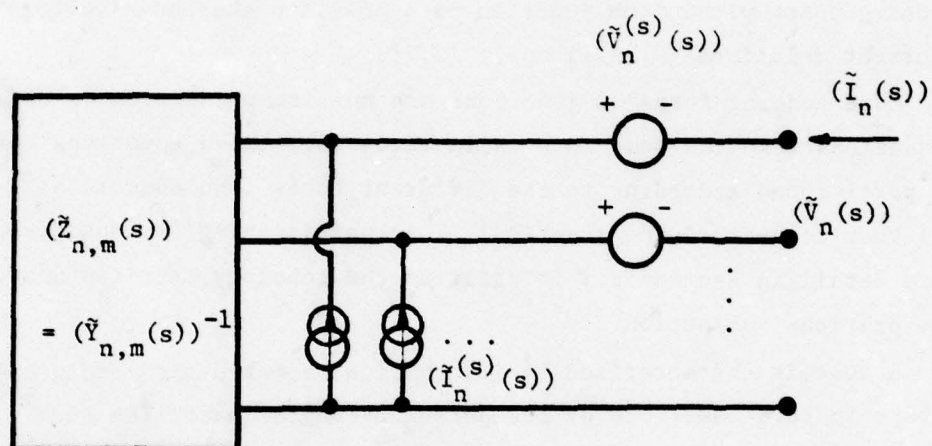


Fig. 2.4. Terminating Network

and for the open-circuited case

$$(\tilde{I}'_n(s)) = (0_n) \quad (2.33)$$

A more general type of junction is one that connects to many tubes, and connections between wires of the tubes are by direct electrical contacts. This type is extremely relevant in modeling the case of branching. As is well known, branches connected at a node have equal voltages and the sum of currents leaving the node is zero. Thus, each connecting point within the junction is a node and the above voltage and current relations (2.9-11) apply [2.7].

More general forms of junctions are multitube junctions. While the equations take the same form as in (2.34,35), these equations need to be partitioned according to the different tubes (and associated waves) that connect to the junction. This partitioning is considered in some detail in Section VI; it utilizes the topology matrices discussed in the previous subsection.

A tube is characterized by its physical construction and geometry. These are in turn described by the per-unit-length quantities such as the per-unit-length impedance matrix  $(\tilde{Z}'_{n,m}(s))$  and the per-unit-length admittance matrix  $(\tilde{Y}'_{n,m}(s))$  for the general case, or the per-unit-length inductance matrix  $(L'_{n,m})$  and the per-unit-length capacitance matrix  $(C'_{n,m})$  for the lossless case.

Based on the per-unit-length series impedance  $(\tilde{Z}'_{n,m}(s))$  and shunt admittance  $(\tilde{Y}'_{n,m}(s))$ , a per-unit-length electrical network can be developed. It illustrates the electrical model of the tube at a point on the tube. This is shown in Fig. 2.5 where for completeness two sets of distributed sources are also shown.

Note that the per-unit-length sources  $(\tilde{V}_n^{(s)'})$  and  $(\tilde{I}_n^{(s)'})$ , as well as the voltage  $(\tilde{V}'_n)$  and current  $(\tilde{I}'_n)$  vectors, are functions of the coordinate  $z$  along the tube as well as the complex frequency  $s$ . The equations governing these variables on a tube are considered in detail in Section III.

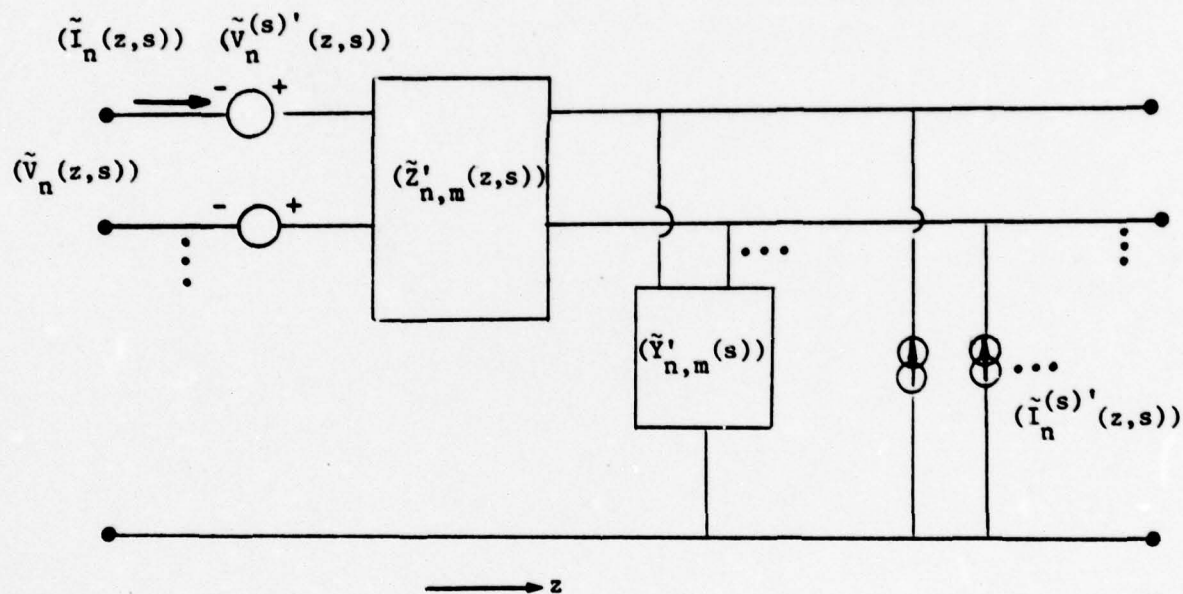


Fig. 2.5 The per-unit-length model of a multi-conductor transmission line.

#### E. Other Related Topologies

The development of scatterer topology and the hierarchical scatterer topology is useful in dealing with scattering and penetration problems [2.2, 2.3, 2.4]. For an aircraft, missile or other systems, there are many cable bundles enclosed inside the walls of the system. The use of hierarchical scatterer topological concepts is well-suited to aid in the solution of these kinds of problems. Here one deals with the problem layer-by-layer, dividing it into many subproblems of coupling, propagation and penetration. The details are treated in the above-cited references and are not described here.

## F. Topology Summary

The various types of topologies and their associated quantities are summarized in Table 2.1, which was first presented in ref. [2.3].

As mentioned earlier, the hierarchical scatterer problem can be divided into the following subproblems corresponding to the electromagnetic processes associated with each layer (principal volume) in the transport of signals into the system:

### 1. coupling

This relates the response of each system layer to the electromagnetic fields coming from the layer external to the one under consideration. Quantitatively coupling can be identified with the source terms in the equations used to describe the response of the layer of interest.

### 2. propagation

This deals with the distribution of signals within the layer of interest in the system. It is concerned with the operator (integral, differential, etc.) in the equations describing the response of the layer as well as the resulting response itself.

### 3. penetration

This deals with the excitation of the signals in the next layer (going to the interior). Specifically penetration is concerned with the conversion of the response within a layer into an appropriate set of parameters which can be used for the coupling process in the next layer. It is then the transition from one layer to the next.

In the hierarchical decomposition of a system one or more of the layers of interest may be represented as transmission line networks, in which case the above breakdown is relevant to transmission-line problems. The above breakdown within a layer is summarized in Table 2.2.





	Topology	Basic Topological Quantity and Symbol	Interconnecting Topological Quantity and Symbol	Diagrammatic form of Topology
1	Graph (Generalized)	Vertex	Edge	
2	Circuit	Node $N_n$	Branch $B_{n,m}^{(T)}$	
3	Transmission Line	Junction $J_n$	Tube $T_{n,m}^{(T)}$	
4	Scatterer	Volume $V_n$	Surface $S_{n,m}$	
5	Hierarchical Scatterer	Principal $(V)_{\lambda}^{(\lambda')}$ Volume	Principal $(S)_{\lambda}^{(\lambda')}$ Surface (closed but sometimes in more than one part)	
		Elementary $(V)_{\lambda,\tau}^{(\lambda')}$ Volume	Elementary $(S)_{\lambda,T;\lambda_2,T_2}^{(\lambda',\lambda_2')}$ Surface (usually open but sometimes closed)	

Table 2.1 Various topologies

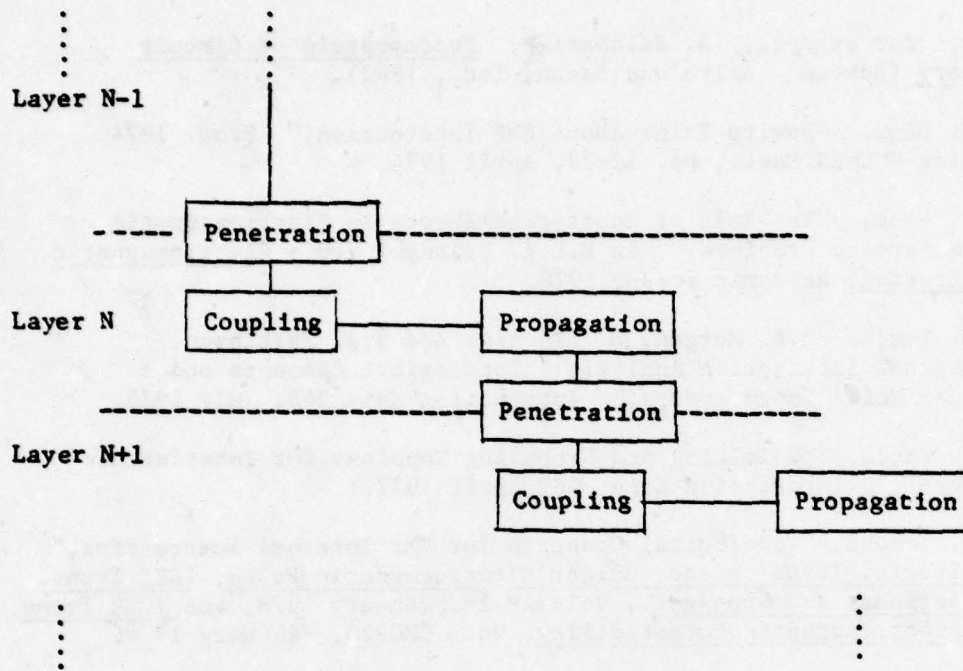


Table 2.2 Hierarchical decomposition of a system

## References

- 2.1 See, for example, N. Balabanian, Fundamentals of Circuit Theory (Boston, Allyn and Bacon, Inc., 1962).
- 2.2 C.E. Baum, "How to Think About EMP Interaction," Proc. 1974 Spring FULMEN Meet., pp. 12-23, April 1974.
- 2.3 C.E. Baum, "The Role of Scattering Theory in Electromagnetic Interference Problems," in P.L.E. Uslenghi (ed.) Electromagnetic Scattering, Academic Press, 1978.
- 2.4 F.M. Tesche, M.A. Morgan, B. Fishbine and E.R. Parkinson, "Internal Interaction Analysis: Topological Concepts and Needed Model Improvements," Interaction Note 248, July 1975.
- 2.5 E.F. Vance, "Shielding and Grounding Topology for Interference Control," Interaction Note 306, April 1977.
- 2.6 F.M. Tesche, "Topological Concepts for EMP Internal Interaction," in Special Issue on the Nuclear Electromagnetic Pulse, IEEE Trans. on Antennas and Propagat., Vol. AP-26, January 1978, and IEEE Trans. on Electromagnetic Compatibility, Vol. EMC-20, February 1978.
- 2.7 C.E. Baum, T.K. Liu, F.M. Tesche and S.K. Chang, "Numerical Results for Multiconductor Transmission-Line Networks," Interaction Note 322, September 1977.
- 2.8 F.M. Tesche and T.K. Liu, "An Electric Model for a Cable Clamp," Interaction Note 307, December 1976.
- 2.9 S. Coen, T.K. Liu and F.M. Tesche, "Calculation of the Equivalent Capacitance of a Rib near a Single Wire Transmission Line," Interaction Note 310, February 1977.
- 2.10 K.S.H. Lee and F.C. Yang, "A Wire Passing by a Circular Aperture in an Infinite Ground Plane," Interaction Note 317, February 1977.

### III. PROPAGATION ON AN N-WIRE TRANSMISSION LINE TUBE

In this section the phenomena of waves propagating on a single section, N-wire transmission-line tube are considered. An N-wire transmission line is one that consists of  $n$  conductors and a reference which may be infinity or ground. As will be derived later, such a system has  $N$  modes of propagation.

The equations governing the voltage and current propagation on an N-wire transmission line, i.e., the generalized transmission equations are the current change equation

$$\frac{d}{dz}(\tilde{I}_n(z,s)) = -(\tilde{Y}'_{n,m}(s)) \cdot (\tilde{V}_n(z,s)) + (\tilde{I}_n^{(s)})'(z,s) \quad (3.1)$$

and the voltage change equation

$$\frac{d}{dz}(\tilde{V}_n(z,s)) = -(\tilde{Z}'_{n,m}(s)) \cdot (\tilde{I}_n(z,s)) + (\tilde{V}_n^{(s)})'(z,s) \quad (3.2)$$

where

$z$  = position along the tube

$(\tilde{I}_n(z,s))$  = current vector at  $z$

$(\tilde{V}_n(z,s))$  = voltage vector at  $z$  (3.3)

$(\tilde{Y}'_{n,m}(s))$  = per-unit-length shunt admittance matrix

$(\tilde{Z}'_{n,m}(s))$  = per-unit-length series impedance matrix

$(\tilde{I}_n^{(s)})'(z,s)$  = per-unit-length shunt current source vector

$(\tilde{V}_n^{(s)})'(z,s)$  = per-unit-length series voltage source vector.

It is noted that all vectors are of dimension  $N$ , and all matrices are  $N \times N$ . The per-unit-length equivalent circuit has been given in Figure 2.3.

There are a few ways of solving (3.1) and (3.2). One could reduce the equations to a second order differential equation in either the voltage vector or the current vector, or one could express the voltage-current relations in terms of a transmission supermatrix [3.1]. Still another way is to solve for the unknown propagation vectors that are associated with the waves. Here, the derivation is in terms of a yet undefined combined voltage. This approach, as will be illustrated later, has many definite advantages over other methods.

A. Combined Voltage Equation

Pre-multiplying (3.1) by a matrix  $(\tilde{A}_{n,m}(s))$  which is  $N \times N$  and non-singular and adding (3.2), then

$$\begin{aligned} \frac{d}{dz} [ (\tilde{A}_{n,m}(s)) \cdot (\tilde{I}_n(s)) + (\tilde{V}_n(s)) ] \\ = [ - (\tilde{A}_{n,m}(s)) \cdot (\tilde{V}'_{n,m}(s)) \cdot (\tilde{V}_n(s)) - (\tilde{Z}'_{n,m}(s)) \cdot (\tilde{I}_n(s)) ] \\ + [ (\tilde{A}_{n,m}(s)) \cdot (\tilde{I}_n^{(s)'}(s)) + (\tilde{V}_n^{(s)'}(s)) ] \end{aligned} \quad (3.4)$$

Defining the following quantities:

$$(\tilde{V}_n(z,s))_q \equiv (\tilde{V}_n(z,s)) + (\tilde{A}_{n,m}(s)) \cdot (\tilde{I}_n(z,s)) \quad (3.5)$$

and

$$(\tilde{V}_n^{(s)'}(z,s))_q \equiv (\tilde{V}_n^{(s)'}(z,s)) + (\tilde{A}_{n,m}(s)) \cdot (\tilde{I}_n^{(s)'}(z,s)) \quad (3.6)$$

(3.4) becomes

$$\frac{d}{dz} (\tilde{V}_n(s))_q = - (\tilde{C}_{n,m}(s)) \cdot (\tilde{V}_n(s))_q + (\tilde{V}_n^{(s)'}(s))_q \quad (3.7)$$

where

$$\begin{aligned} (\tilde{C}_{n,m}(s)) \cdot (\tilde{V}_n(z,s))_q &= (\tilde{A}_{n,m}(s)) \cdot (\tilde{V}'_{n,m}(s)) \cdot (\tilde{V}_n(z,s)) \\ &+ (\tilde{Z}'_{n,m}(s)) \cdot (\tilde{I}_n(z,s)) \end{aligned} \quad (3.8)$$

Using (3.8) and definition (3.5), one obtains

$$(\tilde{C}_{n,m}(s)) = (\tilde{A}_{n,m}(s)) \cdot (\tilde{V}'_{n,m}(s)) \quad (3.9)$$

and

$$(\tilde{C}_{n,m}(s)) \cdot (\tilde{A}_{n,m}(s)) = (\tilde{Z}'_{n,m}(s)) \quad (3.10)$$

Equating  $(\tilde{A}_{n,m}(s))$  in (3.9) and (3.10)

$$(\tilde{C}_{n,m}(s)) \cdot (\tilde{Y}'_{n,m}(s))^{-1} = (\tilde{C}_{n,m}(s))^{-1} \cdot (\tilde{Z}'_{n,m}(s)) \quad (3.11)$$

i.e.

$$(\tilde{C}_{n,m}(s))^2 = (\tilde{Z}'_{n,m}(s)) \cdot (\tilde{Y}'_{n,m}(s)) \quad (3.12)$$

One can also write

$$(\tilde{C}_{n,m}(s)) = [(\tilde{Z}'_{n,m}(s)) \cdot (\tilde{Y}'_{n,m}(s))]^{1/2} \quad (3.13)$$

which has many values. One may define a principal value (or matrix)\*  $(\tilde{Y}_{c,n,m}(s))$ , i.e.

$$(\tilde{Y}_{c,n,m}(s)) = \text{principal value of } [(\tilde{Z}'_{n,m}(s)) \cdot (\tilde{Y}'_{n,m}(s))]^{1/2} \quad (3.14)$$

$(\tilde{Y}_{c,n,m}(s))$  is called the propagation matrix. Expressing

(3.7) in this new form, one obtains

$$\begin{aligned} [(1_{n,m}) \frac{d}{dz} + q(\tilde{Y}_{c,n,m}(s))] \cdot (\tilde{V}_n(z,s))_q &= (\tilde{V}_n(s))'_q(z,s)_q \\ 1_{n,m} &= \begin{cases} 1 & \text{for } n=m \\ 0 & \text{for } n \neq m \end{cases} \end{aligned} \quad (3.15)$$

$q = \pm 1$  for forward and backward traveling combined  
N-vector waves, respectively.

Essentially,  $(\tilde{C}_{n,m}(s))$  has been restricted to  $q(\tilde{Y}_{c,n,m}(s))$  in (3.5).

From (3.9), (3.10) and (3.14)

$$\begin{aligned} (\tilde{A}_{n,m}(s)) &= q(\tilde{Y}_{c,n,m}(s)) \cdot (\tilde{Y}'_{n,m}(s))^{-1} \\ &= q(\tilde{Y}_{c,n,m}(s))^{-1} \cdot (\tilde{Z}'_{n,m}(s)) \end{aligned} \quad (3.16)$$

\* see definition under Section III-B.

Thus,  $(\tilde{A}_{n,m}(s))$  is a characteristic of the transmission line and has the dimensions of an impedance. Define

$$\begin{aligned}(\tilde{Z}_{c,n,m}(s)) &\equiv (\tilde{Y}_{c,n,m}(s)) \cdot (\tilde{Y}'_{n,m}(s))^{-1} \\ &= (\tilde{Y}_{c,n,m}(s))^{-1} \cdot (\tilde{Z}'_{n,m}(s))\end{aligned}\quad (3.17)$$

which is called the characteristic impedance matrix. Now, definitions (3.5) and (3.6) are rewritten to be

$$\begin{aligned}(\tilde{V}_n(z,s))_q &\equiv (\tilde{V}_n(z,s)) + q(\tilde{Z}_{c,n,m}(s)) \cdot (\tilde{I}_n(z,s)) \\ (\tilde{V}_n^{(s)'}(z,s))_q &\equiv (\tilde{V}_n^{(s)'}(z,s)) + q(\tilde{Z}_{c,n,m}(s)) \cdot (\tilde{I}_n^{(s)'}(z,s))\end{aligned}\quad (3.18)$$

One can also define the characteristic admittance matrix to be the inverse of the characteristic impedance matrix, viz.

$$(\tilde{Y}_{c,n,m}(s)) \equiv (\tilde{Z}_{c,n,m}(s))^{-1}\quad (3.19)$$

Putting  $q = +1$  and  $q = -1$  in (3.18), one can obtain the following relations

$$(\tilde{V}_n(z,s)) = \frac{1}{2}[(\tilde{V}_n(z,s))_+ + (\tilde{V}_n(z,s))_-]\quad (3.20)$$

$$(\tilde{Z}_{c,n,m}(s)) \cdot (\tilde{I}_n(z,s)) = \frac{1}{2}[(\tilde{V}_n(z,s))_+ - (\tilde{V}_n(z,s))_-]\quad (3.21)$$

Thus, for forward traveling waves

$$(\tilde{V}_n(z,s))_+ = (\tilde{Z}_{c,n,m}(s)) \cdot (\tilde{I}_n(z,s))_+\quad (3.22)$$

and for backward traveling waves

$$(\tilde{V}_n(z,s))_- = -(\tilde{Z}_{c,n,m}(s)) \cdot (\tilde{I}_n(z,s))_-\quad (3.23)$$

This is an important result which allows one to easily separate the voltage and current vectors into forward and backward waves and easily reconstruct the voltage and current vectors from the waves.

B. Eigenmode Expansion

Expression (3.14) for  $(\tilde{Y}_{c_{n,m}}(s))$  clearly indicates the necessity of eigenmode expansion of the matrix product  $(Z'_{n,m}(s)) \cdot (Y'_{n,m}(s))$ . The eigenvalues would yield the values of the propagation constants of the eigenmodes. Corresponding to each eigenmode, there is a complete set of eigenvectors for the combined voltage. These properties are examined in this section.

## 1. Positive real properties

## a. Definitions

A rational function  $f(s)$  which is real for real values of  $s$  and whose real part is positive for all values of  $s$  with a positive real part is called a positive real function (p. r. function) [3.2]. A positive real matrix is one whose eigenvalues are all p.r. functions. Let  $(\tilde{P}_{n,m}(s))$  be a p.r. matrix of size  $N \times N$ , then the eigenvalue problem becomes

$$\begin{aligned} (\tilde{P}_{n,m}(s)) \cdot (\tilde{P}_n^{(r)}(s))_\delta &= \tilde{p}_\delta(s) (\tilde{P}_n^{(r)}(s))_\delta \\ (\tilde{P}_n^{(l)}(s))_\delta \cdot (\tilde{P}_{n,m}(s)) &= \tilde{p}_\delta(s) (\tilde{P}_n^{(l)}(s))_\delta \end{aligned} \quad (3.24)$$

where  $\delta = 1, 2, \dots, N$  is the eigenindex and  $\tilde{p}_\delta(s)$  are the eigenvalues, and  $(\tilde{P}_n^{(r)}(s))_\delta$  and  $(\tilde{P}_n^{(l)}(s))_\delta$  are the eigenvectors. Since  $(\tilde{P}_{n,m}(s))$  is a p.r. matrix,  $\tilde{p}_\delta(s)$  is a p.r. function of  $s$ . If  $\tilde{p}_\delta$  is independent of  $s$ , then  $\tilde{p}_\delta$  is real and  $\tilde{p}_\delta \geq 0$  for all  $\delta$ . For the oft encountered case of symmetric p.r. matrices we can set

$$(\tilde{P}_n^{(r)}(s))_\delta \equiv (\tilde{P}_n^{(l)}(s))_\delta \quad (3.25)$$

$$(\tilde{P}_{n,m}(s)) = (\tilde{P}_{n,m}(s))^T$$

## b. Eigenmode expansion

A p.r. matrix can be expanded as follows [3.3]:

$$(\tilde{P}_{n,m}(s)) = \sum_{\delta} \tilde{p}_{\delta}(s) (P_n^{(r)}(s))_{\delta} (\tilde{P}_n^{(l)}(s))_{\delta} [(\tilde{P}_n^{(r)}(s))_{\delta} \cdot (\tilde{P}_n^{(l)}(s))_{\delta}]^{-1} \quad (3.26)$$

If the matrix is the argument of a scalar function  $F$ , then

$$F[(\tilde{P}_{n,m}(s))] = \sum_{\delta} F[\tilde{p}_{\delta}(s)] (\tilde{P}_n^{(r)}(s))_{\delta} (\tilde{P}_n^{(l)}(s))_{\delta} [(\tilde{P}_n^{(r)}(s))_{\delta} \cdot (\tilde{P}_n^{(l)}(s))_{\delta}]^{-1} \quad (3.27)$$

One assumes that the scalar function  $F$  is single-valued for all complex  $\tilde{p}_{\delta}(s)$ . Otherwise the principal value of  $F[p_{\delta}(s)]$  is defined to define the principal value (or matrix) of  $F[(\tilde{P}_{n,m}(s))]$ .

For example, powers of the matrix can be expressed as

$$(\tilde{P}_{n,m}(s))^{\epsilon} = \sum_{\delta} [\tilde{p}_{\delta}(s)]^{\epsilon} (\tilde{P}_n^{(r)}(s))_{\delta} (\tilde{P}_n^{(l)}(s))_{\delta} [(\tilde{P}_n^{(r)}(s))_{\delta} \cdot (\tilde{P}_n^{(l)}(s))_{\delta}]^{-1} \quad (3.28)$$

where for  $\text{Re}(s) > 0$  and  $\text{Im}(\epsilon) = 0$ ,  $[\tilde{p}(s)]^{\epsilon} > 0$  defines the principal value of the  $\epsilon$ -th power of a p.r. matrix.

## c. Normalized eigenvectors

The normalized eigenvector is defined by

$$(\tilde{P}_n^{(r)}(s))_{\delta} = \frac{(\tilde{P}_n^{(r)}(s))_{\delta}}{\sqrt{(\tilde{P}_n^{(r)}(s))_{\delta} \cdot (\tilde{P}_n^{(l)}(s))_{\delta}}} \quad (3.29)$$

In terms of the normalized quantities, (3.26) and (3.27) become

$$\begin{aligned} (\tilde{P}_{n,m}(s)) &= \sum_{\delta} \tilde{p}_{\delta}(s) (\tilde{P}_n^{(r)}(s))_{\delta} (\tilde{P}_n^{(l)}(s))_{\delta} \\ F[(\tilde{P}_{n,m}(s))] &= \sum_{\delta} F[\tilde{p}_{\delta}(s)] (\tilde{P}_n^{(r)}(s))_{\delta} (\tilde{P}_n^{(l)}(s))_{\delta} \end{aligned} \quad (3.30)$$

Note for symmetric p.r. matrices the normalized eigenvectors can be reduced to

$$(\tilde{p}_n^{(r)}(s))_\delta = (\tilde{p}_n^{(\ell)}(s))_\delta \equiv (\tilde{p}_n(s))_\delta \quad (3.31)$$

d. Transmission line p.r. matrices

Assume that the per-unit-length impedance and admittance matrices  $(Z'_{n,m}(s))$ ,  $(Y'_{n,m}(s))$  are passive. Then they are p.r. matrices.

In the special case of a lossless transmission line,

$$(Z'_{n,m}(s)) = s(L'_{n,m}) \quad (3.32)$$

$$(Y'_{n,m}(s)) = s(C'_{n,m})$$

where

$$\begin{aligned} (L'_{n,m}) &\equiv \text{per-unit-length inductance matrix} \\ (C'_{n,m}) &\equiv \text{per-unit-length capacitance matrix.} \end{aligned} \quad (3.33)$$

which we also assume to be frequency independent (dispersionless) and, hence, constant matrices. The elements  $L'_{n,m}$  and  $C'_{n,m}$  are real, being derivable from quasi-static boundary-value problems (Laplace equation). The p.r. property of the per-unit-length impedance and admittance matrices then implies that the per-unit-length inductance and capacitance matrices are both p.r. and positive semidefinite. Thus,  $(L'_{n,m})$  and  $(C'_{n,m})$  have real non-negative eigenvalues.

If we further assume that  $(L'_{n,m})$  is symmetric, then

$$\begin{aligned} (L'_{n,m}) \cdot (L'_n)_\delta &= \ell'_\delta (L'_n)_\delta \\ (L'_n)_\delta (L'_{n,m}) &= \ell'_\delta (L'_n)_\delta \end{aligned} \quad (3.34)$$

In terms of the normalized eigenvectors  $(\ell'_n)_\delta$ ,  $(\tilde{Z}'_{n,m}(s))$  is expressible as

$$(\tilde{Z}'_{n,m}(s)) = s \sum_{\delta} \ell'_\delta (\ell'_n)_\delta (\ell'_n)_\delta \quad (3.35)$$

Similar expressions exist for symmetric  $(\tilde{Y}'_{n,m}(s))$  and  $(C'_{n,m})$ .

## 2. Propagation matrix $(\tilde{\gamma}_{c_{n,m}}(s))$

The squared quantity of the propagation matrix is equal to the product of two matrices, each of which is typically symmetric (reciprocity), i.e.,

$$(\tilde{\gamma}_{c_{n,m}}(s))_V^2 = (\tilde{z}'_{n,m}(s)) \cdot (\tilde{y}'_{n,m}(s)) \quad (3.36)$$

Let  $(\tilde{v}_{c_n}(s))_\delta$  be the right eigenvector of  $(\tilde{\gamma}_{c_{n,m}}(s))_V^2$

$$(\tilde{z}'_{n,m}(s)) \cdot (\tilde{y}'_{n,m}(s)) \cdot (\tilde{v}_{c_n}(s))_\delta = \tilde{\gamma}_{V_\delta}^2(s) (\tilde{v}_{c_n}(s))_\delta \quad (3.37)$$

The corresponding quantity for the combined current mode is given by

$$(\tilde{\gamma}_{c_{n,m}}(s))_I^2 = (\tilde{y}'_{n,m}(s)) \cdot (\tilde{z}'_{n,m}(s)) \quad (3.38)$$

Let  $(\tilde{l}_{c_n}(s))_\delta$  be the left eigenvector of  $(\tilde{\gamma}_{c_{n,m}}(s))_V^2$

$$(\tilde{l}_{c_n}(s))_\delta \cdot (\tilde{z}'_{n,m}(s)) \cdot (\tilde{y}'_{n,m}(s)) = \tilde{\gamma}_{I_\delta}^2(s) (\tilde{l}_{c_n}(s))_\delta \quad (3.39)$$

In this note, the following simplified notation is used:

$$(\tilde{\gamma}_{c_{n,m}}(s)) \equiv (\tilde{\gamma}_{c_{n,m}}(s))_V \quad (3.40)$$

Defining the normalized eigenvectors by

$$(\tilde{v}_{c_n}(s))_\delta = \frac{(\tilde{v}_{c_n}(s))_\delta}{\sqrt{(\tilde{v}_{c_n}(s))_\delta \cdot (\tilde{l}_{c_n}(s))_\delta}} \quad (3.41)$$

and

$$(\tilde{I}_{c_n}(s))_\delta = \frac{(\tilde{I}_{c_n}(s))_\delta}{\sqrt{(\tilde{V}_{c_n}(s))_\delta \cdot (\tilde{I}_{c_n}(s))_\delta}} \quad (3.42)$$

it is possible to expand the squared propagation matrix into

$$(\tilde{V}_{c_{n,m}}(s))^2 = \sum_{\delta} \gamma_{\delta}^2(s) (\tilde{V}_{c_n}(s)) (\tilde{I}_{c_n}(s)) \quad (3.43)$$

and using (3.31) the propagation matrix is

$$(\tilde{V}_{c_{n,m}}(s)) = \sum_{\delta} \tilde{\gamma}_{\delta}(s) (\tilde{V}_{c_n}(s)) (\tilde{I}_{c_n}(s)) \quad (3.44)$$

where  $\tilde{\gamma}_{\delta}(s)$  is the principal value of  $[\gamma_{\delta}^2(s)]^{1/2}$ .

Here principal value means for

$$\tilde{f}(s) \geq 0 \quad \text{for } s \geq 0 \quad (3.45)$$

and then

$$\tilde{f}^{1/2}(s) \geq 0 \quad \text{for } s \geq 0 \quad (3.46)$$

with analytic continuation away from the  $s \geq 0$  axis. We then assume

$$\tilde{\gamma}_{\delta}^2(s) \geq 0 \quad \text{for } s \geq 0 \quad (3.47)$$

so that we may choose

$$\tilde{\gamma}_{\delta}(s) \geq 0 \quad \text{for } s \geq 0, \delta = 1, 2, \dots, N \quad (3.48)$$

We further assume that the  $\tilde{\gamma}_{\delta}(s)$  are p.r. functions so that

$$\left. \begin{array}{l} \operatorname{Re}[\tilde{\gamma}_{\delta}(s)] \geq 0 \quad \text{for } s \geq 0 \\ \tilde{\gamma}_{\delta}(s) \text{ analytic for } s > 0 \end{array} \right\} \delta = 1, 2, \dots, N \quad (3.49)$$

Note that  $\tilde{\gamma}_\delta(s)$  having this property corresponds to a + or right-going wave, since a positive real part corresponds to an attenuation in the + direction. A p.r. propagation constant is then a causal propagation constant. However, other more general forms are perhaps possible. For present purposes, p.r. propagation constants are assumed.

The necessity of choosing which square root to use for the propagation matrix is potentially troublesome. The matrix transmission-line equations may have buried in them certain mathematical problems, such as related to existence and uniqueness of solutions, representation of solutions, etc. The diagonalization of the square of the propagation matrix may depend on certain properties of the per-unit-length impedance and admittance matrices; this in turn influences the nature of the square root of the square of the propagation matrix. The problems in choice of the propagation constants may lead to some restrictions to situations that such choices are applicable or even possible. There are then some open questions requiring further research.

With the above definitions we obtain two sets of waves propagating in opposite directions along  $z$ . For all modes we have

$$\begin{aligned} \exp[-(\tilde{\gamma}_{c_{n,m}}(s))z] & \text{ is + propagating} \\ \exp[(\tilde{\gamma}_{c_{n,m}}(s))z] & \text{ is - propagating} \end{aligned} \quad (3.50)$$

For a function  $F$  of  $(\tilde{\gamma}_{c_{n,m}}(s))$ , assuming nondegenerate modes, one can express

$$F[(\tilde{\gamma}_{c_{n,m}}(s))] = \sum_{\delta} F[\tilde{\gamma}_{\delta}(s)] (\tilde{v}_{c_n}(s)) (\tilde{i}_{c_n}(s)) \quad (3.51)$$

Specifically, we have

$$\begin{aligned}
(\tilde{\gamma}_{c_n, m}(s)) &= \sum_{\delta} \tilde{\gamma}_{\delta}(s) (\tilde{v}_{c_n}(s))_{\delta} (\tilde{i}_{c_n}(s))_{\delta} \\
(\tilde{\gamma}_{c_n, m}(s))^{-1} &= \sum_{\delta} \tilde{\gamma}_{\delta}^{-1}(s) (\tilde{v}_{c_n}(s))_{\delta} (\tilde{i}_{c_n}(s))_{\delta} \\
e^{-q(\gamma_{c_n, m}(s))z} &= \sum_{\delta} e^{-q\tilde{\gamma}_{\delta}(s)z} (\tilde{v}_{c_n}(s))_{\delta} (\tilde{i}_{c_n}(s))_{\delta} \\
(\tilde{\gamma}_{c_n, m}(s))^0 &= (1_{n, m}) = \sum_{\delta} (\tilde{v}_{c_n}(s))_{\delta} (\tilde{i}_{c_n}(s))_{\delta} \quad (\text{identity})
\end{aligned} \tag{3.52}$$

### 3. Properties of $(\tilde{v}_{c_n}(s))_{\delta}$ , $(\tilde{i}_{c_n}(s))_{\delta}$

The two normalized eigenvectors as defined in (3.36), (3.37), (3.41), and (3.42) possess unique properties, which are exploited in this section.

Rewriting (3.36) and (3.37)

$$\begin{aligned}
(\tilde{Z}'_{n, m}(s)) \cdot (\tilde{Y}'_{n, m}(s)) \cdot (\tilde{v}_{c_n}(s))_{\delta} &= \tilde{\gamma}_{\delta}^2(s) (\tilde{v}_{c_n}(s))_{\delta} \\
(\tilde{i}_{c_n}(s))_{\delta} \cdot (\tilde{Z}'_{n, m}(s)) \cdot (\tilde{Y}'_{n, m}(s)) &= \tilde{\gamma}_{\delta}^2(s) (\tilde{i}_{c_n}(s))_{\delta}
\end{aligned} \tag{3.53}$$

First, premultiply the first by  $(\tilde{i}_{c_n}(s))_{\delta}$ , then postmultiply the second by  $(\tilde{v}_{c_n}(s))_{\delta}$  (both in dot product sense). The difference of these two new equations becomes

$$\begin{aligned}
&(\tilde{i}_{c_n}(s))_{\delta} \cdot [(\tilde{Z}'_{n, m}(s)) \cdot (\tilde{Y}'_{n, m}(s)) - (\tilde{Z}'_{n, m}(s)) \cdot (\tilde{Y}'_{n, m}(s))] \cdot (\tilde{v}_{c_n}(s))_{\delta} \\
&= [\tilde{\gamma}_{\delta}^2(s) - \tilde{\gamma}_{\delta'}^2(s)] (\tilde{i}_{c_n}(s))_{\delta} \cdot (\tilde{v}_{c_n}(s))_{\delta} \\
&= 0
\end{aligned} \tag{3.54}$$

There are two possible cases. First, if  $\gamma_{\delta}^2 \neq \gamma_{\delta'}^2$ , then

$$(\tilde{i}_{c_n}(s))_{\delta} \cdot (\tilde{v}_{c_n}(s))_{\delta} = 1_{\delta, \delta'} \tag{3.55}$$

where

$$l_{\delta, \delta'} = \begin{cases} 0 & \text{for } \delta \neq \delta' \\ 1 & \text{for } \delta = \delta' \end{cases} \quad (3.56)$$

are elements of the  $N \times N$  identity matrix  $(l_{\delta, \delta'})$  (or Kronecker delta). Equation (3.55) is called the biorthonormal relation;  $(\tilde{i}_{c_n}(s))_{\delta}$  and  $(\tilde{v}_{c_n}(s))_{\delta}$  are the biorthonormal eigenvectors. Second, if  $\gamma_{\delta}^2 = \gamma_{\delta'}^2$ , i.e., the degenerate case, the orthonormal vectors are constructed by other means such as the Gram-Schmidt procedure.

### C. Solution of Combined Voltage Equations

#### 1. Integration of combined voltage equation

The combined differential equation (3.15), i.e.,

$$\frac{d}{dz} (\tilde{v}_n(s))_q + q(\tilde{\gamma}_{c_{n,m}}(s)) \cdot (\tilde{v}_n(z,s))_q = (\tilde{v}_n^{(s)})'(z,s)_q \quad (3.57)$$

can be readily solved [3.4] to give

$$\begin{aligned} (\tilde{v}_n(z,s))_q &= \exp\{-q(\tilde{\gamma}_{c_{n,m}}(s))[z-z_0]\} \cdot (\tilde{v}_n(z_0,s))_q \\ &+ \int_{z_0}^z \exp\{-q(\tilde{\gamma}_{c_{n,m}}(s))[z-z']\} \cdot (\tilde{v}_n^{(s)})'(z',s)_q dz' \end{aligned} \quad (3.58)$$

For a  $+$  wave (i.e., a wave propagating in the  $+$   $z$  direction), let us assume that  $(\tilde{v}_n(0,s))_+$  is specified, giving

$$\begin{aligned} (\tilde{v}_n(z,s))_+ &= \exp\{-q(\tilde{\gamma}_{c_{n,m}}(s))z\} \cdot (\tilde{v}_n(0,s))_+ \\ &+ \int_0^z \exp\{-q(\tilde{\gamma}_{c_{n,m}}(s))[z-z']\} \cdot (\tilde{v}_n^{(s)})'(z',s)_+ dz' \end{aligned} \quad (3.59)$$

Similarly for a  $-$  wave with  $(\tilde{v}_n(L,s))_-$  assumed specified, we have

$$\begin{aligned}
(\tilde{V}_n(z,s))_- &= \exp\{(\tilde{\gamma}_{c_{n,m}}(s))[z-L]\} \cdot (\tilde{V}_n(L,s))_- \\
&+ \int_L^z \exp\{(\tilde{\gamma}_{c_{n,m}}(s))[z-z']\} \cdot (\tilde{V}_n^{(s)'}(z',s))_- dz'
\end{aligned}
\quad (3.60)$$

These results illustrate one aspect of the simplification introduced by the combined voltage in that the + wave depends only on the left boundary condition and the - wave depends only on the right boundary condition in a very compact way. Note that for the minus wave if we replace  $z$  by  $L-z$  as the coordinate variable, then the - wave has precisely the same form as the + wave, which one would expect by symmetry.

Using (3.52), equation (3.58) can be written in terms of eigenmodes, i.e.,

$$\begin{aligned}
(\tilde{V}_n(z,s))_q &= \sum_{\delta} \left\{ e^{-q\tilde{\gamma}_{\delta}(s)[z-z_0]} [(\tilde{I}_{c_n}(s))_{\delta} \cdot (\tilde{V}_n(z_0,s))_q] (\tilde{v}_{c_n}(s))_{\delta} \right. \\
&+ \left. \int_{z_0}^z e^{-q\tilde{\gamma}_{\delta}(s)(z-z_0)} [(\tilde{I}_{c_n}(s))_{\delta} \cdot (\tilde{V}_n^{(s)'}(z',s))] dz' \right\} (\tilde{v}_{c_n}(s))_{\delta} \\
&= \sum_{\delta} [(\tilde{I}_{c_n}(s))_{\delta} \cdot (\tilde{V}_n(z,s))_q] (\tilde{v}_{c_n}(s))_{\delta}
\end{aligned}
\quad (3.61)$$

Define coefficients of expansion as

$$\tilde{C}_{V_{\delta,q}}(z,s) = (\tilde{I}_{c_n}(s))_{\delta} \cdot (\tilde{V}_n(z,s))_q \quad (3.62)$$

For a + wave, i.e., one that travels from  $z=0$  to  $z=L$  along the transmission line, let us assume that  $(\tilde{V}_n(0,s))_+$  is specified. Then

$$(\tilde{V}_n(z,s))_+ = \sum_{\delta} C_{V_{\delta,+}}(z,s) (\tilde{v}_{c_n}(s))_{\delta} \quad (3.63)$$

and

$$\begin{aligned}
 C_{V_{\delta,+}}(z,s) &= (\tilde{I}_{c_n}(s))_{\delta} \cdot (\tilde{V}_n(z,s))_{+} \\
 &= e^{-\tilde{\gamma}_{\delta}(s)z} [(\tilde{I}_{c_n}(s))_{\delta} \cdot (\tilde{V}_n(0,s))_{+}] \\
 &\quad + \int_0^z e^{-\tilde{\gamma}_{\delta}(s)(z-z')} [(\tilde{I}_{c_n}(s))_{\delta} \cdot (\tilde{V}_n^{(s)'}(z',s))_{+}] dz' \quad (3.64)
 \end{aligned}$$

Similarly for a - wave with  $(\tilde{V}_n(L,s))_{-}$  specified

$$(\tilde{V}_n(z,s))_{-} = \sum_{\delta} C_{V_{\delta,-}}(z,s) (\tilde{V}_{c_n}(s))_{\delta} \quad (3.65)$$

and

$$\begin{aligned}
 C_{V_{\delta,-}}(z,s) &= (\tilde{I}_{c_n}(s))_{\delta} \cdot (\tilde{V}_n(z,s))_{-} \\
 &= e^{\tilde{\gamma}_{\delta}(s)(z-L)} [(\tilde{I}_{c_n}(s))_{\delta} \cdot (\tilde{V}_n(L,s))_{-}] \\
 &\quad + \int_L^z e^{\tilde{\gamma}_{\delta}(s)(z-z')} [(\tilde{I}_{c_n}(s))_{\delta} \cdot (\tilde{V}_n^{(s)'}(z',s))_{-}] dz' \quad (3.66)
 \end{aligned}$$

Equations (3.63) and (3.65) show that there are  $2N$  eigenwaves for a  $N$ -wire transmission line (plus a reference). These waves are characterized by  $\tilde{C}_{V_{\delta,+}}(\tilde{V}_{c_n}(s))_{\delta}$  and  $\tilde{C}_{V_{\delta,-}}(\tilde{V}_{c_n}(s))_{\delta}$ ,  $\delta = 1, 2, \dots, N$ . One could define an eigenmatrix as follows

$$(\tilde{E}_{n,m}(s))_V = ((\tilde{V}_{c_n}(s))_1, (\tilde{V}_{c_n}(s))_2, \dots, (\tilde{V}_{c_n}(s))_N) \quad (3.67)$$

where the columns are the voltage eigenvectors. The eigenmode coefficient vector is defined by

$$(\tilde{C}_V(z,s))_q = (\tilde{C}_{V_{1,q}}(z,s), \tilde{C}_{V_{2,q}}(z,s), \dots, \tilde{C}_{V_{N,q}}(z,s)) \quad (3.68)$$

Equation (3.61) can be rewritten as

$$(V_n(z,s))_q = (E_{n,m}(s))_V (C_{V_n}(z,s))_q \quad (3.69)$$

## 2. Semi-infinite transmission line

Many transmission-line properties can be learned by studying the semi-infinite line where the complications due to reflections do not exist. As discussed earlier, the per-unit-length electrical model of a transmission line is given in Figure 2.5.

Assuming that  $(\tilde{V}_n(0,s))_+$  is given and there are no other sources along the line so that only + waves propagate, (3.59) gives

$$(\tilde{V}_n(z,s))_+ = \exp[-(\tilde{Y}_{c_{n,m}}(s))z] \cdot (\tilde{V}_n(0,s))_+ \quad (3.70)$$

At  $z = 0$ ,

$$\begin{aligned} (\tilde{V}_n(0,s))_+ & \text{ is specified} \\ (\tilde{V}_n(0,s))_- & = (0_n) \end{aligned} \quad (3.71)$$

from (3.19)

$$(\tilde{V}_n(0,s))_- = (\tilde{V}_n(0,s)) - (\tilde{Z}_{c_{n,m}}(s)) \cdot (\tilde{I}_n(0,s)) = (0_n) \quad (3.72)$$

Thus

$$(\tilde{V}_n(0,s)) = (\tilde{Z}_{c_{n,m}}(s)) \cdot (\tilde{I}_n(0,s)) \quad (3.73)$$

Or, from (3.20)

$$(\tilde{I}_n(0,s)) = (\tilde{Y}_{c_{n,m}}(s)) \cdot (\tilde{V}_n(0,s)) \quad (3.74)$$

As is well-known, waves propagate in only one direction on a semi-infinite line driven at the one end, with voltage and current related by the characteristic impedance (Equation 3.73). Thus, the effect of a semi-infinite multiconductor transmission line can be represented by an equivalent impedance network that is equivalent to the characteristic impedance matrix  $(\tilde{Z}_{c_{n,m}}(s))$ .

3. Normalization relation of  $(\tilde{v}_{c_n}(s))_\delta$  and  $(\tilde{i}_{c_n}(s))_\delta$  in terms of  $(\tilde{Z}_{c_{n,m}}(s))$  and  $(\tilde{Y}_{c_{n,m}}(s))$  and associated modal expansions

For forward traveling waves only, (3.22) gives

$$(\tilde{v}_n(z,s)) = (\tilde{Z}_{c_{n,m}}(s)) \cdot (\tilde{i}_n(z,s)) \quad (3.75)$$

For  $(\tilde{v}_n(z,s))$  chosen as a single mode, (3.63) gives

$$(\tilde{v}_n(z,s)) = C_{v_{\delta,+}} (\tilde{v}_{c_n}(s))_\delta \quad (3.76)$$

Hence

$$(\tilde{i}_n(z,s)) = C_{v_{\delta,+}} (\tilde{Y}_{c_{n,m}}(s)) \cdot (\tilde{v}_{c_n}(s))_\delta \quad (3.77)$$

Therefore, the  $\delta$ -th mode for the current can be normalized as

$$(\tilde{i}_{c_n}(s))_\delta \equiv (\tilde{Y}_{c_{n,m}}(s)) \cdot (\tilde{v}_{c_n}(s))_\delta \quad (3.78)$$

$$(\tilde{v}_{c_n}(s))_\delta \equiv (\tilde{Z}_{c_{n,m}}(s)) \cdot (\tilde{i}_{c_n}(s))_\delta$$

Together with (3.55) this specifies  $(\tilde{v}_{c_n}(s))$  and  $(\tilde{i}_{c_n}(s))$  including their units.

For nondegenerate modes (3.53), (3.55), and (3.78), give

$$\begin{aligned}
 (\tilde{v}_{c_n}(s))_{\delta} \cdot (\tilde{I}_{c_n}(s))_{\delta'} &= (\tilde{v}_{c_n}(s))_{\delta} \cdot (\tilde{Y}_{c_{n,m}}(s)) \cdot (\tilde{v}_{c_n}(s))_{\delta'} = 1_{\delta, \delta'} \\
 (\tilde{I}_{c_n}(s))_{\delta} \cdot (\tilde{v}_{c_n}(s))_{\delta'} &= (\tilde{I}_{c_n}(s))_{\delta} \cdot (\tilde{Z}_{c_{n,m}}(s)) \cdot (\tilde{I}_{c_n}(s))_{\delta'} = 1_{\delta, \delta'}
 \end{aligned} \quad (3.79)$$

For the first of these equations left dyadic by  $(\tilde{v}_{c_n}(s))_{\delta}$  and right dyadic multiply by  $(\tilde{I}_{c_n}(s))_{\delta'}$  and sum over  $\delta, \delta'$ .

$$\begin{aligned}
 \sum_{\delta, \delta'} (\tilde{v}_{c_n}(s))_{\delta} (\tilde{I}_{c_n}(s))_{\delta'} 1_{\delta, \delta'} &= \sum_{\delta} (\tilde{v}_{c_n}(s))_{\delta} (\tilde{I}_{c_n}(s))_{\delta} \\
 &= (1_{n,m}) \\
 &- \sum_{\delta, \delta'} (\tilde{v}_{c_n}(s))_{\delta} (\tilde{v}_{c_n}(s))_{\delta'} \cdot (\tilde{Y}_{c_{n,m}}(s)) \cdot (\tilde{v}_{c_n}(s))_{\delta'} (\tilde{I}_{c_n}(s))_{\delta'} \\
 &- \left[ \sum_{\delta} (\tilde{v}_{c_n}(s))_{\delta} (\tilde{v}_{c_n}(s))_{\delta} \right] \cdot (\tilde{Y}_{c_{n,m}}(s)) \cdot \left[ \sum_{\delta'} (\tilde{v}_{c_n}(s))_{\delta'} (\tilde{I}_{c_n}(s))_{\delta'} \right] \\
 &- \left[ \sum_{\delta} (\tilde{v}_{c_n}(s))_{\delta} (\tilde{v}_{c_n}(s))_{\delta} \right] \cdot (\tilde{Y}_{c_{n,m}}(s)) \cdot (1_{n,m}) \\
 &- \left[ \sum_{\delta} (\tilde{v}_{c_n}(s))_{\delta} (\tilde{v}_{c_n}(s))_{\delta} \right] \cdot (\tilde{Y}_{c_{n,m}}(s))
 \end{aligned} \quad (3.80)$$

From which we conclude

$$(\tilde{Z}_{c_{n,m}}(s)) = (\tilde{Y}_{c_{n,m}}(s))^{-1} = \sum_{\delta} (\tilde{v}_{c_n}(s))_{\delta} (\tilde{v}_{c_n}(s))_{\delta} \quad (3.81)$$

In a similar manner from the second of (3.78) dyadic multiplication by  $(\tilde{v}_{c_n}(s))_{\delta}$  on the left and  $(\tilde{I}_{c_n}(s))_{\delta'}$  on the right and summing over  $\delta, \delta'$  gives

$$\begin{aligned}
\sum_{\delta, \delta'} (\tilde{v}_{c_n}(s))_{\delta} (\tilde{i}_{c_n}(s))_{\delta'} 1_{\delta, \delta'} &= \sum_{\delta} (\tilde{v}_{c_n}(s))_{\delta} (\tilde{i}_{c_n}(s))_{\delta} \\
&= (1_{n,m}) \\
&= \sum_{\delta, \delta'} (\tilde{v}_{c_n}(s))_{\delta} (\tilde{i}_{c_n}(s))_{\delta} \cdot (\tilde{Z}_{c_{n,m}}(s)) \cdot (\tilde{i}_{c_n}(s))_{\delta'} (\tilde{i}_{c_n}(s))_{\delta'} \\
&= \left[ \sum_{\delta} (\tilde{v}_{c_n}(s))_{\delta} (\tilde{i}_{c_n}(s))_{\delta} \right] \cdot (\tilde{Z}_{c_{n,m}}(s)) \cdot \left[ \sum_{\delta'} (\tilde{i}_{c_n}(s))_{\delta'} (\tilde{i}_{c_n}(s))_{\delta'} \right] \\
&= (1_{n,m}) \cdot (\tilde{Z}_{c_{n,m}}(s)) \cdot \left[ \sum_{\delta'} (\tilde{i}_{c_n}(s))_{\delta'} (\tilde{i}_{c_n}(s))_{\delta'} \right] \\
&= (\tilde{Z}_{c_{n,m}}(s)) \cdot \left[ \sum_{\delta} (\tilde{i}_{c_n}(s))_{\delta} (\tilde{i}_{c_n}(s))_{\delta} \right] \tag{3.82}
\end{aligned}$$

from which we conclude

$$(\tilde{Y}_{c_{n,m}}(s)) = (\tilde{Z}_{c_{n,m}}(s))^{-1} = \sum_{\delta} (\tilde{i}_{c_n}(s))_{\delta} (\tilde{i}_{c_n}(s))_{\delta} \tag{3.83}$$

These results are quite illuminating. Specifically, they show that the characteristic impedance matrices are symmetric, i.e.,

$$\begin{aligned}
(\tilde{Z}_{c_{n,m}}(s))^T &= (\tilde{Z}_{c_{n,m}}(s)) \\
(\tilde{Y}_{c_{n,m}}(s))^T &= (\tilde{Y}_{c_{n,m}}(s)) \tag{3.84}
\end{aligned}$$

This is evident from (3.81) and (3.83) which expand these as sums of symmetric dyads. The form in (3.84) is usually referred to as reciprocity, but this property was not assumed in the beginning, but is required by our results. Again, this is possibly associated with the assumed characteristics of the propagation matrix.

AD-A074 265

AIR FORCE WEAPONS LAB KIRTLAND AFB NM  
ELECTROMAGNETIC PULSE INTERACTION NOTES-EMP 3-39.(U)  
JUL 79 C E BAUM

F/G 20/14

UNCLASSIFIED

AFWL-TR-79-402

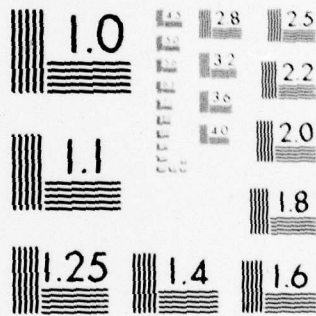
SBIE-AD-E200 363

NL

4 OF 5

AD  
A074265





MICROCOPY RESOLUTION TEST CHART  
NATIONAL BUREAU OF STANDARDS-1963-A

4. Expansion of  $(\tilde{Z}'_{n,m}(s))$  and  $(\tilde{Y}'_{n,m}(s))$  in terms of  $(\tilde{v}_{c_n}(s))_\delta$  and  $(\tilde{i}_{c_n}(s))_\delta$

From (3.58) for the case of no sources along the semi-infinite line,  $z \geq 0$ , with only + waves, we have

$$\begin{aligned}(\tilde{V}_n(z,s))_+ &= \exp\{-(\tilde{\gamma}_{c_{n,m}}(s))z\} \cdot (\tilde{V}_n(0,s))_+ \\ (\tilde{V}_n(z,s))_- &= (0_n)\end{aligned}\quad (3.85)$$

$$(\tilde{V}_n(z,s)) = (\tilde{Z}_{c_{n,m}}(s)) \cdot (\tilde{I}_n(z,s))$$

Expanded in modal form we have

$$\begin{aligned}(\tilde{V}_n(z,s))_+ &= \left\{ \sum_{\delta} e^{-\tilde{\gamma}_{\delta}(s)z} (\tilde{v}_{c_n}(s))_{\delta} (\tilde{i}_{c_n}(s))_{\delta} \right\} \cdot (\tilde{V}_n(0,s))_+ \\ \frac{d}{dz} (\tilde{V}_n(z,s))_+ &= - \left\{ \sum_{\delta} \tilde{\gamma}_{\delta}(s) e^{-\tilde{\gamma}_{\delta}(s)z} (\tilde{v}_{c_n}(s))_{\delta} (\tilde{i}_{c_n}(s))_{\delta} \right\} \cdot (\tilde{V}_n(0,s))_+\end{aligned}\quad (3.86)$$

Noting the special relation between the voltage and current vectors we can then write equations for the voltage vector the same as for the combined voltage vector, i.e.,

$$\begin{aligned}(\tilde{V}_n(z,s)) &= \left\{ \sum_{\delta} e^{-\tilde{\gamma}_{\delta}(s)z} (\tilde{v}_{c_n}(s))_{\delta} (\tilde{i}_{c_n}(s))_{\delta} \right\} \cdot (\tilde{V}_n(0,s)) \\ \frac{d}{dz} (\tilde{V}_n(z,s)) &= - \left\{ \sum_{\delta} \tilde{\gamma}_{\delta}(s) e^{-\tilde{\gamma}_{\delta}(s)z} (\tilde{v}_{c_n}(s))_{\delta} (\tilde{i}_{c_n}(s))_{\delta} \right\} \cdot (\tilde{V}_n(0,s))\end{aligned}\quad (3.87)$$

Similarly, for the current vector we have by multiplication (dot product) by the characteristic admittance matrix

$$(\tilde{I}_n(z,s)) = (\tilde{Y}_{c_{n,m}}(s)) \cdot \left\{ \sum_{\delta} e^{-\tilde{\gamma}_{\delta}(s)z} (\tilde{v}_{c_n}(s))_{\delta} (\tilde{i}_{c_n}(s))_{\delta} \right\} \cdot (\tilde{Z}_{c_{n,m}}(s)) \cdot (\tilde{I}_n(0,s))\quad (3.88)$$

Then using the modal expansions for the characteristic admittance and impedance matrices in (3.83) and (3.81) respectively, together with the biorthonormal modal relation in (3.55) we have

$$\begin{aligned} (\tilde{I}_n(z,s)) &= \left\{ \sum_{\delta} e^{-\tilde{\gamma}_{\delta}(s)z} (\tilde{I}_{c_n}(s))_{\delta} (\tilde{v}_{c_n}(s))_{\delta} \right\} \cdot (\tilde{I}_n(0,s)) \\ \frac{d}{dz} (\tilde{I}_n(z,s)) &= - \left\{ \sum_{\delta} \tilde{\gamma}_{\delta}(s) e^{-\tilde{\gamma}_{\delta}(s)z} (\tilde{I}_{c_n}(s))_{\delta} (\tilde{v}_{c_n}(s))_{\delta} \right\} \cdot (\tilde{I}_n(0,s)) \end{aligned} \quad (3.89)$$

Recall (3.1) and (3.2) without sources

$$\frac{d}{dz} (\tilde{I}_n(z,s)) = -(\tilde{Y}'_{n,m}(s)) \cdot (\tilde{V}_n(z,s)) \quad (3.90)$$

$$\frac{d}{dz} (\tilde{V}_n(z,s)) = -(\tilde{Z}'_{n,m}(s)) \cdot (\tilde{I}_n(z,s))$$

Comparing these to the above modal expansions of the derivatives we have first, considering the current derivative

$$\begin{aligned} &- \left\{ \sum_{\delta} \tilde{\gamma}_{\delta}(s) e^{-\tilde{\gamma}_{\delta}(s)z} (\tilde{I}_{c_n}(s))_{\delta} (\tilde{v}_{c_n}(s))_{\delta} \right\} \cdot (\tilde{Y}_{c_{n,m}}(s)) \cdot (\tilde{V}_n(0,s)) \\ &= - \left\{ \sum_{\delta} \tilde{\gamma}_{\delta}(s) e^{-\tilde{\gamma}_{\delta}(s)z} (\tilde{I}_{c_n}(s))_{\delta} (\tilde{I}_{c_n}(s))_{\delta} \right\} \cdot (\tilde{V}_n(0,s)) \\ &= -(\tilde{Y}'_{n,m}(s)) \cdot (\tilde{V}_n(z,s)) \end{aligned} \quad (3.91)$$

Evaluating this at  $z=0$  and noting that  $(\tilde{V}_n(0,s))$  is an arbitrary N vector, we have

$$(\tilde{Y}'_{n,m}(s)) = \sum_{\delta} \tilde{\gamma}_{\delta}(s) (\tilde{I}_{c_n}(s))_{\delta} (\tilde{I}_{c_n}(s))_{\delta} \quad (3.92)$$

Similarly, using the voltage derivative equations

$$\begin{aligned}
& - \left\{ \sum_{\delta} \tilde{Y}_{\delta}(s) e^{-\tilde{Y}_{\delta}(s)z} (\tilde{v}_{c_n}(s))_{\delta} (\tilde{I}_{c_n}(s))_{\delta} \right\} \cdot (\tilde{Z}_{c_{n,m}}(s)) \cdot (\tilde{I}_n(0,s)) \\
& = - \left\{ \sum_{\delta} \tilde{Y}_{\delta}(s) e^{-\tilde{Y}_{\delta}(s)z} (\tilde{v}_{c_n}(s))_{\delta} (\tilde{v}_{c_n}(s))_{\delta} \right\} \cdot (\tilde{I}_n(0,s)) \\
& = (\tilde{Z}'_{n,m}(s)) \cdot (\tilde{I}_n(z,s))
\end{aligned} \tag{3.93}$$

Evaluating this at  $z=0$  and noting that  $(\tilde{I}_n(0,s))$  is an arbitrary  $N$  vector, we have

$$(\tilde{Z}'_{n,m}(s)) = \sum_{\delta} \tilde{Y}_{\delta}(s) (\tilde{v}_{c_n}(s))_{\delta} (\tilde{v}_{c_n}(s))_{\delta} \tag{3.94}$$

Note now that (3.92) explicitly illustrates that  $(\tilde{Y}'_{n,m}(s))$  is symmetric and (3.94) does the same for  $(\tilde{Z}'_{n,m}(s))$ , i.e.,

$$\begin{aligned}
(\tilde{Z}'_{n,m}(s))^T &= (\tilde{Z}'_{n,m}(s)) \\
(\tilde{Y}'_{n,m}(s))^T &= (\tilde{Y}'_{n,m}(s))
\end{aligned} \tag{3.95}$$

As in (3.84) for the characteristic impedance and admittance matrices, this symmetry is a statement of reciprocity for the impedance and admittance per-unit-length matrices. While this was not explicitly assumed at the start, it is a consequence of the development. This may be associated with the assumed diagonalization characteristics of the propagation matrix. Then let us consider the reciprocity (symmetry) of the impedance and admittance per-unit-length matrices as one of our assumptions for the present development.

Taking (3.94) and left or right dot multiplying by a current eigenmode, we have

$$\begin{aligned}
\tilde{Y}_{\delta}(s) (\tilde{v}_{c_n}(s))_{\delta} &= (\tilde{Z}'_{n,m}(s)) \cdot (\tilde{I}_{c_n}(s))_{\delta} \\
&= (\tilde{I}_{c_n}(s))_{\delta} \cdot (\tilde{Z}'_{n,m}(s))
\end{aligned} \tag{3.96}$$

A dot product with the  $\delta'$ -th current mode gives

$$\tilde{Y}_\delta(s) 1_{\delta,\delta'} = (\tilde{I}_{c_n}(s))_\delta \cdot (\tilde{Z}'_{n,m}(s)) \cdot (\tilde{I}_{c_n}(s))_{\delta'} \quad (3.97)$$

Given  $\tilde{Y}_\delta(s)$  this normalizes the  $(\tilde{I}_{c_n}(s))_\delta$  in terms of  $(\tilde{Z}'_{n,m}(s))$ . Note also the relationship of the voltage and current modes via  $(\tilde{Z}'_{n,m}(s))$  and  $\tilde{Y}_\delta(s)$ .

Similarly, dot multiplying (3.92) on left or right by a voltage eigenmode gives

$$\begin{aligned} \tilde{Y}_\delta(s) (i_{c_n}(s))_\delta &= (\tilde{Y}'_{n,m}(s)) \cdot (\tilde{v}_{c_n}(s))_\delta \\ &= (\tilde{v}_{c_n}(s))_\delta \cdot (\tilde{Y}'_{n,m}(s)) \end{aligned} \quad (3.98)$$

A dot product with the  $\delta'$ -th voltage mode gives

$$\tilde{Y}_\delta(s) 1_{\delta,\delta'} = (\tilde{v}_{c_n}(s))_\delta \cdot (\tilde{Y}'_{n,m}(s)) \cdot (\tilde{v}_{c_n}(s))_{\delta'} \quad (3.99)$$

This normalizes the  $(\tilde{v}_{c_n}(s))_\delta$  in terms of  $(\tilde{Y}'_{n,m}(s))$  and the  $\tilde{Y}_\delta(s)$ . Note also the relationship of the voltage and current modes via  $(\tilde{Y}'_{n,m}(s))$  and  $\tilde{Y}_\delta(s)$ .

## 5. Termination condition of a tube

A transmission line is usually terminated at the two ends  $z=0$  and  $z=L$ . The termination could be a lumped impedance, a distributed network, open-circuit or short-circuit. If sources are included, these conditions can be represented by a generalized Thévenin equivalent network or a generalized Norton equivalent network.

Passive terminations can be specified as an impedance matrix  $(\tilde{Z}_{T,n,m}(z,s))$  or an admittance matrix  $(\tilde{Y}_{T,n,m}(z,s))$  where  $z=0$  or  $L$ . The condition  $(\tilde{Z}_{T,n,m}(L,s)) = (\tilde{Z}_{c_n,m}(s))$ , or equivalently  $(\tilde{Y}_{T,n,m}(L,s)) = (\tilde{Y}_{c_n,m}(s))$  specifies a perfectly matched line and the transmission line behaves like a semi-infinite line for  $0 \leq z \leq L$  (with an equivalent single end at  $z=0$ ).

Alternatively, the terminating conditions can be specified by scattering matrices  $(\tilde{S}_{n,m}(z,s))$  where  $z=0$  or  $L$ . Consider at  $z=L$  (see Figure 3.1); let the incoming waves be designated by a superscript  $-$  and the outgoing waves  $+$ . The scattering matrix is defined by

$$(\tilde{W}_n^{(+)}(s)) = (\tilde{S}_{n,m}(z,s)) \cdot (\tilde{W}_n^{(-)}(s)) \quad (3.100)$$

For the case illustrated in Figure 3.1, one observes that if this termination is taken as  $z=L$ , then

$$\begin{aligned} (\tilde{W}_n^{(+)}(s)) &= (\tilde{V}_n(L,s))_- \\ (\tilde{W}_n^{(-)}(s)) &= (\tilde{V}_n(L,s))_+ \end{aligned} \quad (3.101)$$

One can then rewrite (3.94) as

$$(\tilde{V}_n(L,s))_- = (\tilde{S}_{n,m}(L,s)) \cdot (\tilde{V}_n(L,s))_+ \quad (3.102)$$

which in this terminating case is the same as the definition of a reflection matrix given by

$$(\tilde{S}_{n,m}(L,s)) = [(\tilde{Z}_{T,n,m}(L,s)) + (\tilde{Z}_{c,n,m}(s))]^{-1} \cdot [(\tilde{Z}_{T,n,m}(L,s)) - (\tilde{Z}_{c,n,m}(s))] \quad (3.103)$$

Similarly, at  $z=0$  the termination conditions are

$$(\tilde{V}_n(0,s))_+ = (\tilde{S}_{n,m}(0,s)) \cdot (\tilde{V}_n(0,s))_- \quad (3.104)$$

and

$$(\tilde{S}_{n,m}(0,s)) = [(\tilde{Z}_{T,n,m}(0,s)) + (\tilde{Z}_{c,n,m}(s))]^{-1} \cdot [(\tilde{Z}_{T,n,m}(0,s)) - (\tilde{Z}_{c,n,m}(s))] \quad (3.105)$$

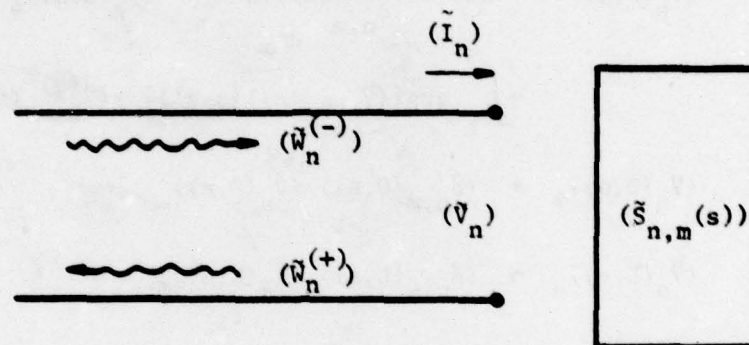


Figure 3.1. Incoming and outgoing wave at a junction

## 6. Solution of combined voltages

Combination of (3.58), (3.102) and (3.104) gives the solution of the combined voltage equation. Rewriting these equations

$$\begin{aligned}
 (\tilde{V}_n(z,s))_+ &= \exp \{ - (\tilde{\gamma}_{c_{n,m}}(s)z) \cdot (\tilde{V}_n(0,s))_+ \\
 &\quad + \int_0^z \exp \{ - (\tilde{\gamma}_{c_{n,m}}(s))[z-z'] \} \cdot (\tilde{V}_n^{(s)'}(z',s))_+ dz' \\
 (\tilde{V}_n(z,s))_- &= \exp \{ (\tilde{\gamma}_{c_{n,m}}(s))[z-L] \} \cdot (\tilde{V}_n(L,s))_- \\
 &\quad + \int_L^z \exp \{ (\tilde{\gamma}_{c_{n,m}}(s))[z-z'] \} \cdot (\tilde{V}_n^{(s)'}(z',s))_- dz' \\
 (\tilde{V}_n(0,s))_+ &= (\tilde{S}_{n,m}(0,s)) \cdot (\tilde{V}_n(0,s))_- \\
 (\tilde{V}_n(L,s))_- &= (\tilde{S}_{n,m}(L,s)) \cdot (\tilde{V}_n(L,s))_+
 \end{aligned} \tag{3.106}$$

These equations can be solved by substitutions, or can be arranged in a matrix form, as described later in the BLT equation. As written here, these correspond to the special case of a transmission-line network consisting of two junctions (or terminations) connected by a single tube.

## 7. Reconstruction of total voltages and total currents

Once the combined voltages are evaluated, the total voltages and total currents are readily obtained.

From (3.18), one obtains

$$\begin{aligned}
 (\tilde{V}_n(z,s)) &= \frac{1}{2} [(\tilde{V}_n(z,s))_+ + (\tilde{V}_n(z,s))_-] \\
 (\tilde{I}_n(z,s)) &= \frac{1}{2} (\tilde{\gamma}_{c_{n,m}}(s)) \cdot [(\tilde{V}_n(z,s))_+ - (\tilde{V}_n(z,s))_-]
 \end{aligned} \tag{3.107}$$

Hence, if one knows  $(\tilde{V}_n(z,s))_+$  and  $(\tilde{V}_n(z,s))_-$  for a given tube, as well as  $(\tilde{Y}_{cn,m}(s))$  or  $(\tilde{Z}_{cn,m}(s))$  (being measurable or conceivably even calculable), then the measurable voltage and current vectors are directly reconstructable.

#### D. Sign Convention of $q$

It is noted that in the definitions of the combined voltage, the convention  $q = +1$  is chosen to represent the wave propagating from  $z=0$  to  $z=L$ . Correspondingly,  $q = -1$  represents the wave propagating from  $z=L$  to  $z=0$ .

Let us further denote the above quantities with a subscript  $u$ , i.e.,  $q_u = +1$  corresponds to wave propagating from left to right, i.e., from  $z_u = 0$  to  $z_u = L$ . This is shown in Figure 3.2.

It is also permissible to choose, on the same tube, a different convention. Let  $z_v = L - z_u$  be a new coordinate, as shown in Figure 3.2. The new  $q$  convention,  $q_v$ , is now opposite to  $q_u$ . Here,  $q_v = +1$  corresponds to a wave traveling from right to left (i.e.,  $z_v = 0$  to  $z_v = L$ ).

This convention will prove useful and is recalled in deriving the BLT equation.

The subsequent sections deal with multitube multiconductor transmission-line networks. More general notations, primarily in the form of additional subscripts denoting either the tube or the junction, are used.

#### E. Summary

Since there are so many expressions, relations, etc., introduced in this section, it is useful to summarize them in tabular form, as presented in Tables 3.1-4.

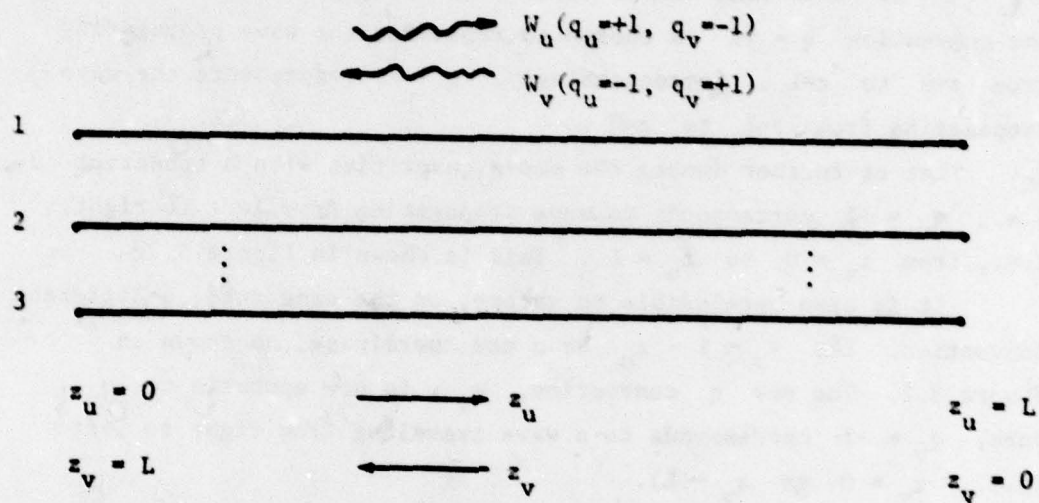


Figure 3.2 Left and right traveling waves

Table 3.1 Transmission-Line Equations

Name	Symbol	Relation
Trans. line eqns. (telegrapher eqns.)		$\frac{d}{dz} (\tilde{V}_n(z,s)) = -(\tilde{Z}'_{n,m}(s)) \cdot (\tilde{I}_n(z,s)) + (\tilde{V}_n^{(s)})'(z,s)$ $\frac{d}{dz} (\tilde{I}_n(z,s)) = -(\tilde{Y}'_{n,m}(s)) \cdot (\tilde{V}_n(z,s)) + (\tilde{I}_n^{(s)})'(z,s)$
Combined Voltage Vector	$(\tilde{V}_n(z,s))_q$	$= (\tilde{V}_n(z,s)) + q(\tilde{Z}_{c,n,m}(s)) \cdot (\tilde{I}_n(z,s))$
Combined Per-Unit-Length Source Vector	$(\tilde{V}_n^{(s)})'(z,s)_q$	$= (\tilde{V}_n^{(s)})'(z,s) + q(\tilde{Z}_{c,n,m}(s)) \cdot (\tilde{I}_n(z,s))$
Voltage Vector Reconstruction	$(\tilde{V}_n(z,s))$	$= \frac{1}{2} [(\tilde{V}_n(z,s))_+ + (\tilde{V}_n(z,s))_-]$
Current Vector Reconstruction	$(\tilde{I}_n(z,s))$	$= \frac{1}{2} (\tilde{Y}_{c,n,m}(s)) \cdot [(\tilde{V}_n(z,s))_+ - (\tilde{V}_n(z,s))_-]$
Separation Index	$q$	$= \pm 1$
Combined Voltage Equation		$\left[ (\tilde{I}_{n,m}) \frac{d}{dz} + q(\tilde{Y}_{c,n,m}(s)) \right] \cdot (\tilde{V}_n(z,s))_q = (\tilde{V}_n^{(s)})'(z,s)_q$
Propagation Matrix	$(\tilde{Y}_{c,n,m}(s))$	$= [(\tilde{Z}'_{n,m}(s)) \cdot (\tilde{Y}'_{n,m}(s))]^{\frac{1}{2}} \text{ (principal or p.r. value)}$
Characteristic Impedance Matrix	$(\tilde{Z}_{c,n,m}(s))$	$= (\tilde{Y}_{c,n,m}(s)) \cdot (\tilde{Y}'_{n,m}(s))^{-1} = (\tilde{Y}_{c,n,m}(s))^{-1} \cdot (\tilde{Z}'_{n,m}(s))$
Characteristic Admittance Matrix	$(\tilde{Y}_{c,n,m}(s))$	$= (\tilde{Z}_{c,n,m}(s))^{-1} = (\tilde{Y}'_{n,m}(s)) \cdot (\tilde{Y}_{c,n,m}(s))^{-1}$ $= (\tilde{Z}'_{n,m}(s))^{-1} \cdot (\tilde{Y}_{c,n,m}(s))$
General Solution (referenced to arbitrary position $z_0$ )	$(\tilde{V}_n(z,s))_q$	$= \exp \left\{ -q(\tilde{Y}_{c,n,m}(s)) [z-z_0] \right\} \cdot (\tilde{V}_n(z_0,s))_q$ $+ \int_{z_0}^z \exp \left\{ -q(\tilde{Y}_{c,n,m}(s)) [z-z'] \right\} \cdot (\tilde{V}_n^{(s)})'(z',s)_q dz'$
Solution for tube $0 \leq z \leq L$ in terms of boundary values	$\left\{ \begin{array}{l} + \text{ or right wave } (\tilde{V}_n(z,s))_+ \\ - \text{ or left wave } (\tilde{V}_n(z,s))_- \end{array} \right.$	$= \exp \left\{ -(\tilde{Y}_{c,n,m}(s))z \right\} \cdot (\tilde{V}_n(0,s))_+ +$ $+ \int_0^z \exp \left\{ -(\tilde{Y}_{c,n,m}(s)) [z-z'] \right\} \cdot (\tilde{V}_n^{(s)})'(z',s)_+ dz'$ $= \exp \left\{ (\tilde{Y}_{c,n,m}(s)) [z-L] \right\} \cdot (\tilde{V}_n(L,s))_-$ $+ \int_L^z \exp \left\{ (\tilde{Y}_{c,n,m}(s)) [z-z'] \right\} \cdot (\tilde{V}_n^{(s)})'(z',s)_- dz'$

Table 3.2 Diagonalization of Propagation Matrix

Name	Symbol	Relation
Square of Propagation Matrix	$(\tilde{\gamma}_{c_{n,m}}(s))^2$	$= (\tilde{\gamma}'_{n,m}(s)) \cdot (\tilde{\gamma}'_{n,m}(s))$
Normalized Voltage Eigenvector	$(\tilde{v}_c(s))_\delta$	$(\tilde{\gamma}_{c_{n,m}}(s))^2 \cdot (\tilde{v}_c(s))_\delta = \tilde{\gamma}_\delta^2(s) (\tilde{v}_c(s))_\delta$
Normalized Current Eigenvector	$(\tilde{i}_c(s))_\delta$	$(\tilde{i}_c(s))_\delta \cdot (\tilde{\gamma}_{c_{n,m}}(s))^2 = \tilde{\gamma}_\delta^2(s) (\tilde{i}_c(s))_\delta$
Eigenvalue of Propagation Matrix	$\tilde{\gamma}_\delta(s)$	$= [\tilde{\gamma}_\delta^2(s)]^{1/2}$ (principal or p.r. value assumed)
Eigenindex	$\delta$	$= 1, 2, \dots, N$ ( $N \times N$ matrices)
Biorthonormal Property (used for normalization)		$(\tilde{v}_c(s))_\delta \cdot (\tilde{i}_c(s))_{\delta'} = 1_{\delta, \delta'}$ (N independent eigenvectors assumed of both voltage and current types)
Function of Propagation Matrix	$F(\tilde{\gamma}_{c_{n,m}}(s))$	$= \sum_{\delta} F(\tilde{\gamma}_\delta(s)) (\tilde{v}_c(s))_\delta (\tilde{i}_c(s))_\delta$
Special Cases	Propagation Matrix $(\tilde{\gamma}_{c_{n,m}}(s))$	$= \sum_{\delta} \tilde{\gamma}_\delta(s) (\tilde{v}_c(s))_\delta (\tilde{i}_c(s))_\delta$
	Transpose $(\tilde{\gamma}_{c_{n,m}}(s))^T$	$= \sum_{\delta} \tilde{\gamma}_\delta(s) (\tilde{i}_c(s))_\delta (\tilde{v}_c(s))_\delta$
Special Cases	Inverse $(\tilde{\gamma}_{c_{n,m}}(s))^{-1}$	$= \sum_{\delta} \tilde{\gamma}_\delta^{-1}(s) (\tilde{v}_c(s))_\delta (\tilde{i}_c(s))_\delta$
	Identity $(1_{n,m})$	$= (\tilde{\gamma}_{n,m}(s))^0 = \sum_{\delta} (\tilde{v}_c(s))_\delta (\tilde{i}_c(s))_\delta$ $= \sum_{\delta} (\tilde{i}_c(s))_\delta (\tilde{v}_c(s))_\delta$

Table 3.3 Normalization of Voltage and Current Eigenmodes

Name	Symbol	Relation
Normalization via Characteristic Impedance and Admittance Matrices	Interrelation of voltage and current eigenmodes	$(\tilde{v}_{c_n}(s))_\delta = (\tilde{Z}_{c_{n,m}}(s)) \cdot (\tilde{i}_{c_n}(s))_\delta = (\tilde{i}_{c_n}(s))_\delta \cdot (\tilde{Z}_{c_{n,m}}(s))$
		$(\tilde{i}_{c_n}(s))_\delta = (\tilde{Y}_{c_{n,m}}(s)) \cdot (\tilde{v}_{c_n}(s))_\delta = (\tilde{v}_{c_n}(s))_\delta \cdot (\tilde{Y}_{c_{n,m}}(s))$
	Separate voltage and current eigenmode normalization	$1_{\delta,\delta} = (\tilde{i}_{c_n}(s))_\delta \cdot (\tilde{Z}_{c_{n,m}}(s)) \cdot (\tilde{i}_{c_n}(s))_\delta$
		$1_{\delta,\delta} = (\tilde{v}_{c_n}(s))_\delta \cdot (\tilde{Y}_{c_{n,m}}(s)) \cdot (\tilde{v}_{c_n}(s))_\delta$
Normalization via Per-Unit-Length Impedance and Admittance Matrices	Interrelation of voltage and current eigenmodes	$\tilde{y}_\delta(s) (\tilde{v}_{c_n}(s))_\delta = (\tilde{Z}'_{n,m}(s)) \cdot (\tilde{i}_{c_n}(s))_\delta = (\tilde{i}_{c_n}(s))_\delta \cdot (\tilde{Z}'_{n,m}(s))$
		$\tilde{y}_\delta(s) (\tilde{i}_{c_n}(s))_\delta = (\tilde{Y}'_{n,m}(s)) \cdot (\tilde{v}_{c_n}(s))_\delta = (\tilde{v}_{c_n}(s))_\delta \cdot (\tilde{Y}'_{n,m}(s))$
	Separate voltage and current eigenmode normalization	$1_{\delta,\delta} = \tilde{y}_\delta^{-1}(s) (\tilde{i}_{c_n}(s))_\delta \cdot (\tilde{Z}'_{n,m}(s)) \cdot (\tilde{i}_{c_n}(s))_\delta$
		$1_{\delta,\delta} = \tilde{y}_\delta^{-1}(s) (\tilde{v}_{c_n}(s))_\delta \cdot (\tilde{Y}'_{n,m}(s)) \cdot (\tilde{v}_{c_n}(s))_\delta$

Table 3.4 Representation of Other Matrices in Terms of Voltage and Current Normalized Eigenmodes (indicating assumed reciprocity)

Name	Symbol	Relation
Characteristic Impedance Matrix	$(\tilde{Z}_{c_{n,m}}(s))$	$= \sum_{\delta} (\tilde{v}_{c_n}(s))_\delta (\tilde{v}_{c_n}(s))_\delta$
Characteristic Admittance Matrix	$(\tilde{Y}_{c_{n,m}}(s))$	$= \sum_{\delta} (\tilde{i}_{c_n}(s))_\delta (\tilde{i}_{c_n}(s))_\delta$
Per-Unit-Length Impedance Matrix	$(\tilde{Z}'_{n,m}(s))$	$= \sum_{\delta} \tilde{y}_\delta(s) (\tilde{v}_{c_n}(s))_\delta (\tilde{v}_{c_n}(s))_\delta$
Per-Unit-Length Admittance Matrix	$(\tilde{Y}'_{n,m}(s))$	$= \sum_{\delta} \tilde{y}_\delta(s) (\tilde{i}_{c_n}(s))_\delta (\tilde{i}_{c_n}(s))_\delta$

## References

- [3.1] C. R. Paul, "Efficient Numerical Computation of the Frequency Response of Cables Illuminated by an Electromagnetic Field," IEEE Trans. on Microwave Theory and Technique, vol. MTT-22, pp. 456-457, April 1974.
- [3.2] E. A. Guillemin, The Mathematics of Circuit Analysis. MIT Press, 1949.
- [3.3] C. E. Baum, "On the Eigenmode Expansion Method for Electromagnetic Scattering and Antenna Problems, Part I: Some Basic Relations for Eigenmode Expansions and Their Relation to the Singularity Expansion," Interaction Note 229, January 1975.
- [3.4] E.A. Coddington and H. Levinson, Theory of Ordinary Differential Equations, McGraw-Hill, 1965.

## IV. SUPERMATRICES AND SUPERVECTORS

Define a supermatrix, or more specifically, a dimatrix or tensor of rank four, as a partitioned matrix or matrix of matrices in the form

$$((D_{n,m})_{u,v}) \quad (4.1)$$

with elementary matrices or blocks

$$(D_{n,m})_{u,v} \quad (4.2)$$

and elements

$$D_{n,m;u,v} \quad (4.3)$$

such that the blocks or elementary matrices are  $N_u \times M_v$ , i.e.,

$$\begin{aligned} n &= 1, 2, \dots, N_u \\ m &= 1, 2, \dots, M_v \end{aligned} \quad (4.4)$$

and the dimatrix is  $N \times N$ , i.e.,

$$\begin{aligned} u &= 1, 2, \dots, N \\ v &= 1, 2, \dots, M \end{aligned} \quad (4.5)$$

Note that this corresponds to a matrix with

$$\begin{aligned} \sum_{n=1}^N N_u & \text{ rows} \\ \sum_{v=1}^M M_v & \text{ columns} \end{aligned} \quad (4.6)$$

which has been partitioned into blocks or elementary matrices by a partitioning of the row and column indices. Pictorially this corresponds to drawing horizontal and vertical lines completely through the matrix between selected adjacent rows and selected adjacent columns.

For our purposes, the dimatrices will be square, i.e.,

$$N = M \quad (4.7)$$

Furthermore, the partitioning will be symmetric, i.e.,

$$N_u = M_v \quad \text{for } u = v \quad (4.8)$$

Hence the diagonal blocks

$$(D_{n,m})_{u,u}, \text{ size } N_u \times N_u \quad (4.9)$$

are square and off-diagonal blocks are symmetrically rectangular, i.e.,

$$(D_{n,m})_{u,v}, \text{ size } N_u \times N_v \quad (4.10)$$

$$(D_{n,m})_{v,u}, \text{ size } N_v \times N_u$$

Supervectors or divectors are similarly defined in the form

$$((V_n)_u) \quad (4.11)$$

with elementary vectors as

$$(V_n)_u$$

$$n = 1, 2, \dots, N_u \quad (4.12)$$

$$u = 1, 2, \dots, N$$

remembering that  $n, m$  and  $u, v$  are merely dummy indices. Note that the elements are designated as

$$V_{n;u} \quad (\text{not } V_{n,u}) \quad (4.13)$$

Define supermatrix multiplication in the dot product or contraction sense as

$$\begin{aligned} ((A_{n,m})_{u,v}) : ((B_{n,m})_{u,v}) \\ &= \left( \sum_{u'=1}^N (A_{n,m})_{u,u'} (B_{n,m})_{u',v} \right) \\ &= \left( \left( \sum_{u'=1}^N \sum_{n'=1}^{N_{u'}} A_{n,n';u,u'} B_{n',m;u',v} \right) \right) \\ &= ((C_{n,m})_{u,v}) \end{aligned} \quad (4.14)$$

Here we note contraction is done twice involving the second indices of the two pairs of indices for the first matrix, and the first indices of the two pairs of indices for the second matrix; this is denoted by two levels of dot product : , noting the two dots one above the other.

In (4.14) the two dimatrices are not necessarily square. It is merely required that the second indices  $m, v$  of the first dimatrix have the same range (hence same partitioning) as the first indices of the second dimatrix. Two dimatrices with this property are said to be of compatible order, for multiplication in the double dot product sense in this case, with order of multiplication specified.

In the present note all dimatrices are taken as being of symmetric compatible order, i.e., (4.7,8) apply and  $N$  and the  $N_u$  have the same values for all dimatrices in the particular discussion (i.e., describing a given physical situation). Furthermore, the divectors are also taken as having the same compatible order. Thus we can form any such operations as

$$\begin{aligned}
 ((A_{n,m})_{u,v}) + ((B_{n,m})_{u,v}) & \quad \text{dimatrix} \\
 ((A_{n,m})_{u,v}) : ((B_{n,m})_{u,v}) & \quad \text{dimatrix} \\
 ((B_{n,m})_{u,v}) : ((A_{n,m})_{u,v}) & \quad \text{dimatrix} \\
 ((A_{n,m})_{u,v}) : ((V_n)_u) & \quad \text{divector} \\
 ((V_n)_u) : ((A_{n,m})_{u,v}) & \quad \text{divector} \\
 ((V_n)_u) : ((W_n)_u) & \quad \text{scalar}
 \end{aligned}
 \tag{4.15}$$

where dimatrix-divector and divector-divector multiplication in the double dot product sense are obvious specializations of (4.14).

## V. IDENTITY SUPERMATRIX

Before continuing the supermatrices of the previous sections to yield an equation, it is necessary to define an identity supermatrix

$$((l_{n,m})_{u,v}) .$$

The identity supermatrix is such that its diagonal element matrices are all identity matrices, and all off-diagonal element matrices are zero matrices, i.e.,

$$(l_{n,m})_{u,v} = l_{u,v} (l_{n,m})$$

$$l_{n,m} = \begin{cases} 1 & \text{for } n=m \\ 0 & \text{for } n \neq m \end{cases} \quad (5.1)$$

involving Kronecker deltas. The individual elements can be written as

$$l_{n,m;u,v} = \begin{cases} 1 & \text{for both } n=m \text{ and } u=v \\ 0 & \text{for either } n \neq m \text{ or } u \neq v \end{cases} \quad (5.2)$$

as a sort of super Kronecker delta or superidentity element. Note the identity supermatrix is then a symmetric dimatrix as in (4.7,8).

For a supermatrix  $((M_{n,m})_{u,v})$  of symmetric compatible order, then

$$((l_{n,m})_{u,v}) : ((M_{n,m})_{u,v}) = ((M_{n,m})_{u,v}) : ((l_{n,m})_{u,v}) = ((M_{n,n})_{u,v}) \quad (5.3)$$

Also, an inverse  $((M_{n,m})_{u,v})^{-1}$  of  $((M_{n,m})_{u,v})$  exists such that

$$((M_{n,m})_{u,v})^{-1} : ((M_{n,m})_{u,v}) = ((M_{n,m})_{u,v}) : ((M_{n,m})_{u,v})^{-1}$$

$$= ((l_{n,m})_{u,v}) \quad (5.4)$$

provided

$$\det[(M_{n,n})_{u,v}] \neq 0 \quad (5.5)$$

Note that  $((M_{n,m})_{u,v})^{-1}$  is of symmetric compatible order with  $((M_{n,m})_{u,v})$ .

## VI. SCATTERING SUPERMATRIX

The concept of scattering matrices introduced in Section III for a terminated tube is extended here for junctions where more than one tube is connected. Collections and suitable ordering of scattering matrices at all junctions of the transmission-line network form a scattering supermatrix.

### A. Junction Scattering Supermatrix

Consider the  $v$ th junction  $J_v$  with tube ends denoted by  $J_{v;r}$  with index  $r$  as discussed in subsection IID. Let this junction be characterized by an impedance matrix

$$(\tilde{Z}_{n,m}(s))_v = (\tilde{Y}_{n,m}(s))_v^{-1} \quad (6.1)$$

The junction scattering matrix is defined so that

$$(\tilde{V}_n(s))_{v,+} = (\tilde{S}_{n,m}(s))_v \cdot (\tilde{V}_n(s))_{v,-} \quad (6.2)$$

where the subscripts  $+$  and  $-$  refer to the aggregate of respectively outgoing and incoming waves ( $N$ -waves) on the various tubes in the form of combined voltage vectors; remember that the current convention for outgoing waves is positive direction outward, and for incoming waves is positive direction inward.

In the supermatrix form partition according to waves on the  $r_v$  tube ends connected to  $J_v$  as

$$\begin{aligned} ((\tilde{V}_n^{(0)}(s))_r)_v &= ((\tilde{Z}_{n,m}(s))_{r,r'})_v : ((\tilde{I}_n^{(0)}(s))_r)_v \\ ((\tilde{Y}_{n,m}(s))_{r,r'})_v &\equiv ((\tilde{Z}_{n,m}(s))_{r,r'})_v^{-1} \end{aligned} \quad (6.3)$$

where

$$(\tilde{V}_n^{(0)}(s))_{r;v}, (\tilde{I}_n^{(0)}(s))_{r;v} \quad (6.4)$$

$$r = 1, 2, \dots, r$$

are the voltage and current vectors on the  $r$ th tube ends at  $J_v$  with current convention into  $J_v$ .

The tube associated with the  $r$ th tube end at  $J_v$  has characteristic impedance and admittance matrices which can be put in supermatrix form for  $J_v$  as

$$(\tilde{Z}_{c,n,m}(s))_{r,r'}_v \equiv \begin{array}{l} \text{tube-end characteristic-impedance} \\ \text{supermatrix for } J_v \end{array}$$

$$(\tilde{Y}_{c,n,m}(s))_{r,r'}_v \equiv \begin{array}{l} \text{tube-end characteristic-admittance} \\ \text{supermatrix for } J_v \end{array}$$

$$= ((\tilde{Z}_{c,n,m}(s))_{r,r'}_v)^{-1} \quad (6.5)$$

where

$$(\tilde{Z}_{c,n,m}(s))_{r,r'}_v \equiv \begin{cases} \text{characteristic-impedance matrix for } r\text{th tube} \\ \text{end at } J_v \text{ for } r=r' \text{ (square)} \\ (0_{n,m}) \text{ for } r \neq r' \text{ (rectangular)} \end{cases}$$

$$(\tilde{Y}_{c,n,m}(s))_{r,r'}_v \equiv \begin{cases} \text{characteristic-admittance matrix for } r\text{th tube end at} \\ J_v \text{ for } r=r' \text{ (square)} \\ (0_{n,m}) \text{ for } r \neq r' \text{ (rectangular)} \end{cases}$$

$$(\tilde{Y}_{c,n,m}(s))_{r,r;v} = (\tilde{Z}_{c,n,m}(s))_{r,r;v}^{-1} \quad (6.6)$$

Thus, these impedance and admittance supermatrices for the tube ends at a given junction are block diagonal and may be represented in terms of the direct sum  $\oplus$  as

$$\begin{aligned}
 ((\tilde{Z}_{c_{n,m}}(s))_{r,r'})_v &\equiv (\tilde{Z}_{c_{n,m}}(s))_{1,1;v} \oplus (\tilde{Z}_{c_{n,m}}(s))_{2,2;v} \oplus \dots \oplus (\tilde{Z}_{c_{n,m}}(s))_{r_v,r_v;v} \\
 &\equiv \bigoplus_{r=1}^{r_v} (\tilde{Z}_{c_{n,m}}(s))_{r,r;v} \\
 ((\tilde{Y}_{c_{n,m}}(s))_{r,r'})_v &\equiv (\tilde{Y}_{c_{n,m}}(s))_{1,1;v} \oplus (\tilde{Y}_{c_{n,m}}(s))_{2,2;v} \oplus \dots \oplus (\tilde{Y}_{c_{n,m}}(s))_{r_v,r_v;v} \\
 &\equiv \bigoplus_{r=1}^{r_v} (\tilde{Y}_{c_{n,m}}(s))_{r,r;v}
 \end{aligned} \tag{6.7}$$

where the convention used here is to maintain the partitioning according to the two pairs of indices  $(n,m)$  and  $(r,r')$  instead of combining them in one pair as in a regular matrix (or monomatrix). Note the subscript  $v$  on the supermatrices; the elementary matrices are also identified with  $v$  and the  $r,r'$  indices range over the tube ends at  $J_v$ , not over the wave indices  $u,v$ .

The scattering supermatrix for  $J_v$  is defined by

$$\begin{aligned}
 ((\tilde{V}_n(s))_r)_{v,+} &\equiv ((\tilde{S}_{n,m}(s))_{r,r'})_v : ((\tilde{V}_n(s))_r)_{v,-} \\
 ((\tilde{V}_n(s))_r)_{v,+} &\equiv ((\tilde{V}_n^{(0)}(s))_r)_v - ((\tilde{Z}_{c_{n,m}}(s))_{r,r'})_v : ((\tilde{I}_n^{(0)}(s))_r)_v \\
 &\equiv \text{outgoing wave supervector at } J_v \\
 ((\tilde{V}_n(s))_r)_{v,-} &\equiv ((\tilde{V}_n^{(0)}(s))_r)_v + ((\tilde{Z}_{c_{n,m}}(s))_{r,r'})_v : ((\tilde{I}_n^{(0)}(s))_r)_v \\
 &\equiv \text{incoming wave supervector at } J_v
 \end{aligned} \tag{6.8}$$

Again note that the  $J_V$  current convention is positive current into  $J_V$  so that the usual Ohm's law convention in (6.3) holds for  $J_V$ . Solving (6.8) for the voltage and current supervectors at  $J_V$

$$\begin{aligned} ((\tilde{V}_n^{(0)}(s))_r)_V &= \frac{1}{2} [((\tilde{V}_n(s))_r)_{V,+} + ((\tilde{V}_n(s))_r)_{V,-}] \\ ((\tilde{I}_n^{(0)}(s))_r) &= \frac{1}{2} ((\tilde{Y}_{c_{n,m}}(s))_{r,r'})_V : [((\tilde{V}_n^{(0)}(s))_r)_{V,-} - ((\tilde{V}_n^{(0)}(s))_r)_{V,+}] \end{aligned} \quad (6.9)$$

Now we can compute the junction scattering supermatrix for  $J_V$  by combining (6.8) and (6.9) with (6.3) to give

$$\begin{aligned} ((\tilde{S}_{n,m}(s))_{r,r'})_V &= [((\tilde{Z}_{n,m}(s))_{r,r'})_V : ((\tilde{Y}_{c_{n,m}}(s))_{r,r'})_V + ((1_{n,m})_{r,r'})_V]^{-1} \\ &\quad : [((\tilde{Z}_{n,m}(s))_{r,r'})_V : ((\tilde{Y}_{c_{n,m}}(s))_{r,r'})_V - ((1_{n,m})_{r,r'})_V] \\ &= [((1_{n,m})_{r,r'})_V + ((\tilde{Z}_{c_{n,m}}(s))_{r,r'})_V : ((\tilde{Y}_{n,m}(s))_{r,r'})_V]^{-1} \\ &\quad : [((1_{n,m})_{r,r'})_V - ((\tilde{Z}_{c_{n,m}}(s))_{r,r'})_V : ((\tilde{Y}_{n,m}(s))_{r,r'})_V] \end{aligned} \quad (6.10)$$

Note the identity supermatrix corresponding to  $J_V$ ; it is of course partitioned in the same symmetric compatible order as are the various impedance and admittance supermatrices and the scattering supermatrix for  $J_V$ .

For the junction  $J_V$  let the  $r$ th tube end have  $N_{V;r}$  conductors (plus the reference) so that the wave on this tube end is a vector of dimension  $N_{V;r}$ . The supervectors then have dimension for  $J_V$  as

$$N_V = \sum_{r=1}^{I_V} N_{V;r} \quad (6.11)$$

The associated supermatrices are  $r_V \times r_V$  in terms of the blocks or elementary matrices; the corresponding matrices (unpartitioned) are  $N_V \times N_V$ . The reader may consult fig. 2.3 for an example of tube ends connecting to a junction.

### B. Reindexing of Elementary Matrices in the Collection of Junction Scattering Supermatrices

Having considered the junction scattering supermatrix for  $J_v$  and noting that  $v = 1, 2, \dots, N_j$  gives all the junctions, we then have the elementary scattering matrices from one tube to another wherever there is such a connection at any junction. The problem is one of rearranging the equations so as to combine the results for junctions and tubes to obtain a description of the overall transmission-line network.

To convert the junction scattering supermatrix to a network scattering supermatrix, consider the tube-end-wave matrix  $(t_{r,u})_{v;E-W}$  which relates the tube ends  $(r)$  at junction  $J_v$  to the waves  $W_u$  on those tubes. Recall the definition from (2.26) of the elements of the tube-end-wave matrix as

$$t_{r,u;v;E-W} \equiv \begin{cases} 0 & \text{if } W_u \text{ does not connect to } J_v \text{ via the } r\text{th} \\ & \text{tube end (i.e., } J_{v;r}) \\ -1 & \text{if } W_u \text{ enters } J_v \text{ via the } r\text{th tube} \\ & \text{end (i.e., } J_{v;r,-}) \\ +1 & \text{if } W_u \text{ leaves } J_v \text{ via the } r\text{th tube end} \\ & \text{(i.e., } J_{v;r,+}) \end{cases} \quad (6.12)$$

Once can then construct this matrix for each  $J_v$  for  $v = 1, 2, \dots, N_j$  from the topological diagram (graph) for the transmission-line network giving the junction  $J_v$  numbering and wave  $W_u$  numbering (as in the example in fig. 2.2b), and from the corresponding diagram for each junction  $J_v$  including tube-end labeling  $(r \text{ or } J_{v;r})$  (as in the example for  $J_3$  in fig. 2.3).

Now to associate an elementary scattering matrix  $(\tilde{S}_{n,m}(s))_{r,r';v}$  for two tube ends,  $J_{v;r}$  and  $J_{v;r'}$  with  $(\tilde{S}_{n,m}(s))_{u,v}$  corresponding to two waves,  $W_u$  and  $W_v$ , in the overall network is straightforward; one must associate

$$\begin{aligned} r' \text{ (or } J_{v;r'}) &\rightarrow v \text{ (or } W_v) \text{ for the incoming wave} \\ r \text{ (or } J_{v;r}) &\rightarrow u \text{ (or } W_u) \text{ for the outgoing wave} \end{aligned} \quad (6.13)$$

However, this is what the tube-end-wave matrix does.

Consider incoming waves corresponding to the second index,  $v$ , in  $(\tilde{S}_{n,m}(s))_{u,v}$ . For one and only one  $J_v$  there is a negative entry in  $(t_{r',v})_{v;E-W}$  under the  $v$ th column; the corresponding row is the value of  $r'$ . Hence, for each  $v$

$$r' \text{ (in } J_{v;r'}) \text{ is that } r' \ni t_{r',v;v;E-W} = -1 \quad (6.14)$$

which is readily found and even automated on a computer. Said another way,  $v$  is a function (an integer function) of  $v$  and  $r'$ . To aid in the search for  $J_{v;r'}$  the value of  $v$  (or junction  $J_v$ ) is found from the junction-wave matrix  $(t_{v,v})_{J-W}$  (as in (2.21)) by finding those values of  $v$  for which  $t_{v,v;J-W}$  is nonzero; there are at most two such values of  $v$  corresponding to the  $W_v$  leaving one junction and entering another junction, except in the case of a self tube where  $W_v$  both leaves and enters the same junction. Considering the one or two possible  $J_v$  the value of  $v$  and  $r'$  are readily found as in (6.14) or via a diagram. After going through  $v = 1, 2, \dots, N_W$  one can construct a table in the form

$v$	$v$	$r'$
1		
2		
$\vdots$		
$N_W$		

(6.15)

Table of Correspondence of incoming waves  $W_v$  to junctions  $J_v$  and tube ends  $J_{v;r'}$

with the values of  $v$  and  $r'$  filled in for every  $v$ .

Similarly for outgoing waves corresponding to the first index  $u$  in  $(\tilde{S}_{n,m}(s))_{u,v}$ , we have a value of  $r$  given by

$$r \text{ (in } J_{v;r}) \text{ is that } r \ni t_{r,u;v;E-W} = +1 \quad (6.16)$$

Hence,  $u$  is a function of  $v$  and  $r$ . Again utilizing the junction-wave matrix  $(t_{v,j})_{J-W}$  and finding the values of  $t_{v,u;J-W}$  which are nonzero, one reduces the consideration to at most two values of the junction index  $v$ . The values of  $v$  and  $r$  are then readily found from the tube-end-wave matrices as in (6.16). After going through  $u = 1, 2, \dots, N_W$  one can construct a table in the form

$u$	$v$	$r$
1		
2		
$\vdots$		
$N_W$		

Table of correspondence of outgoing waves  $W_u$  to junctions  $J_v$  and tube ends  $J_{v;r}$

with the values of  $v$  and  $r$  filled in for every  $u$ .

Hence, with each pair  $(u, v)$  we associate the pair  $(J_{v_1;r}, J_{v_2;r'})$ . Now we have

$$v_1 = v_2 \equiv v \quad \text{for } W_v \text{ scattering into } W_u \text{ at junction } J_v$$

$$v_1 \neq v_2 \quad \text{for } W_v \text{ not scattering into } W_u \text{ (no interconnection) at any } J_v$$

(6.18)

Then we form the network elementary scattering matrices as

$$(\tilde{S}_{n,m}(s))_{u,v} \equiv \begin{cases} (\tilde{S}_{n,m}(s))_{r,r';v} & \text{for } v_1 = v_2 = v \text{ or } W_v \\ & \text{scattering into } W_u \text{ at } J_v \\ (0_{n,m}) = (0_{n,m})_{u,v} & \text{for } v_1 \neq v_2 \text{ or } W_v \\ & \text{not scattering into } W_u \end{cases} \quad (6.19)$$

This gives an explicit algorithm for constructing the  $(\tilde{S}_{n,m}(s))_{u,v}$  from the collection of junction scattering supermatrices  $((\tilde{S}_{n,m}(s))_{r,r'})_v$ .

The reader will also note the correspondence of these results with the wave-wave matrix  $(W_{u,v})$  as defined in (2.24) as

$$W_{u,v} = \begin{cases} 1 & \text{for } v_1 = v_2 \equiv v \text{ and } W_v \text{ scattering into} \\ & W_u \text{ at } J_v \\ 0 & \text{for } v_1 \neq v_2 \text{ or } W_v \text{ not scattering} \\ & \text{into } W_u \end{cases} \quad (6.20)$$

The wave-wave matrix then indicates which  $(u,v)$  pairs must be considered for finding nonidentically zero scattering matrices, thereby simplifying the search among the elementary matrices comprising the junction scattering supermatrices.

### C. Scattering Supermatrix

The proper ordering of all the junction scattering matrices into one large matrix forms the system (or network) scattering supermatrix  $((\tilde{S}_{n,m}(s))_{u,v})$ . This supermatrix is a collection of the junction scattering matrices, which themselves are collections of individual tube scattering matrices. The latter are matrices containing reflection and transmission coefficients of individual wires within the tubes. Thus,  $((\tilde{S}_{n,m}(s))_{u,v})$  is a dimatrix (or tensor of rank four).

The wave-wave matrix  $(W_{u,v})$  gives the structure of the scattering supermatrix since the scattering supermatrix is in general block sparse as

$$(\tilde{S}_{n,m}(s))_{u,v} = (0_{n,m})_{u,v} \text{ for } W_{u,v} = 0 \quad (6.21)$$

Hence, also, the scattering supermatrix is  $N_W \times N_W$  in terms of the  $u,v$  indices, i.e.,

$$u,v = 1, 2, \dots, N_W \quad (6.22)$$

The elementary scattering matrices  $(\tilde{S}_{n,m}(s))_{u,v}$  are  $N_u \times N_v$ , i.e.,

$$n = 1, 2, \dots, N_u \quad (6.23)$$

$$m = 1, 2, \dots, N_v$$

where

$$N_u = \text{number of conductors (not including reference) on the tube with } u\text{th wave} \quad (6.24)$$

and likewise for  $N_v$ .

As a special case, it is interesting to note that if there are no self tubes (with both ends connected to the same junction), then

$$W_{u,u} = 0 \quad \text{for } u = 1, 2, \dots, N_u \quad \text{for no self tubes} \quad (6.25)$$

$$(\tilde{S}_{n,m}(s))_{u,u} = (0_{n,m})_{u,u} \quad \text{for } n, m = 1, 2, \dots, N_u \text{ (square)}$$

In this case the scattering supermatrix has zero matrices for its diagonal blocks; this will complement the identity supermatrix which has, as its only nonzero elementary matrices, the diagonal blocks which are identity matrices (as discussed in Section V). This case is anticipated to be quite common in practice.

# VII. DEFINITIONS OF SOME IMPORTANT SUPERMATRIX AND SUPERVECTOR QUANTITIES BASED ON RESULTS FOR WAVES ON A TUBE

This section takes the results for the combined voltages on a tube and separates them into the wave variables for the network. The resulting equation for a general combined voltage wave  $W_u$  is used to relate the combined voltages at both ends of the tube with the sources along the tube. Each term is generalized to a form appropriate to the transmission-line network, i.e., supermatrices and supervectors, by aggregating the results for all  $W_u$  for  $u = 1, 2, \dots, N_W$ .

## A. Common Equation for the Two Waves on a Tube

Let us take the results for the propagation on a single tube developed in subsection IIIC from (3.59) and (3.60) as

$$\begin{aligned}
 (\tilde{V}_n(z, s))_+ &= \exp\{-(\tilde{\gamma}_{c_{n,m}}(s))z\} \cdot (\tilde{V}_n(0, s))_+ \\
 &+ \int_0^z \exp\{-(\tilde{\gamma}_{c_{n,m}}(s))[z-z']\} \cdot (\tilde{V}_n^{(s)'}(z', s))_+ dz' \\
 (\tilde{V}_n(z, s))_- &= \exp\{(\tilde{\gamma}_{c_{n,m}}(s))[z-L]\} \cdot (\tilde{V}_n(L, s))_- \\
 &+ \int_L^z \exp\{\tilde{\gamma}_{c_{n,m}}(s)[z-z']\} \cdot (\tilde{V}_n^{(s)'}(z', s))_- dz'
 \end{aligned}
 \tag{7.1}$$

Then, as discussed in subsection IIID, let us identify the two waves on the tube with two waves of the transmission-line network, say  $W_u$  and  $W_v$ .

Consider the  $+$  wave; call this  $W_u$  and set the coordinate and dimension variables as

$L_u \equiv L \equiv$  length of path for  $W_u$

$z_u \equiv z \equiv$  wave coordinate for  $W_u$

$$0 \leq z_u \leq L_u$$

$N_u \equiv N \equiv$  number of conductors (less reference) on tube  
and dimension of vectors for  $W_u$  (7.2)

The wave and source conventions are then

$$(\tilde{V}_n(z_u, s))_u \equiv (\tilde{V}_n(z, s))_+ = (\tilde{V}_n(z_u, s)) + (\tilde{Z}_{c_{n,m}}(s))_u \cdot (\tilde{I}_n(z_u, s))$$

$\equiv$  combined voltage for  $W_u$

$$(\tilde{V}_n^{(s)'}(z_u, s))_u \equiv (\tilde{V}_n^{(s)'}(z, s))_+ = (\tilde{V}_n^{(s)'}(z_u, s)) + (\tilde{Z}_{c_{n,m}}(s))_u \cdot (\tilde{I}_n^{(s)'}(z_u, s))$$

$\equiv$  combined voltage source per unit length for  $W_u$

$$(\tilde{Z}_{c_{n,m}}(s))_u \equiv (\tilde{Y}_{c_{n,m}}(s))_u^{-1} \equiv \text{characteristic impedance matrix for } W_u$$

$$(\tilde{Y}_{c_{n,m}}(s))_u \equiv (\tilde{Y}_{c_{n,m}}(s)) \equiv \text{propagation matrix for } W_u \quad (7.3)$$

Note that for  $W_u$  the current  $(\tilde{I}_n(z_u, s))$  convention is taken as positive in the direction of increasing  $z_u$  (as in fig. 2.5). Likewise, the voltage source per unit length  $(\tilde{V}_n^{(s)'}(z_u, s))$  (including any discrete voltage sources) is taken as positive increasing in the direction of increasing  $z_u$ . The first of (7.1) then takes the form for  $W_u$  as

$$\begin{aligned} (\tilde{V}_n(z_u, s))_u &= \exp\{-(\tilde{Y}_{c_{n,m}}(s))_u z_u\} \cdot (\tilde{V}_n(0, s))_u \\ &+ \int_0^{z_u} \exp\{-(\tilde{Y}_{c_{n,m}}(s))_u [z_u - z'_u]\} \cdot (\tilde{V}_n^{(s)'}(z'_u, s))_u dz'_u \end{aligned} \quad (7.4)$$

Next consider the - wave; call this  $W_v$  and set the coordinate dimension variables as

$$L_v \equiv L \equiv \text{length of path for } W_v$$

$$z_v \equiv L - z \equiv \text{wave coordinate for } W_v$$

$$0 \leq z_v \leq L_v$$

$$N_v \equiv N \equiv \text{number of conductors (less reference) on tube and} \\ \text{and dimension of vectors for } W_v \quad (7.5)$$

The wave and source conventions are then

$$(\tilde{V}_n(z_v, s))_v \equiv (\tilde{V}_n(z, s))_- = (\tilde{V}_n(z_v, s)) + (\tilde{Z}_{c_{n,m}}(s))_v \cdot (\tilde{I}_n(z_v, s))$$

$$\equiv \text{combined voltage for } W_v$$

$$(\tilde{V}_n^{(s)'}(z_v, s))_v \equiv -(\tilde{V}_n^{(s)'}(z, s))_- = (\tilde{V}_n^{(s)'}(z_v, s)) + (\tilde{Z}_{c_{n,m}}(s))_v \cdot (\tilde{I}_n^{(s)'}(z_v, s))$$

$$\equiv \text{combined voltage source per unit length for } W_v$$

$$(\tilde{Z}_{c_{n,m}}(s))_v \equiv (\tilde{Y}_{c_{n,m}}(s))_v^{-1} \equiv \text{characteristic impedance matrix for } W_v$$

$$(\tilde{Y}_{c_{n,m}}(s))_v \equiv (\tilde{Y}_{c_{n,m}}(s)) \equiv \text{propagation matrix for } W_v \quad (7.6)$$

Now for  $W_v$  the current  $(\tilde{I}_n^{(s)}(z_v, s))$  convention is taken as positive in the direction of increasing  $z_v$  and, hence, of decreasing  $z$  (opposite to that for  $W_u$ ). Similarly, the voltage source per unit length is taken as positive in the direction of increasing  $z_v$  which is the direction of decreasing  $z$ . This is so that for  $W_v$  the conventions are defined with respect to  $z_v$  in the same manner as for  $W_u$  they have been defined with respect to  $z_u$ . The second of (7.1) then takes the form for  $W_v$  as

$$\begin{aligned}
(\tilde{v}_n(z_v, s))_v &= \exp\{-(\tilde{\gamma}_{c_{n,m}}(s))_v z_v\} \cdot (\tilde{v}_n(0, s))_v \\
&+ \int_0^{z_v} \exp\{-(\tilde{\gamma}_{c_{n,m}}(s))_v [z_v - z'_v]\} \cdot (\tilde{v}_n^{(s)'}(z'_v, s))_v dz'_v
\end{aligned} \quad (7.7)$$

which is exactly the same as for  $W_u$  in (7.4). Hence, only one such equation need be considered; it is applicable for all  $u = 1, 2, \dots, N_w$  thereby applying to all waves in the transmission-line network.

The chosen conventions for  $W_u$  and  $W_v$  to have the same form with respect to  $z_u$  and  $z_v$  are then important to simplifying the formulation of the network equations. With these choices we have relations between the two waves  $W_u$  and  $W_v$  on the same tube for coordinates and dimensions as

$$\begin{aligned}
L_u &\equiv L_v \equiv L \\
z_u + z_v &= L \\
N_u &= N_v = N
\end{aligned} \quad (7.8)$$

The wave and source relations are (for uncombined quantities)

$$\begin{aligned}
(\tilde{v}_n(z_u, s)) &= (\tilde{v}_n(z_v, s)) \\
(\tilde{i}_n(z_u, s)) &= -(\tilde{i}_n(z_v, s)) \\
(\tilde{v}_n^{(s)'}(z_u, s)) &= -(\tilde{v}_n^{(s)'}(z_v, s)) \\
(\tilde{i}_n^{(s)'}(z_u, s)) &= (\tilde{i}_n^{(s)'}(z_v, s)) \\
(\tilde{Z}_{c_{n,m}}(s))_u &= (\tilde{Z}_{c_{n,m}}(s))_v = (\tilde{Z}_{c_{n,m}}(s)) \\
(\tilde{\gamma}_{c_{n,m}}(s))_u &= (\tilde{\gamma}_{c_{n,m}}(s))_v = (\tilde{\gamma}_{c_{n,m}}(s))
\end{aligned} \quad (7.9)$$

### B. Relation of Combined-Voltage Waves on Both Ends of a Tube

Now in (7.4) (or equivalently, (7.7)) we have the combined voltage at any  $z_u$  in terms of the value (boundary condition) at  $z_u = 0$ . Setting  $z_u = L_u$  we introduce the boundary value there as giving

$$(\tilde{V}_n(L_u, s))_u = \exp\{-(\tilde{\gamma}_{c_{n,m}}(s))_u L_u\} \cdot (\tilde{V}_n(0, s))_u + \int_0^{L_u} \exp\{-(\tilde{\gamma}_{c_{n,m}}(s))_u [L_u - z'_u]\} \cdot (\tilde{V}_n^{(s)'}(z'_u, s))_u dz'_u \quad (7.10)$$

This evidently relates  $(\tilde{V}_n(0, s))_u$  which is an outgoing wave from the junction at  $z_u = 0$ , to  $(\tilde{V}_n(L_u, s))_u$  which is an incoming wave to the junction at  $z_u = L_u$ . This is used later with the scattering supermatrix to form the BLT equation for the transmission-line network.

As a matter of convention, let all sources be considered as being present in the tubes instead of the junctions. If one has a junction with an equivalent circuit containing sources, as for example in fig. 2.4, then the sources can be moved just across the terminals into the tube, a movement of zero distance. Note then that the boundary values  $(\tilde{V}_n(0, s))_u$  and  $(\tilde{V}_n(L_u, s))_u$  are combined voltages on the junction "side" of the connections to the junction. Given this convention again, note the different conventions for sources for the two different waves on a tube, as discussed above.

### C. Propagation Characteristic Supermatrix

Considering the various terms in (7.10), let us first aggregate all the propagation terms not associated with the sources into a block diagonal propagation supermatrix as

$$\begin{aligned} & ((\tilde{\Gamma}_{n,m}(s))_{u,v}) \\ & \equiv \exp\{-(\tilde{\gamma}_{c_{n,m}}(s))_{1L_1}\} \oplus \exp\{-(\tilde{\gamma}_{c_{n,m}}(s))_{2L_2}\} \oplus \dots \oplus \exp\{-(\tilde{\gamma}_{c_{n,m}}(s))_{N_W L_{N_W}}\} \\ & \equiv \bigoplus_{u=1}^{N_W} \exp\{-(\tilde{\gamma}_{c_{n,m}}(s))_{uL_u}\} \\ & \equiv \text{propagation supermatrix} \end{aligned} \quad (7.11)$$

where the elementary matrices (blocks) are given by

$$\begin{aligned}
 (\tilde{\Gamma}_{n,m}(s))_{u,v} &= \begin{cases} \exp\{-(\tilde{\gamma}_{c_{n,m}}(s))_u L_u\} & \text{for } u = v \\ (0_{n,m}) & \text{for } u \neq v \end{cases} \\
 &= 1_{u,v} \exp\{-(\tilde{\gamma}_{c_{n,m}}(s))_u L_u\}
 \end{aligned} \tag{7.12}$$

#### D. Source Supervector and Supermatrix Integral Operator

Again from (7.10) let us define a source vector for  $W_u$  in traveling from  $z_u = 0$  to  $z_u = L_u$  as

$$(\tilde{v}_n^{(s)}(s))_u \equiv \int_0^{L_u} \exp\{-(\tilde{\gamma}_{c_{n,m}}(s))_u [L_u - z'_u]\} \cdot (\tilde{v}_n^{(s)'}(z'_u, s))_u dz'_u \tag{7.13}$$

The source supervector is then merely

$$((\tilde{v}_n^{(s)}(s))_u) \equiv \left( \int_0^{L_u} \exp\{-(\tilde{\gamma}_{c_{n,m}}(s))_u [L_u - z'_u]\} \cdot (\tilde{v}_n^{(s)'}(z'_u, s))_u dz'_u \right) \tag{7.14}$$

Once can factor the above result by the use of a supermatrix integral operator. Define the elementary matrix blocks of this operator as

$$\begin{aligned}
 &(\tilde{\Lambda}_{n,m}(z'_u, s; (\cdot)))_{u,v} \\
 &\equiv \begin{cases} \int_0^{L_u} \exp\{-(\tilde{\gamma}_{c_{n,m}}(s))_u [L_u - z'_u]\} (\cdot) dz'_u & \text{for } u = v \\ (0_{n,m}) & \text{for } u \neq v \end{cases} \\
 &= 1_{u,v} \int_0^{L_u} \exp\{-(\tilde{\gamma}_{c_{n,m}}(s))_u [L_u - z'_u]\} (\cdot) dz'_u
 \end{aligned} \tag{7.15}$$

where the argument  $(\cdot)$  indicates the place to put the expression following the operator in order to perform the operation. This is defined so that

$$\begin{aligned}
 & (\tilde{\Lambda}_{n,m}(z'_u, s; (\cdot)))_{u,v} \cdot (\tilde{V}_n^{(s)'}(z'_u, s))_v \\
 & = 1_{u,v} (\tilde{V}_n^{(s)}(s))_v \\
 & = 1_{u,v} \int_0^L \exp\{-(\tilde{\gamma}_{c_{n,m}}(s))_v [L_v - z'_v]\} \cdot (\tilde{V}_n^{(s)'}(z'_v, s)) dz'_v \quad (7.16)
 \end{aligned}$$

with the multiplication which is part of the operation taken in the dot product sense. We can then readily form

$$((\tilde{V}_n^{(s)}(s))_u) = ((\tilde{\Lambda}_{n,m}(z'_u, s; (\cdot)))_{u,v}) : ((\tilde{V}_n^{(s)'}(z'_u, s))_u)$$

$$((\tilde{\Lambda}_{n,m}(z'_u, s; (\cdot)))_{u,v})$$

$$\begin{aligned}
 & \equiv \bigoplus_{u=1}^{N_W} (\tilde{\Lambda}_{n,m}(z'_u, s; (\cdot)))_{u,v} \\
 & \equiv \bigoplus_{u=1}^{N_W} \int_0^L \exp\{-(\tilde{\gamma}_{c_{n,m}}(s))_u [L_u - z'_u]\} (\cdot) dz'_u
 \end{aligned}$$

$\equiv$  propagation supermatrix integral operator

$$((\tilde{V}_n^{(s)'}(z'_u, s))_u) \equiv \text{distributed source supervector} \quad (7.17)$$

Note that the propagation supermatrix integral operator in (7.17) is a generalization of the propagation supermatrix in (7.11) to allow for continuous combined voltage sources along the wave coordinates instead of just the boundary conditions (equivalent sources) at the set of  $z_u = 0$ .

E. Combined Voltage Supervector

For completeness we have the aggregate of combined voltage vectors in (7.10) as

$((\tilde{V}_n(0,s))_u) \equiv$  combined voltage supervector of outgoing waves at the junctions

$((\tilde{V}_n(L_u,s))_u) \equiv$  combined voltage supervector of incoming waves at the junctions (7.18)

In this note we will formulate the BLT equation in terms of the outgoing waves at the junctions, but other forms are also possible.

## VIII. BLT EQUATION

Combining the results of the previous derivations we can write the BLT equation for the description of the transmission-line network. We begin with the scattering supermatrix in Section VI which relates the incoming waves to the outgoing waves as

$$((\tilde{V}_n(0,s))_u) = ((\tilde{S}_{n,m}(s))_{u,v}):((\tilde{V}_n(L_u,s))_u) \quad (8.1)$$

using the combined voltage supervectors from subsection VII E. Note the distinction between incoming waves ( $z_u = L_u$ ) and outgoing waves ( $z_u = 0$ ) at the set of junctions or tube ends.

Next, relate the incoming waves at the output ends of the tubes ( $z_u = L_u$ ) to the same waves at the input end of the same tubes ( $z_u = L_u$ ), albeit at different junctions in general. Taking (7.10) in supermatrix form, we have

$$\begin{aligned} ((\tilde{V}_n(L_u,s))_u) &= ((\tilde{\Gamma}_{n,m}(s))_{u,v}):((\tilde{V}_n(0,s))_u) + ((\tilde{V}_n^{(s)}(s))_u) \\ &= ((\tilde{\Gamma}_{n,m}(s))_u):((\tilde{V}_n(0,s))_u) + ((\tilde{\Lambda}_{n,m}(z'_u,s;(\cdot)))_{u,v}):((\tilde{V}_n^{(s)'}(z'_u,s))_u) \end{aligned} \quad (8.2)$$

Combining (8.1) and (8.2) we have

$$\begin{aligned} ((\tilde{V}_n(0,s))_u) &= ((\tilde{S}_{n,m}(s))_{u,v}):((\tilde{\Gamma}_{n,m}(s))_{u,v}):((\tilde{V}_n(0,s))_u) + ((\tilde{S}_{n,m}(s))_{u,v}):((\tilde{V}_n^{(s)}(s))_u) \end{aligned} \quad (8.3)$$

That is rearranged by use of the supermatrix identity as

$$\begin{aligned}
 [((1_{n,m})_{u,v}) - ((\tilde{S}_{n,m}(s))_{u,v}) : ((\tilde{\Gamma}_{n,m}(s))_{u,v})] : ((\tilde{V}_n(0,s))_u) \\
 = ((\tilde{S}_{n,m}(s))_{u,v}) : ((\tilde{V}_n^{(s)}(s))_u) \\
 = ((\tilde{S}_{n,m}(s))_{u,v}) : ((\tilde{\Lambda}_{n,m}(z'_u, s; (\cdot)))_{u,v}) : ((\tilde{V}_n^{(s)})'(z'_u, s))_u
 \end{aligned}$$

(8.4)

This is one form of the BLT equation with the unknowns taken as the combined voltage waves leaving the junctions. Note again that all sources are given a convention as being on the tubes in the wave coordinates  $0 \leq z_u \leq L_u$  so that they are picked up in the integration along the wave coordinates and are not included in the combined voltages at the junctions  $((\tilde{V}_n(0,s))_u)$  which are being computed.

For computational purposes the BLT equation is one large matrix equation with square matrices of size  $N \times N$  and vectors of dimension  $N$  where

$$N = \sum_{u=1}^{N_w} N_u \quad (8.5)$$

Noting, however, the sparse nature of these matrices with blocks of zeros, one may be able to take advantage of the partitioning used to construct the supermatrices to simplify computations.

## IX. RECONSTRUCTION OF VOLTAGES AND CURRENTS

Having solved the BLT equation as in (8.4) in some form or other, we have a set of combined voltages such as the outgoing combined voltages  $((\tilde{V}_n(0,s))_u)$  at the junctions. From these one can find voltages and currents essentially everywhere, including at the junction terminals (tube ends) and at arbitrary positions on the tubes.

Consider the important case of voltages and currents at the tube ends (junctions). Let the two waves on a particular tube be  $W_u$  and  $W_v$  as in subsection VIIA. Using the conventions established there we have

$$N_u = N_v = N \equiv \text{dimension of vectors}$$

$$L_u = L_v = L \equiv \text{length}$$

$$z_u + z_v = L \equiv \text{relation between two wave coordinates}$$

$$z = z_u = L - z_v \equiv \text{tube coordinate} \quad (9.1)$$

Then we have at  $z=0$

$$\begin{aligned} (\tilde{V}_n(0,s)) &= \frac{1}{2} [(\tilde{V}_n(0,s))_u + (\tilde{V}_n(L_v,s))_v] \\ (\tilde{I}_n(0,s)) &= \frac{1}{2} (\tilde{Y}_{c_{n,m}}(s)) \cdot [(\tilde{V}_n(0,s))_u - (\tilde{V}_n(L_v,s))_v] \end{aligned} \quad (9.2)$$

with the current positive in the  $+z$  direction or out of the junction at  $z=0$ . At the other end with  $z=L$  we have

$$\begin{aligned} (\tilde{V}_n(L,s)) &= \frac{1}{2} [(\tilde{V}_n(L_u,s))_u + (\tilde{V}_n(0,s))_v] \\ (\tilde{I}_n(L,s)) &= \frac{1}{2} (\tilde{Y}_{c_{n,m}}(s)) \cdot [(\tilde{V}_n(L_u,s))_u - (\tilde{V}_n(0,s))_v] \end{aligned} \quad (9.3)$$

with current positive in the  $+z$  direction or into the junction at  $z=L$ . For substitution into the above equations, one uses

$$\begin{aligned}
(\tilde{V}_n(L_u, s))_u &= (\tilde{\Gamma}_{n,m}(s))_{u,u} \cdot (\tilde{V}_n(0, s))_u + (\tilde{\Lambda}_{n,m}(z'_u, s; (\cdot)))_{u,u} \cdot (\tilde{V}_n^{(s)'}(z'_u, s))_u \\
(\tilde{V}_n(L_v, s))_v &= (\tilde{\Gamma}_{n,m}(s))_{v,v} \cdot (\tilde{V}_n(0, s))_v + (\tilde{\Lambda}_{n,m}(z'_v, s; (\cdot)))_{v,v} \cdot (\tilde{V}_n^{(s)'}(z'_v, s))_v
\end{aligned}
\tag{9.4}$$

so that  $W_u$  has  $z_u = L_u$  related to  $z_u = 0$  and  $W_v$  has  $z_v = L_v$  related to  $z_v = 0$ . In this form the current and voltage vectors at the tube ends can be computed from the combined voltage vectors leaving the junctions (i.e.,  $(\tilde{V}_n(0, s))_u$ ) from the BLT equation (8.4) and the combined sources along the tube via (9.4) for the two waves on the tube.

For more general positions along the tube of interest we have

$$\begin{aligned}
(\tilde{V}_n(z, s)) &= \frac{1}{2} [(\tilde{V}_n(z_u, s))_u + (\tilde{V}_n(z_v, s))_v] \\
(\tilde{I}_n(z, s)) &= \frac{1}{2} (\tilde{\Gamma}_{c,n,m}(s)) \cdot [(\tilde{V}_n(z_u, s))_u - (\tilde{V}_n(z_v, s))_v]
\end{aligned}
\tag{9.5}$$

with current positive in the  $+z$  direction which is equivalent to the  $+z_u$  direction and to the  $-z_v$  direction. For substituting into (9.5), one uses (7.4) and (7.7) repeated here as

$$\begin{aligned}
(\tilde{V}_n(z_u, s))_u &= \exp\{-(\tilde{\gamma}_{c,n,m}(s))_u z_u\} \cdot (\tilde{V}_n(0, s))_u \\
&\quad + \int_0^{z_u} \exp\{-(\tilde{\gamma}_{c,n,m}(s))_u [z_u - z'_u]\} \cdot (\tilde{V}_n^{(s)'}(z'_u, s))_u dz'_u \\
(\tilde{V}_n(z_v, s))_v &= \exp\{-(\tilde{\gamma}_{c,n,m}(s))_v z_v\} \cdot (\tilde{V}_n(0, s))_v \\
&\quad + \int_0^{z_v} \exp\{-(\tilde{\gamma}_{c,n,m}(s))_v [z_v - z'_v]\} \cdot (\tilde{V}_n^{(s)'}(z'_v, s))_v dz'_v
\end{aligned}
\tag{9.6}$$

In this form the combined voltage supervectors  $(\tilde{V}_n(0, s))_u$  leaving the junctions as computed from the BLT equation (8.4) and the combined sources  $(\tilde{V}_n^{(s)'}(z'_u, s))_u$  along the tubes (or waves) can be used to compute the combined voltages and thereby the voltages and currents at any position  $z = z_u = L_u - z_v$  along any tube of interest.

## X. SOME FORMS OF SOLUTIONS OF BLT EQUATIONS

Having formulated the BLT equation (8.4), one can represent its solution in various ways. The reader should note that the particular form in (8.4) is only one of many forms the BLT equation can take; in this case the unknowns are the combined voltages scattered from (outward propagation from) the junctions.

Since the BLT equation has been cast in the form of a supermatrix equation, the solution can be written directly as

$$\begin{aligned}
 & ((\tilde{V}_n(0,s))_u) \\
 &= [((1_{n,m})_{u,v}) - ((\tilde{S}_{n,m}(s))_{u,v}) : ((\tilde{\Gamma}_{n,m}(s))_{u,v})]^{-1} \\
 & : ((\tilde{S}_{n,m}(s))_{u,v}) : ((\tilde{\Lambda}_{n,m}(z'_u, s; (\cdot)))_{u,v}) : ((\tilde{V}_n^{(s)'}(z'_u, s))_u) \quad (10.1)
 \end{aligned}$$

For each complex frequency  $s$  this solution can be directly computed via integration (for the distributed sources), supermatrix multiplication, and supermatrix inversion, typically by computer. However, this approach may have limited utility for some kinds of problems due to a desire for the transient behavior and/or the characterization of the solution (such as bounding it) for a large class of excitations  $((\tilde{V}_n^{(s)'}(z'_u, s))_u)$ .

Considerable work has been done in representing the solution of electromagnetic scattering problems, as formulated in integral equations, in terms of the eigenmode expansion method (EEM) and the singularity expansion method (SEM). The literature on SEM and EEM is quite extensive and the reader can consult two review book chapters [10.1,2] concerning this subject and obtain a bibliography. While the SEM and EEM concepts have been cast in terms of electromagnetic integral equations, there is a direct connection to matrix equations because of the moment method (MoM) which is used to matricize the integral equations, i.e., put the integral equations in a form for numerical evaluation as on a computer [10.3]. In fact, some of the original developments in SEM and EEM theory and application used matrix concepts to arrive at the needed ideas and techniques [10.4-6]. Hence, SEM and EEM are directly applicable to the

BLT equation, as in (8.4) or in other related forms of it. A few of the results are presented here to indicate the forms of some of the basic results as applicable to the supermatrix BLT equation.

In EEM form one defines eigenmode supervectors and eigenvalues via

$$\begin{aligned} [((1_{n,m})_{u,v}) - ((\tilde{S}_{n,m}(s))_{u,v}) : ((\tilde{\Gamma}_{n,m}(s))_{u,v})] : ((\tilde{V}_n(s))_u)_\beta &= \tilde{\lambda}_\beta(s) ((\tilde{V}_n(s))_u)_\beta \\ ((\tilde{L}_n(s))_u)_\beta : [((1_{n,m})_{u,v}) - ((\tilde{S}_{n,m}(s))_{u,v}) : ((\tilde{\Gamma}_{n,m}(s))_{u,v})] &= \tilde{\lambda}_\beta(s) ((\tilde{L}_n(s))_u)_\beta \\ \beta &= 1, 2, \dots, N \end{aligned} \quad (10.2)$$

where for distinct eigenvalues we have the biorthogonal property

$$((\tilde{L}_n(s))_u)_\beta : ((\tilde{V}_n(s))_u)_{\beta'} = 0 \quad \text{for } \beta \neq \beta' \quad (10.3)$$

This result also applies in the weaker case of independent eigensupervectors. From (8.5) we have  $N$  eigenvalues and assume the existence of  $N$  independent eigensupervectors (of both left and right kinds separately). The right eigenmodes are used to expand  $(\tilde{V}_n(0,s))$  which gives the outgoing waves at the junctions. The left eigenmodes appear to be related to the incoming waves at the junctions, and this aspect will hopefully be considered in a future note.

Defining normalized eigensupervectors as

$$\begin{aligned} ((\tilde{V}_n(s))_u)_\beta &\equiv [((\tilde{L}_n(s))_u)_\beta : ((\tilde{V}_n(s))_u)_\beta]^{-1/2} ((\tilde{V}_n(s))_u)_\beta \\ ((\tilde{L}_n(s))_u)_\beta &\equiv [((\tilde{L}_n(s))_u)_\beta : ((\tilde{V}_n(s))_u)_\beta]^{-1/2} ((\tilde{L}_n(s))_u)_\beta \end{aligned} \quad (10.4)$$

we have the biorthonormal property

$$((\tilde{L}_n(s))_u)_\beta : ((\tilde{V}_n(s))_u)_{\beta'} = 1_{\beta, \beta'} \quad (10.5)$$

This allows us to write the expansion

$$\begin{aligned}
((1_{n,m})_{u,v}) - ((\tilde{S}_{n,m}(s))_{u,v}) : ((\tilde{\Gamma}_{n,m}(s))_{u,v}) \\
= \sum_{\beta} \tilde{\lambda}_{\beta}(s) [((\tilde{L}_n(s))_u)_{\beta} : ((\tilde{V}_n(s))_u)_{\beta}]^{-1} ((\tilde{V}_n(s))_u)_{\beta} ((\tilde{L}_n(s))_u)_{\beta} \\
= \sum_{\beta} \tilde{\lambda}_{\beta}(s) ((\tilde{V}_n(s))_u)_{\beta} ((\tilde{L}_n(s))_u)_{\beta}
\end{aligned} \tag{10.6}$$

which is an example of a dyadic expansion using a dyadic or outer product of supervectors. The inverse is

$$\begin{aligned}
[ ((1_{n,m})_{u,v}) - ((\tilde{S}_{n,m}(s))_{u,v}) : ((\tilde{\Gamma}_{n,m}(s))_{u,v}) ]^{-1} \\
= \sum_{\beta} \tilde{\lambda}_{\beta}^{-1}(s) ((\tilde{V}_n(s))_u)_{\beta} ((\tilde{L}_n(s))_u)_{\beta}
\end{aligned} \tag{10.7}$$

and the identity is

$$\begin{aligned}
((1_{n,m})_{u,v}) &= \sum_{\beta} ((\tilde{V}_n(s))_u)_{\beta} ((\tilde{L}_n(s))_u)_{\beta} \\
&= \sum_{\beta} ((\tilde{L}_n(s))_u)_{\beta} ((\tilde{V}_n(s))_u)_{\beta}
\end{aligned} \tag{10.8}$$

Combining (10.6) with (10.8) also gives

$$((\tilde{S}_{n,m}(s))_{u,v}) : ((\tilde{\Gamma}_{n,m}(s))_{u,v}) = \sum_{\beta} [1 - \tilde{\lambda}_{\beta}(s)] ((\tilde{V}_n(s))_u)_{\beta} ((\tilde{L}_n(s))_u)_{\beta} \tag{10.9}$$

The solution of the BLT equation (8.4) can then be written as a sum of eigensupervector contributions as

$$((\tilde{V}_n(s))_u)$$

$$= \sum_{\beta} \tilde{\lambda}_{\beta}^{-1}(s) [((\tilde{\lambda}_n(s))_u)_{\beta} : ((\tilde{S}_{n,m}(s))_{u,v}) : ((\tilde{\Lambda}_{n,m}(z'_u, s; (\cdot)))_{u,v}) : ((\tilde{V}_n(s))' (z'_u, s))_u] \\ ((\tilde{V}_n(s))_u)_{\beta} \quad (10.10)$$

Note that this solution expresses the outgoing combined voltages at the junctions in terms of eigenmodes at the junctions. These eigenmodes can be extended throughout the tubes of the transmission-line network by the techniques discussed in Section IX; these extended eigenmodes can then be used to construct the combined voltages and voltages and currents throughout the tubes. However, these eigenmodes are not anticipated to be simply related to the tube eigenmodes (Section III) which may be more appropriate for extending the combined voltages at the junctions to the combined voltages, voltages, and currents throughout the network tubes.

Concerning the SEM representation of the solution, there is much that can be adapted from the work on electromagnetic scattering and antenna problems. The general form of the solution of the BLT equation in the form expressed in (8.4) is

$$((\tilde{V}_n(0,s))_u) = \sum_{\alpha} \tilde{f}(s_{\alpha}) \tilde{\eta}_{\alpha}(s) ((v_n)_u)_{\alpha} (s-s_{\alpha})^{-n_{\alpha}} \\ + \text{other singularity terms} \quad (10.11)$$

where  $\tilde{f}(s)$  (or  $f(t)$ ) is some excitation waveform which appears in the combined sources  $((\tilde{V}_n(s))' (z'_u, s))_u$  and which is taken out so as to give some equivalent delta-function response in defining the coupling coefficients  $\tilde{\eta}_{\alpha}(s)$ . For present purposes, we can set  $\tilde{f}(s) = 1$  assuming that the excitation has been appropriately normalized. The order of the pole is  $n_{\alpha} = 1, 2, \dots$ , but here only the first order is considered; second order can be adapted from [10.2].

The natural mode supervectors are found from

$$\begin{aligned}
 & [((1_{n,m})_{u,v}) - ((\tilde{S}_{n,m}(s_\alpha))_{u,v}) : ((\tilde{\Gamma}_{n,m}(s_\alpha))_{u,v})] : ((v_n)_u)_\alpha = ((0_n)_u) \\
 & ((\ell_n)_u)_\alpha : [((1_{n,m})_{u,v}) - ((\tilde{S}_{n,m}(s_\alpha))_{u,v}) : ((\tilde{\Gamma}_{n,m}(s_\alpha))_{u,v})] = ((0_n)_u)
 \end{aligned} \tag{10.12}$$

where the left mode supervectors are also referred to as the coupling supervectors. The natural frequencies are found as the solutions of

$$\det[((1_{n,m})_{u,v}) - ((\tilde{S}_{n,m}(s_\alpha))_{u,v}) : ((\tilde{\Gamma}_{n,m}(s_\alpha))_{u,v})] = ((0_n)_u) \tag{10.13}$$

These can be related to the eigenvalues via

$$D(s, \lambda) = \det[(1-\lambda)((1_{n,m})_{u,v}) - ((\tilde{S}_{n,m}(s))_{u,v}) : ((\tilde{\Gamma}_{n,m}(s))_{u,v})] \tag{10.14}$$

for which we have

$$\begin{aligned}
 D(s, \tilde{\lambda}_\beta(s)) &= 0 \\
 D(s_\alpha, 0) &= 0
 \end{aligned} \tag{10.15}$$

from which we set

$$\alpha = (\beta, \beta') \tag{10.16}$$

such that

$$\tilde{\lambda}_\beta(s_{\beta, \beta'}) = 0 \tag{10.17}$$

associates the natural frequencies with the zeros of eigenvalues. The natural modes are similarly related to the eigenmodes as

$$\begin{aligned}
 ((v_n)_u)_{\beta, \beta'} &= N_{\beta, \beta'} ((\tilde{v}_n(s_{\beta, \beta'}))_u)_\beta \\
 ((\ell_n)_u)_{\beta, \beta'} &= M_{\beta, \beta'} ((\tilde{\ell}_n(s_{\beta, \beta'}))_u)_\beta
 \end{aligned} \tag{10.18}$$

where  $N_{\beta, \beta'}$  and  $M_{\beta, \beta'}$  are complex constants related to the normalization chosen for the natural modes.

The class 1 coupling coefficients are given by

$$\begin{aligned}
 \tilde{\eta}_\alpha(s) &= \frac{((\ell_n)_u)_\alpha : ((\tilde{\Lambda}_{n,m}(z'_u, s_\alpha; (\cdot)))_{u,v}) : ((\tilde{V}_n^{(s)})'(z'_u, s_\alpha))_u e^{-(s-s_\alpha)t_0}}{((\ell_n)_u)_\alpha : \frac{\partial}{\partial s} [((1_{n,m})_{u,v}) - ((\tilde{S}_{n,m}(s))_{u,v}) : ((\tilde{\Gamma}_{n,m}(s))_{u,v})] \Big|_{s=s_\alpha} : ((v_n)_u)_\alpha} \\
 &= N_{\beta,\beta'}^{-1} \left[ \frac{\partial}{\partial s} \lambda_\beta(s) \Big|_{s=s_{\beta,\beta'}} \right]^{-1} ((\tilde{\ell}_n(s_{\beta,\beta'}))_u) : ((\tilde{\Lambda}_{n,m}(z'_u, s_{\beta,\beta'}; (\cdot)))_{u,v}) \\
 &\quad : ((\tilde{V}_n^{(s)})'(z'_u, s_{\beta,\beta'}))_u e^{-(s-s_{\beta,\beta'})t_0} \quad (10.19)
 \end{aligned}$$

where the turn-on time  $t_0$  can be taken as a function of position (n and u indices) in the network. With this class 1 coupling coefficient, the time-domain form of (10.11) is

$$\begin{aligned}
 ((v_n(0,t))_u) &= \sum_{\alpha} \tilde{f}(s_\alpha) \tilde{\eta}_\alpha(s_\alpha) ((v_n)_u)_\alpha e^{s_\alpha t} u(t-t_0) \\
 &\quad + \text{other singularity terms} \quad (10.20)
 \end{aligned}$$

The class 2 coupling coefficients (corresponding to the SEM representation of the inverse matrix in (10.1)) are given by

$$\begin{aligned}
 \tilde{\eta}_\alpha(s) &= \frac{((e^{-(s-s_\alpha)t_0} \ell_n)_u)_\alpha : ((\tilde{\Lambda}_{n,m}(z'_u, s; (\cdot)))_{u,v}) : ((\tilde{V}_n^{(s)})'(z'_u, s))_u)}{((\ell_n)_u)_\alpha : \frac{\partial}{\partial s} [((1_{n,m})_{u,v}) - ((\tilde{S}_{n,m}(s))_{u,v}) : ((\tilde{\Gamma}_{n,m}(s))_{u,v})] \Big|_{s=s_\alpha} : ((v_n)_u)_\alpha} \\
 &= N_{\beta,\beta'}^{-1} \left[ \frac{\partial}{\partial s} \tilde{\lambda}_\beta(s) \Big|_{s=s_{\beta,\beta'}} \right]^{-1} ((e^{-(s-s_{\beta,\beta'})t_0} \tilde{\ell}_n(s_{\beta,\beta'}))_u) : ((\tilde{\Lambda}_{n,m}(z'_u, s; (\cdot)))_{u,v}) \\
 &\quad : ((\tilde{V}_n^{(s)})'(z'_u, s))_u \quad (10.21)
 \end{aligned}$$

where the turn-on time  $t_0$  can be taken as a function of two sets of position variables ( $n$  and  $u$ ) in the network corresponding to both the summation with the left mode supervectors and the position of observation. In time domain the class 2 coupling coefficients give more complicated results than (10.20) for class 1 due to the appearance of a time convolution.

Like the eigenmodes, the natural modes can be extended throughout the transmission-line network and made a function of the  $z_u$  coordinates. These can then be used for representing voltage and current supervectors throughout the tubes in the network.

This section has merely indicated some of the properties of BLT equations, particularly due to their formal similarity to electromagnetic integral equations. This analogy should provide much insight and future results.

References

- 10.1 C.E. Baum, "The Singularity Expansion Method", in L. Felsen (ed.), Transient Electromagnetic Fields, Springer Verlag, 1976.
- 10.2 C.E. Baum, "Toward an Engineering Theory of Electromagnetic Scattering: The Singularity and Eigenmode Expansion Methods", in P.L.E. Uslenghi (ed.), Electromagnetic Scattering, Academic Press, 1978.
- 10.3 R.F. Harrington, Field Computation by Moment Methods, MacMillan, 1968.
- 10.4 C.E. Baum, "On the Singularity Expansion Method for the Solution of Electromagnetic Interaction Problems", Interaction Note 88, December 1971.
- 10.5 F.M. Tesche, "On the Singularity Expansion Method as Applied to Electromagnetic Scattering from Thin Wires", Interaction Note 102, April 1972.
- 10.6 C.E. Baum, "On the Eigenmode Expansion Method for Electromagnetic Scattering and Antenna Problems, Part I: Some Basic Relations for Eigenmode Expansions and Their Relation to the Singularity Expansion", Interaction Note 229, January 1975.

## XI. CONCLUSION

This has been a long quest. While we have found a few things of apparent significance, the quest is not finished. As with many results the answers raise as many, if not more, questions. There are several general areas for future development that come to mind.

The BLT equation (including its alternate forms) expresses the characteristics of a multiconductor transmission-line network in a single supermatrix equation. In this form various properties of the network can be explored. Various properties related to energy and reciprocity can be formulated. In this regard, the symmetry properties of the various impedance and admittance matrices in the network need to be explored. This appears to have some relation to the diagonalizability properties of the propagation matrices.

A development parallel to transmission-line network topology is scatterer topology. In scatterer topology a hierarchical topology related to shielding concepts has been introduced. Perhaps this hierarchical topology can be introduced into some kinds of transmission-line networks to simplify their analysis and/or synthesis. Turning the question around, perhaps the transmission-line network topology and the BLT equation can aid in developing new insights into scatterer topology and the associated equations describing the electromagnetic scattering.

## EPILOGUE

"Then he subdued the Pisidians who made head against him, and conquered the Phrygians, at whose chief city, Gordium, which is said to be the seat of the ancient Midas, he saw the famous chariot fastened with cords made of the rind of the cornel-tree, which whosoever should untie, the inhabitants had a tradition, that for him was reserved the empire of the world. Most authors tell the story that Alexander finding himself unable to untie the knot, the ends of which were secretly twisted round and folded up within it, cut it asunder with his sword. But Aristobulus tells us it was easy for him to undo it, by only pulling the pin out of the pole, to which the yoke was tied, and afterwards drawing off the yoke itself from below."

---

From The Lives of the Noble Grecians and Romans, by Plutarch, translated by John Dryden, revised by Arthur Hugh Clough, Modern Library, Random House, reprint of Clough edition (1864), from the section on Alexander the Great.

☆U.S. Government Printing Office: 1979 - 678-488/301

NOTE 351

FIELD EXCITATION OF  
MULTICONDUCTOR TRANSMISSION LINES

by

Fred M. Tesche  
Tom K. Liu  
Steve K. Chang  
David V. Giri

September 1978

FIELD EXCITATION OF  
MULTICONDUCTOR TRANSMISSION LINES

ABSTRACT

This note discusses the excitation of a multiconductor transmission line by an incident electromagnetic field. Specific relations in terms of field-induced voltage and current sources which are distributed along the transmission line. It is shown how these sources are derived from a knowledge of the incident (or free space) fields by using a field coupling parameter. The components of the exciting fields along the line are then given explicitly for the special case of an incident plane wave with arbitrary angle of incidence.

## SECTION I INTRODUCTION

Recently there has been a renewed interest in transmission-line theory and its application to the internal interaction problems involving electromagnetic pulse (EMP) excitation of aerospace systems. One new development in this area has been the formulation of an analysis procedure to study large interconnected networks of multi-conductor transmission lines. This analysis, which is described in refs. (1) and (2), and the resulting computer program (ref. 3), will permit not only simple branching of transmission lines within the network, but also complicated looping of lines. Thus, an arbitrarily interconnected set of transmission lines can be analyzed using this approach.

The analysis of the transmission-line networks described in refs. (1) and (2) is based on the network excitation being due to lumped (or discrete) voltage and current sources located at a source position somewhere along each transmission-line section (tube). While this specification of sources may be useful for certain applications, it is not particularly useful for EMP studies, where the transmission-line network is excited by an incident, transient electromagnetic field. In the EMP case, not only is the transmission-line excitation distributed along the line, but the fundamental excitation quantities are the incident electric and magnetic fields ( $\vec{E}$  and  $\vec{B}$ ), not the current and voltage sources. Thus, it is necessary to modify the past analysis to permit distributed field excitation of the transmission lines.

Field excitation of simple open two-wire lines has been considered by a number of authors and two separate, but equivalent, approaches used. Taylor, Satterwhite and Harrison (ref. 4) and Smith (ref. 5) derive a coupling model based on the incident tangential electric fields on both wires of the transmission line and on the short wires of the loads at the ends of the line. This approach is based on the integral form of Maxwell's equations as applied to the closed loop formed by the two parallel wires of the transmission

line and the two loads at the ends. In this formulation, there appear distributed voltage sources in both wires of the transmission line, as well as voltage sources at both loads terminating the line.

A different approach has been used by Lee (ref. 6) to determine the distributed field excitation. This is based on the differential forms of Maxwell's equations and yields distributed current and voltage sources along the line, with the voltage source being proportional to the  $\bar{H}$  field and the current source being related to the  $\bar{E}$  field.

Both of these formulations yield identical results for computing the TEM currents flowing on a two-wire line excited by an incident field. The former approach has been extended to the case of multiconductor transmission lines by Paul (ref. 7) and Frankel (ref. 8), and is similar to that discussed in this report. A slightly different approach has been employed by Kajfez and Wilton in ref. (9), where the concepts of reciprocity have been used to obtain the multiconductor transmission-line response to a small aperture excitation of the line. The method of refs. (4) and (5) has been applied to multiconductor systems by Strawe (ref. 10), but his report is not widely distributed.

The present report discusses in detail the excitation of multiconductor transmission lines by an incident electromagnetic field using the differential formulation. Section II presents the derivation of the equations describing the terminal, or load, current responses of a multiconductor transmission line. These equations have, as sources, both distributed voltage and current generators which are induced by incident magnetic and electric fields. Section III first discusses the derivation of these local sources in terms of the local fields and transmission-line geometry. The concept of an "equivalent separation" between conductors, as commonly used for two-wire lines, is then developed for an arbitrary multiconductor transmission line. Finally, in Section IV, the incident field components which contribute to the distributed sources are given for an incident plane wave striking the line at an arbitrary angle of incidence.

## SECTION II

## MULTICONDUCTOR TRANSMISSION-LINE RESPONSE TO DISTRIBUTED SOURCES

As discussed in ref. (1), the response of a general transmission-line network may be calculated by decomposing the currents on each tube of the transmission line into forward and reverse propagating components. At every junction within the network, a scattering matrix can be derived to express all scattered components of current in terms of the incident components. These two sets of relations can be combined to form a large matrix equation for the incident currents. This equation, called the BLT equation, can be inverted numerically and the incident currents determined. Through the scattering matrices, the scattered and, thus, the total currents on the lines, can be determined.

A basic element of the above network analysis is the determination of the propagation properties of the forward and backward waves on the line, as well as their relative excitation by sources along the line. For the purpose of this section, therefore, we will consider only a single section (tube) of multiconductor transmission line.

Consider a lossless section of multiconductor transmission line having no sources, as shown in Figure 1. The length of the line is denoted by  $l$  and it contains  $N$  wires with the  $N+1^{\text{st}}$  wire being the reference conductor. The  $N+1$  wires are required to be parallel, but not necessarily coplanar. For such a line, its electrical properties are determined by a capacitive coefficient matrix,  $(C'_{n,m})$ , and an inductive coefficient matrix,  $(L'_{n,m})$ , which depend only on line geometry and dielectric properties around the line. For this line, these matrices are nonsingular matrices of order  $N$ .

As discussed in ref. (1), the voltages and currents on this line without sources must obey a coupled set of partial differential equations as

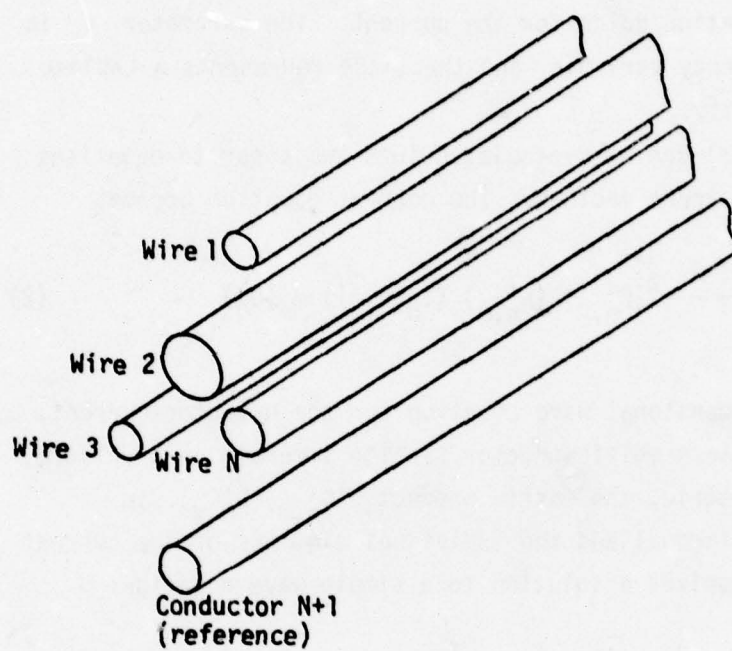


Figure 1. Section of multiconductor transmission line.

$$\frac{\partial}{\partial z} \begin{pmatrix} (\tilde{V}_n(z,s)) \\ (\tilde{I}_n(z,s)) \end{pmatrix} = -s \begin{pmatrix} (0_{n,m}) & (L'_{n,m}) \\ (C'_{n,m}) & (0_{n,m}) \end{pmatrix} \begin{pmatrix} (\tilde{V}_n(z,s)) \\ (\tilde{I}_n(z,s)) \end{pmatrix} \quad (1)$$

where the notation  $(\tilde{V}_n)$  represents an N-vector for the line voltage and a similar notation holds for the current. The parameter  $s$  is the complex frequency variable, and the tilde represents a Laplace transformed quantity.

Equation (1) can be manipulated into two separate equations for voltage and current vectors. The current equation becomes

$$\frac{\partial^2 (\tilde{I}_n(z,s))}{\partial z^2} - s^2 (C'_{n,m}) (L'_{n,m}) (\tilde{I}_n(z,s)) = (0_n) \quad (2)$$

which is a one-dimensional wave equation for the N-vector current.

For a lossless multiconductor section immersed in a uniform, homogeneous dielectric, the matrix product  $(C'_{n,m})(L'_{n,m})$  in Equation (2) is diagonal and the individual elements of the current N-vector are themselves a solution to a simple wave equation:

$$\frac{\partial^2 I_n(z,s)}{\partial z^2} - \frac{s^2}{v^2} \tilde{I}_n(z,s) = 0$$

where  $v$  is the velocity of wave propagation on the line.

A more general line, however, does not have a diagonal result for the  $(C'_{n,m})(L'_{n,m})$  matrix, although it is possible to diagonalize it through the use of a nonsingular  $N \times N$  transformation matrix, denoted by  $(T_{n,m})$ , which consists of the current eigenmodes,  $(\phi_n)_i$ , as columns. The  $\phi_n$ 's are solutions to the eigenvalue equation

$$s^2 (C'_{n,m}) (L'_{n,m}) (\phi_n)_i = \tilde{\gamma}_i^2 (\phi_n)_i \quad (3)$$

where  $\tilde{\gamma}_i^2$  is the  $i^{\text{th}}$  eigenvalue corresponding to the eigenmode  $(\phi_n)_i$ .

By introducing a change of variables as

$$(\tilde{I}_n(z,s)) = (T_{n,m})(\tilde{i}_n(z,s)) \quad (4)$$

where  $(\tilde{i}_n(z,s))$  represents the modal currents, the wave equation for the modal currents becomes

$$\frac{\partial^2 (\tilde{i}_n(z,s))}{\partial z^2} = s^2 (T_{n,m})^{-1} (C'_{n,m}) (L'_{n,m}) (T_{n,m}) (\tilde{i}_n) = (\tilde{\gamma}_{n,m})^2 (\tilde{i}_n) \quad (5)$$

where  $(\tilde{\gamma}_{n,m})^2$  is a diagonal matrix containing the  $\tilde{\gamma}_i^2$  terms as elements.

Since the matrix  $(\tilde{\gamma}_{n,m})^2$  in Equation (5) is diagonalized, the solution for the modal currents can be expressed directly as exponential functions of position, and the total solution for the line currents becomes

$$(\tilde{I}_n(z,s)) = (T_{n,m}) \left( e^{-(\tilde{\gamma}_{n,m})z} (\tilde{\alpha}_n^+) + e^{(\tilde{\gamma}_{n,m})z} (\tilde{\alpha}_n^-) \right) \quad (6)$$

where  $(\tilde{\alpha}_n^+)$  and  $(\tilde{\alpha}_n^-)$  are N-vectors which define the amplitudes of each of the propagating modes on the line and which depend on the line termination and excitation. The terms  $e^{\pm(\tilde{\gamma}_{n,m})z}$  are diagonal matrices having as elements  $e^{\pm\tilde{\gamma}_i z}$ , where  $\tilde{\gamma}_i = +\sqrt{\tilde{\gamma}_i^2}$ .

A similar development for the line voltage  $(\tilde{V}_n(z,s))$  can be carried out to determine voltage modes and a propagation equation similar to Equation (6). By defining a characteristic impedance matrix as

$$(Z_{C_{n,m}}) = s^{-1} (C'_{n,m})^{-1} (T_{n,m}) (\tilde{\gamma}_{n,m}) (T_{n,m})^{-1} \quad (7)$$

the line voltage N-vector can be expressed using the same constants  $(\tilde{\alpha}_n^+)$  and  $(\tilde{\alpha}_n^-)$  as in Equation (6):

$$(\tilde{V}_n(z,s)) = (\tilde{Z}_{C_{n,m}})(T_{n,m}) \left( e^{-(\tilde{\gamma}_{n,m})z} (\tilde{\alpha}_n^+) - e^{(\tilde{\gamma}_{n,m})z} (\tilde{\alpha}_n^-) \right) \quad (8)$$

The unknown constants  $(\tilde{\alpha}_n^+)$  and  $(\tilde{\alpha}_n^-)$  are determined by taking into account the loads at each end of the line, as well as the excitation. Consider the line shown in Figure 2, which has lumped voltage and current sources at  $z = z_s$ , as well as load impedances  $(\tilde{Z}_{1n,m})$  and  $(\tilde{Z}_{2n,m})$  at  $z = 0$  and  $z = \ell$  respectively. On the section of the line  $0 \leq z \leq z_s$  Equations (6) and (8) are valid, since this section of the line is source free. Similarly, for  $z_s \leq z \leq \ell$  similar equations are valid, but with different constants,  $(\tilde{\alpha}_n)$ . By relating  $(\tilde{V}_n(z,s))$  to  $(\tilde{I}_n(z,s))$  at  $z = 0$ , and  $z = \ell$  through the load impedance matrices and by relating the discontinuities of  $(\tilde{V}_n(z,s))$  and  $(\tilde{I}_n(z,s))$  to the voltage and current sources at  $z = z_s$ , a set of linear equations can be developed with the  $(\tilde{\alpha}_n)$  constants for each section of line as unknowns.

Of special interest are the load currents, i.e.,  $(\tilde{I}_n(0,s))$  and  $(\tilde{I}_n(\ell,s))$ . Using the solutions for the  $(\tilde{\alpha}_n)$  as well as Equation (6) for  $z = 0$  and  $z = \ell$ , the load currents may be expressed as:

$$\begin{bmatrix} (\tilde{I}_n(0,s)) \\ (\tilde{I}_n(\ell,s)) \end{bmatrix} = \begin{bmatrix} (\delta_{n,m}) + (\tilde{\Gamma}_{1n,m}) & (0_{n,m}) \\ (0_{n,m}) & (\delta_{n,m}) + (\tilde{\Gamma}_{2n,m}) \end{bmatrix} \cdot \begin{bmatrix} -(\tilde{\Gamma}_{1n,m}) & (T_{n,m}) \cdot e^{(\tilde{\gamma}_{n,m})z} \cdot (T_{n,m})^{-1} \\ (T_{n,m}) \cdot e^{(\tilde{\gamma}_{n,m})\ell} \cdot (T_{n,m})^{-1} & -(\tilde{\Gamma}_{2n,m}) \end{bmatrix}^{-1} \begin{bmatrix} (\tilde{J}_n^-(s)) \\ (\tilde{J}_n^+(s)) \end{bmatrix} \quad (9)$$

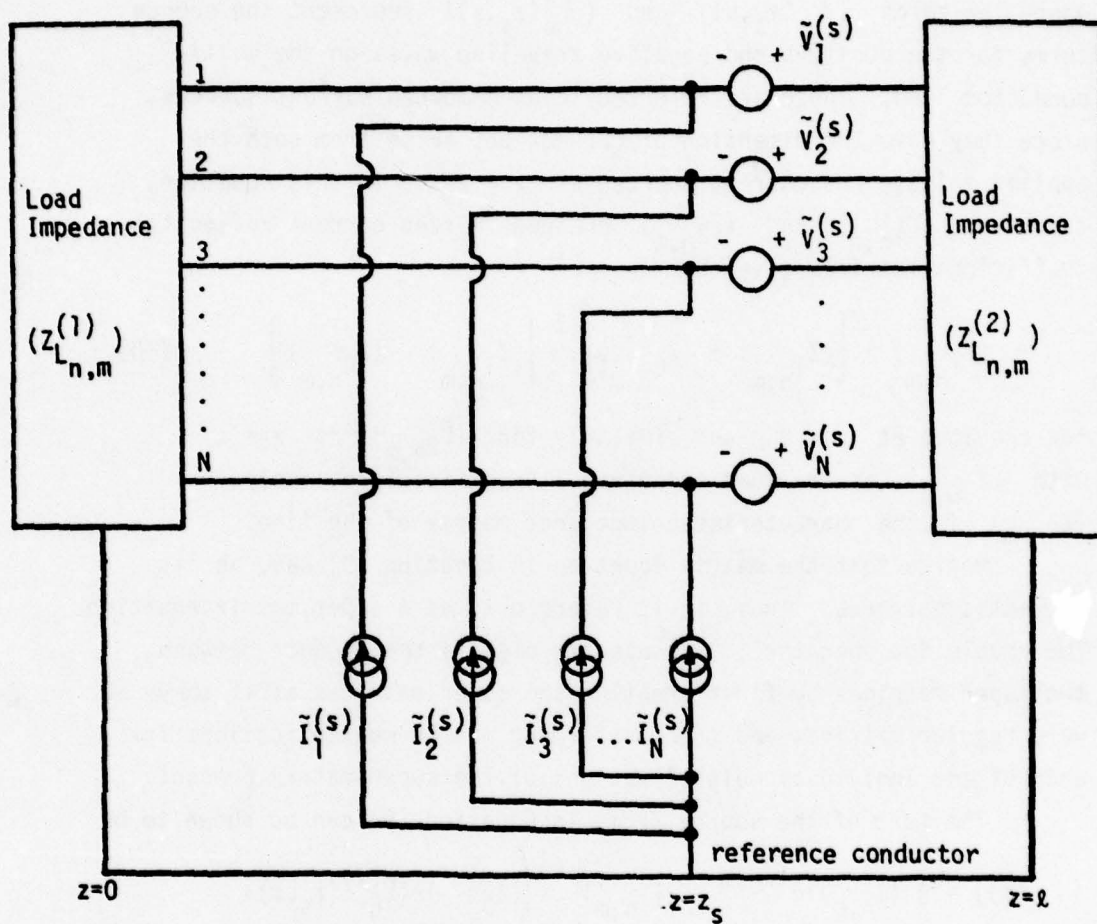


Figure 2. Single length of multiconductor transmission line with loads and lumped sources at  $z = z_s$ .

where the terms  $(\tilde{f}_n^+(z_s, s))$  and  $(\tilde{f}_n^-(z_s, s))$  represent the source terms for the positive and negative traveling waves on the multi-conductor line. Those are referred to as combined current sources, since they have the dimension of current but arise from both the applied voltage and current sources at  $z = z_s$ . In this equation, the terms  $(\tilde{\Gamma}_{1n,m})$  and  $(\tilde{\Gamma}_{2n,m})$  are generalized current reflection coefficient matrices given by

$$(\tilde{\Gamma}_{1n,m}) = \left[ (\tilde{Z}_{1n,m}) + (Z_{Cn,m}) \right]^{-1} \cdot \left[ (\tilde{Z}_{1n,m}) - (Z_{Cn,m}) \right] \quad (10)$$

for the load at  $z = 0$ , and similarly for  $(\tilde{\Gamma}_{2n,m})$  at  $z = \ell$  with  $(\tilde{Z}_{2n,m})$  as the load impedance. As defined previously,  $(Z_{Cn,m})$  is the characteristic impedance matrix of the line.

Notice that the matrix equation in Equation (9) has, as its elements, matrices. Thus, it is referred to as a super matrix equation. The double dot operator  $(:)$  is used to signify the product between two super matrices by first treating the super matrices as if they were regular matrices and then performing matrix multiplications for each of the individual multiplications of the super matrix product.

The form of the source terms in Equation (9) can be shown to be

$$(\tilde{f}_n^-(s)) = \frac{1}{2} (T_{n,m}) \cdot e^{(\tilde{Y}_{n,m})z_s} \cdot (T_{n,m})^{-1} \cdot \left( (Z_{Cn,m}) \cdot (\tilde{V}_n^{(s)}(z_s, s)) + (\tilde{I}_n^{(s)}(z_s, s)) \right) \quad (11)$$

and

$$(\tilde{f}_n^+(s)) = \frac{1}{2} (T_{n,m}) \cdot e^{(\tilde{Y}_{n,m})(\ell - z_s)} \cdot (T_{n,m})^{-1} \cdot \left( (Z_{Cn,m})^{-1} \cdot (\tilde{V}_n^{(s)}(z_s, s)) - (\tilde{I}_n^{(s)}(z_s, s)) \right) \quad (12)$$

With these source terms, the terminal response of the transmission line can be determined for lumped voltage and current sources at  $z = z_s$ . For field excitation of the transmission line, it is

necessary to consider distributed excitation, as opposed to the discrete excitation discussed above. This can be regarded as a simple extension of Equations (11) and (12) by integrating over the source terms  $(\tilde{V}_n^{(s)})$  and  $(\tilde{I}_n^{(s)})$ . Doing this, the combined current sources become

$$(\tilde{J}_n^-(s)) = \frac{1}{2} \int_0^l \left( (T_{n,m}) \cdot e^{(\tilde{Y}_{n,m})\xi} \cdot (T_{n,m})^{-1} \cdot ((Z_{c_{n,m}})^{-1} \cdot (\tilde{V}_n^{(s)}(\xi, s)) + (\tilde{I}_n^{(s)}(\xi, s))) \right) d\xi \quad (13)$$

$$(\tilde{J}_n^+(s)) = \frac{1}{2} \int_0^l \left( (T_{n,m}) \cdot e^{(\tilde{Y}_{n,m})(l-\xi)} \cdot (T_{n,m})^{-1} \cdot ((Z_{c_{n,m}})^{-1} \cdot (\tilde{V}_n^{(s)}(\xi, s)) - (\tilde{I}_n^{(s)}(\xi, s))) \right) d\xi \quad (14)$$

which follows directly from superposition. Notice that now the voltage and current sources are per-unit-length quantities, and hence denoted by a prime. These quantities must be determined given a knowledge of the incident electromagnetic field on the line, as well as a knowledge of the transmission line cross-sectional geometry. This is discussed in the next section of this report.

## SECTION III

## DETERMINATION OF DISTRIBUTED VOLTAGE AND CURRENT SOURCES

As indicated in the previous section, the terminal (or load) currents of a multiconductor transmission line can be evaluated using Equations (9), (13) and (14) if the distributed voltage and current sources  $(\tilde{V}_n^{(s)}(z,s))$  and  $(\tilde{I}_n^{(s)}(z,s))$  are known everywhere along the line. In some instances, such as a small aperture or other localized source close to the transmission line, it is possible to approximate the solution using a discrete source position, as in ref. (9). For an arbitrarily incident plane wave, however, this is not possible. Sources distributed over the entire line are necessary.

Consider the case of a single multiconductor cable in free space and with impedance terminations at each end, as shown in Figure 3. Assume that in this bundle there are  $n+1$  wires, with the  $n+1^{\text{st}}$  wire being the reference conductor. The electric and magnetic fields in the vicinity of the line can be divided into two parts. These are the incident components,  $\tilde{E}^{\text{inc}}$  and  $\tilde{H}^{\text{inc}}$  and the scattered components  $\tilde{E}^s$  and  $\tilde{H}^s$ , such that

$$\tilde{E} = \tilde{E}^{\text{inc}} + \tilde{E}^s \quad (15a)$$

$$\tilde{H} = \tilde{H}^{\text{inc}} + \tilde{H}^s \quad (15b)$$

The scattered field components are caused entirely by the induced currents and charges on the  $n+1$  wires, as well as by the currents on the terminations. The scattered fields from the line can be further subdivided into three different classes. There are TEM, TE and TM transmission line modes, which are produced by "transmission line" currents, having the property that the components of the total current on each of the conductors sum to zero.

In addition to these currents, there are "antenna mode" currents. These are currents which flow on each wire (but with a different magnitude

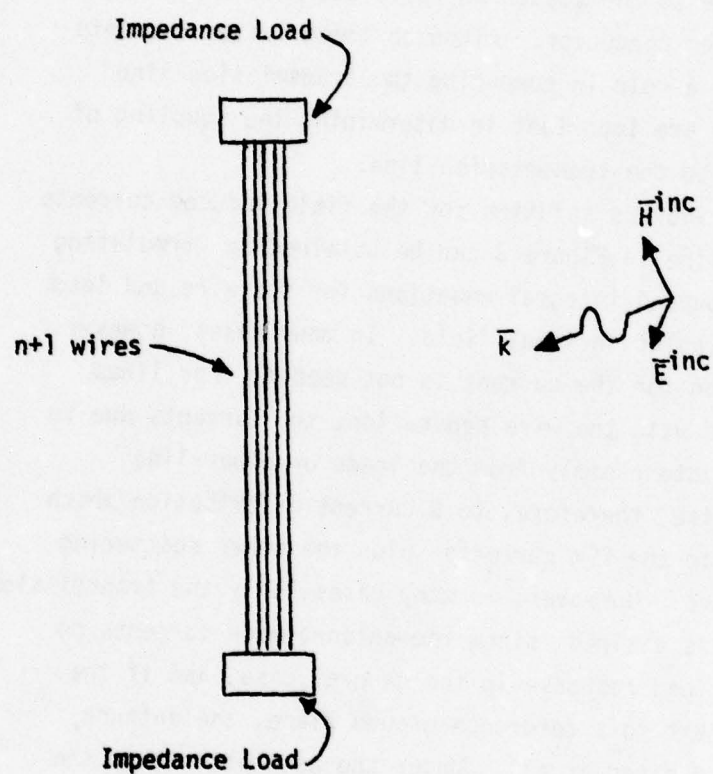


Figure 3. Isolated multiconductor line excited by incident plane wave.

for each wire, in general) and are subject to the constraint that the voltage difference between any two conductors in a transverse plane is zero. Furthermore, these currents go to zero at the ends of the line.

Finally, there can exist quasi-static current and charge distributions which contribute to the scattered field but have a net current or charge of zero on each conductor. Although these latter currents and charges do not play a role in computing the transmission-line response directly, they are important in determining the coupling of electromagnetic fields to the transmission line.

A complete and rigorous solution for the field induced currents on the multiconductor line in Figure 3 can be obtained by formulating and solving a set of coupled integral equations for the wire and load currents, given a particular incident field. In many cases, however, such a complete solution for the current is not needed. For lines which are long compared with the wire separation, the currents due to TE and TM fields attenuate rapidly from the loads or other line terminations, giving rise, therefore, to a current distribution which corresponds primarily to the TEM currents plus the other scattering currents mentioned above. Moreover, in many cases, only the transmission-line current response is desired since the antenna mode currents do not contribute to the load response in the general case, and if the transmission line is next to a reference ground plane, the antenna mode currents are not excited at all. Under the assumption that the TE and TM currents are negligible and neglecting the effects of load currents, the total  $\vec{E}$  and  $\vec{H}$  fields in the vicinity of the transmission line can be written as

$$\vec{E} = \vec{E}^{inc} + \vec{E}^{ant} + \vec{E}^{TEM} + \vec{E}^{st} \quad (16a)$$

and

$$\vec{H} = \vec{H}^{inc} + \vec{H}^{ant} + \vec{H}^{TEM} + \vec{H}^{st} \quad (16b)$$

where the subscript (inc) refers to the incident (or free space) fields, (ant) denotes the fields produced by the antenna mode currents, (TEM) stands for the fields due to the transmission-line currents, and (st) is for the portion of the fields caused by the static distribution of current and charge on the wires, determined with the condition that the total current and charge be zero on each wire.

Following the approach used in ref. (11) for single-wire lines and in ref. (7) for multiconductor lines, Maxwell's equations can be used to derive a  $v-i$  relation for the transmission line currents. Consider a uniform section of multiconductor line shown in Figure 4. For a time dependence of  $e^{st}$ , Maxwell's equation may be written as

$$\nabla \times \tilde{\mathbf{E}} = -s \tilde{\mathbf{B}} \quad (17)$$

and on a path  $C_1$ , from the reference conductor to wire 1 (where  $d\bar{\ell}_1$  represents an element of the path, and  $\hat{n}_1$  is the normal to the path), we can integrate Equation (17) to yield the following:

$$-\frac{d}{dz} \int_a^b \tilde{\mathbf{E}} \cdot d\bar{\ell} = s \int_a^b \tilde{\mathbf{B}} \cdot \hat{n} d\ell \quad (18)$$

This result is standard, and its derivation will not be repeated here.

Noting that the line integral of the electric field in Equation (18) is the negative of the voltage between the two conductors, this equation may be written as

$$\begin{aligned} \frac{d\tilde{V}_1}{dz} = & j\omega \int_a^b \tilde{\mathbf{B}}^{\text{TEM}} \cdot \hat{n} d\ell + j\omega \int_a^b \tilde{\mathbf{B}}^{\text{ant}} \cdot \hat{n} d\ell \\ & - j\omega \int_a^b (\tilde{\mathbf{B}}^{\text{inc}} + \tilde{\mathbf{B}}^{\text{st}}) \cdot \hat{n} d\ell \end{aligned} \quad (19)$$

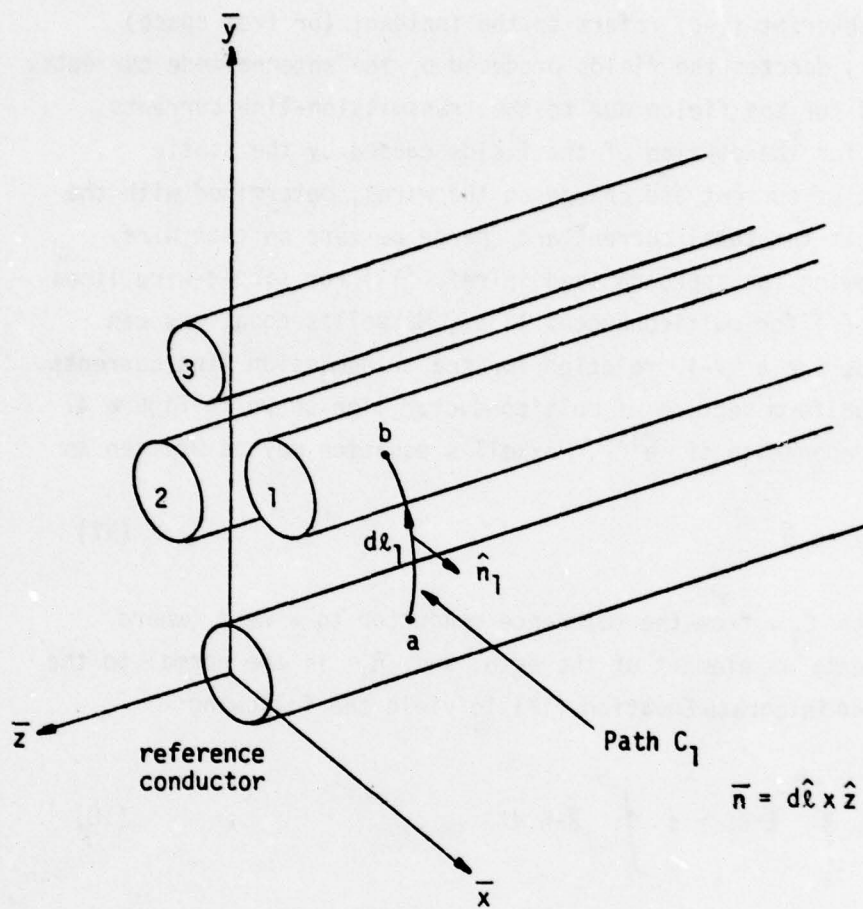


Figure 4. Cross section of multiconductor line showing integration path  $C_1$  from point  $a$  to  $b$ .

As discussed by Paul in ref. (7), the term involving the  $\tilde{B}^{\text{TEM}}$  field, which arises from all TEM currents on the multiconductor line and is a magnetic flux per unit length, can be computed in terms of the inductance coefficient matrix elements as

$$-\int_a^b \tilde{B}^{\text{TEM}} \cdot \hat{n} \, d\ell \equiv \phi_1 = L_{11} \tilde{I}_1 + L_{12} \tilde{I}_2 + \dots L_{1n} \tilde{I}_n \quad (20)$$

where  $\tilde{I}_1 \dots \tilde{I}_n$  represent the currents on the  $n$  (non-reference) conductors.

From our definition of the "antenna mode" currents, the voltage between wire 1 and the reference is zero for these currents, which implies that the antenna current flux term is also zero. See ref. (12). Thus, we have the relation

$$\int_a^b \tilde{B}^{\text{ant}} \cdot \hat{n} \, d\ell \equiv 0 \quad (21)$$

With these substitutions, Equation (19) can be written as

$$\frac{d\tilde{V}_1}{dz} = -j\omega (L'_{11} \tilde{I}_1 + L'_{12} \tilde{I}_2 + \dots L'_{1n} \tilde{I}_n) + s \int_a^b (\tilde{B}^{\text{inc}} + \tilde{B}^{\text{st}}) \cdot \hat{n} \, d\ell \quad (22)$$

This procedure may be repeated for each of the  $n$  wires in the bundle, and the resulting equations expressed in matrix form are

$$\frac{d(\tilde{V}_n)}{dz} = -s (L'_{n,m}) \cdot (\tilde{I}_n) + s \left( \int_n^b (\tilde{B}^{inc} + \tilde{B}^{st}) \cdot \hat{n}_n d\ell_n \right) \quad (23)$$

The last term in this equation has dimensions of (volts/unit length) and is essentially a distributed voltage source for the transmission line. Denoting this by  $(\tilde{V}'_n(s))$ , we then have

$$(\tilde{V}'_n(s)) = s\mu_0 \left( \int_n^b (\tilde{H}^{inc} + \tilde{H}^{st}) \cdot \hat{n}_n d\ell_n \right) \quad (24)$$

where the relation  $\tilde{B} = \mu_0 \tilde{H}$  has been used. The differential equation for voltage and current in Equation (23) then becomes

$$\frac{d(\tilde{V}_n)}{dz} + s(L'_{n,m}) \cdot (\tilde{I}_n) = (\tilde{V}'_n(s)) \quad (25)$$

A similar manipulation can be performed using the other Maxwell equation

$$\nabla \times \tilde{H} = s\epsilon \tilde{E} \quad (26)$$

to obtain the second telegrapher's equation containing sources. Applying this to the contour  $C_1$  in exactly the same manner as in ref. (11), the following relation may be derived.

$$- \frac{d}{dz} \int_1^b \tilde{H} \cdot \hat{n} d\ell = s\epsilon \int_1^b \tilde{E} \cdot d\bar{\ell} \quad (27)$$

By inserting Equation (16a) into this last equation and noting that the antenna mode contributions vanish, since by definition of the antenna currents,  $\oint \tilde{\mathbf{E}}^{\text{ant}} \cdot d\tilde{\mathbf{l}} = 0$  and  $\oint \tilde{\mathbf{H}}^{\text{ant}} \cdot \hat{\mathbf{n}} d\ell = 0$ , this equation can be written as

$$-\frac{d}{dz} \int_a^b (\tilde{\mathbf{H}}^{\text{inc}} + \tilde{\mathbf{H}}^{\text{st}} + \tilde{\mathbf{H}}^{\text{TEM}}) \cdot \hat{\mathbf{n}} d\ell = s \epsilon \int_a^b \tilde{\mathbf{E}} \cdot d\tilde{\mathbf{l}} \quad (28)$$

or, as done by Lee (ref. 11), expressed as

$$-\frac{d}{dz} \int_a^b \tilde{\mathbf{H}}^{\text{TEM}} \cdot \hat{\mathbf{n}} d\ell = s \epsilon \int_a^b \tilde{\mathbf{E}} \cdot d\tilde{\mathbf{l}} - s \epsilon \int_a^b (\tilde{\mathbf{E}}^{\text{inc}} + \tilde{\mathbf{E}}^{\text{s}}) \cdot d\tilde{\mathbf{l}} \quad (29)$$

Using Equation (20) and recognizing that  $\int_a^b \tilde{\mathbf{E}} \cdot d\tilde{\mathbf{l}}$  is the voltage  $-V_1$ , Equation (29) becomes

$$\frac{1}{\mu} \frac{d}{dz} (L'_{11} \tilde{I}_1 + \dots L'_{1n} \tilde{I}_n) = -s \epsilon \tilde{V}_1 - s \epsilon \int_a^b (\tilde{\mathbf{E}}^{\text{inc}} + \tilde{\mathbf{E}}^{\text{s}}) \cdot d\tilde{\mathbf{l}} \quad (30)$$

for the first wire. This process can be repeated for each wire, and the following matrix equation can be developed for the transmission line currents  $(\tilde{I}_n)$  and voltages  $(\tilde{V}_n)$ :

$$\frac{1}{\mu} (L'_{n,m}) \cdot \frac{d(\tilde{I}_n)}{dz} = -s \epsilon (\tilde{V}_n) - s \epsilon \left( \int_n^{b_n} (\tilde{\mathbf{E}}^{\text{inc}} + \tilde{\mathbf{E}}^{\text{s}}) \cdot d\tilde{\mathbf{l}}_n \right) \quad (31)$$

Rearranging terms slightly yields the second telegrapher's equation

$$\frac{d(\tilde{I}_n)}{dz} + s(C'_{n,m}) \cdot (\tilde{V}_n) = (\tilde{I}_n'(s)) \quad (32)$$

where the source term  $(\tilde{I}_n'(s))$  is given by

$$(\tilde{I}_n'(s)) = -s(C'_{n,m}) \cdot \left( \int_a^{b_n} (\tilde{E}^{inc} + \tilde{E}^s) \cdot d\vec{l}_n \right) \quad (33)$$

Note that in deriving this relation, the assumption that

$$(L'_{n,m}) \cdot (C'_{n,m}) = \mu_0 \epsilon \quad (34)$$

has been employed, a result which implies that the lines are within a uniform, homogeneous dielectric medium.

In an inhomogeneous dielectric region, say for the case of each conductor having a separate dielectric jacket, it is known that true TEM modes cannot exist. However, an approximate analysis can be carried out by assuming that Equations (25) and (32) are applicable. The validity of this "quasi-TEM" assumption lies in the reasonable comparison of theoretical and experimental results for the multi-conductor system (ref. 13).

It is to be noted that the basic telegrapher's equations derived here for the transmission line currents and voltages are different in form than those developed by Paul (ref. 7). This is due to the fact that Paul has integrated from the center of one conductor to the other center, not from one surface to another of the thin, widely spaced conductors which he considers. For the more general case of fat, closely spaced wires, the total static electric and magnetic field in

any transverse plane must be used to compute the equivalent line sources.

Aside from a difference in the definition of the unit normal vector  $\hat{n}$ , the major difference between the formulation of Lee in ref. (11) and the present analysis is the existence of an additional antenna mode source term in Lee's two-wire analysis. This two-wire analysis could be extended to a multiwire case, and thus would imply the existence of similar source terms in the present multiconductor analysis. As discussed by Frankel (ref. 12), the apparent discrepancy arises out of different choices for the "antenna current" by Lee, which thus has an effect on the remaining transmission-line current.

As stated earlier, our choice of the "antenna current" is that current flowing in each wire which produces a voltage difference of zero between any conductor and another at any transverse plane in the line. This choice is also used by Uchida (ref. 14), and thus leads to a decoupling of the transmission line currents from the antenna mode currents.

Although explicit expressions for the voltage and current sources have been developed in Equations (24) and (33), it still remains necessary to evaluate the scattered static fields  $\tilde{E}^s$  and  $\tilde{H}^s$ , before the source terms can be used in Equations (13) and (14) to determine the load response of the multiconductor line. To determine these source terms, it is necessary to solve two static boundary value problems. To determine the current source in Equation (33), it is necessary to solve the two-dimensional static problem illustrated in Figure 5. An incident (free space) electric field strikes a collection of conductors, on which the net charges are zero. A static scattered field is produced by the local charges induced on each wire, and the

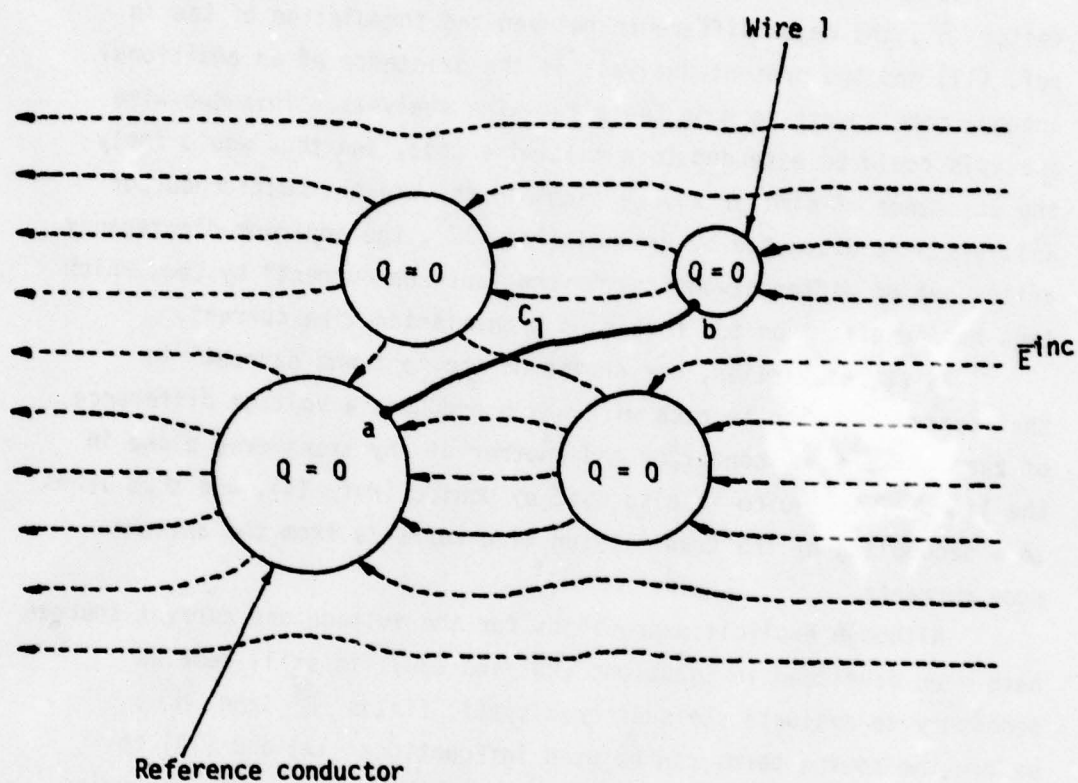


Figure 5. Cross section of multiconductor cable in incident  $E$  field showing typical field distribution and integration path from a to b. Each conductor has zero net charge.

integrals in Equation (33) are then evaluated along any contour from point  $a$  to  $b$ , using the total scattered field,  $\vec{E}^{inc} + \vec{E}^s$ .

The solution to this problem for the multiconductor case is similar to the two-wire problem discussed by Lee, but extended to more wires. It is solved by looking for the solution to

$$\nabla^2 \phi = 0 \quad (34)$$

exterior to the wires, with the condition that  $\phi = \text{constant}$  on each of the conductors subject to the constraint that

$$\oint \frac{\partial \phi_i}{\partial n_i} dS_i = 0 \quad (35)$$

on each conductor,  $i$ , and that at infinity, the potential is

$$\phi \Rightarrow \phi^{inc} = -\vec{r} \cdot \vec{E}^{inc} \quad (36)$$

Here  $\phi^{inc}$  represents the incident or free-space potential field in the absence of the transmission line. Once this equation is solved (usually by numerical means) the potentials of each wire,  $\phi_i$ , can be determined, and the integrals of Equation (33) can be determined directly

$$\int_a^{b_i} (\vec{E}^{inc} + \vec{E}^s) \cdot d\vec{l}_i = -(\phi_i - \phi_{n+1}) \quad (37)$$

It is possible, however, to express the integral in Equation (37) in a simpler form, using only the incident field,  $\vec{E}^{inc}$ , and a vector equivalent distance,  $\vec{h}_i$ , in a manner similar to that of ref. (11). Consider an auxiliary problem which has a potential field given by  $\phi^*$  and is defined by the relations

$$\nabla^2 \phi^* = 0 \quad (38)$$

with  $\phi_j^* = \text{constant}$  (but unknown) on each of the  $i$  conductors of

the multiconductor bundle, and with

$$\oint \frac{\partial \phi_j}{\partial n_j} dS_j = 0 \quad (39)$$

for all conductors except for the  $i^{\text{th}}$  conductor and the reference conductor, where we have the constraint

$$\oint_{\text{wire } i} \frac{\partial \phi_i}{\partial n} dS_i = - \frac{Q_i^*}{\epsilon} \quad (40)$$

and

$$\oint_{\text{reference}} \frac{\partial \phi_{n+1}}{\partial n_{n+1}} dS_{n+1} = \frac{Q_i^*}{\epsilon} \quad (41)$$

The solution to this auxiliary problem can be used to find the field excitation of the transmission line by using Green's identity,

$$\phi^* \nabla^2 \phi - \phi \nabla^2 \phi^* = 0 \quad (42)$$

and applying Gauss' theorem to give the expression

$$\oint_{\text{all conductors}} \left( \phi^* \frac{\partial \phi}{\partial n} - \phi \frac{\partial \phi^*}{\partial n} \right) dS + \oint_{S_\infty} \left( \phi^* \frac{\partial \phi}{\partial n} - \phi \frac{\partial \phi^*}{\partial n} \right) dS = 0 \quad (43)$$

where  $S_\infty$  is a closed surface at infinity. Using the facts that  $\phi$  and  $\phi^*$  are constant on the conductors, that

$$\oint \frac{\partial \phi_j^*}{\partial n_j} dS = 0 \quad (44)$$

for all conductors except the  $i^{\text{th}}$  and the reference conductor, and that

$$\oint_{S_\infty} \left( \phi^* \frac{\partial \phi}{\partial n} - \phi \frac{\partial \phi^*}{\partial n} \right) dS = \int_{\text{wires}} \left( \phi^{\text{inc}} \frac{\partial \phi^*}{\partial n} \right) dS = - \frac{1}{\epsilon} \int_{\text{wires}} \phi^{\text{inc}} \sigma^* dS \quad (45)$$

where

$$\sigma_j^* = -\epsilon \frac{\partial \phi_j^*}{\partial n} \quad (46)$$

is the charge density on each conductor for the auxiliary problem and is a known quantity. Equation (43) can then be expressed as

$$\frac{1}{\epsilon} (\phi_i - \phi_{n+1}) \int_{S_i} \sigma_i dS_i = -\frac{1}{\epsilon} \int_{S_1} \phi^{inc} \sigma_1^* dS_1 - \frac{1}{\epsilon} \int_{S_2} \phi^{inc} \sigma_2^* dS_2 - \dots \quad (47)$$

Using Equation (40) and the relation  $\phi^{inc} = -\bar{E} \cdot \bar{r}$ , this last equation takes the form

$$(\phi_i - \phi_{n+1}) = -\bar{E}^{inc} \cdot \bar{h}_i \quad (48)$$

where the vector  $\bar{h}_i$  is defined as

$$\bar{h}_i = \frac{\int_{S_1} r \sigma_1^* dS_1 + \int_{S_2} r \sigma_2^* dS_2 + \dots + \int_{S_{n+1}} r \sigma_{n+1}^* dS_{n+1}}{\int_{S_i} \sigma_i^* dS_i} \quad (49)$$

With this expression, Equation (37) can be conveniently expressed as

$$\int_a^b (\bar{E}^{inc} + \bar{E}^s) \cdot d\bar{l}_i = \bar{E}^{inc} \cdot \bar{h}_i \quad (50)$$

and the  $N$  vector equivalent current source becomes

$$(\tilde{I}_n'(s)) = -s(C_{n,m}') \cdot (\bar{E}^{inc} \cdot \bar{h}_n)_m \quad (51)$$

The vectors  $\bar{h}_i$  are referred to as the "field coupling vectors" for the line, and also as the "effective height" of the conductors.

Physically, they correspond to the vector distance between the charge centroids on the multiconductor system, given a total charge  $Q$  on the  $i^{\text{th}}$  conductor,  $-Q$  on the reference conductor and zero net charge on all others. Figure 6 illustrates these relationships.

For the case of thin, widely separated wires, the vectors  $\bar{h}_i$  are simply the distances from the center of the reference conductor to each of the wires' centers. For more closely spaced wires, the field coupling parameters must be calculated, using the integral equation approach outlined by Giri in ref. (15).

A similar procedure can be carried out for determining the distributed voltage source in Equation (24) by solving a magnetostatic problem. The details of this are identical to that described by Lee (ref. 11), modified by the presence of more than just two conductors. The results are that the same field coupling parameters,  $\bar{h}_i$ , that are used for the electric field calculations may be used for the magnetic fields. This results in the following equation for the distributed voltage source.

$$(\tilde{V}_n'(s)) = s\mu_0 \left( (\bar{h}_n \times \hat{1}_z) \cdot \bar{H}^{\text{inc}} \right) \quad (52)$$

The preceding discussion has been for the field excitation of an isolated multiconductor line, in which one of the conductors in the bundle serves as the reference. An often encountered situation, however, is not this configuration, but one with an  $n$ -wire bundle next to a flat, conducting ground plane. For this case, the ground plane serves as the reference conductor, and the antenna mode currents are not excited.

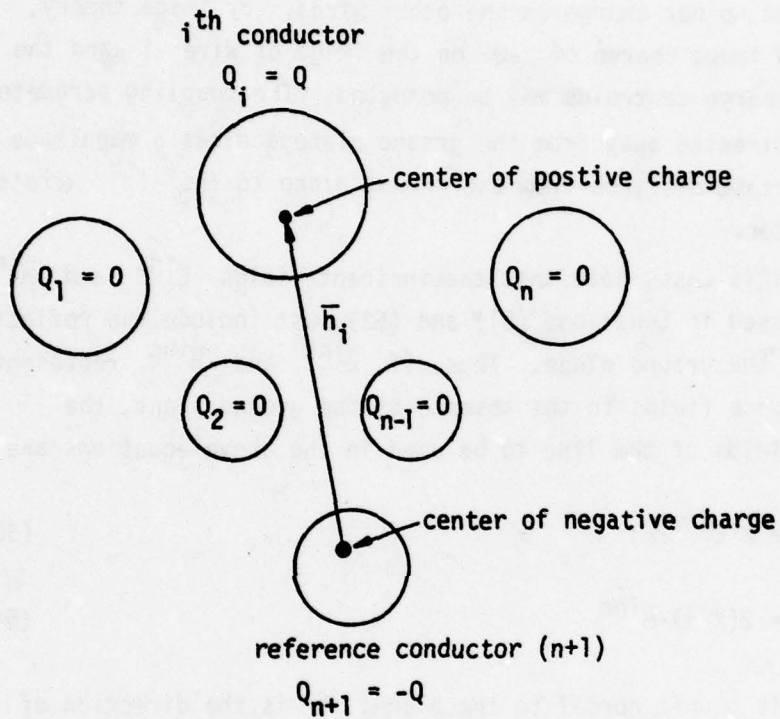


Figure 6. Cross section of isolated  $n+1$  wire multiconductor line, showing field coupling vector for the  $i^{\text{th}}$  conductor.

For this case, the field coupling parameters are still calculated as above. For example, as shown in Figure 7, the coupling parameter  $\bar{h}_i$  is calculated by placing a charge  $Q$  on wire  $i$  and no net charge on the other wires. By image theory, there is an image charge of  $-Q$  on the image of wire  $i$  and the resulting charge centroids may be computed. The coupling parameter vector is directed away from the ground plane and has a magnitude equal to the shortest distance from the ground plane to the  $i^{\text{th}}$  wire's charge center.

In this case, note that the incident fields  $\bar{E}^{\text{inc}}$  and  $\bar{H}^{\text{inc}}$  which are used in Equations (51) and (52) must include the reflection effects of the ground plane. Thus, if  $\bar{E}^{\text{inc}}$  and  $\bar{H}^{\text{inc}}$  represent the free space fields in the absence of the ground plane, the exciting fields of the line to be used in the above equations are

$$E_n = 2(\bar{E}^{\text{inc}} \cdot \hat{n}) \quad (53)$$

and

$$H_t = 2(\hat{k} \times \hat{n}) \cdot \bar{H}^{\text{inc}} \quad (54)$$

where  $\hat{n}$  is a unit normal to the plane,  $\hat{k}$  is the direction of propagation of the incident wave and the subscripts  $n$  and  $t$  represent field components normal to and parallel to the ground plane, respectively.

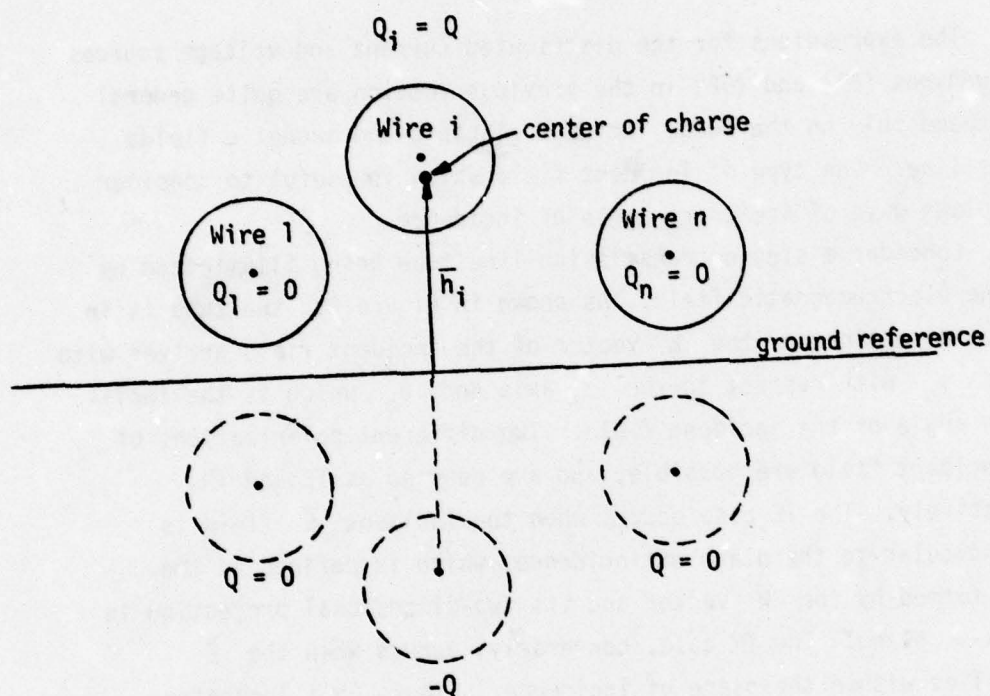


Figure 7. Field coupling vector for Wire i of multiconductor line over a ground plane.

#### SECTION IV EXCITATION FIELDS DUE TO INCIDENT PLANE WAVE

The expressions for the distributed current and voltage sources in Equations (51) and (52) in the previous section are quite general and depend only on the local incident electric and magnetic fields on the line. One type of incident field which is useful to consider is a plane wave of arbitrary angle of incidence.

Consider a single transmission-line tube being illuminated by a plane electromagnetic field. As shown in Figure 8a, the tube is in the  $\hat{z}$  direction and the  $\bar{k}$  vector of the incident field arrives with angles  $\psi_0$  with respect to the  $\hat{z}$  axis and  $\theta_0$ , which is the inclination angle of the incident field. Two different polarizations of the incident field are possible, and are denoted as TE and TM, respectively. The TE case occurs when the incident  $\bar{E}$  field is perpendicular to the plane of incidence, which is defined as the plane formed by the  $\bar{k}$  vector and its two-dimensional projection in the x-y plane. The TM case, conversely, occurs when the  $\bar{E}$  field lies within the plane of incidence. Figure 8b illustrates these different polarizations.

For both of these polarizations, the field components at the multiconductor tube can be expressed as follows:

##### TE Fields

$$H_z^{inc} = -H^{inc} \sin \psi_0$$

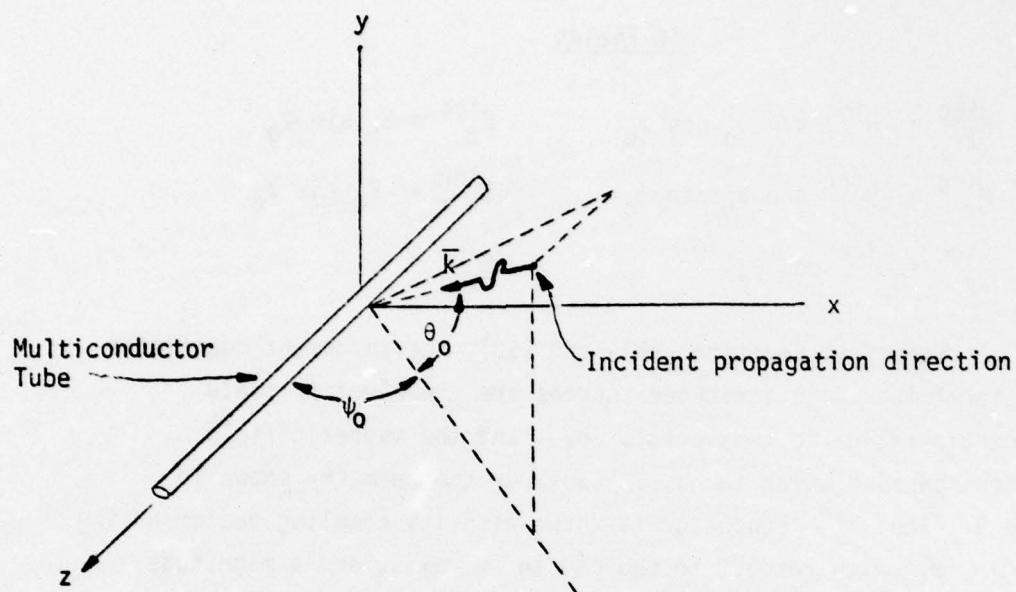
$$H_x^{inc} = H^{inc} \cos \psi_0$$

$$H_y^{inc} = 0$$

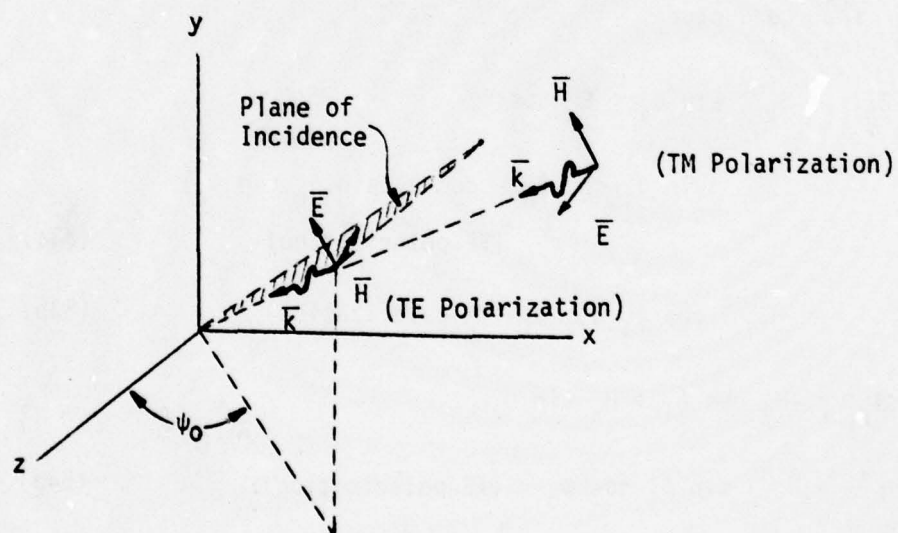
$$E_z^{inc} = -E^{inc} \sin \theta_0 \cos \psi_0$$

$$E_x^{inc} = -E^{inc} \sin \theta_0 \sin \psi_0$$

$$E_y^{inc} = E^{inc} \cos \theta_0$$



(a)



(b)

Figure 8. Geometry and polarization of the incident plane wave.

TE Fields

$$\begin{aligned}
 H_z^{inc} &= -H^{inc} \sin \theta_0 \cos \psi_0 & E_z^{inc} &= E_0 \sin \psi_0 \\
 H_x^{inc} &= -H^{inc} \sin \theta_0 \sin \psi_0 & E_x^{inc} &= -E_0 \cos \psi_0 \\
 H_y^{inc} &= H^{inc} \cos \theta_0 & E_y^{inc} &= 0
 \end{aligned}$$

As seen from Equations (51) and (52), the important quantities for determining the distributed sources are the electric field component parallel to the vectors  $\bar{h}_i$ , and the magnetic field component perpendicular to  $\bar{h}_i$ . Consider the geometry shown in Figure 9. The  $i^{\text{th}}$  conductor is shown with its coupling vector having an angle  $\theta_i$  with respect to the chosen  $x$  axis, and a magnitude  $h_i$ . For this case, the components of the electric field in the direction parallel to  $\bar{h}_i$  are given by the following expressions for the  $i^{\text{th}}$  conductor:

$$\begin{aligned}
 E_{||i} &= E_y^{inc} \sin \theta_i + E_x \cos \theta_i \\
 &= E^{inc} (\sin \theta_i \cos \theta_0 - \cos \theta_i \sin \theta_0 \sin \psi_0) \\
 &\quad \text{(TE polarization)} \qquad (53a)
 \end{aligned}$$

$$= -E^{inc} \cos \theta_i \cos \psi_i \text{ (TM polarization)} \qquad (53b)$$

and

$$\begin{aligned}
 H_{\perp i} &= -H_y \cos \theta_i + H_x \sin \theta_i \\
 &= H^{inc} \sin \theta_i \cos \psi_0 \quad \text{(TE polarization)} \qquad (54a)
 \end{aligned}$$

$$\begin{aligned}
 &= -H^{inc} (\cos \theta_i \cos \theta_0 + \sin \theta_i \sin \theta_0 \sin \psi_0) \\
 &\quad \text{(TM polarization)} \qquad (54b)
 \end{aligned}$$

With these field components, the distributed vector current and voltage sources take the form

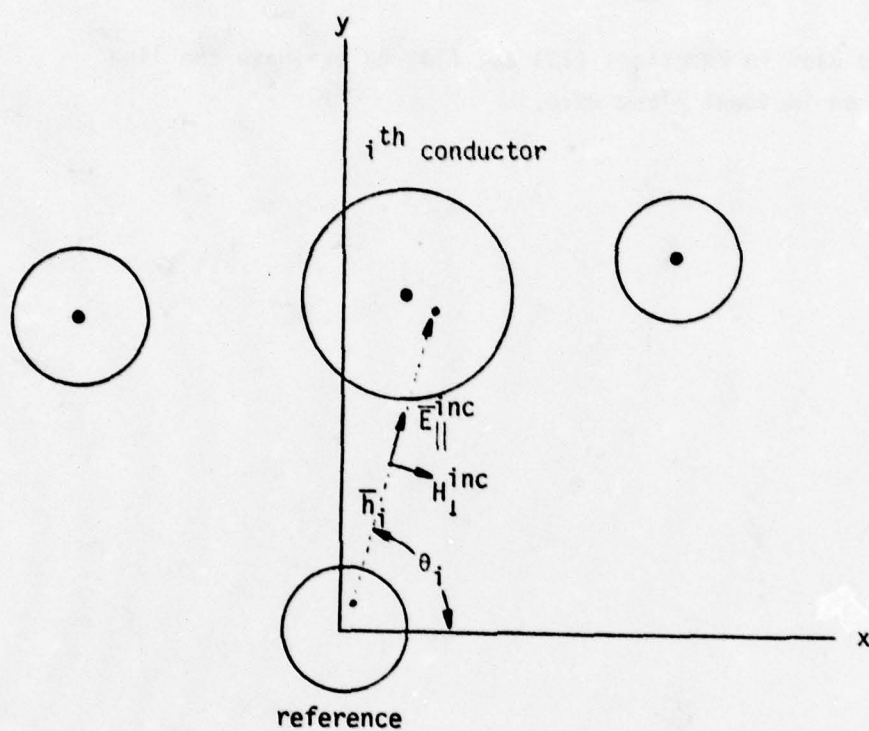


Figure 9. Cross section of multiconductor line showing field coupling parameter and pertinent field components.

$$\text{and } (\tilde{I}_n'(s)) = -s (\bar{C}_{n,m}') (h_n E_{||n}) \quad (55)$$

$$(\tilde{V}_n'(s)) = s\mu_0 (h_n H_{\perp n}) \quad (56)$$

and should be used in Equations (13) and (14) to evaluate the line response for an incident plane wave.

## SECTION V CONCLUSIONS

This report has presented a discussion of the field excitation of multiconductor transmission lines. First, a general expression for the current response at the terminations of an N-wire multiconductor cable has been developed in terms of distributed voltage and current sources. In Section III relationships between these sources and the total static electric and magnetic fields in the vicinity of the transmission line are then derived. These are then related to the free space (or incident) fields through a vector field coupling parameter or equivalent separation of the lines. Finally, Section IV expresses the distributed source terms for the multiconductor line in terms of the angles of incidence and polarization of an incident plane wave.

This work expands upon the past studies of field excitation of two-wire transmission lines. The field coupling parameters for a multiconductor line are seen to be determined from a series of calculations involving specifying a zero net charge on all conductors except the reference and the conductor for which the coupling parameter is being determined. It is noted, furthermore, that the excitation of the line depends strongly on the line's orientation with respect to the incident fields.

## REFERENCES

1. Baum, C.E., et al. "Numerical Results for Multiconductor Transmission Line Networks," AFWL EMP Interaction Notes, Note 322, September 1977.
2. Baum, C.E., T.K. Liu and F.M. Tesche, "On the General Analysis of Multiconductor Transmission Line Networks," AFWL EMP Interaction Notes, Note 130, November 1978.
3. Tesche, F.M. and T.K. Liu, "User Manual and Code Description for QV7TA: A General Multiconductor Transmission Line Analysis Code," AFWL Interaction Application Memos, Memo 26, August 1978.
4. Taylor, C.D., R.S. Satterwhite and C.W. Harrison, Jr., "The Response of a Terminated Two-Wire Transmission Line Excited by a Nonuniform Electromagnetic Field," AFWL EMP Interaction Notes, Note 66, November 1965; also, IEEE Trans. A.P., Vol. AP-13, pp. 987-989.
5. Smith, A.A., Coupling of External Electromagnetic Fields to Transmission Lines, John Wiley and Sons, New York, 1977.
6. Lee, K.S.H., "Balanced Transmission Lines in External Fields," AFWL EMP Interaction Notes, Note 115, July 1972.
7. Paul, C.R., "Frequency Response of Multiconductor Transmission Lines Illuminated by an Electric Field," IEEE Trans. EMC, Vol. EMC-18, No. 4, pp. 183-186, November 1976.
8. Frankel, S., Multiconductor Transmission Line Analysis, Artech House, 1977.
9. Kajfez, D. and D.R. Wilton, "Small Aperture on a Multiconductor Transmission Line Filled with Inhomogeneous Dielectrics," AFWL Interaction Note 347, November 1977.
10. Strawe, D.F., "Analysis of Uniform Multiwire Transmission Lines," Boeing Report D2-26088-1 under Contract F04701-72-C-0210, November 1972.
11. Lee, K.S.H., "Two Parallel Terminated Conductors in External Fields," IEEE Trans. EMC, Vol. EMC-20, No. 2, pp. 288-296, May 1978. (A revision of ref. 6.)
12. Frankel, S., "Evaluation of Certain Transmission-Line Forcing Functions," AFWL Interaction Note to be published.

13. Chang, S.K., F.M. Tesche, D.V. Giri, and T.K. Liu, "A Comparison of Experimental and Numerical Results for Multiconductor Transmission Line Networks," AFWL Interaction Application Memos, Memo 27, August 1978.
14. Uchida, H. Fundamentals of Coupled Lines and Multiwire Antennas, Sasaki Publishing, Ltd., Sendai, Japan, 1967.
15. Giri, D.V., F.M. Tesche, and S.K. Chang, "A Note on Transverse Distributions of Surface Charge Densities on Multiconductor Transmission Lines," AFWL Interaction Notes, Note 337, April 1, 1978.

NOTE 352

DIFFRACTION THROUGH A CIRCULAR APERTURE  
IN A SCREEN SEPARATING TWO DIFFERENT MEDIA

by

Harvey J. Fletcher  
Alan Harrison

December 1978

DIFFRACTION THROUGH A CIRCULAR APERTURE  
IN A SCREEN SEPARATING TWO DIFFERENT MEDIA

TABLE OF CONTENTS

<u>SECTION</u>	<u>PAGE</u>
1.0 INTRODUCTION . . . . .	352-3
2.0 MATHEMATICAL FORMULATION OF THE PROBLEM. . . . .	352-4
3.0 DERIVATION OF THE SOLUTION . . . . .	352-8
4.0 REFERENCES . . . . .	352-20

DIFFRACTION THROUGH A CIRCULAR APERTURE  
IN A SCREEN SEPARATING TWO DIFFERENT MEDIA

Harvey J. Fletcher and Alan Harrison

1.0 INTRODUCTION

The classic problem of the diffraction of a plane electromagnetic wave through a circular aperture has been treated by many authors. Exact solutions for arbitrary incident direction and arbitrary frequency have been given by Meixner and Andrejewski<sup>(1)</sup> (1950), Flammer<sup>(2)</sup> (1950), Lure<sup>(3)</sup> (1960), Nomura and Katsura<sup>(4)</sup> (1955). Some of these solutions were published by Bowman, Senior, Uslenghi<sup>(5)</sup> (1969). Thomas<sup>(6)</sup> (1969) derived the integral equations which would give the solution of the diffraction of a plane electromagnetic wave by a circular aperture in an infinite plane screen which separates two different media. He assumed a low frequency and gave an approximate numerical result for the special case of zero conductivity. Butler and Umashankar (1976) generalized the problem to an aperture of arbitrary shape and described a numerical procedure by the method of moments to find a solution. In this paper, we shall derive an exact solution to the problem with arbitrary frequency and arbitrary media. We will specialize the result to the case of a circular aperture illuminated by a plane wave normally incident. The special case of the two media being equal reduces to the solution given by Flammer.

## 2.0 MATHEMATICAL FORMULATION OF THE PROBLEM

The problem at hand is illustrated in Figure 1.

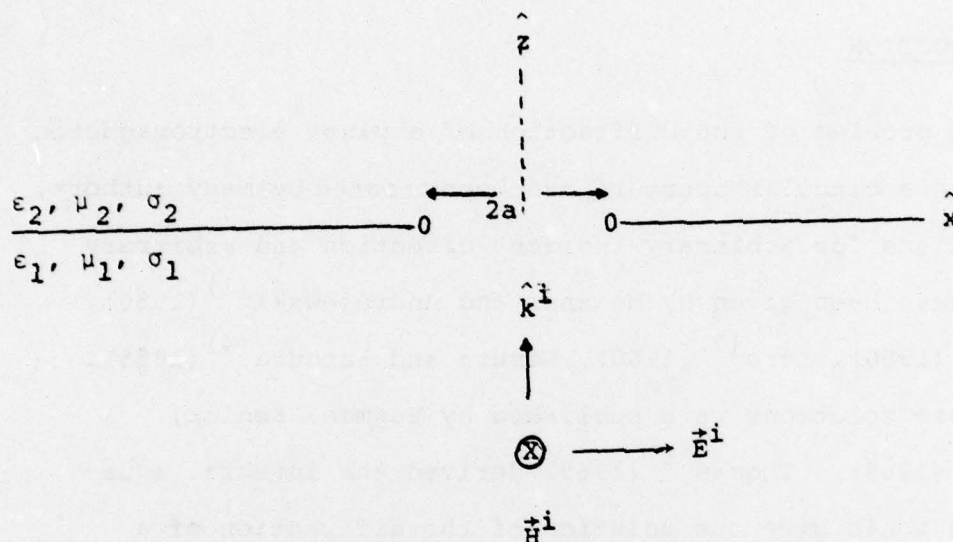


Figure 1 Incident Plane Wave On Circular Aperture

A plane wave is travelling in medium I with permittivity, permeability and conductivity  $\epsilon_1$ ,  $\mu_1$ , and  $\sigma_1$ . The wave illuminates an infinite perfectly conducting screen at  $z=0$  with a circular aperture whose center is at the origin. On the shadow side of the screen is a medium with permittivity, permeability, and conductivity given by  $\epsilon_2$ ,  $\mu_2$ ,  $\sigma_2$ .

We shall assume the incident wave is sinusoidal and suppress the factor  $e^{-i\omega t}$ . The general impulse can be found by Fourier Transforms. Maxwell's Equations are given by:

$$\nabla \times \vec{E} = i\omega\mu\vec{H}$$

$$\nabla \times \vec{H} = -i\omega\epsilon^*\vec{E}$$

$$\nabla \cdot \vec{H} = \nabla \cdot \vec{E} = 0$$

$$\epsilon^* = \epsilon - \sigma/i\omega$$

Subscript 1 will indicate the incident medium and subscript 2 will indicate the medium on the shadow side of the screen. The incident wave will be travelling in the z direction with the electric field in the x direction. The incident electric and magnetic fields are given by

$$\vec{E}^i = E_0(\omega)e^{ik_1 z} \hat{x}$$

$$\vec{H}^i = H_0(\omega)e^{ik_1 z} \hat{y}$$

where

$$k_\ell = \frac{\omega}{c_\ell(\omega)}$$

$$c_\ell(\omega) = \frac{1}{(\epsilon_\ell^* \mu_\ell)^{1/2}}$$

$$H_0(\omega) = E_0(\omega)/Z_1$$

$$Z_\ell(\omega) = (\mu_\ell/\epsilon_\ell^*)^{1/2}$$

$$\epsilon_\ell^*(\omega) = \epsilon_\ell - \sigma_\ell/i\omega$$

$$\ell = 1, 2$$

Real parts of Square

Roots are Positive.

The boundary conditions are the following:

1. The scattered wave satisfies the radiation boundary condition at large distances from the aperture.
2. The tangential electric field is zero on the screen.
3. The tangential electric and magnetic fields are zero at the aperture.
4. The tangential electric field goes to zero as the rim is approached from the aperture.

There is a unique solution of Maxwell's Equations which satisfy the above boundary conditions.

Let us introduce oblate spheroidal coordinates defined by

$$x = a \sqrt{(1 + \xi^2)(1 - \eta^2)} \cos \phi$$

$$y = a \sqrt{(1 + \xi^2)(1 - \eta^2)} \sin \phi$$

$$z = a\xi\eta \operatorname{sign} z$$

so that  $\xi = 0$  is the equation of the surface of the aperture and  $\eta = 0$  is the surface of the screen.

The range of the variables is

$$0 \leq \xi < \infty$$

$$0 \leq \eta \leq 1$$

If there were no aperture, the wave would be reflected so as to satisfy the boundary condition at the screen..

$$\vec{E}^r = -E_0(\omega) e^{-ik_1 z} \hat{x}$$

$$\vec{H}^r = H_0(\omega) e^{-ik_1 z} \hat{y}$$

The fields on the incident side with an aperture present are given by

$$\vec{E}_1 = \vec{E}^i + \vec{E}^r + \vec{E}_1^s$$

$$\vec{H}_1 = \vec{H}^i + \vec{H}^r + \vec{H}_1^s$$

where  $\vec{E}^s$  and  $\vec{H}^s$  are the scattered electric and magnetic fields, on the incident side of the screen. The mathematic description of the boundary conditions is:

$$E_{1x}(\xi, 0, \phi) = E_{1y}(\xi, 0, \phi) = E_{2x}(\xi, 0, \phi) = E_{2y}(\xi, 0, \phi) = 0$$

$$E_{1x}(0, \eta, \phi) = E_{2x}(0, \eta, \phi) \quad E_{1y}(0, \eta, \phi) = E_{2y}(0, \eta, \phi)$$

$$H_{1x}(0, \eta, \phi) = H_{2x}(0, \eta, \phi) \quad H_{1y}(0, \eta, \phi) = H_{2y}(0, \eta, \phi)$$

$$\lim_{\eta \rightarrow 0} \phi \cdot \vec{E}(0, \eta, \phi) = 0$$

$$\lim_{\xi \rightarrow \infty} E_2(\xi, \eta, \phi) e^{-ik_2 \xi} = \text{constant}$$

$$\lim_{\xi \rightarrow \infty} \vec{E}_1^s(\xi, \eta, \phi) e^{-ik_1 \xi} = \text{constant}$$

AD-A074 265

AIR FORCE WEAPONS LAB KIRTLAND AFB NM  
ELECTROMAGNETIC PULSE INTERACTION NOTES-EMP 3-39.(U)  
JUL 79 C E BAUM

F/G 20/14

UNCLASSIFIED

AFWL-TR-79-402

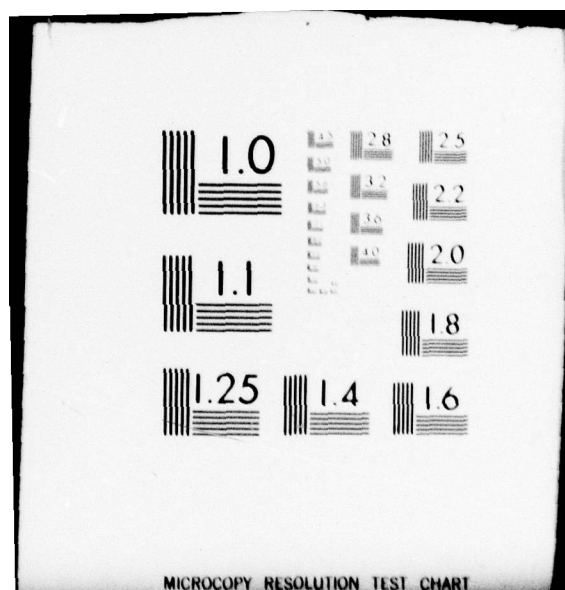
SBIE-AD-E200 363

NL

5 OF 5

AD  
A074265





### 3.0 DERIVATION OF THE SOLUTION

Let us introduce a vector potential  $\vec{\Pi} = \alpha \Pi_x \hat{x} + \beta \Pi_z \hat{z}$ . The electric and magnetic fields are then given by <sup>(s)</sup>

$$\vec{H}_2 = -i\omega\epsilon_2^* \nabla \times \vec{\Pi}_2 \quad \vec{H}_1^{(s)} = -i\omega\epsilon_1^* \nabla \times \vec{\Pi}_1$$

$$\vec{E}_2 = \nabla \times \nabla \times \vec{\Pi}_2 \quad \vec{E}_1^{(s)} = \nabla \times \nabla \times \vec{\Pi}_1$$

$\Pi_x$  and  $\Pi_z$  both satisfy the wave equation but with different velocities in different regions. Thus,

$$\nabla^2 \Pi_{1x} = -k_1^2 \Pi_{1x} \quad \nabla^2 \Pi_{1z} = -k_1^2 \Pi_{1z}$$

$$\nabla^2 \Pi_{2x} = -k_2^2 \Pi_{2x} \quad \nabla^2 \Pi_{2z} = -k_2^2 \Pi_{2z}$$

All of Maxwell's Equations are automatically satisfied. If  $\Pi_{1x}$  and  $\Pi_{2x}$  and  $\frac{\partial \Pi_{2z}}{\partial z}$  and  $\frac{\partial \Pi_{2z}}{\partial z}$  are chosen to be zero at  $\eta=0$ , then all of the screen boundary are satisfied. A separable solution of the wave equation in Oblate Spheroidal coordinates is

$$R_{mn}^{(p)}(-ic, i\xi) S_{mn}^{(q)}(-ic, \eta) \phi_m^{(k)}(\phi)$$

$$p=1,2,3,4, \quad q=1,2 \quad k=1,2$$

where

$$\phi_m^{(1)}(\phi) = \cos m\phi$$

$$\phi_m^{(2)}(\phi) = \sin m\phi$$

where  $R_{mn}^{(p)}(-ic, i\xi)$  are the radial spheroidal wave functions, (see Abramowich<sup>(8)</sup>) and where  $S_{mn}^{(q)}(-ic, \eta)$  are the angular wave functions (see appendix). If the fields are to be finite on the axis,  $(\eta=1)$ , then  $q=1$ , and also  $\eta$  is an integer. If the fields are to satisfy the radiation boundary conditions at  $\xi=\infty$ , then  $p=3$ .

$$\text{The functions } S_{mn}^{(1)}(-ic, \eta) = \sum_{r=0,1}^{\infty} f_r^m(c) P_{m+n}^m(\eta)$$

where the sum is over the odd integers if  $n-m$  is odd and over the even integers if  $n-m$  is even.  $P_{m+n}^m(\eta)$  is the Associated Legendre's Function. If this is to vanish at  $\eta=0$ , then  $n-m$  must be odd. If the derivative of this is to vanish at  $\eta=0$ , then  $n-m$  must be even.

Let us find  $\Pi_x$  satisfying all the boundary conditions except the rim condition

$$\Pi_{1x} = \Sigma (A_{mn} \cos m\phi + B_{mn} \sin m\phi) R_{mn}^{(3)}(-ic, i\xi) S_{mn}^{(1)}(-ic, \eta)$$

$$\Pi_{2x} = \Sigma (C_{mn} \cos m\phi + D_{mn} \sin m\phi) R_{mn}^{(3)}(-ic_2, i\xi) S_{mn}^{(1)}(-ic, \eta)$$

where the sum is such that  $n-m$  is an odd integer. The scattered fields are given by

$$E_{\ell x} = \frac{\partial^2 \Pi_{\ell x}}{\partial x^2} + k_{\ell}^2 \Pi_{\ell x} \quad E_{\ell y} = \frac{\partial^2 \Pi_{\ell x}}{\partial x \partial y} \quad E_{\ell z} = \frac{\partial^2 \Pi_{\ell x}}{\partial x \partial z}$$

$$H_{\ell x} = 0 \quad H_{\ell y} = -i\omega\epsilon_{\ell} \frac{\partial \Pi_{\ell x}}{\partial z} \quad H_{\ell z} = i\omega\epsilon_{\ell} \frac{\partial \Pi_{\ell x}}{\partial y}$$

The continuity of E is assured at  $\xi=0$ , if  $\Pi_{1x} = \Pi_{2x}$  at  $\xi=0$ .

The continuity of H is assured at  $\xi=0$ , if

$$2H_0 - i\omega\epsilon_1 \frac{\partial \Pi_{1x}}{\partial z} = i\omega\epsilon_2^* \frac{\partial \Pi_{2x}}{\partial z} \text{ at } \xi=0$$

The partial with respect to z is given by

$$\frac{\partial}{\partial z} = \pm \left[ \frac{n(1+\xi^2)}{a(\xi^2 + n^2)} \frac{\partial}{\partial \xi} + \frac{\xi(1-n^2)}{a^2(\xi^2 + n^2)} \frac{\partial}{\partial n} \right]$$

where the plus sign is used if  $z>0$  and the minus sign if  $z<0$ .

It follows that

$$\frac{-2H_0 a n}{i\omega} = \epsilon_2 \frac{\partial \Pi_{2x}}{\partial \xi} + \epsilon_1 \frac{\partial \Pi_{1x}}{\partial \xi} \text{ at } \xi=0$$

Substituting the series in the above two boundary conditions leads to

$$B_{mn} = D_{mn} = 0 \quad \text{and} \quad m = 0 \text{ so that}$$

$$\Sigma A_{on} R_{on}^{(3)}(-ic_1, io) S_{on}^{(1)}(-ic_1, n) = \Sigma C_{on} R_{on}^{(3)}(-ic_2, io) S_{on}^{(1)}(-ic_2, n)$$

$$\epsilon_1 \Sigma A_{on} R_{on}^{(3)'}(-ic_1, io) S_{on}^{(1)}(-ic_1, n) + \epsilon_2 \Sigma C_{on} R_{on}^{(3)'}(-ic_2, io) S_{on}^{(1)}(-ic_2, n)$$

$$= \frac{-2H_0 a n}{i\omega} = \frac{-2H_0 a}{i\omega} P_1(n)$$

where the prime indicates a derivative with respect to  $\xi$ . Since the  $S_{on}$  functions are orthogonal, we can multiply both sides by  $S_{on}$  and integrate

$$A_{on} = \frac{+1}{R_{on}^{(3)}(-ic_1, io) I_n} \sum_{\substack{n=1 \\ \text{odd}}}^{\infty} C_{on} R_{on}^{(3)}(-ic_2, io) I_{nn}$$

and

$$A_{on} = \frac{1}{R_{on}^{(3)' }(-ic_1, io) \epsilon_1 I_n} \left\{ - \frac{2H_o a f_1^{01}}{j\omega 3} - \epsilon_2 \sum_{\substack{n=1 \\ \text{odd}}}^{\infty} C_{on} R_{on}^{(3)' }(-ic_2, io) I_{nn} \right\}$$

Eliminate  $A_{on}$  and obtain

$$\Sigma C_{on} E_{nn} = F_n$$

where

$$E_{nn} = \left[ \epsilon_1 R_{on}^{(3)}(-ic_1, io) R_{on}^{(3)'}(-ic_2, io) + \epsilon_2 R_{on}^{(3)}(-ic_2, io) R_{on}^{(3)'}(-ic_1, io) \right] J_{n\bar{n}}$$

$$I_{n\bar{n}}(c_1, c_2) = I_{n\bar{n}} = \int_0^1 S_{on}^{(1)}(-ic_1, \eta) S_{on}^{(1)}(-ic_2, \eta) d\eta \quad (n, \bar{n} = \text{odd})$$

$$F_n = -\frac{2}{3} a H_0 f_1^{01}(c_1) R_{on}^{(3)}(-ic_1, io) / i\omega$$

$$I_n = I_{nn}(c_1, c_1)$$

The solution of this infinite set of equations can be substituted in the equation for  $A_{on}$ ,  $\Pi_{2x}$ ,  $\vec{E}_2$ , and  $\vec{H}_2$  to give the diffracted fields. However, the rim condition is not satisfied ( $E\phi \rightarrow \infty$ ).

Let us look for another solution involving  $\Pi_2$ .

$$\Pi_{1z} = \Sigma (G_{mn} \cos m\phi + H_{mn} \sin m\phi) R_{mn}^{(3)}(-ic_1, i\xi) S_{mn}^{(1)}(-ic_1, \eta)$$

$$\Pi_{2z} = \Sigma (J_{mn} \cos m\phi + K_{mn} \sin m\phi) R_{mn}^{(3)}(-ic_2, i\xi) S_{mn}^{(1)}(-ic_2, \eta)$$

where the sum is such that  $n-m$  is even.

The fields are given by

$$E_{lx} = \frac{\partial^2 \pi_{lz}}{\partial x \partial z} \quad E_{ly} = \frac{\partial^2 \pi_{lz}}{\partial y \partial z} \quad E_{lz} = -\frac{\partial^2 \pi_{lz}}{\partial x^2} - \frac{\partial^2 \pi_{lz}}{\partial y^2} + k^2 \pi_{lz}$$

$$H_x = 0 \quad H_y = i\omega \epsilon_l \frac{\partial \pi_{lz}}{\partial x} \quad H_z = -i\omega \epsilon_l \frac{\partial \pi_{lz}}{\partial y}$$

The continuity boundary conditions are

$$\frac{\partial \pi_{1z}}{\partial \xi} = \frac{\partial \pi_{2z}}{\partial \xi} \quad \text{at} \quad \xi = 0$$

$$\epsilon_2 \pi_{2z} - \epsilon_1 \pi_{1z} = \frac{2H_0 x}{i\omega} = \frac{2H_0 a}{i\omega} \sqrt{1-\eta^2} \cos \phi = -\frac{2H_0 a P_1^1(\eta) \cos \phi}{i\omega} \quad \text{at } \xi=0$$

In order that both sides have the same  $\theta$  dependence, choose

$$H_{mn} = K_{mn} = 0 \quad \text{and } m=1$$

It follows that

$$\sum_{\substack{n=1 \\ \text{odd}}}^{\infty} G_{1n} R_{1n}^{(3)'}(-ic_1, io) S_{1n}^{(1)}(-ic_1, o) = \sum_{\substack{n=1 \\ \text{odd}}}^{\infty} J_{1n} R_{1n}^{(3)'}(-ic_2, io) S_{1n}^{(1)}(-ic_2, o)$$

$$-\epsilon_1 \sum_{\substack{n=1 \\ \text{odd}}}^{\infty} G_{1n} R_{1n}^{(3)}(-ic_1, io) S_{1n}^{(1)}(-ic_1, o) + \epsilon_1 \sum_{\substack{n=1 \\ \text{odd}}}^{\infty} J_{1n} R_{1n}^{(3)}(-ic_2, io)$$

$$S_{1n}^{(1)}(-ic_2, o) = -\frac{2H_0 a P_1^1(\eta)}{i\omega}$$

solve both equations for  $G_{1n}$

$$G_{1n} = \frac{-1}{R_{1n}^{(3)'} (-ic_1, io) L_n} \sum_{\substack{\bar{n}=1 \\ \text{odd}}}^{\infty} J_{1\bar{n}} R_{1\bar{n}}^{(3)'} (-ic_2, io) L_{n\bar{n}}$$

$$G_{1n} = \frac{1}{-\epsilon R_{1n}^{(3)} (-ic_1, io) L_n} \left[ -\frac{4H_o a}{3i\omega} - \epsilon_2 \sum_{\substack{\bar{n}=1 \\ \text{odd}}}^{\infty} J_{1\bar{n}} R_{1\bar{n}}^{(3)} (-ic_2, io) L_{n\bar{n}} \right]$$

Eliminate  $G_{1n}$  and obtain

$$\sum_{\substack{\bar{n}=1 \\ \text{odd}}}^{\infty} J_{1\bar{n}} M_{n\bar{n}} = N_n$$

where

$$M_{n\bar{n}} = L_{n\bar{n}} \left[ \epsilon_1 R_{1\bar{n}}^{(3)'} (-ic_2, io) R_{1n}^{(3)} (-ic_1, io) + \epsilon_2 R_{1\bar{n}}^{(3)} (-ic_2, io) R_{1n}^{(3)'} (-ic_1, io) \right]$$

$$L_{n\bar{n}} = \int_0^1 S_{1n}(-ic_1, 0) S_{1\bar{n}}(-ic_2, 0) dn$$

$$N_n = - \frac{4aH_0 f_0^{ln}}{3i\omega} R_{1n}^{(3)'}(-ic_1, io)$$

$$L_n = L_{nn}(c_1, c_1)$$

This again gives an infinite set of linear equations to solve for  $J_{1n}$ . Substitution of these constants in the above equations will give the fields. To get a unique solution, we take

$$\vec{\Pi} = \alpha \Pi_x \hat{x} + \beta \Pi_z \hat{z} \quad \text{where } \alpha + \beta = 1$$

This will satisfy all the boundary conditions except the condition that  $E_\phi = 0$  on the rim.

$E_\phi$  is given by (2)

$$\begin{aligned} E_\phi = c\phi \left\{ \frac{-\alpha(1-\eta^2)^{\frac{1}{2}}(\xi^2+1)^{\frac{1}{2}}}{ka^2(\xi^2+\eta^2)} \right\} \Sigma' c_{on} \left\{ \frac{R_{on}^{(3)}(-ic_2, io)}{(\xi^2+1)^{\frac{1}{2}}} \frac{d}{dn} \left[ (1-\eta^2)^{\frac{1}{2}} \frac{dS_{on}}{dn} \right] \right. \\ + \frac{S_{on}^{(1)}(-ic_2, \eta)}{(1-\eta^2)^{\frac{1}{2}}} \frac{d}{d\xi} \left[ (\xi^2+1)^{\frac{1}{2}} \frac{dR_{on}^{(3)}}{d\xi}(-ic_2, i\xi) \right] \\ + \beta \frac{(1-\eta^2)^{\frac{1}{2}}(\xi^2+1)^{\frac{1}{2}}}{ka^2(\xi^2+\eta^2)} \Sigma' J_{1n} \frac{\xi R_{1n}^{(3)}(-ic_2, i\xi) S_{1n}'(-ic_2, \eta)}{\xi^2+1} \\ \left. + \frac{\eta}{1-\eta^2} S_{1n}^{(1)}(-ic_2, \eta) \frac{dR_{1n}^{(3)}}{d\xi}(-ic_2, i\xi) \right\} \end{aligned}$$

The differential equations for R and S are

$$\frac{d}{d\xi} (\xi^2 + 1) \frac{dR_{mn}}{d\xi} + \left( -\lambda_{mn} + c^2 \xi^2 + \frac{m^2}{\xi^2 + 1} \right) R_{mn} = 0$$

$$\frac{d}{d\eta} (1 - \eta^2) \frac{dS_{mn}}{d\eta} + \left( \lambda_{mn} + c^2 \eta^2 - \frac{m^2}{1 - \eta^2} \right) S_{mn} = 0$$

$$\text{Since } S_{on}^{(1)}(-ic_2, \eta) = \sum_{\substack{r=1 \\ \text{odd}}}^{\infty} f_r^{on}(c_2) P_r(\eta)$$

$$\text{and } P_r(0) = 0$$

$$\text{it follows that } S_{on}^{(1)}(-ic_2, \eta) = 0.$$

Put  $\eta=0$  in the differential equation and get

$$S_{on}^{(1)''}(-ic_2, 0) = 0$$

Expand in a Taylor Series

$$S_{on}^{(1)}(-ic_2, \eta) = S_{on}^{(1)}(-ic_2, 0)\eta + S_{on}^{(1)'''}(-ic_2, 0) \frac{\eta^3}{6} + \dots$$

Further expansion leads to

$$\frac{d}{dn} (1-n^2)^{\frac{1}{2}} \frac{dS_{on}^{(1)}}{dn} = \left[ S'''(-ic_2, 0) - S'(-ic_2, 0) \right] n + O(n^3)$$

$$\text{and } \frac{d}{d\xi} (\xi^2+1)^{\frac{1}{2}} \frac{dR_{on}^{(3)}}{d\xi} = R_{on}^{(3)''}(-ic_2, i0) + O(\xi^2)$$

Using the differential equations

$$R_{on}^{(3)''}(-ic_2, i0) = \lambda_{on} R_{on}^{(3)}(-ic_2, i0)$$

$$S_{on}^{(1)'''}(-ic_2, i0) = (2-\lambda_{on}) S_{on}^{(1)'}(-ic_2, i0)$$

Collect the highest power of  $\eta$  in the expression for  $E_\phi$ .

$$\begin{aligned}
 E_\phi &= \frac{c\phi}{ka^2\eta} \left\{ -\alpha \sum C_{on} \left\{ R_{on}^{(3)}(0) (1-\lambda_{on}) S_{on}^{(1)'}(0) \right. \right. \\
 &\quad \left. \left. + S_{on}^{(1)'}(0) \lambda_{on} R_{on}^{(3)}(0) \right. \right. \\
 &\quad \left. \left. + \beta \sum J_{ln} S_{ln}^{(1)}(0) R_{ln}^{(3)'}(0) \right\} \right\} \\
 &= \frac{c\phi}{k^2 a \eta} \left\{ -\alpha \sum C_{on} R_{on}^{(3)}(0) S_{on}^{(1)'}(0) \right. \\
 &\quad \left. + \beta \sum J_{ln} R_{ln}^{(3)'}(0) S_{ln}^{(1)}(0) \right. \\
 &\quad \left. + o(\eta^2) \right\}
 \end{aligned}$$

This is infinite as  $\eta \rightarrow 0$  unless  $\alpha$  and  $\beta$  are chosen so that

$$\begin{aligned}
 &\alpha \sum C_{on} R_{on}^{(3)}(0) S_{on}^{(1)'}(0) \\
 &= \beta \sum J_{ln} R_{ln}^{(3)'}(0) S_{ln}^{(1)}(0)
 \end{aligned}$$

In this case

$$\alpha = \frac{\sum J_{ln} R_{ln}^{(3)'}(0) S_{ln}^{(1)}(0)}{\sum J_{ln} R_{ln}^{(3)'}(0) S_{ln}^{(1)}(0) + \sum C_{on} R_{on}^{(3)}(0) S_{on}^{(1)'}(0)}$$

and  $\beta = 1 - \alpha$  and  $E_\phi = 0$  at  $\xi = \eta = 0$ .

In the special case when  $\epsilon_1^* = \epsilon_2^*$  and  $\mu_1 = \mu_2$ , then  $I_{nn}^- = I_n \delta_n^{\bar{n}}$

and  $L_{nn}^- = \delta_n^{\bar{n}} L_n$

$$L_{nn}^- = 2\epsilon^* R_{on}^{(3)}(0) R_{on}^{(3)'}(0) \delta_n^{\bar{n}} I_n$$

$$A_{on} = C_{on} = \frac{ia H_o f_1^{on}}{3\omega \epsilon^* R_{ln}^{(3)'}(0) I_n}$$

$$M_{nn}^- = 2\epsilon R_{ln}^{(3)'}(0) R_{ln}^{(3)}(0) \delta_n^{\bar{n}} I_n$$

$$-G_{ln} = J_{l\bar{n}} = \frac{2E_o a i f_o^{ln}}{3k I_n R_{ln}^{(3)}(0)}$$

These check the values given by Flammer<sup>(2)</sup>. Thus, we have found a solution which generalizes that of Flammer to the case of arbitrary medium.

#### 4.0 REFERENCES

- (1) Meixner, J. and W. Andrejewski, Ann Physik, 7, 1950, pp. 157-168.
- (2) Flammer, C., J. App. Phys., 24, 1953, pp. 1224-1231.
- (3) Lur'e, K. A., Soviet Physics, 4, 1960, pp. 1313-1325.
- (4) Nomura, Y., and S. Katsura, J. Phys. Soc. Japan, 10, 1955, pp. 285-304.
- (5) Bowman, J. J., and T. B. A. Senior and P. T. E. Uslenghi, Electromagnetic and Acoustic Scattering By Simple Shapes, North Holland Pub. Co., 1969, pp. 564-568.
- (6) Thomas, D. P., Canadian J. of Physics, 47, 1968, pp. 921-930.
- (7) Butler, C. M., and K. R. Umashankar, Radio Science, 11, 1976, pp. 611-619.
- (8) Abramowitz, M. and I. A. Stegun, Handbook of Mathematical Functions, Dover Pub. Inc., 1965, pp. 752-759.
- (9) Stratton, J. A., P. M. Morse, L. J. Chu, J. D. C. Little, F. J. Corbato, Spheroidal Wave Functions, The M.I.T. Press, 1956.
- (10) C. Flammer, Spheroidal Wave Functions, Stanford Univ. Press, 1957

NOTE 353

THE RECEIVING PROPERTIES OF THE SMALL ANNULAR SLOT ANTENNA

by

David E. Merewether  
Roger B. Cook  
Robert Fisher

29 September 1978

THE RECEIVING PROPERTIES OF  
THE SMALL ANNULAR SLOT ANTENNA

ABSTRACT

An analytical formula for the effective height of an annular slot antenna is determined using the reciprocity theorem. This result generalizes the previously available monochromatic result and yields an equivalent circuit valid for computing the transient response of the small annular slot antenna.

## THE RECEIVING PROPERTIES OF THE SMALL ANNULAR SLOT ANTENNA

## 1. INTRODUCTION

The annular slot antenna (Figure 1) has been a subject of continuing interest because it is a low profile antenna [1] and because it is a tractable model for the inadvertant antenna formed by the recessed connectors used on some missiles [2]. The problem of predicting the receiving properties of this antenna is complicated by the fact that the field distribution in the aperture is not strictly TEM (ie.,  $E_r \sim \frac{1}{r}$ ). Although the exact distribution of the field in the aperture is not required for predicting the radiated field, the contribution of higher order TM modes to the equivalent antennna capacity is not negligible [3].

The problem can be circumvented by locating the drive terminals at a distance below the ground plane where the TM modes have all disappeared. An apparent antenna admittance and an apparent effective height referred to the ground plane is calculated in this way. This approach was used by Chang and Harrison to find the effective height of an annular slot as observed across a conjugate matched load located one helf of a wavelength from the opening [4]. While their results may have been suitable for continuous wave

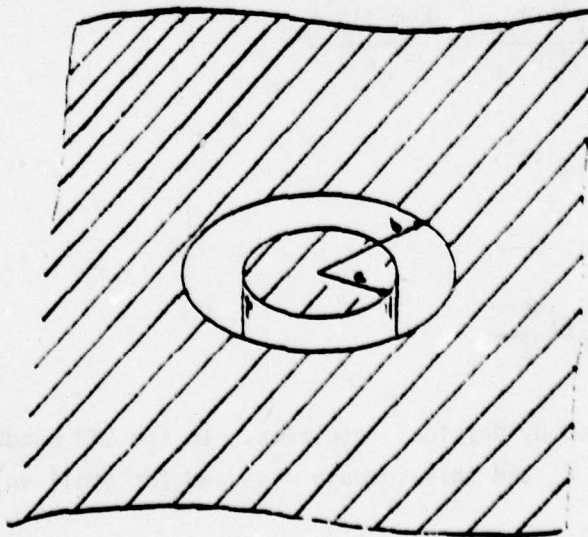


Figure 1. Annular Slot Antenna

analysis, for pulse response analysis a less restrictive result is required. In their own work, Chang and Harrison used a formula for the short circuit current ([5] eq. 23),

$$I_0 = -j4\pi a E_0 \epsilon_0^{-1} J_1(k_0 a \sin \theta_0) \quad (1)$$

where common definitions are used,  $k_0 = \omega/c$ ,  $\epsilon_0 = \sqrt{\frac{\mu_0}{\epsilon_0}}$ , etc. This result was expected to be true for the thin slot with  $(b-a) \ll b$ .

Evidently, in (1)  $E_0$  is the incident field at the observer location without the ground plane or the antenna present. For most problems the ground plane would exist with or without the antenna present. For these problems a more natural incident field is the normal component of the total electric field observed at the antenna location without the antenna present,

$$E^{\text{norm}} = 2 E_0 \sin \theta_0. \quad (2)$$

Noting that for small arguments  $J_1(x) = \frac{x}{2}$  (1) becomes

$$I_0(\omega) = -j4\pi a \frac{E^{\text{norm}}}{2 \sin \theta_0} \epsilon_0^{-1} \frac{k_0 a \sin \theta_0}{2} \quad (3)$$

$$= -j\omega \epsilon_0 E_{\text{norm}} \pi a^2. \quad (4)$$

So that

$$I_0(t) = -\text{Area} \epsilon_0 \frac{dE^{\text{norm}}}{dt} \quad (5)$$

which is the result expected by physical intuition. In the EMP handbook [2] the data was normalized to  $E_0$  and this formula was used for small values of  $a/b$ .

Here, we derive a new formula for the effective height, based on the reciprocity theorem that is valid for pulse analysis and is not restricted to very thin slots.

Following this development, the formula for antenna capacity is examined to determine its limitations. Parametrically determined data is given to provide a complete description of the equivalent circuit for a range of  $a/b$  values from 0.3 to 1.

In the final section, a finite difference approach was used to obtain supporting data for the new effective height formulas.

## 2. DERIVATION OF EFFECTIVE HEIGHT FORMULA

Consider the annular slot antenna driven by a continuous wave current source  $I_1$ , located some distance below the exit plane (Figure 2). Consider that a small current element  $I_2(2h_2)$  is simultaneously radiating at the same frequency and that its direction is along the hemisphere centered on the antenna. Then, according to the reciprocity theorem ([6], p. 322), we may expect that

$$\int_V \vec{E}_2 \cdot \vec{J}_1 dv = \int_V \vec{E}_1 \cdot \vec{J}_2 dv \quad (6)$$

Here,  $E_1$  and  $E_2$  are the electric fields produced by the distributed currents source density  $\vec{J}_1$ , and  $\vec{J}_2$  respectively and the volume integral includes both sources. Since the current source  $\vec{J}_1$  exists only at the load inside the coax  $\vec{J}_1 = I_1 (2\pi r)^{-1} \vec{a}_r \delta(z+d)$ , and the left side of (6) is

$$\begin{aligned} \int_V \vec{E}_2 \cdot \vec{J}_1 dv &= I_1 \int_a^b E_{2r} dr \\ &= I_1 * (\text{Voltage across load due to source \#2}) \end{aligned} \quad (7)$$

Assuming that this voltage is induced at the end of the coax, then

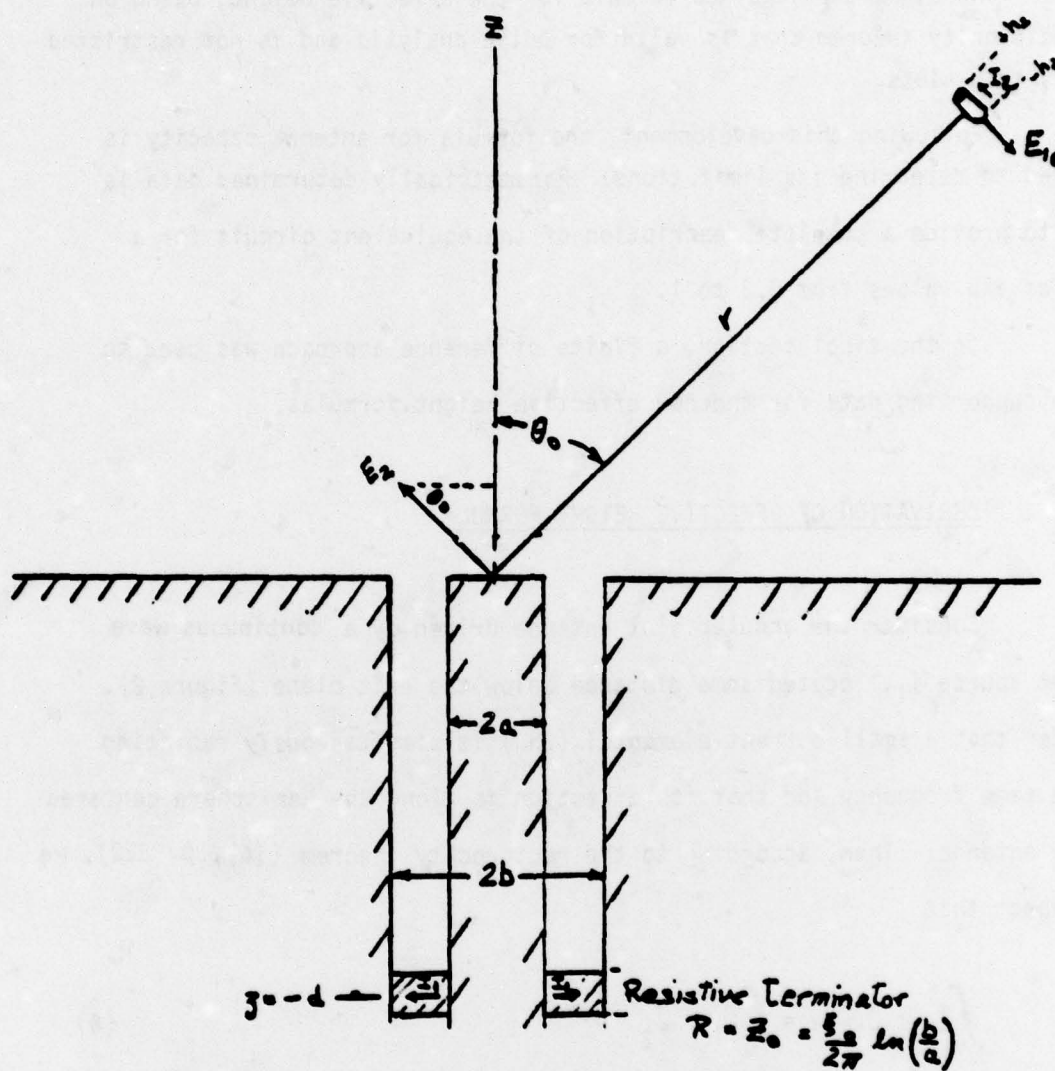


Figure 2: Driven Annular Slot Antenna with Test Source

$$\int_V \vec{E}_2 \cdot \vec{J}_1 \, dv = I_1 + h_e E_2^{\text{norm}} + \frac{Z_0}{Z_a + Z_0} e^{-jk_0 d} \quad (8)$$

Here,  $Z_a$  is the effective antenna impedance, and  $Z_0$  is the characteristic impedance of the transmission line and  $E_2^{\text{norm}}$  is the normal component of the incident field due to the test source ([6], p. 310) and its image at the top of the annular slot.

$$E^{\text{norm}} = -j \frac{\omega \mu_2 + I_2 + 2h_2}{4\pi r} e^{-jk_0 r} \sin \theta_0 \quad (9)$$

Finally, the left side of (6) is

$$\int_V \vec{E}_2 \cdot \vec{J}_1 \, dv = \frac{-I_1 h_e Z_0}{Z_a + Z_0} + e^{-jk_0(r+d)} \frac{j\omega \mu_2 I_2 h_2 \sin \theta_0}{\pi r} \quad (10)$$

The right side of equation 6 is evaluated by noting that the test source is oriented along the  $-\vec{a}_\theta$  direction so that only the  $E_\theta$  component of  $\vec{E}_1$  is important:

$$\int_V \vec{E}_1 \cdot \vec{J}_2 \, dv = I_2 \int_{-h_2}^{h_2} E_1 \cdot (-\vec{a}_\theta) dz' = -I_2 2h_2 E_{1\theta} \quad (11)$$

$E_{1\theta}$  has been determined by Harrison and Chang [4, Eq. 24].

$$E_{1\theta} = -\frac{V_a e^{-jk_0 r}}{r \ln b/a} [J_0(k_0 b \sin \theta_0) - J_0(k_0 a \sin \theta_0)], \quad (12)$$

which is computed assuming that  $E_{1r}$  is TEM at the aperture:

$$E_{1r} = \frac{V_a}{\rho \ln(b/a)} \quad (13)$$

Now if the aperture voltage  $V_a$  is due to a source,  $J_1$  at  $z = -d$ , we have

$$V_a = \frac{I_1 Z_0 Z_a}{Z_0 + Z_a} e^{-jk_0 d} \quad (14)$$

Using (11), (12) and (14), the right side of equation (6) becomes

$$\int_V \vec{E}_1 \cdot \vec{J}_2 dv = \frac{+I_2 2h_2 e^{-jk_0(r+d)}}{r \ln b/a} \left[ J_0(k_0 b \sin \theta_0) - J_0(k_0 a \sin \theta_0) \right] \frac{I_1 Z_0 Z_a}{Z_0 + Z_a} \quad (15)$$

Substituting (10) and (15) into (6), the effective height is determined to be

$$h_e = \frac{-2\pi Z_a [J_0(k_0 b \sin \theta_0) - J_0(k_0 a \sin \theta_0)]}{j\omega \mu \ln(b/a) \sin \theta_0} \quad (16)$$

If the antenna is small,  $k_0 b < 1$ , then  $Z_a = \frac{1}{j\omega C_a}$  and  $J_0(x) = 1 - \frac{x^2}{4}$  such that

$$h_e = \frac{\pi \epsilon (b^2 - a^2)}{2 C_a \ln(b/a)} \sin \theta_0 \quad (17)$$

The form of (16) is similar to the monochromatic result given by Harrison and Chang ([4]eq. 61). However, the assumptions used here are less restrictive so that the effective height given by (16) is valid for computing the voltage measured across any impedance at a reasonable distance ( $d > 5b$ ) below a ground plane using transmission line theory. Equation (17) is suitable for pulse response studies provided that  $k_0 b < 1$  at the highest frequency of interest.

### 3. EQUIVALENT CIRCUIT FOR AN ANNULAR SLOT ANTENNA

The voltage or current equivalent circuit of an annular slot antenna is useful for determining the electromagnetic energy that is coupled into cables with arbitrary loads on the far end. This section presents the frequency domain formulation of the equivalent circuits, with the inherent assumptions that only TEM modes exist. The time domain formulation, including TEM and TM modes, is derived in Section 4 of this report.

The equivalent circuits consist of a current (or voltage) source in parallel (or series) with the aperture capacitance as shown in Figure 3. Both time and frequency domain sources are shown.

The aperture admittance was derived by Levine and Papas [7], and is given by the following equation:

$$Y_a = G_a + j\omega C_a \quad (18)$$

with

$$G_a = \frac{Y_0}{\ln b/a} \int_0^{\pi/2} \frac{d\theta}{\sin \theta} \left[ J_0(k_0 a \sin \theta) - J_0(k_0 b \sin \theta) \right]^2 \quad (19)$$

$$\omega C_a = \frac{Y_0}{\pi \ln b/a} \left[ 2 \int_0^\pi d\psi S_1 \left\{ k_0 a \left[ 1 + (b/a)^2 - 2(b/a) \cos \psi \right]^{1/2} \right\} \right. \\ \left. - \int_0^\pi d\psi S_1 \left( 2k_0 a \sin \frac{\psi}{2} \right) - \int_0^\pi d\psi S_1 \left( 2k_0 b \sin \frac{\psi}{2} \right) \right] \quad (20)$$

with  $S_1$  representing the sine integral, and  $Y_0 = \frac{1}{60 \ln b/a}$ , the characteristic admittance of the cable. For EMP and lightning calculations, and for typical annular slot antenna geometries, the small argument expansion ( $k_0 b \ll 1$ ) is valid, and these equations reduce to the following:

$$G_a = \frac{2Y_0}{3\ln b/a} \left( \frac{k_0 a}{2} \right)^4 \left[ (b/a)^2 - 1 \right]^2 \quad (21)$$

and

$$\omega C_a = \frac{2k_0 a Y_0}{\pi \ln b/a} \left( \int_0^\pi d\psi \left[ 1 + (b/a)^2 - 2(b/a) \cos \psi \right]^{1/2} - 2(1 + b/a) \right). \quad (22)$$

The conductance  $G_a$  is frequency dependent, and can not be represented in a time domain circuit; however,  $G_a$  is small and can usually be neglected except when the load connected to the equivalent circuit is a very high impedance.

The normalized  $C_a$ , calculated from (22) is shown in Figure 3, along with the normalized  $h_e$  obtained from (17).

Since the antenna capacity is very small, the current equivalent circuit would be appropriate for most problems involving cables terminated in realistic impedances. The product  $C_{ant} h_e$  needed for this equivalent is also given on Figure 3.

The effect of recessing the center post of the antenna was not considered in this work. The depth dependence shown on Figure 3 was taken from Reference 2.

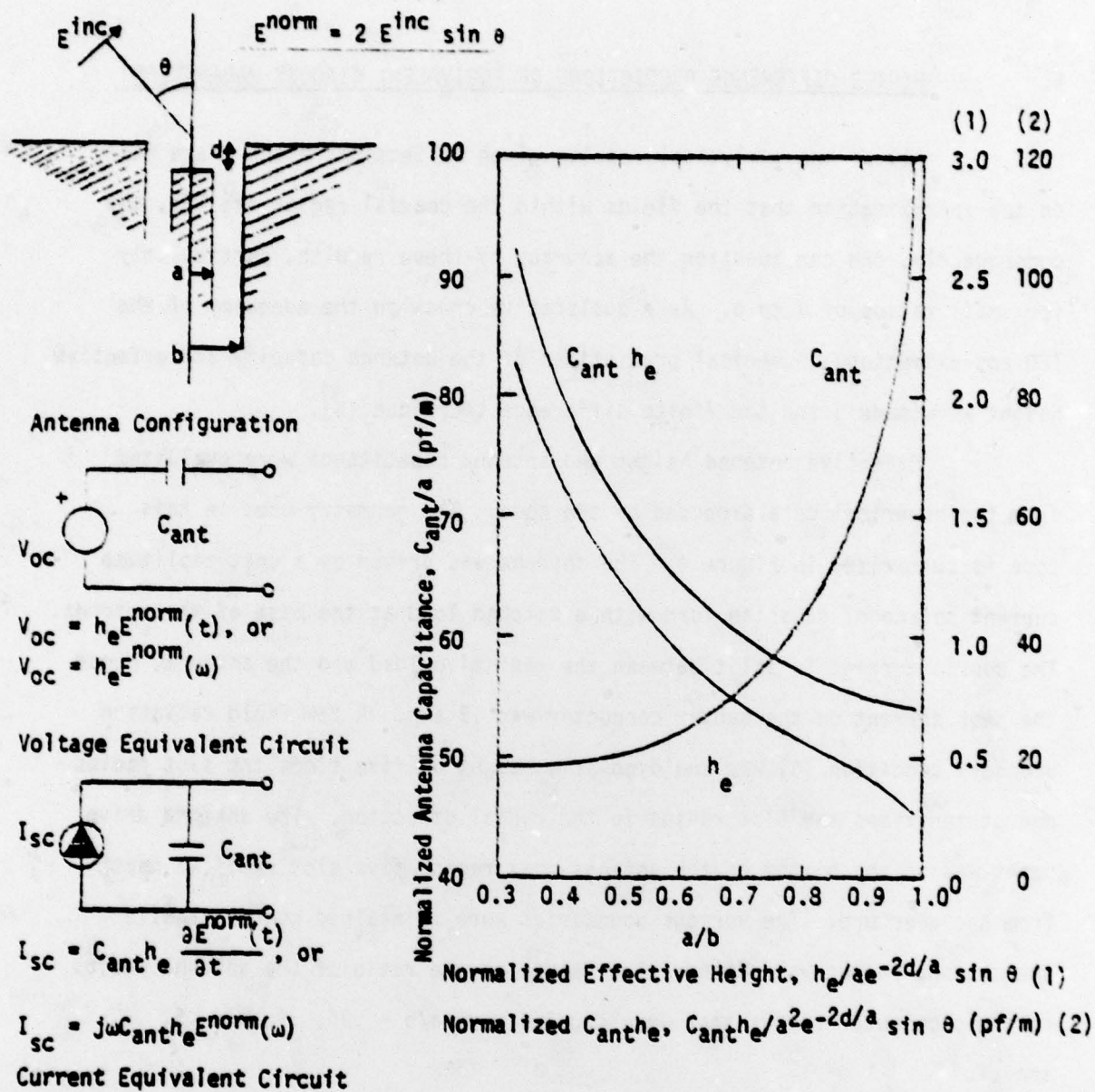


Figure 3: The Equivalent Circuits

#### 4. FINITE DIFFERENCE PREDICTIONS OF EQUIVALENT CIRCUIT PARAMETERS

All of the analytical results given in Sections 2 and 3 are based on the approximation that the fields within the coaxial region are TEM, and consequently, one can question the accuracy of these results, particularly for small ratios of  $a$  to  $b$ . As a qualitative check on the adequacy of the TEM approximations, numerical predictions of the antenna capacity and effective height were made using the finite difference technique [8].

Effective antenna height and antenna capacitance were evaluated from the numerical data produced by the code. The geometry used in this code is summarized in Figure 4. The antenna was driven by a unit amplitude current source of gaussian form with a matched load at the base of the antenna. The source current is split between the resistive load and the antenna, hence the peak current on the center conductor was .5 amp. A far field radiation boundary condition [8] was employed at a height of five times the slot radius and at ten times the slot radius in the radial direction. The antenna drive point was at the bottom of the antenna coax region five slot radii in depth from the aperture. The various boundaries were maintained constant while the antenna radius was varied. The values of the ratio of the antenna radius to the slot outer radius that were studied were  $a/b = .95, .9, .7, .5, .3$ , and  $.1$ .

In order to evaluate the effective antenna height and the capacitance from the finite difference data, it is necessary to relate these parameters to the fields predicted by the computer code. We will develop here the relationships providing these parameters. Consider first the antenna capacitance. This capacitance is given by

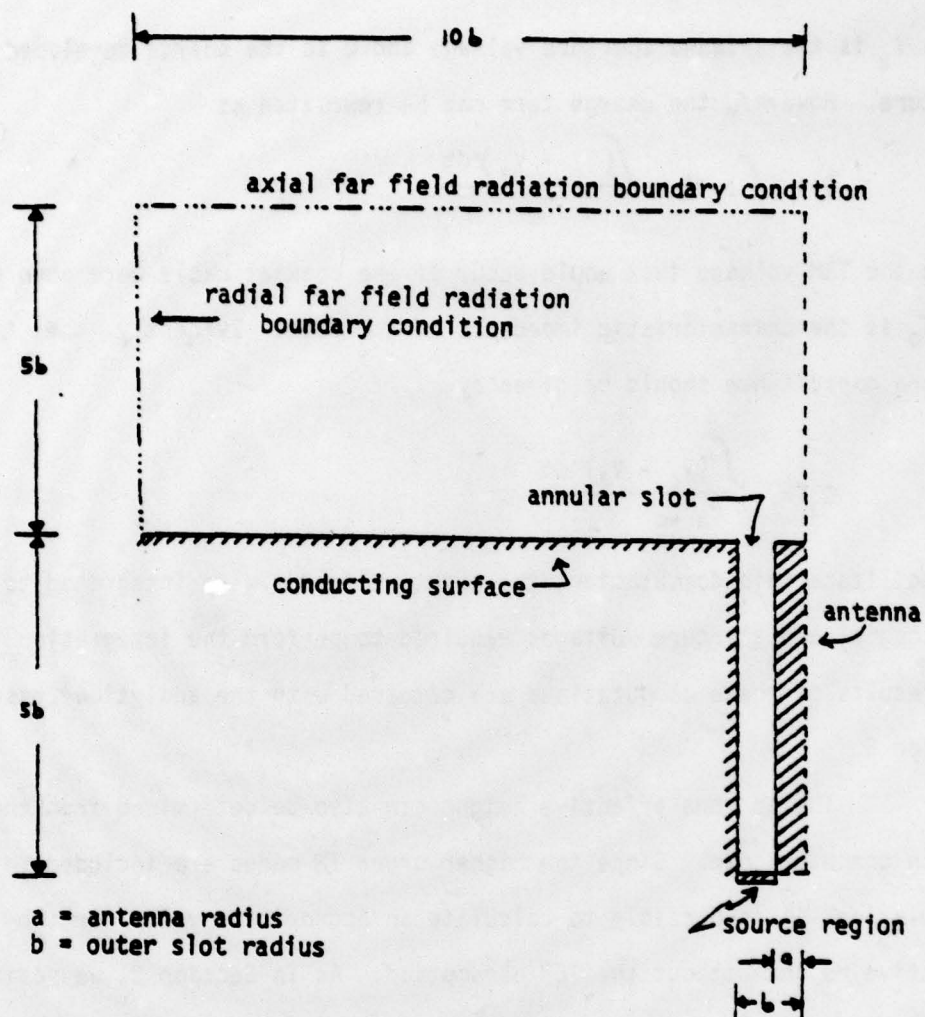


Figure 4: Geometry for finite difference computations

$$C_a = \frac{Q}{V_a}, \quad (23)$$

where  $V_a$  is the antenna aperture voltage and  $Q$  is the charge developed at the aperture. However, the charge term can be rewritten as

$$Q = \int I \, dt = \frac{\int (V_c - V_a) \, dt}{Z_0} \quad (24)$$

$V_c$  is the TEM voltage that would occur if the coaxial cable were open circuited and  $Z_0$  is the characteristic impedance of the slot. Evidently, the antenna capacitance should be given by,

$$C_a = \frac{\int (V_c - V_a) \, dt}{V_a Z_0}. \quad (25)$$

To facilitate this computation, the aperture fields were integrated to compute the coaxial and aperture voltages required to perform the integration in (25). The results of these computations are compared with the analytical results in Section 5.

The antenna effective height can also be determined from the time domain computer code. Since the higher order TM modes are included in this calculation, it is possible to calculate an approximate value for the effective height without the TEM assumption. As in Section 2, we position a TEM exciting source far enough away from the groundplane that the TEM assumption can be expected to be valid for both the transmitted and received fields. We return to (6) and define a new effective height  $h_{eZ_0}$  such that  $h_{eZ_0} E_{inc}$  = the voltage across a resistor equal to the characteristic impedance of the coaxial cable. With this assumption (10) becomes

$$\int E_2 I_1 \, dr = I_1 h_{eZ_0} \left( \frac{j\omega\mu_0 I_2 2h_2}{4\pi r} \right) e^{-jk_0(r+d)}, \quad (26)$$

where the test source is a monopole of height  $h_2$  located on the ground plane  $\theta_0 = \pi/2$  (Figure 2). For the right side of equation (6), we are to use the numerically predicted radiated field at the point  $r$ , then (15) becomes

$$\int E_1 \cdot I_2 \, dv = E_{z1}(r) I_2 h_2 \quad (27)$$

and applying (6), we have

$$h_e Z_0 = \frac{2\pi r E_{z1}(r)}{j\omega\mu_0 I_1 e^{-jk_0(r+d)}} \quad (28)$$

The results of these calculations can be related to the open circuit effective height by substitution into the equivalent circuit of Figure 3.

$$\frac{h_e E^{\text{norm}} \cdot Z_0 e^{-jk_0 d}}{Z_a + Z_0} = h_e Z_0 E^{\text{norm}} \quad (29)$$

Recognizing that  $Z_a = \frac{1}{j\omega C_a} \gg Z_0$ ,

$$h_e = h_e Z_0 \frac{Z_a}{Z_0} e^{-jk_0 d} + \frac{2\pi r E_{z1}(r)}{\mu_0 C_a Z_0 (j\omega)^2 I_1} \quad (30)$$

The results of the computer predictions made using a Gaussian input pulse showed that  $E_{z1}(r)$  was similar in shape to the second derivative of  $I_1(t)$  (Figure 5). However, the pulse that was used as an input was too short to satisfy the requirement that  $k_0 b \ll 1$  at every frequency. As a result, Fourier transforms of the field predictions were substituted into (30) to obtain the results given in Section 5.

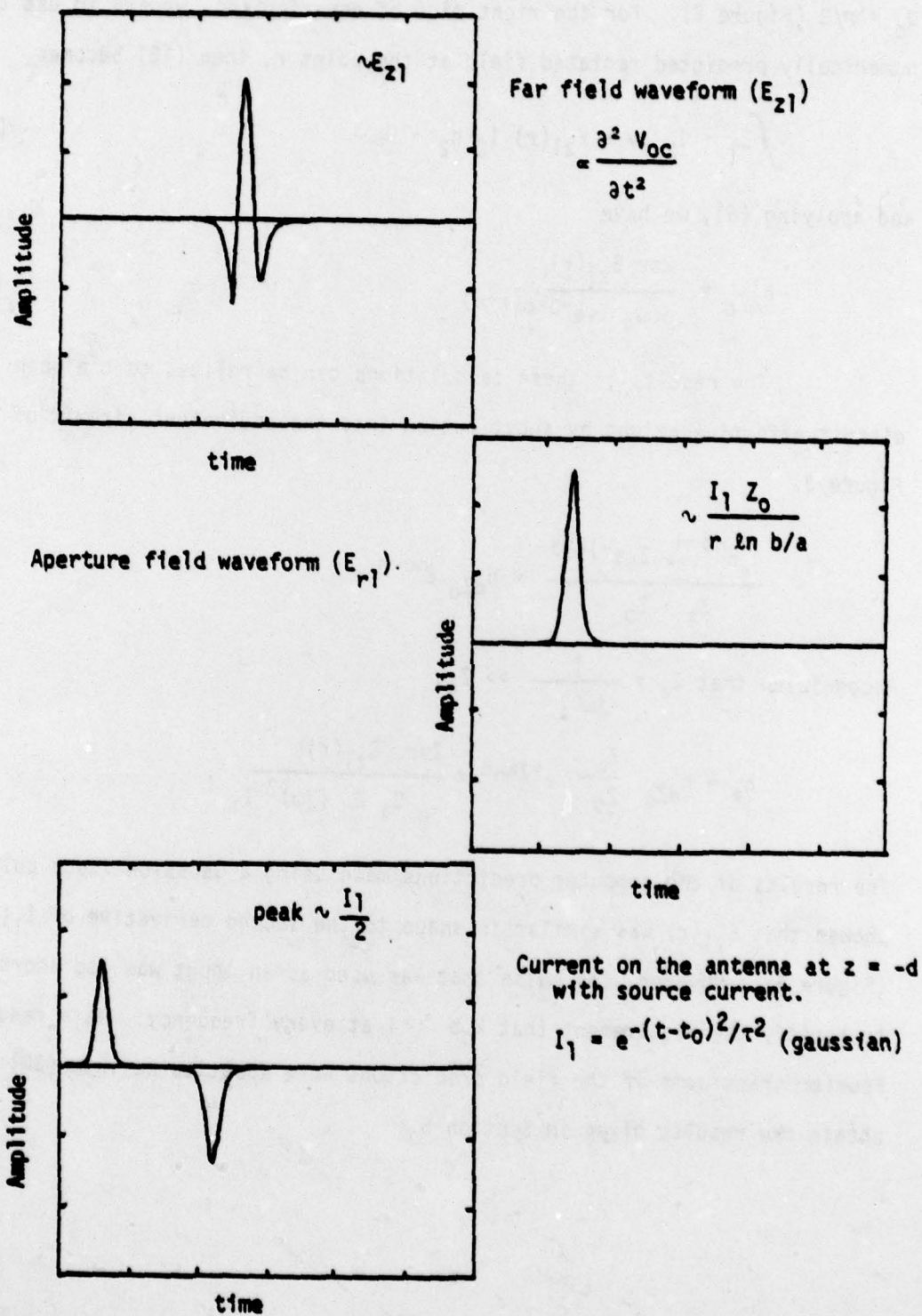


Figure 5: Typical waveforms from the finite difference code

## 5. COMPARISON OF RESULTS AND CONCLUSIONS

The two solution approaches used here both are based on the reciprocity theorem. However, the analytical results for both effective height and antenna capacity assume that only TEM fields exist in the coaxial cable, while the finite difference approach approximately accounts for all TM modes. The accuracy of the finite difference calculations improves as the slot width increases, since there are more finite difference cells in the aperture, while the accuracy of the analytical result should decrease as the slot width increases.

The results of the two prediction techniques are compared in Figure 6. The antenna capacity for this type of antenna is very small, so it was expected to be difficult to extract from the finite difference results. However, the disagreement between the two predictions of antenna capacity was less than 25% over the entire range of  $a/b$ . The calculations of the effective height and the short circuit current disagree by less than 10%. We conclude, therefore, that the most serious inaccuracies are in the computation of the antenna capacity.

In any event, the comparisons suggest that the analytical formulas given in Sections 2 and 3 (or shown in Figure 3) are sufficiently accurate to use for EM susceptibility analysis across the range of  $.3 < a/b < .9$ .

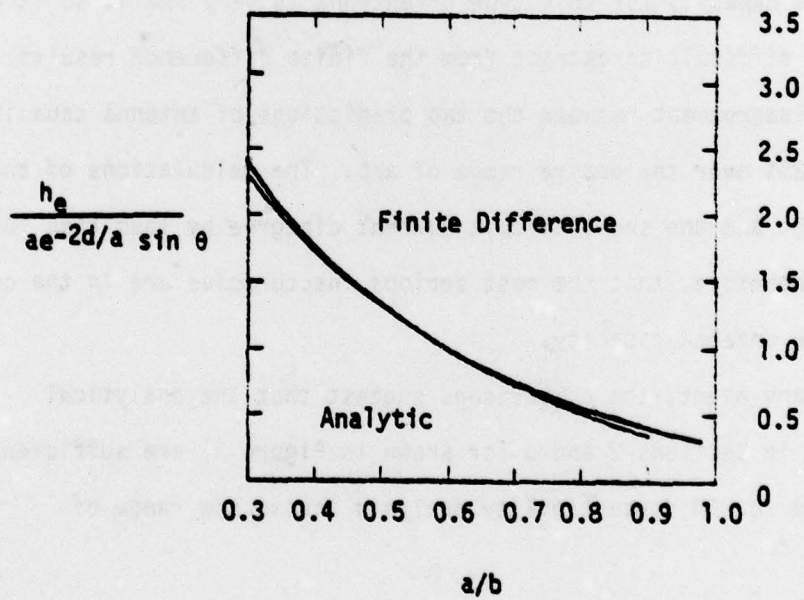
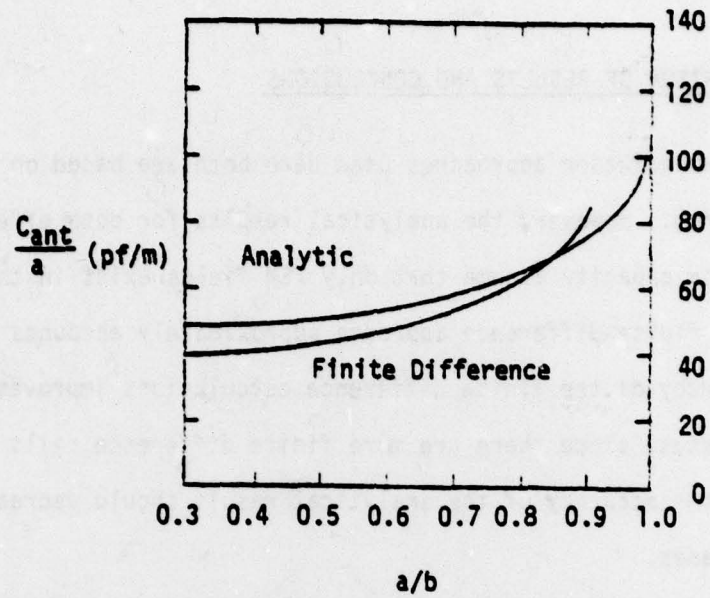


Figure 6: Comparison of Frequency and Time Domain Results

## REFERENCES

1. Jones, J. E. and Richmond, J. H., "Application of an Integral Equation Formulation to the Prediction of Space Shuttle Annular Slot Antenna Radiation Patterns," IEEE Trans. on Antennas and Propagation, Vol. AP 22, No. 1, January 1974, pp 109-111.
2. Sandia Labs, "Electromagnetic Pulse Handbook for Missiles and Aircraft in Flight", Air Force Weapons Lab, EMP Interaction 1-1, September 1972.
3. Chang, D. C. "Input Impedance and Complete Near Field Distribution of an Annular Aperture Antenna Driven by a Coaxial Line," IEEE Transactions on Antennas and Propagation, Vol. AP-18, No. 5, September 1970, pp 610-616.
4. Harrison, C. W. and D. C. Chang, "Theory of the Annular Slot Antenna Based on Duality," IEEE Transactions on EMC, Vol. EMC-13, No. 1, February 1971, pp 8-14.
5. Chang, D. C. and C. W. Harrison, "On the Pulse Response of a Flush Mounted Coaxial Aperture", IEEE Transactions on EMC, Vol. EMC-13, No. 1, February 1971, pp 14-18.
6. Weeks, W. L. Electromagnetic Theory for Engineering Applications, John Wiley and Sons, Inc., New York, 1964.
7. Levine, H. and Papas, C. H., "Theory of the Circular Diffraction Antenna", Journal of Applied Physics, Vol. 22, Jan. 1951, pp 29-43.
8. Merewether, D. E., "Transient Currents Induced on a Body of Revolution by an Electromagnetic Pulse", IEEE Transactions on EMC, Vol. EMC-13, No. 2, May 1971, pp 41-46, and also Interaction Note 93, May 1971.